UNIVERSITÉ DU QUÉBEC

THÈSE PRÉSENTÉE À
L'UNIVERSITÉ DU QUÉBEC À CHICOUTIMI
COMME EXIGENCE PARTIELLE
DU DOCTORAT EN INGÉNIERIE

Par

YU LI

STUDY OF THE INFLUENCE OF ALTITUDE ON THE CHARACTERISTICS OF THE ELECTRICAL ARC ON POLLUTED ICE SURFACE

L'ÉTUDE DE L'INFLUENCE DE L'ALTITUDE SUR LES CARACTÉRISTIQUES DE L'ARC ÉLECTRIQUE À LA SURFACE DE GLACE POLLUÉE

Juin 2002

Mise en garde/Advice

ABSTRACT

In cold mountainous regions, both low air pressure and atmospheric icing can decrease the electrical insulation strength of outdoor insulators used in power transmission networks. This decrease in insulator strength can lead to insulator flashovers and consequent power disruptions. This thesis aims to study the fundamental processes and mechanisms of flashover on the polluted ice surfaces at low air pressure. This study will contribute to the understanding of flashover phenomena observed on ice surfaces at low air pressure, the development of a numerical model for predicting the flashover voltage of ice-covered insulators and the determination of external insulation levels of power networks in cold high altitude regions.

Two physical models of ice were used in this study: a plane triangular ice sample and a real short post insulator covered with wet-grown ice. A series of experimental investigations were systematically carried out in a low air pressure chamber located in the climatic room in the laboratories of industrial chair CIGELE at UQAC. Using a high speed frame camera and a data acquisition system, the flashover process on an ice surface was studied in detail at low air pressure and related parameters were recorded and analyzed. These parameters included the applied voltage, the leakage current, the flashover time, the arc length and the arc root radius. Subsequently, the effects of specific factors on the flashover performance of the two physical models and the corresponding exponent m were determined. These factors included air pressure, applied voltage type and polarity, freezing water conductivity as well as insulator profile. Utilizing a measuring electrode, the voltage-current characteristics of an arc on an ice surface were studied under both AC and DC voltages at low air pressures. The arc constants A, n as well as the electrode voltage drop were determined under various conditions.

The experimental results from this study and the subsequent theoretical analyses suggested specific physical mechanisms of arc propagation on an ice surface: the thermal ionization of the air in front of an arc root resulted in arc movement; the electrostatic force had an auxiliary effect of impelling arc

propagation; the electrical breakdown only occurred during the final jump period of the flashover.

Intriguingly, a decrease in flashover voltage was observed with ice-covered insulators at high altitudes. Four deductions are proposed to explain this observation: a decrease in the arc voltage gradient-current, E-I, characteristics, an increase in current density in the arc core root, a decrease in the electrode voltage drop and, finally, the arc floating phenomena.

Based on the results and deductions from this study, several recommendations were proposed for the future studies.

RÉSUMÉ

Dans les régions froides et montagneuses, la présence d'une pression atmosphérique plus faible ainsi que la présence de glace atmosphérique peuvent diminuer la performance électrique des isolateurs extérieurs utilisés dans les réseaux de transport d'énergie. Cette diminution de la performance électrique peut mener à des contournements d'isolateurs pouvant entraîner des interruptions partielles, voire totales, de la distribution électrique. Cette thèse a donc pour but d'étudier les processus et les mécanismes fondamentaux des contournements électriques d'isolateurs recouverts de glace polluée dans des conditions de pression atmosphérique faible. Cette étude contribuera à la compréhension du phénomène de contournement en haute altitude observé sur surface de glace polluée, au développement d'un modèle numérique de prédiction de la tension de contournement des isolateurs recouverts de glace et à la détermination des niveaux d'isolation externe des réseaux de distribution dans les régions froides en haute altitude.

Pour mener à bien cette recherche, deux modèles physiques de glace ont été utilisés: un échantillon de glace de forme triangulaire et un isolateur réel court recouvert de glace en régime humide. Une série d'études expérimentales systématiques a été effectuée à l'aide d'une chambre de basse pression utilisée à l'intérieur d'une chambre climatique aux laboratoires de la chaire industrielle CIGELE à l'UQAC. Le processus de contournement sous basse pression atmosphérique sur surface de glace a été étudié en détail, et les paramètres associés ont été enregistrés en utilisant une caméra à haute vitesse et un système d'acquisition. Ces paramètres incluent la tension appliquée, le courant de fuite, le temps de contournement, la longueur d'arc et le rayon de racine d'arc. Par la suite, l'influence des facteurs spécifiques tels que la pression atmosphérique, le type et la polarité de la tension appliquée, la conductivité de l'eau formant la glace ainsi que le profil de l'isolateur sur les performances de contournement des deux modèles physiques utilisés ont été déterminés, ainsi que leur influence sur les exposants m (la valeur de m indique le degré de l'influence de la pression atmosphérique sur la tension de contournement) correspondants à chaque modèle. En utilisant une électrode de mesure, les caractéristiques de tension-courant de l'arc électrique se propageant à la surface de la glace en condition de

basse pression atmosphérique ont été étudiées sous des tensions CC et CA. Les constantes *A*, *n* d'arc ainsi que la chute de tension aux électrodes ont été déterminées pour des conditions diverses.

L'étude des résultats expérimentaux et les analyses théoriques ultérieures ont permis de proposer les mécanismes physiques spécifiques à la propagation de l'arc à la surface de la glace. Ces mécanismes physiques se traduisent par : l'ionisation thermique de l'air devant le pied de l'arc entraînant un mouvement de l'arc; la force électrostatique avec un effet auxiliaire d'entraînement de la propagation de l'arc et enfin, le claquage électrique ne se produisant que pendant le saut final du contournement.

De plus, une diminution de la tension de contournement a aussi été observée dans le cas des isolateurs recouverts de glace en condition de haute altitude. Ainsi, les quatre propositions d'explication de ce phénomène sont les suivantes: une diminution des caractéristiques de gradient de tension-courant d'arc, une augmentation de la densité du courant dans le pied d'arc, une diminution de la chute de tension des électrodes et finalement, les phénomènes d'arc flottant.

Basées sur les résultats et les déductions de cette étude, plusieurs recommandations ont été proposées pour de futures études.

ACKNOWLEDGMENTS

I would like to take this opportunity to convey my great appreciation to those who helped me complete this thesis through their technical and moral support.

First of all, I would like to express my deepest gratitude to my director, Professor Masoud Farzaneh, for his supervision, support, patience and confidence during my PhD project.

I would like to acknowledge the staff of the CIGELE and GRIEA, in particular Mr. Sylvain Desgagnés, for their useful ideas and technical assistance in the laboratory.

Finally, I would like to thank my husband, Jianhui, for his continuous encouragement and assistance in test works and for his inspired advice in the writing of this thesis.

TABLE OF CONTENTS

LIST OF FIGURES

LIST OF TABLES

LIST OF ABBREVIATIONS AND SYMBOLS

AC   Alternative current

CA   Courant alternatif (in French)

CC   Courant continu (in French)

CIGELE   NSERC/Hydro-Québec/UQAC Chair on Atmospheric Icing of Power Network Equipment

DAS   Data acquisition system

DC   Direct current

DC+   Positive direct current

DC-   Negative direct current

E-I   Voltage gradient-current

ESDD   Equivalent salt deposit density

EHV   Extra-high Voltage

GRIEA   Research Group on Atmospheric Environment Engineering

HV   High voltage

IEC   International Electrotechnical Commission

IEEE   Institute of Electrical and Electronics Engineers

NaCl   Sodium chloride

SDD	Salt deposit density
UQAC	Université du Quebéc à Chicoutimi (in French)
V-I	Voltage-current

A	Arc constant
d	Distance between electrodes
E	Voltage gradient or electric field stress
F	Electrostatic force
h	Humidity
h_0	Absolute humidity (11 g/m^3)
I	Current
I_c	Critical current
I_{cf}	Critical flashover current
I_m	Peak value of leakage current
J	Current density of arc root
k_1	Air density correction factor
k_2	Humidity correction factor
K_t	Atmospheric correction factor
L	Length of leakage path
L_{arc}	Arc length
L_M	Maximum arc length during the half cycle

m	Exponent
n	Arc constant
P	Ambient air pressure
P_0	Standard atmospheric pressure (101.3 kPa)
R	Correlation coefficient
R_r	Residual resistance
r_p	Residual resistance per unit leakage length
r	Arc root radius
T	Ambient temperature
T_0	Temperature (20 °C)
t	Time
V	Voltage
V_0	Voltage under standard atmospheric pressure condition
V_{arc}	Voltage along arc
V_c	Critical voltage
V_e	Electrode voltage drop
V_F	Estimated flashover voltage
V_{MF}	Minimum flashover voltage, the lowest voltage level at which 2 flashovers occur out of a maximum of 3 tests
V_m	Voltage on the measuring electrode
V_{total}	Voltage including the electrode voltage drop and the voltage drop along the arc itself

V_{WS}	Maximum withstand voltage, the highest voltage level at which at least three withstand tests out of four can be obtained
v	Arc propagation velocity
v_{max}	Maximum instant velocity of arc propagation
x	Arc length
x_c	Critical arc length
x_P	Pollution layer length
α	First Townsend coefficient
γ	Second Townsend coefficient
δ	Relative air density
σ	Freezing water conductivity
ε_0	Air permittivity

LIST OF PAPERS PUBLISHED FROM THIS PH. D THESIS WORK

[1]   Farzaneh, M., Li, Y. and Zhang, J., "Effect of High Altitude on DC Flashover Process on an Ice Surface", *International Journal of Offshore and Polar Engineering*, Vol. 11, No. 4, pp. 304-309, December 2001.

[2]   Farzaneh, M., Li, Y. and Zhang, J., "Process of AC Arc Propagation on an Ice Surface at Low Air Pressure", *Submitted to the Conference of the International Association of Science and Technology for Development (IASTED 2002)*, Marina Del Rey, USA, May 2002.

[3]   Shu, L., Farzaneh, M., Li, Y., Zhang, J., Sima, W. and Sun, C., "Effects of Low air Pressure and Contamination on Flashover Performance of Ice-covered Insulators", *Submitted to the 10th International Workshop on Atmospheric Icing of Structures (IWAIS 2002)*, Brno, Czech Republic, June 2002.

[4]   Shu, L., Farzaneh, M., Li, Y. and Sun, C., "AC flashover performance of polluted insulators covered with artificial ice at low atmospheric pressure",

Proceedings of IEEE Conference on Electrical Insulation and Dielectric Phenomena (CEIDP 2001), Kitchener, Canada, pp. 609-612, October 2001.

[5]   Li, Y., Farzaneh, M. and Zhang, J., "Behavior of DC Arcs on an Ice Surface at Low Air Pressure ", *Proceedings of 12th International Symposium on High Voltage Engineering (ISH 2001)*, Bangalore, India, Vol. 3, Paper 5-42, August 2001.

[6]   Farzaneh, M., Li, Y., Zhang, J. and Fikke, S.M., " Effect of Low Pressure on V-I Characteristics of AC Arc on Ice Surfaces", *Proceedings of IEEE Conference on Electrical Insulation and Dielectric Phenomena (CEIDP 2000)*, Victoria, Canada, Vol. 1, Paper 3A-15, October 2000.

[7]   Farzaneh, M., Li, Y., Zhang, J. and Mercure, H., "E-I Characteristics of DC Arc on an Ice Surface under Low Atmospheric Pressure ", *Proceedings of 9th International Workshop on Atmospheric Icing of Structures (IWAIS 2000)*, Chester, UK, pp. 1-4, June 2000.

[8]   Farzaneh, M., Li, Y., Fikke, S. M. and Mercure, H., "DC Flashover of artificial Ice-Covered Insulators at Low Atmospheric Pressure", *Proceedings of 9th International Offshore and Polar Engineering Conference (ISOPE 1999)*, Brest, France, Vol. 2, pp. 612-615, May 1999.

[9]   Li, Y., Farzaneh, M. and Zhang, J., "Critical Flashover Voltage of Short HV Insulator Covered with Ice at Low Atmospheric Pressure", *Proceedings of*

1998 International Conference on Power System Technology (POWERCON 1998), Beijing, China, Vol. 1, pp. 520-523, August 1998.

[10] Farzaneh, M., Li, Y. and Zhang, J., "DC Flashover on Ice Surface at Low Atmospheric Pressure", *Proceedings of 8th International Workshop on Atmospheric Icing of Structures (IWAIS 1998)*, Iceland, pp.209-212, June 1998.

[11] Li, Y., Farzaneh, M. and Zhang, J., "Effects of Voltage Type and Polarity on Flashover Performances at Low Atmospheric Pressure on an Ice Surface", *Proceedings of 8th International Offshore and Polar Engineering Conference (ISOPE 1998)*, Montreal, Canada, pp. 543-546, May 1998.

[12] Farzaneh, M., Li, Y. and Zhang, J., "Effects of Altitude on AC Flashover on Ice Surfaces", *Proceedings of 10th International Symposium on High Voltage Engineering (ISH 1997)*, Montreal, Canada, pp.73-76, August 1997.

CHAPTER 1

INTRODUCTION

CHAPTER 1

INTRODUCTION

1.1 GENERAL

The first central electricity-generating station, the Pearl Street Station, was inaugurated by Edison to light New York City in 1882. This station was able to energize 400 lamps each lamp consuming 83 W. In the same year the first transmission line from Miesbach to Munich, providing 1343 V DC, was designed by Miller and Duprez. Today, the electricity industry has spread all over the world. Long distance power transmission lines and the high voltage level substations have been widely used in the electric power networks due to increase of the need for electric power, which makes the insulation components in electrical equipments, in particular various insulators, play an increasingly important role in power system operation.

Insulators are devices that are used in electrical supply networks to support, separate or contain conductors at high voltages. Insulators function to electrically separate and mechanically connect two conductors with different electric

potentials. Normally, most insulators are used in high voltage overhead transmission lines and substations. They are called outdoor insulators and are required to withstand extreme changes in the environmental conditions.

1.2 PROBLEM DEFINITION

In cold regions, atmospheric ice can accumulate on overhead transmission lines due to freezing rain or drizzle, in-cloud icing, icing fog, wet snow or frost during winter. This ice will endanger the normal operation of electric power systems and may result in the power disruption, which will bring troubles into community services and daily life.

The most serious power accident in Canadian history occurred in January 1998 [9]. A sequence of three ice storms hit successively the areas of southern and western Quebec, eastern Ontario and part of the Atlantic Provinces. Over the period of January 5-9, about 100 mm of freezing rain fell on these regions. Ice accretion resulted in the collapse of more than 1,000 power transmission steel towers (including 735 kV level towers), and 30,000 wooden poles. Close to 1.4 million people in Quebec and 230,000 in Ontario were without power for several days. A month after the ice storm, 700,000 people were still without electricity. The direct economic loss for a single power company, Hydro-Québec, was

approximately one billion Canadian dollars. Social cost may have exceeded three times that amount [56].

There are two main negative effects of accumulated ice or snow on electrical equipment. The first is excessive mechanical loading of towers, transmission lines and substations hardware that can either lead to impeding proper operation of apparatus or, in extreme cases, to major collapsing of the lines with dramatic consequences. The second is a change in the insulation performance of insulating material and structures that sometimes may result in flashover faults and the consequent power outages. Such events have been reported by many authors in various countries such as Canada [7] [16] [57] [94], United States [11] [72] [74], Japan [91], Norway [36], China [138], England [39] and Finland [71].

A typical example of an insulator flashover incident occurred on March 9-10, 1986 within the Ontario Hydro network [94]. Due to freezing rain and fog, the surface of the insulators accumulated ice and short icicles, which resulted in 57 successive flashovers. Of these, 27 involved transmission line insulators in the area just west of Toronto. Most of the 500 kV transmission systems in southern Ontario were collapsed in this incident. Other flashover events took place on April 18, 1988 at the Arnaud substation in the Hydro-Québec network [57]. A series of

six flashovers, which caused by insulators covered with wet snow, resulted in a major power interruption for a large part of the province of Québec.

Power outages in the United States were also reported by **Kawai** [72]. Some of which occurred during a warm morning after an ice storm in the west coast area and others were recorded during snow or ice storms in the northeast area. An ice flashover was cited as the cause of a major disturbance in an EHV substation in the Southern area [72]. An ice storm caused numerous 345 kV post insulators to flash over in a non-contaminated station in 1976 according to **Charneski** [11]. Similar flashovers were experienced from post insulators on February 1, 1980 at the Monroe Power Plant 345 kV station, USA.

With increased industrialization and expansion, the development of new power systems called for the construction of transmission lines and substations in high altitude regions (higher than 1000 m). In such areas, the electrical performance of insulators is influenced not only by low air pressure, but also, in many cases, by atmospheric icing. This is because the ice accretion rates generally increase with altitude on mountains due to higher wind speeds and greater cloud frequencies [119] [127]. Serious icing conditions together with the low air pressure make a dangerous situation for power transmission lines. A number of power outages, reported from several countries as Japan [128], Norway

[35] [36], Switzerland [93] and China [122] [123] [124] [125], were attributed to the coinciding presence of atmospheric ice and low air pressure.

Fikke [35] described several accidents occurred in southern Norway, where a transmission line crosses a 1000 -1100 m mountain range with a peak of 1400 m. From January 1981 to February 1989, 21 flashovers were detected that were probably caused by contaminated ice on insulators.

In the winter of 1966/1967, **Meier et al** [93] reported several grounding faults that they attributed to ice and snow accumulations on a 400 kV line crossing the alpine chain in Switzerland. The altitude of this area is more than 2500 m above sea level, and the highest peak is about 2750 m.

Some outages in southwest China were reported by **Su et al** [124] [125]. In this region most overhead transmission lines are built in cold mountainous districts where the altitude ranges from 1000 m to 4000 m above sea level. Ice-accumulations resulted in frequent power system accidents from November to February of each year. Since 1961, about 98 icing accidents were recorded from more than twenty transmission lines in mountainous districts within Yunnan province. A small number of flashovers on insulator strings covered with contaminated-ice were observed by linemen on 110 kV and 220kV transmission lines.

The above-mentioned power system problems have motivated a large number of important studies concerning the effects of either atmospheric ice or altitude on the insulator flashover.

Studies on the flashover of ice-covered insulators may be traced back approximately 40 years [65] [74]. Published results have been typically concerned with the flashover performance of ice-covered insulators as well as the factors influencing flashover voltage. The mechanisms underlying phenomenon of flashover on ice-covered insulators have not yet to be fully understood. Up until now, only some tentative explanations have been proposed.

Most of the previous studies focus on the flashover on polluted insulators under high altitude conditions. Only a few of initial studies examined the combined effects of altitude and ice accretion. To the best of our knowledge, there has been no detailed and systematic study on the flashover on ice-covered insulators under high altitude conditions.

A more thorough review of previous studies is presented in Chapter 3 of this thesis.

1.3 RESEARCH OBJECTIVES

In order to advance our knowledge on the flashover mechanisms of ice-covered insulators under high altitude conditions, this PhD thesis aims to study of the effects of low air pressure on the flashover process, the performance of ice-covered insulators and the arc characteristics and behavior on ice surfaces. More specifically, the objectives are as follows:

- Investigation of the influence of low air pressure on flashover on ice surfaces. Specifically, the value of exponent m, which was used in the literature extensively to account for the variation of the flashover voltage with ambient pressure, will be determined under various conditions, including the voltage types and polarity, the conductivity of freezing water and the different profiles of insulators

- Examination of the effects of the low air pressure on the voltage-current characteristics of AC and DC arcs. Specifically, the arc constants A, n and the electrode voltage drop V_e at different air pressures will be determined

- Investigation of the influence of low air pressure on the behavior of arcs on ice surface. In particular, arc propagation velocity and arc root radius will be determined

- Revelation of the flashover mechanisms of ice-covered insulators, particularly at low air pressure, and the identification of the factors that contribute to the decrease of flashover voltage at low air pressure

1.4 METHODOLOGY

In order to attain the objectives of this study, a series of laboratory experiments were initially carried out in a climatic room and the results were subjected to a theoretical and statistical analysis. The main methods used in this study are summarized as follows:

- With the purpose of simulating a high altitude atmospheric condition, an evacuated chamber (low air pressure chamber) was set up. Inside this chamber, the air pressure was able to be adjusted from 101 kPa to 30 kPa (corresponding to altitudes of 0 to 9000 m).

- For studying the effects of insulator profile on the flashover phenomena under ice and low air pressure conditions, a real short post type insulator and a simplified physical ice model, namely a plane triangular ice sample, were used.

- The maximum withstand voltage, the highest voltage level at which at least three withstand tests out of four can be obtained, of ice samples

or ice-covered insulators was determined under various conditions using the method developed and adapted by CIGELE at UQAC [22] based on that of IEC 507 [60].

− In order to make it possible to accurately and easily measure arc characteristics, the plane triangular ice sample was also used for determining arc parameters.

− A high-speed frame camera and a data acquisition system were utilized to record the arc propagation velocity, its behavior on ice surface, as well as the corresponding voltage and leakage current waveforms.

− The characteristics of an arc on an ice surface were determined under various conditions by utilizing a measuring electrode, the high-speed camera and the data acquisition system.

− The regression analysis (the least squares method) was applied to the test results from the investigation of flashover performance to determine the value of exponent m and the study of arc characteristics to determine the arc constants A, n.

− Physical mechanisms of flashover on ice-covered insulators, particularly at low air pressure, are proposed based on the observation of flashover phenomena and the analysis of the results in this study.

1.5 STATEMENT OF ORIGINALITY

In this work, the phenomenon that the flashover voltage of ice-covered insulators at high altitude decreases with ambient air pressure was systematically studied in detail for the first time.

The author designed an experiment setup to duplicate the reduced air density and cold climate conditions in high altitude regions and carried out a series of more than 1300 tests. Effects of low air pressure on the flashover performance of ice sample and ice-covered insulators, the V-I characteristics of an arc on an ice surface as well as the propagation process of an arc were investigated for the first time.

From the obtained results, certain novel facts and phenomena were discovered concerning arc propagation on an ice surface at low air pressure. Consequently, physical mechanisms of flashover on ice-covered insulators at standard and low air pressure were discussed. Additionally few deductions were used in an attempt to explain the fact that the flashover voltage of ice-covered insulators decreases with the decrease of the air pressure were proposed based on the analysis of the results.

1.6 ORGANIZATION OF THE THESIS

This thesis contains nine chapters.

The present chapter is an overall introduction for this PhD thesis. In this chapter the research objectives, methods used, and main contributions of this study are briefly described.

Some related fundamental theories, particularly those related to electric discharge in gases and on dielectric surfaces, are presented in the second chapter.

A literature review is arranged in the third chapter. This chapter summarizes the results from the previous study related to this thesis work from two aspects: atmospheric icing and low air pressure.

The flashover performance results from the short type post insulator and the plane triangular ice sample respectively under various air pressures are presented in Chapters 4 and 5. From these experimental results, values of exponent m are deduced for different conditions. Factors affecting the value of m are discussed.

Chapter 6 focuses mainly on the effects of low air pressure on the V-I characteristics of an arc on an ice surface. The electrode voltage drops and the arc constants A and n were all determined at different air pressures.

In Chapter 7, the behavior of an arc on an ice surface at low air pressure is discussed. The arc propagation velocity and arc root radius under various conditions are presented and demonstrated in this chapter.

In Chapter 8, the flashover process on ice-covered insulators at low air pressure is investigated. The flashover mechanisms of ice-covered insulators at low air pressure are discussed and four deductions explaining the decrease of flashover voltage at low air pressure are proposed.

Finally, in Chapter 9, some general conclusions are summarized from analyses and discussions of the results reported in the previous chapters. In addition, some recommendations are provided for the future research.

CHAPTER 2

FUNDAMENTAL THEORIES ON ELECTRICAL DISCHARGES AT LOW AIR PRESSURE

CHAPTER 2

FUNDAMENTAL THEORIES ON ELECTRICAL DISCHARGES AT LOW AIR PRESSURE

2.1 INTRODUCTION

Flashover faults on the insulators of power systems caused by some severe climatic and environmental conditions take place occasionally. In fact, this flashover phenomenon is a type of electrical discharge. More precisely, it is a surface discharge.

This chapter will provide a brief review of the fundamental physics underlying electric discharges in gases and along gas-solid interfaces. Some basic types of electric discharge in gases as well as their mechanisms and characteristics will be introduced followed by the principal theories concerning discharges along polluted surfaces. The effects of certain parameters, in particular air pressure, will also be discussed.

2.2 ELECTRIC DISCHARGE IN GASES

2.2.1 Definition of Electric Discharge in Gases

A gas in its normal state is almost a perfect insulating material. However, when a high enough electric field is established in a gas between two electrodes, the gas can become a conductor. Electric discharge in gases is a phenomenon induced by an electron current flowing through the gas.

A gas can exhibit conductivity only when it possesses free charged particles. Ionization and electron emission are two main ways to generate the free charged particles where [102]:

- ionization is the process of liberating an electron from a gas particle in the gaseous space, and
- electron emission is the process of liberating an electron from the surface of a solid electrodes.

2.2.2 Electric Discharge Types

Electric discharges may exist as many types. The classification of electric discharge differs according to specific criteria.

Based on its appearance, electric discharge can be roughly divided into four main types [8] [102]:

- Glow discharge is a phenomenon where luminous diffusion takes place in the space between two electrodes.

- Corona discharge is a type of partial discharge observed within a non-uniform electric field. It has a luminous zone surrounding the smaller electrode as the corona surrounding the sun during an eclipse.

- Arc channel is a region of completely ionized gas. It is also a very hot plasma state that is extremely bright and has a very high current density. Amongst complete V-I characteristics of gaseous discharges, an arc occupies a zone where the current is highest.

- Spark discharge is also a completely ionized gas, but it is transient. If the power supply is not sufficiently powerful, there is a bright, thin yet intermittent spark observed between the electrodes.

The discharge can also be divided into non-self-sustaining and self-sustaining discharges as follows [62]:

- Non-self-sustaining discharge requires certain external factors, (such as natural or artificial radiation), to maintain ionization. The external factors are essential to the continuation of the discharge.

− Self-sustaining discharge does not depend on external factors to maintain ionization. On the contrary, it is maintained by the electric field alone.

2.2.3 Breakdown Mechanisms

If the discharge completely bridges the gap, which reduces the voltage between the electrodes to near zero, it is called an electrical breakdown. There are two basic theories that explain a process of electrical breakdown. The first is called the Townsend discharge mechanism and the second is called the streamer discharge mechanism [86].

2.2.3.1 Townsend mechanism

The Townsend discharge mechanism can be summarized as follows:

1). Current resulting from the α process

When an electron moves through a gas it will collide and may ionize the gas molecules, which generates novel free electrons. This process is called the α process. The novel free electrons may generate other free electrons in the same way during their movement in electric field. Such a group of electrons named an avalanche.

In the case of a uniform electric field, the current, I, increases exponentially with electrode separation, x, as follows:

$$I = I_0 e^{\alpha x} \qquad (2.1)$$

where I_0 is the current caused by the initial electrons from the emission from the cathode. α is the Townsend first ionization coefficient and it indicates the number of collision ionizations that occur when one electron moves one unit length along the electric field strength E. α can be determined by the following relation:

$$\frac{\alpha}{P} = A_0 e^{-\frac{B_0 P}{E}} \qquad (2.2)$$

where P is the air pressure; A_0 and B_0 are constants that depend on the gas temperature [102].

2). Current resulting from both α and γ processes

When positive ions impact a cathode, they may produce a secondary electron emission, which is called the γ process. The coefficient γ indicates the number of free electrons released from a cathode per positive ion impact. Therefore, γ depends on the material and surface state of the cathode. A typical value for γ is in the order of 10^{-2} to 10^{-3} [102] and is 0.01 for air [75].

The current resulting from both the α and γ processes can be determined by the following equation:

$$I = I_0 \frac{e^{\alpha d}}{1 - \gamma \cdot e^{\alpha d}} \qquad (2.3)$$

3). The condition of a self-sustaining discharge

With the increase of applied voltage, the electric field increases, which leads to an increase in both α and $\gamma \cdot e^{\alpha d}$ until $\gamma \cdot e^{\alpha d}$ approaches 1. The denominator in Equation (2.3) then approaches 0 and I approaches infinity. When the current approaches infinity, then the discharge becomes self-sustaining. Therefore, the condition of self-sustaining discharge in a uniform field can be expressed as following [102]:

$$\alpha d = k = \ln \frac{1}{\gamma} \qquad (2.4)$$

In the case of a uniform field, the above equation is also the condition of breakdown within the gas. The value of k is typically within a range of 4 to 7 when γ is in the order of 10^{-2} to 10^{-3} [102].

2.2.3.2 Streamer mechanism

When the product of the air pressure (P) and the distance between electrodes (d), Pd, is greater than 150 mmHg·cm, the effects of space charge on the electric field distribution cannot be neglected. For this reason, the streamer

breakdown mechanism was originally proposed [87] [92] [113] to help develop and augment the Townsend discharge mechanism.

The streamer breakdown mechanism can be summarized as follows:

1). Space charge in the electric avalanche distorts the applied field

Due to different moving velocities of electrons and positive ions, a lot of space charges appear in the primary electric avalanche as shown in Fig. 2.1 (a). These space charges create an evident distortion of the electric field. The electric field strength at the front and tail of the avalanche increases. However, the field strength between the positive and negative space charges in the electric avalanche decreases as shown in Fig. 2.1 (b).

2). Streamer process

The increased electric field at the front of an avalanche will effectively promote the excitation of atoms. Many photons will be emitted when atoms return from their excited states to their normal state. These photons may lead to photoionization of other atoms and auxiliary avalanches will be created. After the main avalanche has crossed the gap, the electrons are swept into the anode where the positive ions remain in a cone-shape volume as shown in Fig. 2.2 (a).
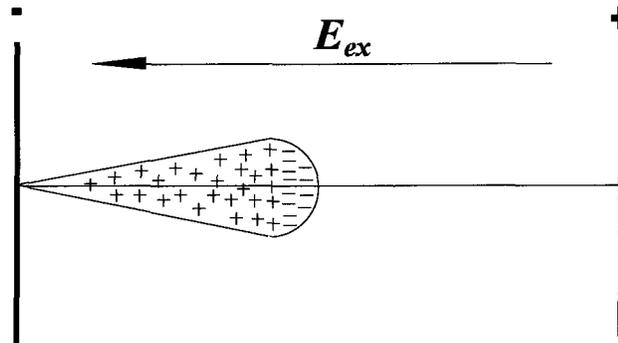
(a) Electric avalanche
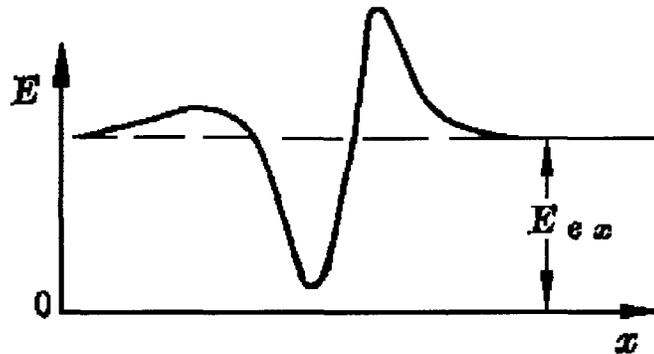
(b) Electric field distorted

Fig. 2.1 Distribution of space charges in the electric avalanche

and distortion of the applied field [134]

E_{ex}: Applied field

A highly localized space charge field is produced and more auxiliary avalanches are created near the anode. The tip of the streamer attracts the oncoming avalanches and its electrons enter the zone of positive ions. This action forms a plasma channel, which extends from the anode toward the cathode. This is called the streamer channel. Fig. 2.2 (b) shows the streamer having crossed half

of the gap length. If the tip of streamer arrives at the cathode, the final breakdown

will occur. Fig. 2.2 (c) illustrates a schematic diagram of the completed streamer
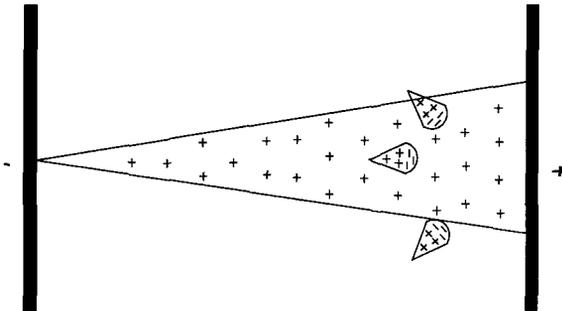
channel.

(a) Main avalanche has crossed the gap
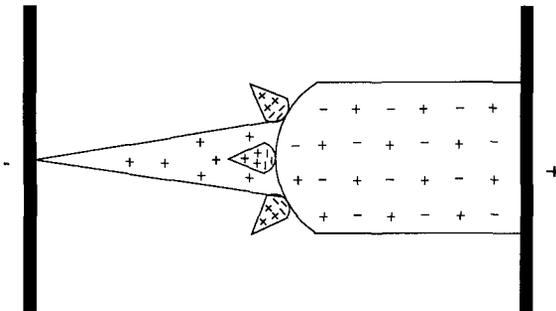
(b) Streamer length equal to half of the gap length
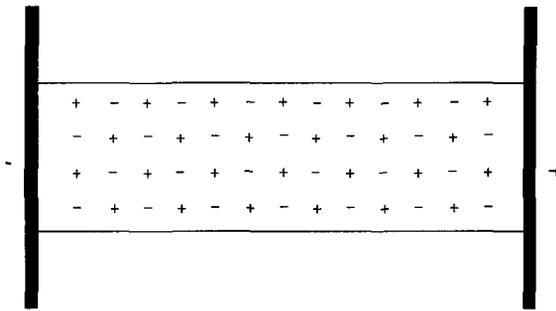
(c) Completed streamer channel

Fig. 2.2 Schematic diagram of the propagation of a streamer

A highly localized space charge field is produced and more auxiliary avalanches are created near the anode. The tip of the streamer attracts the oncoming avalanches and its electrons enter the zone of positive ions. This action forms a plasma channel, which extends from the anode toward the cathode. This is called the streamer channel. Fig. 2.2 (b) shows the streamer having crossed half of the gap length. If the tip of streamer arrives at the cathode, the final breakdown will occur. Fig. 2.2 (c) illustrates a schematic diagram of the completed streamer channel.

Normally, the streamer process has a comparatively narrow spark track compared to the more diffused form of glow obtained in the Townsend process.

3). The condition of self-sustaining discharge

As mentioned above, once the streamer forms, the discharge can be maintained by photoionization, which is created by the discharge itself. From this moment the discharge becomes the self-sustaining discharge. The formation of a streamer is the condition of a self-sustaining discharge in a uniform field, which can also be expressed as follows [86]:

$$e^{\alpha d} = K = const. \tag{2.5}$$

where the constant K is approximately 10^8.

In order to compare the streamer mechanism with the Townsend mechanism, equation (2.5) can be written as follows:

$$\alpha d = k = const. \tag{2.6}$$

It should be noted that equation (2.6) has the same form as the condition of a self-sustaining discharge derived from the Townsend mechanism, as represented by equation (2.4). However, k is equal to 18 to 20 for the streamer formation [86], which is higher than that observed for the Townsend mechanism.

2.3 SURFACE DISCHARGE

2.3.1 Definition of Surface Discharge

When an electric discharge occurs on a surface of a dielectric in a gaseous or liquid medium, it is called a surface discharge. Furthermore, if an electric breakdown occurs along the interface between the gas and liquid, or the gas and solid, it is termed a flashover. In this study, the focus will be on flashover phenomenon observed along an insulator surface, which will be the interface between a gas and a solid.

2.3.2 Surface Flashover Mechanism

Surface flashover on an insulator in a vacuum, can be divided into three stages [97]:

- Initiation: A surface flashover usually begins with the emission of electrons (generally by field or thermal emissions) from a triple junction, where the electrode, insulator and gas meet.

- Development or growth: There are two main theories that describe the development of a surface flashover discharge. They are as follows:

  - Secondary electron emission avalanche. Some of the initial electrons impact the insulator surface and produce additional electrons and, a secondary electron emission avalanche will develop.

  - Electron cascade within a thin surface layer of an insulator. Some electrons are injected into the insulator by tunneling at the cathode. Part of these electrons will be emitted into the vacuum and others will be accelerated by the electric field within the insulator and make inelastic collisions. An electron cascade will be created along the surface (but just inside the insulator) as soon as their energy exceeds the band gap of the insulator.

Both of these processes can cause desorption of the gas, which had been previously absorbed by the insulator surface.

– Final. The desorbed gas is ionized. The existence and movement of the ions then produce further increase in the current along the insulator surface. Finally, surface flashover of the insulator occurs.

2.3.3 Flashover of Polluted Insulators

Flashover on polluted insulators is a type of flashover phenomenon caused by the deposition of pollution on an insulator surface. To investigate this phenomenon, many flashover tests were carried out under natural or artificial pollution conditions, (respectively in a pollution station or in a laboratory) [15] [42] [78]. The International Electrotechnical Commission (IEC) has worked out a series of international standards for artificial pollution tests on high-voltage insulators [60] [61].

2.3.3.1 Flashover process on a polluted surface

Generally, the process of flashover on polluted insulators can roughly be divided into the following four stages [50] [67] [117]:

1). Deposition of pollutant

The pollutant, which is found in aerosol form, can precipitate on an insulator surface and form a pollution layer.

2). Wetting of the pollution layer

The resistance of the pollution layer is very high when it is dry. Therefore, pollution does not cause an obvious decrease in the insulating properties of insulators. However, under some inclement climactic conditions, (such as the fog, dew, drizzle, etc.), the pollution layer, consisting highly soluble electrolytes, will be humidified and its conductivity will get increased. As the result, a leakage current will flow through the pollution layer as illustrated in Fig. 2.3(a).

3). Formation of a dry band and a local arc

Because of the shape of insulators, the current density on the surface is generally non-uniform. In areas of high current density, the heating effect of the current is greater and a local dry zone will appear in these areas. This local dry zone will lead to the constriction of current. The local dry zone will then have a tendency to laterally extend until a complete dry band is formed as shown in Fig. 2.3(b).

A dry band has a high resistance; therefore, the applied voltage will drop primarily along the dry band. If the voltage is high enough, the dry band will be broken down and a local arc will appear across it. In the vicinity of the local arc root, the concentration of the current will lead to a widening of the dry band as shown in Fig. 2.3(c).

(a)

(b)

(b)

(d)

(d)

(f)
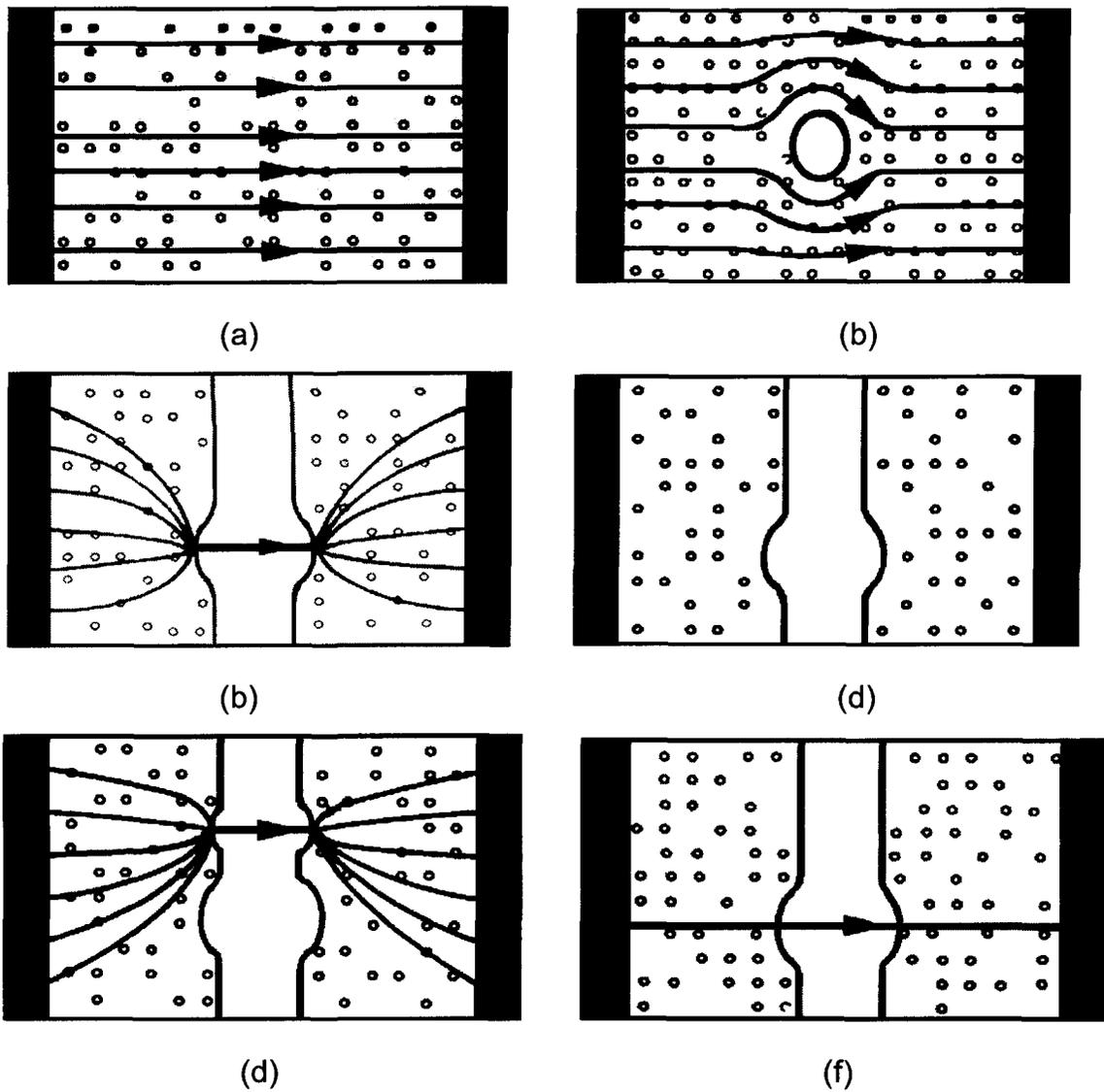
Fig. 2.3 Stages of flashover on polluted surface [79]

4). Development of an arc and completion of a flashover

Depending on the conditions, a surface discharge can evolve into the following possible ways:

- The local arc can extinguish as shown in Fig. 2.3(d).

- The local arc can move laterally to find a more stable position that corresponds to a shorter arc length as shown in Fig. 2.3(e).

- The local arc can extend longitudinally until it reaches the electrodes and causes a complete flashover. In this case, the arc extends along the surface of a humid pollution layer without the dry zone as shown in Fig. 2.3(f).

2.3.3.2 Flashover mechanism of polluted insulators

In order to reveal the mechanisms underlying the flashover phenomenon, some researchers used simple physical models such as a water channel [13] [67] [90] and a plane triangular [63], disc [66] [141] or cylindrical sample [53]. Currently, the mechanisms underlying arc development and the consequent flashover phenomenon are not well understood.

1). Criteria for pollution flashover

Several researchers have proposed certain criteria for arc development and flashover. The first quantitative criterion was proposed by **Obenaus** [107] and completed by **Neumärker** [104], which is known as the extinction theory. The flashover process is modeled as an arc in series with a resistance, which

represents the non-bridged portion of a wet pollution layer as schematically shown in Fig. 2.4.
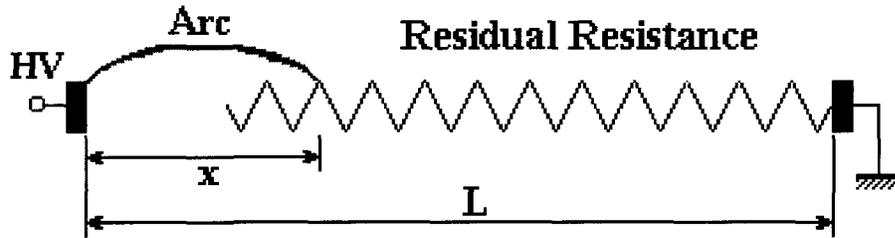
Fig. 2.4 Modeling concept for studying arc development

The corresponding circuit equation can be expressed as follows:

$$V = V_{arc} + IR_r \tag{2.7}$$

where V is the overall voltage between electrodes; I is the leakage current; V_{arc} is the voltage along arc and R_r is the residual resistance of the pollution layer. The arc voltage V_{arc} can be expressed as:

$$V_{arc} = AxI^{-n} \tag{2.8}$$

where A and n are the arc constants. x is the length of arc.

According to Equation (2.7), V was found to have a minimum value, V_c, for arc extension. If the following Equation (2.9) was satisfied, the arc will extend and the flashover will occur.

$$V_{app} \geq V_c \tag{2.9}$$

where V_{app} is the applied voltage. A derivation method was deduced by **Alston** and **Zoledziowski** [2]. The critical voltage V_c, critical current I_c and critical arc length x_c were obtained from the following:

$$\begin{cases} V_c = A^{\frac{1}{n+1}} \cdot L \cdot r_p^{\frac{n}{n+1}} \\ x_c = \dfrac{L}{n+1} \\ I_c = \left(\dfrac{A}{r_p}\right)^{\frac{1}{n+1}} \end{cases} \tag{2.10}$$

where L is the leakage path length and r_p is the pollution resistance per unit of leakage length. However Obenaus' extinction criterion is a necessary rather than a sufficient criterion for flashover.

Hampton [50] and **Hesketh** [52] established the criterion for arc motion as follows:

$$\frac{di}{dx} > 0 \tag{2.11}$$

If this criterion is satisfied for all positions along a possible arc path, then flashover will occur.

Näcke [99] proposed an electrical stability criterion. The change of total voltage for displacement of the discharge root at constant current is considered within this criterion. This can be represented by the following relation:

$$dV = \left(\frac{\partial V_{arc}}{\partial x}\right)_i dx + i\left(\frac{\partial R}{\partial x_P}\right)_i dx_P \qquad (2.12)$$

where x is the arc length and x_P is the length of the pollution layer. It is assumed that the arc will move if $dV < 0$.

With respect to AC voltage, there are three models for arc reignition following current zero.

– Energy reignition model

In the energy reignition model, the breakdown takes place when the residual arc gap is no longer able to dissipate the injected energy. The critical condition for energy breakdown is as follows [89]:

$$V_{cx}^2 = kN_{02}R_m x \qquad (2.13)$$

where V_{cx} is the critical voltage corresponding to the arc length x, N_{02} is the post-zero constant of the arc characteristic, R_m is the residual arc resistance at peak current, k is the thermal diffusivity.

– Dielectric reignition model

Dielectric breakdown takes place when the instantaneous value of the recovery voltage exceeds the dielectric strength of the gap, and is typical of relatively slow rates of recovery voltage. The critical condition for dielectric breakdown is as follows [117]:

$$V_{cx} = xE_{da}f(I_m)$$
(2.14)

where E_{da} is the dielectric strength at ambient temperature.

Using an arc in series with a uniform pollution resistance, the minimum flashover voltage can be obtained as follows [117]:

$$\frac{V_c}{L} = 23r_p^{0.4}$$
(2.15)

– Experimentally based model

These models are based solely on experimental results. One model shows the relationship between the minimum arc reignition voltage, the lowest voltage at which an AC arc reignition following current zero takes place, and the arc current and can be represented as follows [18]:

$$V_{cx} = \frac{800x}{\sqrt{I}}$$
(2.16)

where I is the arc current.

2). Physical mechanism underlying the arc development and flashover

The above criteria for flashover do not consider any of the physical processes involved in pollution flashover. One such physical process involves the external forces that pull the discharge across a surface. Suggested external forces

include electrostatic attraction, electromagnetic forces, thermal buoyant forces [19] [40] [101] [108] [114].

Jolly [67] deduced the external forces acting on an arc root be the following amounts: electrostatic force of 2.8×10^{-6} N; electromagnetic of 1.6×10^{-10} N; thermal buoyant force of 1.3×10^{-7} N. Such a small order of forces could not result in an arc development velocity in the order of $10^2 \sim 10^3$ m/s during the pollution flashover process. Therefore, it was proposed that the pollution flashover is an electric breakdown process. The convergence of current flow lines at the arc root will produce a high local electric field, which accelerates the electron impact and ionized the air in front of the arc head, thus extending the arc. Thermal and photoelectric ionization will increase the ionization process.

Mercure et al [96] measured the current distribution in the arc root during flashover and proposed that a higher current density and arc temperature on the forward side of arc result in an apparent motion of the arc root region and the consequent elongation of the arc at the surface of the electrolyte.

Li [82] and **Zhang** [146] calculated separately the electric field stress at the arc root. **Li** found it too low to cause the electric breakdown of air and proposed that pollution flashover can be caused by the thermal ionization of salt in the column due to high temperatures. **Zhang** concluded that the main factor of making

the arc to propagate forward is the thermal ionization of air and the strong normal component of field strength plays an important role in the resultant temperature increase and the formation of thermal ionization. When the arc length reaches about 90% of leakage length, the electrical field at the arc root is high enough for the electric breakdown of air, which leads to the final flashover of polluted insulators.

3). Velocity of arc propagation

Different types of ionization can lead to different arc propagation velocities. Therefore, the investigations of the mechanisms underlying arc development and flashover need to consider the velocity of arc propagation.

Using a high-speed camera, **Al-Baghdadi** [1] obtained the following empirical formula for DC arc velocity:

$$v = 1.54 \times 10^{-4} r_P^{2.5} \left(i^4 - i_c^4 \right) \text{ cm/s} \tag{2.17}$$

where v is the arc velocity, i is the arc current, i_c is the critical current, r_P is the pollution resistance per unit length.

Assuming that the energy required for the creation of a new arc length comes from the electrode voltage drop at the water surface, **Jolly et al** [68] deduced that:

$$v = \frac{V_e i}{Q} \qquad (2.18)$$

where V_e is the electrode voltage drop and Q is the energy content per unit length

of the arc.

Zoledziowski [149] found that AC stress-duration characteristics of polluted

insulators can be expressed as:

$$\left(V^2 - V_c^2\right) \cdot t = const. \cdot R_r^{\;2} \qquad (2.19)$$

where V_c is the constant (critical voltage) and R_r is the pollution resistance of the

insulator. After assuming and deducting further [117], Equation 2.19 can be

modified to the following:

$$\left(V^2 - V_c^2\right) \cdot t = \frac{\sigma \cdot Q}{3} \cdot r_p^{\;2} \cdot L^3 \qquad (2.20)$$

where σ is the constant conductance at the tip of a discharge .

Rizk [117] assumed that the variables that could influence arc velocity are

the arc constants A and n, the arc time constant θ, the insulator parameters (such

as x_p, L and r), the supply circuit parameters including V, the angular frequency ω

and inductance L_s. Using a dimensional analysis method to the Al-Baghdadi's

experiments results [1], the arc velocity, v was obtained from following relation:

$$v = const. \cdot i^4 \cdot r_p^{\frac{4.5}{1+n}} \qquad (2.21)$$

where i is the arc current and r_p is pollution resistance per unit leakage length.

2.4 ELECTRIC DISCHARGE AT LOW AIR PRESSURE

Section 2.2.3 illustrated that the ionization coefficients α and γ are related to gas pressure. Therefore, air pressure is an important factor affecting breakdown and flashover voltage.

2.4.1 Paschen's Law

In 1889, Paschen's experimental results lead to the conclusion that the breakdown voltage V is solely the function of the product Pd:

$$V = f(Pd) \tag{2.22}$$

This is called Paschen's law, where V is the breakdown voltage, P is the gas pressure and d is the electrode separation. The relation between V and Pd has been sketched in Fig. 2.5. For air, the minimum voltage V_{min} is 327 V and occurs when Pd = 0.567 mm Hg. cm [75].
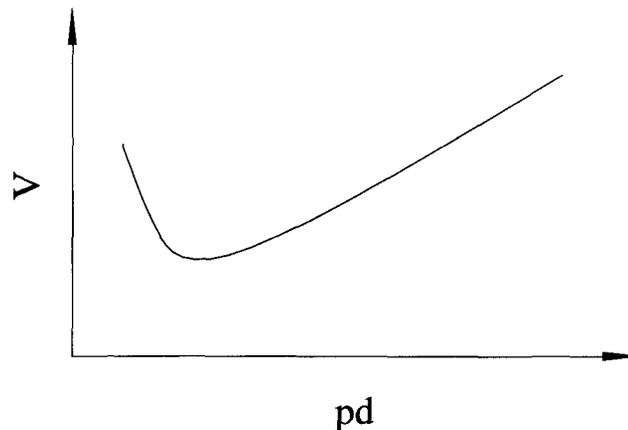
Fig. 2.5 Paschen curve

The general shape of the Paschen curve can be explained from the ionization theory of gases. Within a fixed-space gap at very low pressures (the left branch from the minimum voltage point), the collision frequency is low such that sufficient ionization is maintained only by increasing the probability of ionization at each collision. Consequently, the electron velocity, and thus the electric field must be high. Hence V must increase as P diminishes. At higher pressures (the right branch from the minimum voltage point), the collision frequency is high, which results in a high rate of energy loss. Therefore, the energy gained per free path is low unless the field is high. Correspondingly, V must increase when P increases. Therefore, the curve must show a minimum V. The actual discharge in air is under a relatively high Pd product and, consequently, it can be located on the right branch of the Paschen curve.

2.4.2 Atmospheric Correction Factors

As mentioned above, the breakdown or flashover of external insulation depends upon the atmospheric conditions. At high altitude, the breakdown or flashover voltage decreases usually with the decrease of either air density or humidity. For the case of flashover on ice-covered insulators, the humidity normally reaches saturation around the arcs, and hence only air density is important.

2.4.2.1 Standard reference atmosphere condition

According to IEC international standard [62], the standard reference atmospheric condition is:

- Pressure: $P_0 = 101.3$ kPa (760 mmHg);

- Temperature: $T_0 = 20\ °C$;

- Absolute humidity: $h_0 = 11$ g/m^3.

2.4.2.2 Correction of flashover voltage under different air pressures

By applying certain correction factors, a flashover voltage measured under given test conditions (temperature T, pressure P, humidity h) can be converted to the value that would have been obtained under the standard reference atmospheric conditions (T_0, P_0, h_0).

Without correcting for air humidity, the flashover voltage in a given test condition, V, can be corrected to the corresponding value under standard reference atmosphere condition by using the following:

$$V_0 = k_1 \cdot V \qquad (2.23)$$

where k_1 is the air density correction factor. Both the pressure and temperature will influence air density.

The air density correction factor depends on the relative air density δ and can be generally expressed as:

$$k_1 = \delta^m \qquad (2.24)$$

$$\delta = \frac{P}{P_0}\frac{273+T_0}{273+T} \qquad (2.25)$$

where P_0 and P are the standard atmospheric pressure (101.3 kPa) and the test ambient pressure respectively. T_0 and T are the standard reference temperature of 20 °C and the test ambient temperature respectively. The value of exponent m is still under consideration.

CHAPTER 3

LITERATURE REVIEW

CHAPTER 3

LITERATURE REVIEW

3.1 INTRODUCTION

A review of the literature pertinent to this thesis will be presented in this chapter. With respect to the objectives of this thesis, concerning the flashover on an ice surface under low air pressure, this review will focus on the following:

- studies concerning flashovers under atmospheric icing conditions
- studies concerning flashovers under high altitude conditions

For both of these topics, the studies on the flashover performance of an insulator, the mechanisms underlying flashover and the modeling of arc development on an insulator surface will be summarized.

3.2 STUDIES CONCERNING ATMOSPHERIC ICING ON AN INSULATOR

Atmospheric ice accretion on power transmission lines has been studied for many years. At UQAC, the Research Group on Atmospheric Environment Engineering (GRIEA) and the later created NSERC/Hydro-Québec/UQAC Chair on Atmospheric Icing of Power Network Equipment (CIGELE) have worked in this field for over 25 years. A wealth of valuable results was published and several reviews were completed by **Farzaneh et al** [17] [23] [25] [29]. In general, the previous investigations can be classified into three categories:

- ice accretion

- flashover performance of an insulators covered with ice

- underlying mechanisms and modeling of a flashover on an ice surface

3.2.1 Ice Accretion

It is accepted that the ice accumulated on an insulator surface is formed essentially from the coagulation of supercooled water droplets below 0 °C. Ice accumulation generally requires three conditions, which are as follows:

- The meteorological condition: a sufficient amount of supercooled water droplets must be present in the atmosphere

- The hydrodynamic condition: the supercooled water droplets are attracted to a solid surface

– The thermodynamic condition: the supercooled water droplets are immediately frozen onto the solid surface

The ice formed under different atmospheric and environmental conditions has dissimilar characteristics. **Kuroiwa** [77], **Imai** [58] and **Oguchi** [109] classified ice into three basic types: hard rime, soft rime and glaze, based on air temperature, wind velocity, water droplet size and liquid water content. Hard rime is opaque and has a density between 0.6 and 0.87 g/cm^3. Soft rime is white and opaque, with a density less than 0.6 g/cm^3. Glaze is transparent and has a density of approximately 0.9 g/cm^3. Conditions favoring the formation of various types of ice in nature are summarized in Table 3.1 [58] [76] [77] [109].

Table 3.1 Conditions favoring the formation of various types of ice [109]

Type of Ice	Density (g/cm^3)	Surrounding Temperature (°C)	Wind Velocity (m/s)	Water Droplet Diameter (µm)
Hard Rime	0.6 – 0.87	-3 – -15	5 – 20	5 – 20
Soft Rime	< 0.6	-5 – -25	5 – 20	5 – 20
Glaze	0.8 – 0.9	0 – -3	1 – 20	500 – 6000

All of above conditions of icing are under non-energized, which is different from the situation for an operating ice-covered insulator. To study flashover on an

ice-covered insulator, **Farzaneh et al** [25] formed various types of ice on an energized insulator in a climate room at the Université du Québec à Chicoutimi. The ice was grown under one of two regimes; a wet-grown or a dry-grown regime. Both hard rime and soft rime ice were grown under a dry regime. Under the dry regime, all the water droplets impinging on an insulator surface were completely frozen. In contrast, glaze is grown under a wet regime where icicles formed around the insulator sheds. This type of ice deposition simulated ice accretion during freezing rain precipitation. The experimental parameters for dry-growth and wet-growth ice are listed in Table 3.2.

Table 3.2 Experimental conditions for dry-growth and wet-growth ice [25]

Type of Regime	Surrounding Temperature (°C)	Droplet Size (µm)	Wind Velocity (m/s)	Liquid Water Content (g/m³)
Dry	-12	15	3.3	6.8
Wet	-12	80	3.3	6.8

Two forms of accretions, the icicle form and the curtain form, were observed during a field study of ice accretion on high voltage equipment. This observational study was carried out in a number of geographical regions within the Hydro-Quebec network [22]. Meteorological parameters including air temperature and wind velocity were also recorded. The icicle was the most common form detected.

The conditions for forming icicles were a freezing rain with the range from a few millimeters to 10 mm, and an air temperature between –4 °C and –1 °C. The curtain resulted from a freezing rain precipitation between 30 and 40 mm and an air temperature of approximately –1 °C.

3.2.2 Flashover Performance of an Insulator

The flashover on an ice-covered insulator was a main contributing cause for the power outages recorded in power networks constructed in cold regions. The flashover performance of an ice-covered insulator has been the focus of many investigations in countries with cold climates and a large number of papers have been published on this topic. It is generally accepted that atmospheric ice can decrease the insulating strength of an insulator under AC, DC or impulse voltages [22] [43] [72] [91] [110] [111] [138] The minimum flashover voltage of an insulator covered with ice was found to be less than 30% of the minimum flashover voltage of a wet insulator. This observation was influenced by several factors such as the icing process, environmental condition and applied voltage types.

3.2.2.1 Influence of ice type

Different types of ice have different characteristics. Therefore, ice type is a factor which may influence the insulating strength of an insulator.

Phan et al [110], **Khalifa et al** [74] and **Shu et al** [122] separately examined the minimum flashover voltage of a short insulators string covered with three types of ice: soft rime, hard rime or glaze. The hard rime was considered to be the most severe type of ice.

Fujimura et al [43] measured the withstand voltage of an ice-covered suspension insulator string formed in a cold room and a snow-covered insulator where the snow originated from a mountain. The AC withstand voltage of an ice-covered insulator was approximately 40% lower than the withstand voltage of an insulator covered with snow. The DC withstand voltage of ice-covered an insulator was practically the same as that measured for a snow-covered insulator.

Sugawara et al [129] investigated how the AC withstand voltage varied with ice density for two standard suspension insulator units covered with artificial ice. The withstand voltage decreased slowly with an increase in the ice density from 0.6 to 0.8 g/cm3. For an ice density of 0.9 g/cm3, the withstand voltage was markedly smaller than that observed for an ice density of 0.6 or 0.8 g/cm3.

Farzaneh et al [22] [25] studied the effect of dry and wet grown ice on the maximum withstand voltage gradient of different insulator types. The maximum withstand voltage gradient under wet-grown ice conditions was substantially lower

than the voltage gradient under dry-grown ice conditions. **Renner at al** [115] obtained similar results.

Overall, these results suggest that glaze and hard rime ice were more dangerous to transmission lines than soft rime ice.

3.2.2.2 Influence of the amount of ice

The amount of ice was another factor affecting the flashover voltage of an ice-covered insulator. There is currently no international standard for measuring the amount of ice on insulator surface. Accordingly, different parameters were used in different studies to determine the amount of ice. These parameters included the ice weight or thickness on insulators, the ice weight per unit of insulator dry arc distance [43] [72] [123] and the ice thickness on a monitoring cylindrical conductor [22] [110] [121].

Kawai [72] conducted a series of AC flashover tests on a standard or anti-fog insulator string of five to seven units in a refrigerated room. The thickness of the ice layer around insulators was found to be non-uniform, and the maximum thickness was approximately 0.4 cm, which will likely result in a flashover on today's extra-high voltage lines under operating voltages. **Phan et al** [110] showed that the minimum flashover voltage of insulators covered with hard rime decreased with an increase in ice thickness of up to 2 cm. A thickness of ice larger than 2 cm

resulted in a virtually constant minimum flashover voltage. **Sugawara et al** [129] reported that the withstand voltage, V_{ws}, decrease slightly with an increase in ice thickness. V_{ws} for the sheds with the icicles cut away was found to be substantially higher than the V_{ws} measured for a shed with the same ice thickness but with icicles under the sheds.

The ice thickness on insulators was non-uniform and difficult to measure. Therefore, using the ice weight on insulators to calculate the ice amount, **Fujimura et al** [43] and **Shu et al** [123] studied the flashover performance of a suspension insulator string covered with ice. The withstand voltage became lower and tended to saturation as the weight of ice increased.

In a laboratory setting, the ice weight on an insulator was difficult to measure reliably for every test, especially for a post type insulator. Therefore, **Farzaneh et al** [22] [24] [32] used the thickness of wet ice grown on a rotating monitoring cylinder as a reference parameter to determine the amount of ice. It was found that the maximum withstand stress, V_{ws}/m of an insulator decreases with up to a 2 cm increase in ice thickness for anti-fog insulators, 2.5 cm for IEEE standard and EPDM insulators, 3.0 cm for post insulators. After these thickness markers were reached, V_{ws}/m remained constant. When the ice thickness exceeded 1.5 cm, the probability of flashover on insulators used in EHV transmission lines.

3.2.2.3 Influence of freezing water conductivity

The pollutants in the atmosphere can increase the conductivity of atmospheric ice, which will consequently increase the leakage current of an ice-covered insulator and cause a decrease in insulating strength.

Fikke et al [35] [36] conducted a large number of field studies on the atmospheric conditions connected to flashovers that occurred between 1981 and 1989. Flashover events in the mountainous areas in Norway occurred primarily because of icing conditions combined with a high ion concentration caused by salt or the combustion of fissile fuels.

Kannus et al [70] examined the effect of the resistivity of freezing water on the leakage current of AC flashover tests. When the resistivity of freezing water was decreased from 90 Ωm to 9 Ωm, the leakage current pulses appeared earlier during icing period and the amplitudes increased rapidly. In conclusion, the flashover voltage of two suspension insulator units was found to be linearly proportional to the square root of the resistivity of freezing water.

In Canada, **Chisholm et al** [16] developed a cold-fog test method to reproduce a flashover on an insulator while considering surface contaminations, ice and fog, while the ambient temperature was increasing to 0 °C. A winter fog

flashover was thought to be a common problem for 500-kV substations with light ESDD levels, 230-kV substations with moderate ESDD levels, and 115 kV substations with heavy ESDD levels. They also found a strong influence of ice temperature on flashover voltage in the range of –2 °C to 0 °C

Fujimura et al [43], **Matsuda et al** [91] and **Vouckovic et al** [135] carried out separately flashover tests on insulators covered with ice formed from water with different conductivities. They reported that the flashover voltage of insulators covered with ice depended on the conductivity of the water. When the conductivity was high, the withstand voltage of an insulator was low.

The effect of freezing water conductivity on the withstand voltage of ice-covered post insulator was also studied at CIGELE [22] [24] [25]. The gradient of the maximum withstand voltage decreased with an increase in the freezing water conductivity up to a value of 80 µS/cm. After this level of water conductivity, the gradient of the maximum withstand voltage tended towards a saturation value.

3.2.2.4 Influence of the insulator length

The flashover voltage of an ice-covered insulator string depended on its length. **Farzaneh et al** [22], **Phan et al** [110], **Kannus et al** [70] and **Su et al** [126] separately studied the flashover voltage of a short insulator string and found that

the minimum flashover voltage of an ice-covered insulator string increased more or less linearly with the length of the insulator string up to 1 m.

Kawai [72] tested the flashover voltage of both a long (19 to 25 units) and a short (5 to 7 units) insulator strings covered with ice. No linear relationship between insulation strength and insulator length discovered under mild ice conditions. The flashover voltage per insulator unit was considerably lower for a long insulator string than for a short insulator string. This disparity was attributed to the non-uniform voltage distribution along the insulator string.

3.2.2.5 Influence of ice uniformity

The uniform ice distribution closely depended on the wind velocity during ice accretion on an insulator. One of the effects of ice uniformity was its influence on the leakage distance of insulators covered with ice and the consequent flashover voltage [24].

Farzaneh et al [22] [24] [25] observed that nearly vertical icicles formed when the wind velocity was lower than 3.3 m/s, resulting in a relatively uniform ice distribution along the insulator string or post insulator. Icicles twisted toward the insulator axis and a non-uniform ice distribution formed at higher wind velocities of up to 6.4 m/s. The leakage distance for a one-meter string of IEEE insulators

covered with wet-grown ice increased in a linear manner as the wind velocity increased. Consequently, the maximum withstand voltage gradient rose rapidly with an increase in the leakage distance. Overall, the greater the uniformity of ice distribution along an insulator string, the greater the possibility of a flashover.

3.2.2.6 Influence of leakage current

The leakage current was occasionally used as a parameter to study the performance of ice-covered insulators.

Khalifa et al [74] studied the influence of atmospheric ice accretion on the performance of a high voltage insulator string in 1965. The critical leakage current of an ice-covered insulator was found to be less than the critical leakage current of a polluted insulator.

Hara et al [51] studied the effect of leakage current on the flashover performance of iced insulators. The threshold value for the current of a white arc was approximately 18 mA. This threshold value remained constant during periods of ice deposition and de-icing. The flashover threshold current was practically equal to the observed maximum stable white arc current. This current was above or equal to 120 mA for a long rod insulator and 180 mA for a porcelain insulator.

3.2.2.7 Influence of insulator type

Many different types of insulators have been developed to accomplish a variety of purposes. The insulating performance under icing conditions will be different for different types of insulator.

Using porcelain, glass and composite insulators, **Khalifa** [74] studied the flashover performance of these insulators under icing conditions and found that the insulating performance of a composite insulator was inferior to that of a ceramic insulator string. Contrary to this result, **Cherney** [14] tested five different types of long-rod insulators covered with ice and concluded that the insulating performance of a composite insulator was superior to that of an IEEE standard insulator string. Additionally, a composite insulator with alternative sheds had a better performance than one with uniform sheds. **Wu et al** [142] found that the insulating performance of a composite insulator, such as SIR or EPDM, was superior to that of a glass cap-pin insulator string. Finally, it was discovered that the insulating performance of a long insulator string covered with ice could be improved by using corona rings.

3.2.2.8 Influence of insulator position

An insulator string can be installed in different positions within a transmission line, which can influence the accumulation of ice on insulators and the consequent insulating performance.

Renner at al [115] reported that a suspension insulator installed with a swing angle had higher insulation strength than that observed for an insulator assembled vertically with the same mass of ice. Similar results were obtained by **Lee et al** [80] and **Schneider** [120]. They separately tested an insulator in a vertical, horizontal and V type position. The V type insulator string had a superior performance than that observed for a vertical string under similar ice conditions. However, **Bui et al** [10] discovered that the horizontal position was superior to the other two positions under icing conditions.

3.2.2.9 Influence of voltage polarity

Many researchers have studied the effect of voltage polarity on the flashover performance of an ice-covered insulator since the development of DC transmission lines.

Watanable [138] carried out a series of DC flashover tests on an insulator covered with ice or snow. The minimum flashover voltage of an insulator was found to be higher under negative voltage than that measured under positive voltage under both ice and snow conditions. Contrarily, **Fujimura et al** [43] reported that the flashover voltage of an ice-covered insulator was lower under negative polarity and consequently conducted the experiments exclusively under DC- voltage conditions. However, **Renner et al** [115] found that the flashover voltage of ice-covered insulators under DC- voltage was only slightly lower than the

flashover voltage measured under DC+ voltage. Consequently, the effect of voltage polarity could be neglected.

A number of tests were carried out under DC conditions at CIGELE [28] [31]. The minimum flashover voltage of a short string of four anti-fog insulators was considerably lower under DC- than under DC+ voltage. The minimum flashover voltage disparity between DC- and DC+ voltage conditions was approximately 32% for an ice thickness of 0.5 cm and 47% for an ice thickness of 3 cm or greater.

3.2.3 Flashover Mechanism and Modeling

3.2.3.1 Arc characteristics and flashover mechanism

Because the flashover on an ice surface was influenced by many factors, its mechanism was very complicated. Up until now, most published studies mainly concentrated on determining the flashover performance of an ice-covered insulator and the relevant factors. Only a few studies were concerned with the fundamental aspects of a flashover on an ice-covered insulator.

Jordan et al [69] studied the corona discharge at the surface of an ice needle. Meanwhile, **Phan et al** [112] measured the corona discharge of water drops over the freezing temperature range. The evolution of a corona discharge of

a water drop was studied during its transition from a liquid to a solid phase and vice versa.

Sato et al [120] investigated the flashover performance of a flat plate insulator covered with the three types of ice, (glaze, soft rime and hard rime), formed by spraying a contaminated liquid on an insulator in a cold room. For a given concentration of NaCl-contaminated liquid, the average SDD (Salt Deposit Density) value for an ice state was 5 to 9 times higher than the average SDD value under ice-free conditions, which lead to a 20% reduction in the flashover stress under soft rime conditions when compared to ice-free conditions.

Sugawara et al [130] investigated the AC flashover mechanism of an insulator covered with salt-contaminated ice. A white arc appeared on both the high voltage and earth-facing sides of the insulator with an increase in the test voltage. The white arc melted the ice on the earth-facing side of the insulator. The melt water had a very high conductivity and flowed along the edge of the accreted ice. The arc developed along a path produced by the flow of melt water. Flashover occurred as a consequence of this mechanism.

Using a simple physical model, **Bui et al** [10] studied the characteristics of a DC arc between a metal electrode and an ice surface in a small refrigerated chamber where the temperature could be adjusted to a value between –50 °C and

20 °C. The electrode voltage drop, V_e, and the arc constants A and n did not change with a change in ice temperature yet they did change with a change in the electrode polarity. Table 3.3 illustrates the results of this particular study. The limitation of experiment is that the distance between the HV electrode and measuring electrode is only 3 mm.

Table 3.3 Arc constants under different voltage polarities [10]

Polarity	Positive	Negative
V_e (V)	900	400
A	166	380
n	0.56	0.49

Using a triangular physical model of ice, **Farzaneh et al** [26] [27] [32] [33] carried out a large number of investigations on the characteristics of both a dynamic and a static arc on an ice surface under AC and DC conditions. Under AC conditions, V_e was included in the calculation of the arc constant A. Hence, when the arc length was less than 7 cm, the influence of the arc length on the arc characteristics could not be neglected. Under DC conditions, the E-I characteristics of both a dynamic and a static arc were not affected by the arc length. There was a slight difference between the characteristics of a dynamic and a static arc. Table 3.4 presents the results of this particular study.

Using a cylindrical ice sample, **Chen** [12] similarly investigated the arc V-I characteristics and V_e under both DC and AC voltage conditions. The results for this particular study are presented in Table 3.5.

Table 3.4 Electrode voltage drop and arc constants obtained at

CIGELE using a triangular ice sample [27] [32] [33]

Arc Type		AC	Positive	Negative
Static Arc	V_e (V)	—	—	502
	A	346.4	—	107.5
	n	0.36	—	0.61
Dynamic Arc	V_e (V)	—	799	526
	A	204.7	208.9	84.6
	n	0.56	0.45	0.77

Table 3.5 Electrode voltage drop and arc constants obtained at UQAC

using a cylindrical ice sample [12]

Arc Type	AC	Positive	Negative
V_e (V)	953	735	608
A	152.1	169.1	213.1
n	0.52	0.59	0.53

At CIGELE, **Zhang et al** [144] [145] studied the behavior of an arc on an ice surface under AC and DC conditions. An arc could propagate in two different ways: inside or outside the ice. The arc propagation was divided into two stages. The first stage began the moment a violet arc was established with an initial length of 5% of the total ice sample length and ended when the arc length reached approximately 40% of the total length. The arc extended relatively slowly. The second stage was discernible by an arc length between 40% and 100% of the total length. During this stage, the arc propagation velocity suddenly increased. The maximum velocity was reached immediately before flashover. Table 3.6 illustrates the arc propagation velocity under different voltage types and polarity.

Table 3.6 Arc propagation velocity under different
voltage types and polarities [144]

Arc type		Arc propagation velocity (m/s)		
		First stage	Second stage	Maximum value
Positive arc	outer	0.05 to 0.3	20 to 50	≈ 100
	inner	-	3 to 7	≈ 50
Negative arc	outer	0.05 to 0.3	35 to 60	≈ 100
	inner	-	10 to 20	≈ 50
AC arc	outer	0.04 to 0.15	16 to 30	≈ 440
	inner	-	2 to 7	≈ 260

For both AC and DC arcs, the arc root radius was found to increase in a non-linear manner as the leakage current was increased. The radius of the outer arc root was substantially larger than the radius of the inner arc root. The radius of an AC arc was somewhat smaller than the radius of a DC arc.

3.2.3.2 Electric arc modeling

The field and laboratory investigations concerning a flashover on an ice-covered insulator are costly and time consuming. For this reason, several researchers have attempted to establish a mathematical model to predict the flashover voltage of an ice-covered insulator.

The first mathematical model was based on a series of experiments conducted by CIGELE for calculating the flashover voltage of a short ice-covered insulator string with a length up to 1 m [27] [34]. This model is based on the Obenaus' concept as illustrated in Fig. 2.4. During the flashover process, due to the presence of a water film with relatively high conductivity on the ice surface, the major part of leakage current is conductive and passes through the arc and water film. Therefore, the basic equation, the arc reignition condition and the equation for calculating the residual resistance are as follows:

$$V = V_e + AxI^{-n} + IR_r(x) \tag{3.1}$$

$$I = \left(\frac{kx}{V}\right)^{\frac{1}{b}} \tag{3.2}$$

$$R_r(x) = \frac{1}{2\pi\gamma_e}\left[\frac{4(L-x)}{D+2d} + \ln\left(\frac{D+2d}{4r}\right)\right]$$ (3.3)

where V is the applied voltage, I is the leakage current, k and b are the arc reignition constants, x is the arc length, $R_r(x)$ is residual resistance, γ_e is the surface conductivity of the ice layer, L and D are the length and diameter of the insulator, d is the thickness of the ice layer and, finally, r is the arc root radius.

Using a triangular physical ice model, all the necessary parameters depicted in above equations were empirically determined [26] [27] [33] [34] [143] [144] [145]. The results are depicted in Table 3.7.

Table 3.7 Parameters for calculating the flashover voltage of an ice-covered insulator under AC and DC conditions [27] [34] [143]

	AC	Positive	Negative
V_e (V)	—	799	526
A	204.7	208.9	84.6
n	0.56	0.45	0.77
k	1118	—	—
b	0.5277	—	—
γ_e	$0.0675\sigma + 2.45$	$0.082\sigma + 1.79$	$0.0599\sigma + 2.59$
r	$\sqrt{\dfrac{I}{0.875\pi}}$	$\sqrt{\dfrac{I}{0.648\pi}}$	$\sqrt{\dfrac{I}{0.624\pi}}$

This model was applied to a 5-unit string of IEEE standard insulators covered with ice. The calculating results corresponded well with the experimental results. It was also successfully applied to insulators that ranged in voltage from 44 kV to 500 kV and in leakage distance from 1 to 10 m [34].

At CIGELE, a dynamic mathematical model is currently being established to calculate the flashover voltage, the leakage current and the arc propagation velocity. Initial results have already been published [30] [37] [38].

Sundararajan et al [132] calculated the flashover voltage of an ice-covered insulator using a dynamic arc model, which was previously used to a polluted insulator. The flashover voltage of a standard and EPRI insulator under AC and DC conditions was calculated and compared with the experimental results.

3.3 STUDIES ON THE EFFECT OF HIGH ALTITUDE ON AN INSULATOR

It is accepted that both the electrical breakdown of an air gap and the flashover on an external insulation surface will be influenced by atmospheric conditions.

Previous studies on an insulator situated at high altitude focused primarily on the influence of low air pressure on the flashover voltage of a clean or polluted insulator. For a clean insulator, a large number of studies were conducted and an international standard was established [62].

3.3.1 Polluted Insulators

The studies on the flashover on a polluted insulator under high altitude conditions have been carried out since the 1960's. These studies focused primarily on the observed decrease in the flashover voltage of a polluted insulator. The decrease in flashover voltage of a polluted insulator situated at high altitude was chiefly due to the decrease in the air pressure in such areas.

3.3.1.1 Characterization of the observed decrease in flashover voltage

The relationship between flashover voltage and air pressure was found to be non-linear. In general, this relationship can be expressed as follows:

$$\frac{V}{V_0} = \left(\frac{P}{P_0}\right)^m \tag{3.4}$$

where P_0 and P represent respectively the standard atmospheric pressure (101.3 kPa) and the pressure at high altitude, V_0 and V are the flashover voltages corresponding to pressures P_0 and P respectively, exponent m the degree of

influence of air pressure on the flashover voltage. Exponent m generally depends on the voltage type, insulator profile and pollution severity.

In order to determine the effects of low air pressure on the flashover performance of a polluted insulator, a large number of studies were conducted by many researchers. However, duo to the different experimental facilities and methods, there were some different conclusions. The different values for m suggested by different researchers are listed in Table 3.8.

Table 3.8 Values for m

Voltage type m Countries	AC	DC-	DC+	Notes
Sweden [41]	$0.29_{(1)}$	$0.5_{(1)}$	—	(1) IEEE insulator
Japan [73] [64] [100]	$0.5_{(1)}, 0.55_{(2)}$	$0.35_{(1)}, 0.44,$ $0.32\text{-}0.35_{(6)}$	$0.4_{(1)}$	(2) Anti-fog insulator
USSA [5] [118]	$0.5_{(1)}, 0.6_{(3)}$	$0.5_{(1)}$	—	(3) Complex form insulator
China [46] [47] [48] [54] [146] [148]	$0.42\text{-}0.81_{(2)},$ $0.44, 0.4_{(7)},$ $0.31_{(6)}$	$0.25\text{-}0.4,$ $0.14_{(6)}$	$0.15_{(6)}$	(4) Simple form insulator (5) Rectangular plate sample (6) Triangular plate sample
Mexico [3]	$0.5_{(1)}, 0.8_{(3)}$	—	—	(7) Cylindrical sample
Canada [95]	$0.5_{(1)}$	$0.35_{(5)}$	$0.4_{(1)}$	

Fryxell et al [41] investigated both AC and DC flashover performance of an anti-fog type insulator chain in a vacuum tank. Under dry conditions, the flashover

voltage decreased linearly with a decrease in the air pressure. However, under wet conditions, if the altitude was over 1000 m, a non-linear correction was applied. Pollution density has no visible effect on the high altitude correction factor.

Kawamura et al [73] studied the effect of air pressure, which was set to a value between 13 and 101 kPa, on the DC breakdown voltage of a contaminated porcelain insulator and a glass model. The flashover voltage decreased in a non-linear manner when the pressure was decreased. The flashover voltage under 13 kPa was reduced to approximately 50% to 60% of that measured under 101 kPa. Voltage polarity also had an effect on the insulator strength. Under DC+ voltage, the insulation strength was increased by 15 to 20% compared with DC- voltage. **Ishii et al** [64] obtained the similar results by measuring both AC and DC flashover voltage of contaminated insulators under low air pressure conditions. In addition, they found that the flashover voltage under AC conditions reduced at a faster rate than that observed under DC voltage conditions.

Naito et al [100] studied the effect of air density on the DC pollution flashover of insulators at NGK. The value for exponent m under DC- voltage conditions was approximately 0.44.

Employing reported empirical relations, **Mizuno et al** [98] theoretically investigated the effect of weather conditions such as temperature and pressure on

the flashover voltage of contaminated insulators. The value for m using the conventional evaluation formula was determined to be between 0.35 and 0.55 under DC conditions and between 0.44 and 0.80 under AC conditions. The theoretical value for exponent m was calculated to be 0.2 under DC conditions. A temperature change during an experiment could explain the disparity between the empirical and theoretical results for exponent m. The flashover voltage of a contaminated insulator decreased with a decrease in air pressure or an increase in temperature. The combined effect of a low temperature and a low air pressure effectively cancelled the reduction in flashover voltage of a contaminated insulator.

Bergman et al [5] measured the 50% flashover voltage under polluted conditions for two types of insulators, the complex shape PF6-V and the simple shape PS6-A, under four different levels of air pressure; 101.3, 92, 70.3 and 68 kPa. The observed decrease in the 50% flashover voltage, namely the test voltage at which an insulator has 50% probability to flashover one individual test, with a decrease in air pressure depended on the configuration of the insulator. The average value for m was calculated to be 0.5 for a simple shaped insulator, and 0.6 for a complex shaped insulator.

Rudakova et al [118] conducted a literature review of studies on the high altitude effects on pollution flashover in USSR. This review included field, laboratory and vacuum chamber tests that employed a suspension insulator, post

insulator, or bushing. Among these studies there was a general tendency for the natural pollution severity to be lower in areas of higher elevation. The exponent m was found to be insensitive to pollution severity when pollution severity was set to a value between 2 to 14 µS. For nearly all types of insulators, the value for m was calculated to be 0.5. The following altitude correction formula was proposed:

$$\frac{V}{V_0} \approx 1 - 0.059H \qquad (3.5)$$

where V_0 and V are the flashover voltages corresponding to standard air pressure and low air pressure respectively and H is the altitude in km. For some insulators with deep ribs and small rib spacing, the insulator performance was influenced by the breakdown of air between the ribs and, consequently, the value for m was calculated to be between 0.5 and 0.8.

Long [88] performed a series of tests in an artificial climatic chamber to investigate the effect of altitude on the dry and wet flashover voltage of an insulator. Both the dry and wet flashover voltage decreased with a decrease in air pressure. **Gou** [46] summarized similar conclusion for AC flashover test of contaminated insulators. He suggested that the pollution level should be considered in the air density correction for a polluted insulator. **Zhao et al** [148] carried out AC pollution tests on four types of cap-and-pin insulators under the pressure range of 48 to101 kPa. The exponent m varied from 0.28 to 0.50 for different pollution levels and insulator types. The average value for m was calculated to be 0.44.

Zhang [146] conducted many tests to determine both the AC and DC flashover voltage of a polluted insulator under low air pressure conditions. The value for exponent m increased as SDD was increased from 0.03 to 0.2 mg/cm2. The value for m under AC voltage conditions was larger than that observed under DC conditions for a given degree of pollution. The profile of the insulator had no evident effect on the value for m. In addition, defining $\Delta P = (P_0 - P)/P_0$, Equation (3.4) can be rewritten as

$$V = V_0 (1 - \Delta P)^m \tag{3.6}$$

Deploying Equation (3.6) to Taylor Series and omitting with the high-order terms of ΔP, the relation becomes as follows and was employed to correct the flashover voltage of a polluted insulator at high altitude:

$$V = V_0 (1 - m \cdot \frac{P_0 - P}{P_0}) \tag{3.7}$$

where V_0 and V are the flashover voltage of a polluted insulator under standard and ambient air pressure respectively; P_0 and P respectively the standard and ambient air pressure.

Huang et al [54] carried out the solid-layer tests on a smooth cylindrical insulator and five other post type porcelain insulators in a fog chamber under a pressure set between 50 and 101 kPa and a SDD set between 0.03 and 0.40 mg/cm^2. The value for exponent m was calculated to be approximately 0.4 for the simple insulator profile. For post insulators, m varied with the pollution severity:

exponent m was low when the pollution severity was low or high, (SDD equaled 0.03mg/cm^2 and 0.4mg/cm^2 respectively), whereas exponent m reached its maximum value at a medium pollution severity level. Using a plane triangular glass sample, **Guan et al** [48] found that the flashover voltage of a polluted sample decreased with a decrease in air pressure. The flashover voltage under AC conditions was higher than that measured under DC conditions. A negative polarity (for point electrode) had a higher pollution flashover voltage than the positive polarity. The values for m were calculated to be approximately 0.31 for AC, 0.14 for DC- and 0.15 for DC+ voltage conditions.

Anibal et al [3] conducted the AC flashover tests of two types of polluted insulators; an IEEE standard disk and a NEMA56-1 in a low pressure chamber under four pressure levels of 510, 580, 650 and 760 mmHg and three contamination levels of 0.07, 0.17 and 0.30 mg/cm^2. The value for exponent m was affected by the shape of the insulator. Exponent m was calculated to be 0.5 for a standard suspension insulator and 0.8 for an insulator with a more complicated geometry.

Mercure [95] measured the DC pollution flashover performance of a rectangular sample at low air pressure. The flashover discharge was initiated at an external air gap where a pointed electrode was suspended above an electrolytic solution. The value for m was calculated to be approximately 0.35. Results

obtained by other researchers were also taken into consideration and the final value for m was suggested to be 0.35 for DC-, 0.4 for DC+ and 0.5 for AC voltage conditions. When the elevation was increased up to 4 km , the derating percentage for a polluted insulator performance in a leakage path length were on average approximately 4%/km for DC-, 5%/km for DC+, 6%/km for a standard shape and 7%/km for an anti-fog shape under AC conditions. The dielectric breakdown performance of an air gap was derated by about 10.5%/km.

3.3.1.2 Flashover Mechanism and Modeling at High Altitude

In order to reveal the mechanisms underlying the decrease in flashover voltage of an insulator at high altitude, many studies were carried out to determine the arc characteristics. The voltage-current, V-I, characteristics of an arc at standard and low air pressure can be expressed as follows:

$$V = AxI^{-n} \tag{3.8}$$

where V is the voltage along arc, I is the current through arc, x is arc length, A and n are arc constants that were investigated by several researchers under different conditions. The results are shown in Table 3.9. Under different conditions and using different measuring methods, the results could vary.

Bergman et al [6] performed a study on the static V-I characteristics of an AC arc on a contaminated surface at an air pressure of 70.3 kPa. The constant A

was determined to be 84 and n was determined to be 0.7. However, no data was determined under standard pressure for comparison.

Table 3.9 Arc constants A and n measured by different investigators

Investigations	Voltage type	Pressure (kPa)	A	n
Bergman [6]	AC	70.3	84	0.7
Kawamura [73]	DC-	101	63	0.5
		13	53	1
Ishii [64]	DC	101	40-50	0.83
		40	20-35	0.77
Zhao [148]	AC	—	$(345 \sim 376)*P^{0.65}$	0.67
Huang [55]	Positive arc	—	$120*(P/P_0)^{0.25}$	0.52
	Negative arc		$148*(P/P_0)^{0.25}$	
Gou [46]	AC	99.59	33.2	Irregular
		54.87	22.6	

Using a triangular glass plate, **Kawamura et al** [73] investigated the V-I characteristics of an arc on a contaminated surface at 101 and 13 kPa. The constant A and n were found to be 63 and 0.5 at 101 kPa. They were 35 and 1 at 13 kPa. According to Equation (2.9) presented in section 2.3.3.2 and using above V-I characteristics of arc, the flashover voltage of polluted triangular plate at 101 and 13 kPa was determined. However, the difference between the calculated and

actual value of flashover voltage was notable. Therefore, they could not predict the flashover voltage at low pressure exclusively from the V-I characteristics of arc.

Ishii et al [64] investigated the propagation velocity of a local arc on a polluted surface. At 101 kPa, the extension of an arc was very smooth for DC+ whereas arc extension was stepwise for DC-. The velocity was approximately 1 m/s for both DC+ and DC- at 101 kPa. Two propagation modes were also discovered: a slow mode with the velocity of 1 m/s and a fast mode with the velocity more than 500m/s. For DC arc, a fast mode was seldom exhibited at 101 kPa yet it was consistently observed at low pressure. The AC arc propagated only in the fast mode. The V-I characteristics of an arc on a polluted surface at low pressure were determined using optical and spectroscopic methods. The DC arc constants A and n decreased with a decrease in pressure. At 101 kPa, the constant A was between 40 and 50 and n was 0.83. At 40 kPa, the constant A was between 20 and 35 and n was 0.77. From these results, the flashover voltage of a triangular model was calculated under 101 kPa and 40 kPa. However, because the value of A was given in a range, it is difficult to be used in the prediction of flashover voltage of real industrial insulators.

Zhao et al [148] studied the V-I characteristics of an AC arc on a polluted insulator surface. The relation between the critical AC voltage gradient and the critical current can be expressed as follows:

$$E_c = C \cdot I_c^{-0.67} \cdot P^{0.65} \tag{3.9}$$

where E_c in V/cm is the critical voltage gradient, I_c in A is the critical current, P in atm is the air pressure. The constant C varied within the narrow range of 345–376 according to the insulator type.

Using IEEE standard insulators and post insulators, **Gou** [46] measured the E-I characteristics of an AC arc on polluted insulators at low air pressure. The relation between E and I was affected by air pressure. When the pressure was reduced from 99.59 to 54.87 kPa, the arc constant A decreased from 33.2 to 22.6 and the constant n varied between 0.425 and 0.790. In conclusion, the constant A decreased with a decrease in air pressure and n was irregularly influenced by air pressure.

Using a plane triangular glass sample, **Huang** [55] investigated the flashover on a polluted surface under high altitude conditions. Under DC voltage, n was not influenced by air pressure and the average value calculated for n was 0.16. However, the constant A decreased with a decrease in air pressure as depicted in Table 3.10.For an AC arc, the development condition was proposed to be as follows:

$$\frac{V \cdot I}{x} \geq C \tag{3.10}$$

where x is arc length in cm, V is the voltage along arc in volts, I is the current through an arc in amperes and C is a constant that is influenced by the air pressure and can be expressed as follows:

$$C = 526.7 \left(\frac{P}{P_0} \right)^{0.75} \tag{3.11}$$

Table 3.10 Value for A for DC arcs at different air pressures

Polarity	Positive Arc				Negative Arc			
Pressure	101	70	40	20	101	70	40	20
A	119.8	107.7	97.6	79.7	148.5	138.3	116.4	110.3

The AC flashover voltage of a polluted plane triangular glass sample can be determined using the following formula:

$$V_c = 5.25 \sqrt{\frac{C}{\gamma_e}} \tag{3.12}$$

where V_c is the AC flashover voltage (effective value) and γ_e is the conductivity of the residual polluted layer.

Using an electrolytic solution at low air pressure to simulate the surface of wet polluted insulators of overhead lines in mountains, **Fujishima et al** [44] measured the intensity of photo-emission from the tip of a local discharge and the propagation velocity of a local arc under standard and low air pressure. The propagation velocity increased with the photo-emission intensity and solution

resistivity. However, the influence of both the air pressure and applied voltage waveform on the velocity was very small.

Rizk et al [117] modified the mathematical model for flashover on polluted insulators at standard air pressure and introduced a physical approach to account for the effect of reduced air density on the AC flashover voltage and critical leakage current. The reignition equation and basic circuit equation of an AC polluted insulator at any pressure are as follows:

- Reignition equation:

$$V_{cx} = \frac{716xP^{0.77}}{I_m^{0.526}}$$

(3.13)

- Basic circuit equation:

$$V_{cx} = \frac{xN_0P^{m_0}}{I_m^n} + r_p(L - x)I_m$$

(3.14)

where, V_{cx}, in V, is the peak value for the AC flashover voltage, x, in cm, is the arc length, P, in atm, is the ambient pressure and I_m, in A, is the peak value for the arc current. There was some uncertainty concerning the variation of m_0 and n. Solving Equations (3.13) and (3.14) and searching for the critical point $\left(\frac{dV_{cx}}{dx} = 0 \right)$ yielded the critical arc length x_c, critical current I_c and critical voltage V_c. The results from this model were compared to empirical data and a good correlation was noted. I_c

was observed to be more sensitive to ambient pressure than V_c. x_c reached 65% of the leakage path and pollution severity and ambient pressure had only a slight effect on x_c.

Using a dynamic arc model of a pollution flashover on an insulator and the reignition equation (3.13), **Sundararajan et al** [131] adapted the contamination flashover model to compute the flashover voltage of a contaminated insulator at high altitudes. They reported that the derating of the flashover voltage strength varied at a rate of 1.8% per 1000 ft for AC voltage conditions when the pollution severity was light to moderate or an ESDD of 0.03-0.07.

3.3.2 Ice-Covered Insulators

In high altitude regions, the pollution is not normally severe [118] and, therefore, the influence of atmospheric ice on the performance of an insulator becomes more critical than in other regions. Relative to the large number of studies on the flashover on a polluted insulator at low air pressure, there is a dearth of information on the flashover on an ice-covered insulator under low air pressure.

Shu et al [123] investigated the AC flashover performance of an ice-covered and polluted insulator at low air pressure using 3 units of suspension

insulators in an artificial climate chamber. When the ice weight and the ESDD were held constant, the flashover voltage of an ice-covered insulator dramatically decreased with a decrease in air pressure. When the air pressure was reduced, the diameter of an arc became slightly larger. In conclusion, air pressure, ice weight and pollution had a substantial effect on the AC flashover performance of an ice-covered and polluted insulator.

Zhang [146] studied the effects of ice, pollution and air pressure on the AC and DC flashover performance of a 3-unit-string of suspension insulators. The flashover voltage was found to decrease with a decrease in air pressure. When the altitude was elevated from 232 to 3000 m, the AC and DC flashover voltages decreased approximately 23-32% and 15-28%, respectively. Under the same conditions, the flashover voltage was consistently slightly lower under DC than under AC voltage conditions. The following correction formula was proposed:

$$V = 1.57 V_0 \cdot W^{-0.1365}(1 - 0.9\frac{P_0 - P}{P_0}) \quad \text{for AC} \tag{3.15}$$

$$V = 1.36 V_0 \cdot W^{-0.11110}(1 - 0.8\frac{P_0 - P}{P_0}) \quad \text{for DC} \tag{3.16}$$

where, P_0 and P are the standard and ambient air pressures respectively, V_0 and V are the flashover voltage at P_0 and P, W is the ice weight per insulator in kg/unit.

3.4 CONCLUSION

From the literature reviews presented above, it was observed that the flashover along an ice-covered insulator at standard pressure and along a polluted insulator at low air pressure have received a great deal of attention from many researchers. These studies are summarized as shown in Fig. 3.1.

In Fig. 3.1 the following color scheme illustrates the relative number of investigations: the green block indicates that many investigations have been carried out, the yellow block means that there are some investigations and the red block indicates that very few studies are available. The investigation of a flashover on an insulator under ice and altitude conditions is in the early stage. Currently, two principal questions have yet to be clearly answered:

- The principle underlying the observed decrease in flashover voltage of an ice-covered insulator under high altitude conditions and the factors affecting this decrease such as voltage type and polarity, insulator profile, etc.
- The mechanisms underlying a flashover along an ice-covered insulator under high altitude conditions.
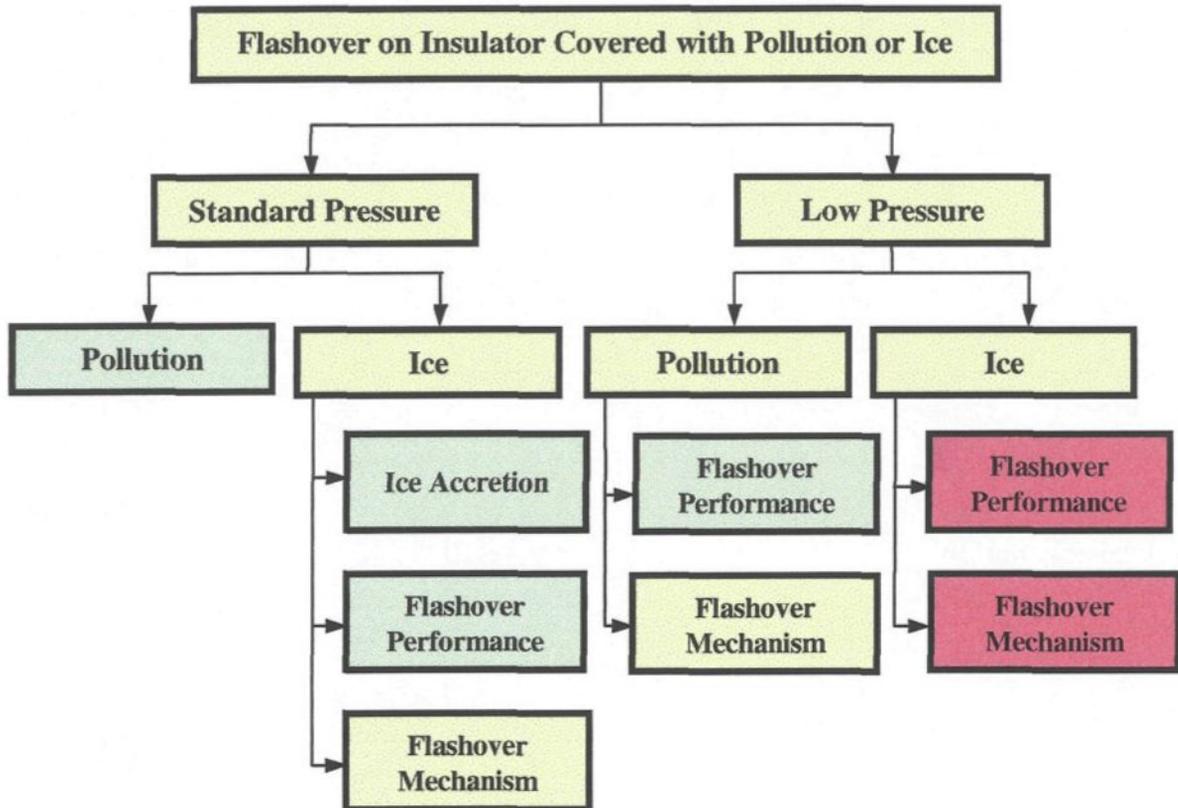
Fig. 3.1 Block diagram listing the investigations of a flashover on an

insulator covered with pollution or ice

These two questions are the motivation behind this PhD thesis, which is a systematic investigation of a flashover along an ice-covered insulator at high altitudes.

CHAPTER 4

FLASHOVER PERFORMANCE OF A SHORT POST INSULATOR AT LOW AIR PRESSURE

CHAPTER 4

FLASHOVER PERFORMANCE OF A SHORT POST INSULATOR AT LOW AIR PRESSURE

4.1 INTRODUCTION

The influence of air pressure on the critical flashover voltage of polluted insulators is generally expressed as follows:

$$\frac{V}{V_0} = \left(\frac{P}{P_0}\right)^m \tag{4.1}$$

where P_0 and P are respectively the standard pressure (101.3 kPa) and the pressure at high altitudes, V_0 and V are the flashover voltages corresponding to the pressures P_0 and P respectively; and exponent m indicates the degree of influence that air pressure has on the critical flashover voltage, as discussed in Chapter 3.

The ice deposited on insulators is occasionally considered as a special type of pollution. Equation (4.1) can also be used to express the influence air pressure has on the critical flashover voltage of ice-covered insulators. The value of m

depends on the voltage type, insulator profile and, particularly, pollution severity, therefore, the values obtained under polluted conditions cannot be simply applied here. In this study, the influence of low air pressure on the values of m will be examined and discussed.

In this chapter, the flashover performance of a real short post insulator at low pressure will be presented. First, the test sample, experimental facilities and methodology will be introduced. Then, the AC and DC flashover voltages of the real short post insulator as well as the exponent m were determined under various conditions. These results will also be analyzed and discussed in this chapter.

4.2 EXPERIMENTAL FACILITIES AND PROCEDURES

4.2.1 Test Sample

It is difficult and costly to investigate in a laboratory setting the flashover performance of long ice-covered insulators at low air pressure. Therefore, experiments were carried out on a short porcelain post insulator (represented in Fig. 4.1), which had the following dimensions: an overall height of 360 mm, a leakage distance of 670 mm and a shed diameter of 155 mm.
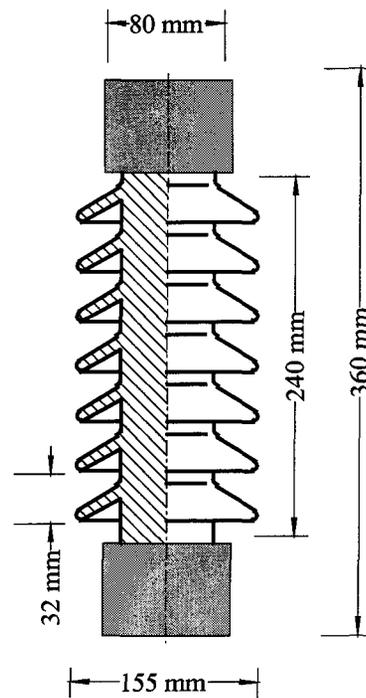
Fig. 4.1 Short post insulator

The insulator was initially covered with ice under normal pressure in a climatic room as illustrated in Fig. 4.2. The procedure for depositing ice on insulators under normal pressure is summarized as follows:

- The insulator was placed in a climatic room maintained at a constant temperature of –12 °C.

- A relatively uniform wind was produced by a series of fans placed behind a honeycomb diffusing panel. Water was fed through nozzles to produce super-cooled water droplets that deposited on the surface

of the insulator. The conductivity of the resultant ice layer was controlled by adding the sodium chloride into the de-ionized water and adjusting its concentration.

− The thickness of the ice layer was confirmed by measuring the ice deposition on a monitoring cylinder, 3.8 cm in diameter, rotating at 1 rpm within the climatic chamber.
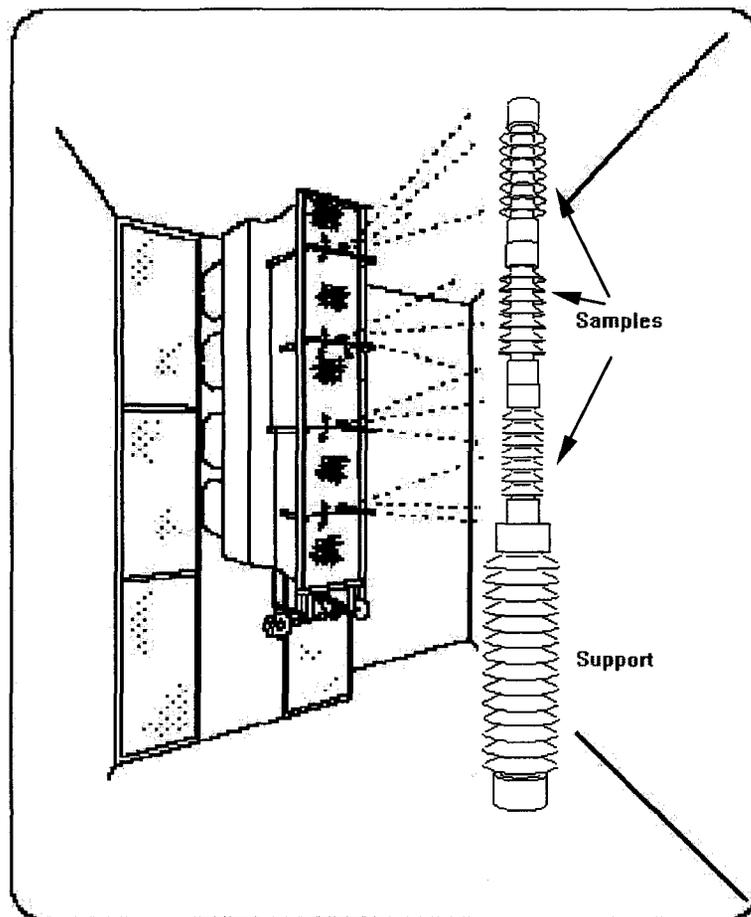
Fig. 4.2 Schematic diagram of ice accumulation

As mentioned in Chapter 3, wet-grown ice with a density of approximately 0.9 g/cm^3 is known to be more dangerous for power systems than dry-grown ice [22] [25]. Therefore, Wet-grown ice was used in the short post insulator flashover experiments in this study. The experimental conditions for wet-growth ice accretion on insulators are listed in Table 4.1.

Table 4.1 Experimental conditions for wet-grown ice accretion

Surrounding Temperature (°C)	Water Droplet Size (μm)	Wind Velocity (m/s)	Liquid Water Content (g/m^3)
-12	80	3.3	6.8

Once the average thickness of the ice layer accumulating on the monitoring cylinder reached 15 mm, the sprays and fans were stopped. The insulator was removed and an air gap with a width of approximately 1 cm was made by cutting out a small fragment of ice near the upper electrode. This air gap simulated the air gaps naturally created on energized industrial insulators either by the heating effect of local arcs or ice falling during ice accretion [22]. Fig. 4.3 shows the physical aspects of an insulator covered with artificial ice after the formation of an air gap. An insulator covered artificially with ice on a single side simulated an insulator covered with ice under natural conditions and exposed to a uniform wind.
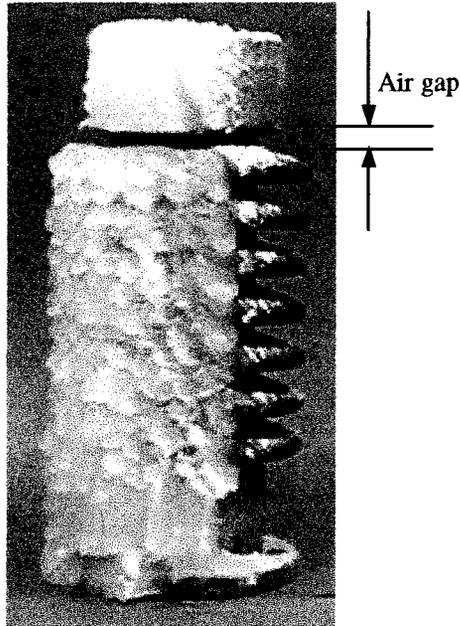
Fig. 4.3 Physical aspect of ice-covered insulator with an air gap

4. 2. 2 Evacuated Chamber

To simulate the low air pressure of high altitudes, tests were carried out in an evacuated cylindrical chamber with a diameter of 610 mm and a height of 760 mm as shown in Fig. 4.4. Using a vacuum system, the air pressure inside this chamber could be adjusted within 5 minutes to any value between 101.3 and 30 kPa corresponding to an altitude range of 0 to 9,000 m respectively. The chamber was transparent to permit visual observation and photographs. The evacuated chamber was placed in a climate room to control the air temperature, which is one of the most important factors influencing the critical flashover voltage of ice-covered insulators.
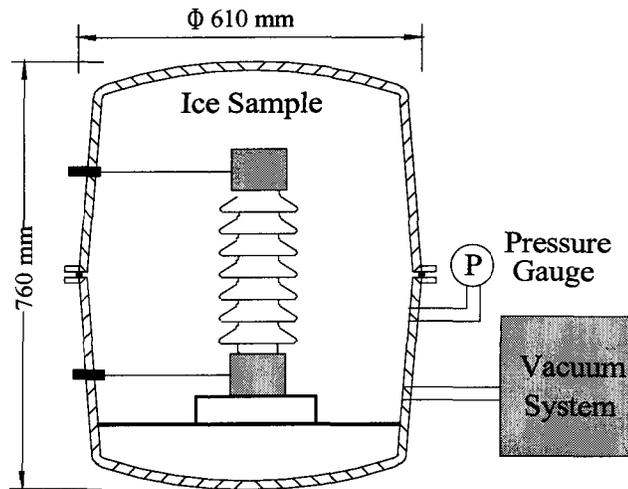
Fig. 4.4 Schematic diagram of the evacuated chamber

4. 2. 3 Experimental Set-Ups and Test Methods

After the ice had accumulated and the air gap was excised, the test sample was placed vertically in the evacuated chamber and the ambient temperature was adjusted to 5 °C. This air temperature was chosen based on the results of a recent study [147] that dealing with the effects of air temperature on the flashover on an ice surface. It was discovered that the flashover voltage of ice-covered insulators decreased as the ambient temperature increased from -12 °C to 5 °C and then leveled off after 5 ° C.

When the desired air temperature was reached, the vacuum system was turned on to adjust the ambient pressure to a specified value. A high voltage was then applied to the top electrode while the bottom electrode was connected to ground as represent in the test circuit in Fig. 4.5.
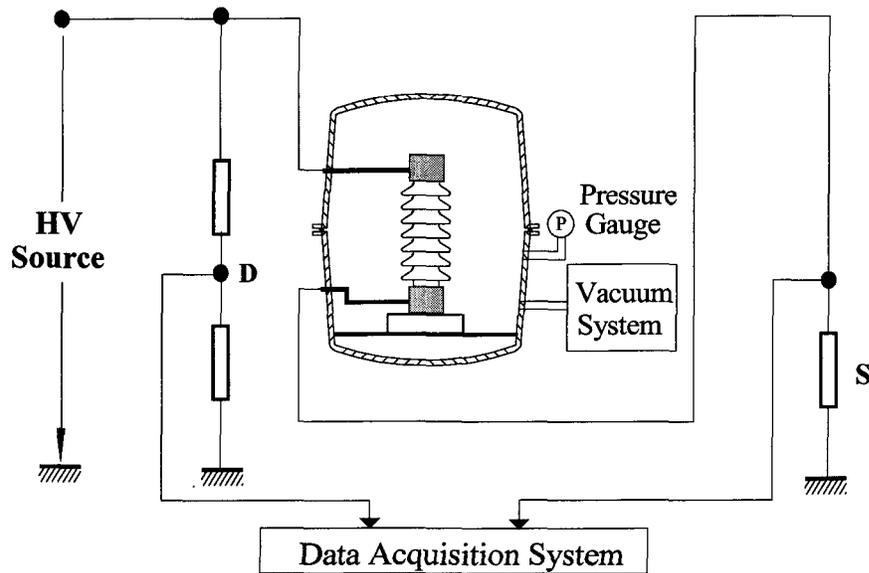
Fig. 4.5 Test Circuit

D — Voltage divider   S — Current Shunt

The AC high voltage system consisted of a 240 kVA/120 kV transformer and a 240 kVA regulator. The overall short-circuit current of this HV system was about 28 A with a maximum operating voltage of 120 kV.

A DC high voltage of up to ±100 kV was supplied by a half-wave rectifying circuit controlled by a thyristor (SCR) feedback system, which ensured a dynamic voltage drop of less than 5% when the load current was 0.5 A.

The high voltage system is shown in Fig. 4.6.
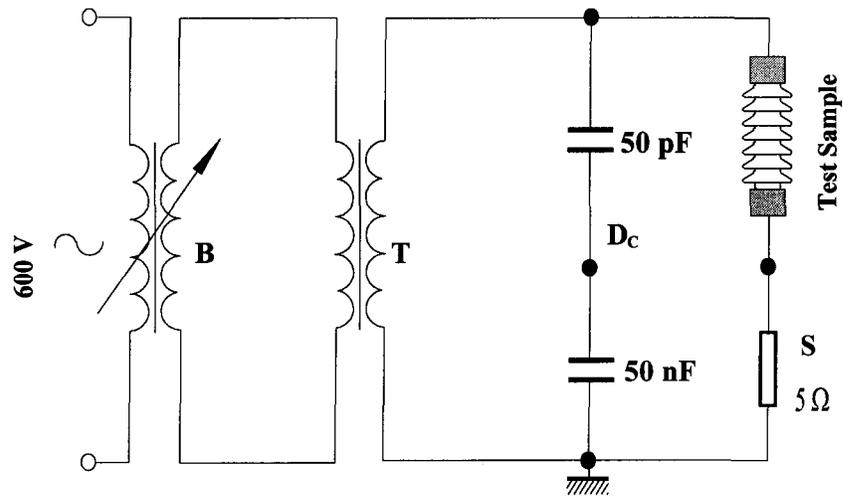
(a) AC
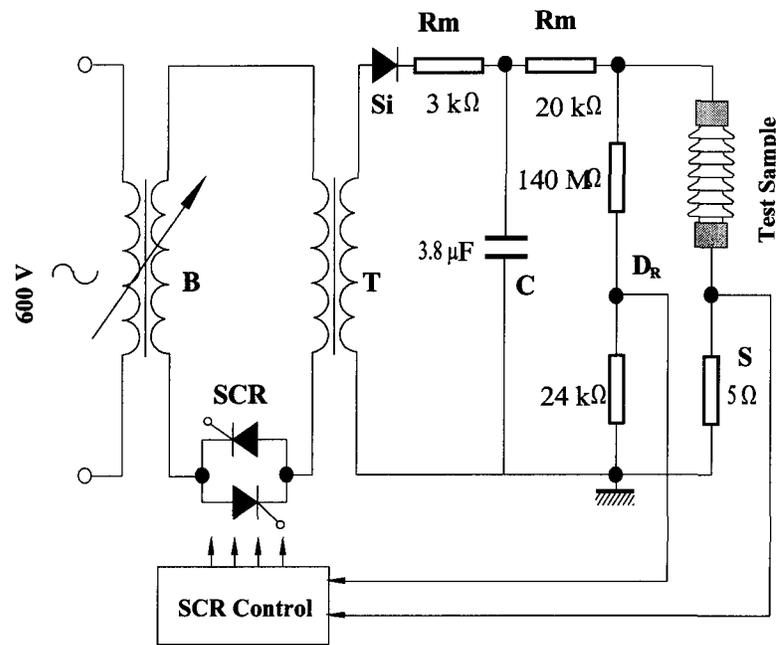
(b) DC

Fig. 4.6 High voltage system of the high voltage laboratory of UQAC

B: Regulator 240 kVA   T: Transformer, 240 kVA/120 KV   Rm: Protecting resistor

S: Current shunt D_C: Capacitive voltage divider D_R: Resistive voltage divider

Si: Rectifier   C: Capacitor   SCR: Thyristor

The output voltage of AC and DC systems was measured using a capacitive (AC) or resistive (DC) voltage divider and a peak voltmeter which was corrected by means of an electrostatic voltmeter with an accuracy of ± 0.1 kV.

A data acquisition system (DAS) was used to simultaneously record the waveforms of the applied voltage and leakage current during the flashover tests.

In order to determine the maximum withstand voltage, V_{WS}, and minimum flashover voltage, V_{MF}, of ice-covered insulators, a method based on and developed from the method described in the standard IEC 507 [60] was used. This method was used in previous research works at CEGELE [22] [24] [26] and can be summarized as follows:

- After the ice-covered insulator was placed in the evacuated chamber and the temperature and air pressure were adjusted to the desired values, a voltage was applied to the HV electrode as depicted in Fig. 4.5. The voltage was increased at a constant rate of 3.9 kV/s until the estimated flashover voltage, V_F, was attained. The voltage was kept for a period of 15 minutes or until flashover occurred.

- The maximum withstand voltage, V_{WS}, was determined by incrementally increasing the applied voltage in steps by 1 kV, which was approximately 5 % of V_F. Each test sample was used only once

for a single flashover test. V_{WS} was considered the maximum level of applied voltage at which flashover failed to occur for a minimum of 3 tests out of 4.

- The minimum flashover voltage, V_{MF}, corresponded to a voltage level that was1 kV higher than V_{WS} where 2 flashovers occurred out of a maximum of 3 tests.

A group of results on AC flashover tests are shown in Fig 4.7 where the air pressure was set to 60 kPa and the freezing water conductivity was adjusted to 80 μS/cm. From these results, V_{WS} and V_{MF} were determined to be 25 $\pm$ 0.1 kV and 26 $\pm$ 0.1 kV respectively.
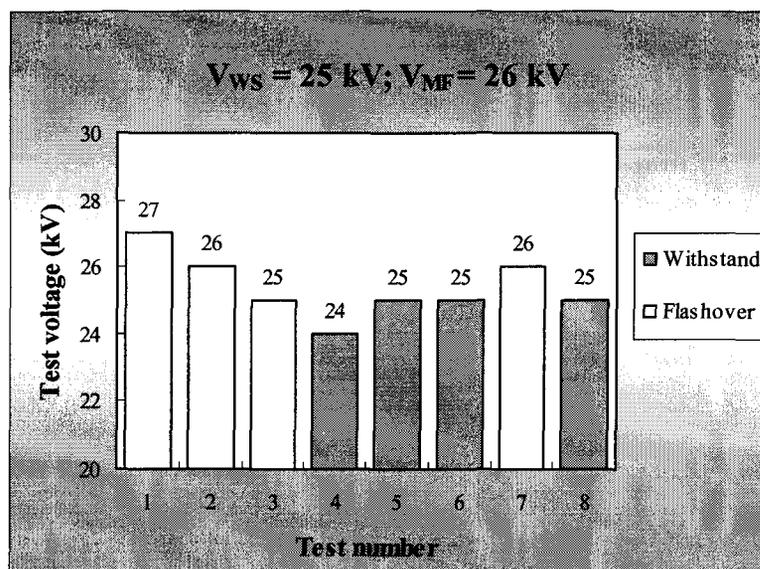
Fig. 4.7 Determination of V_{ws} and V_{MF} under AC conditions

(σ = 80 μS/cm, P= 60 kPa, T = 5°C)

4.3 AC FLASHOVER VOLTAGE AT LOW AIR PRESSURE

In order to understand fully the effects of air pressure on the flashover on an ice surface, a wide range of air pressures were used in this study. For the short post insulator, the air pressure levels tested were 101, 80, 60 and 45 kPa.

Using the methodology described above, the minimum flashover voltage, V_{MF}, was measured for an ice-covered insulator with the freezing water conductivity set to both 80 and 250 μS/cm. Based on the test results, the relation between minimum flashover voltage, V_{MF}, and air pressure, P, was determined as shown in Fig 4.8.
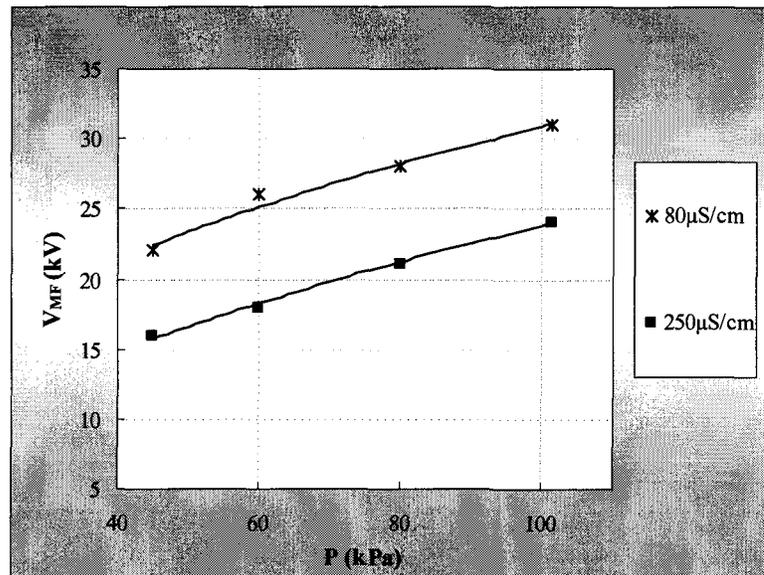
Fig. 4.8 AC Minimum flashover voltage of ice-covered insulators as a

function of air pressure (T = 5°C)

Fig. 4.8 illustrates that the minimum AC flashover voltage, V_{MF}, of ice-covered short insulators decreased with a decrease in air pressure. The decrease in V_{MF} with air pressure became larger as conductivity was increased. The decrease in V_{MF} was approximately 29% and 33% for a conductivity of 80 μS/cm and 250 μS/cm, respectively, when the air pressure was decreased from 101.3 kPa to 45 kPa.

It should be noted that the observed decrease in flashover voltage with an increase in freezing water conductivity was more pronounced at high altitude than that observed at sea level conditions. When the freezing water conductivity was changed from a value of 80 to 250 μS/cm, the flashover voltage decreased approximately 23% at sea level. In contrast, at an altitude of 6500 m (45 kPa) the flashover voltage decreased approximately 27% when the freezing water conductivity was changed from a value of 80 to 250 μS/cm.

4.4 EXPONENT *m* UNDER AC CONDITIONS

The exponent *m* is an important parameter for designing the insulation level of transmission lines in high altitude regions. For determine the value of *m*, Fig. 4.8 was redrawn to employ a logarithmic scales for both axes as illustrated in Fig 4.9. In this figure, R is the correlation coefficient. Using the regression analysis to

these results, the values of exponent *m* were determined and presented in Table 4.2.
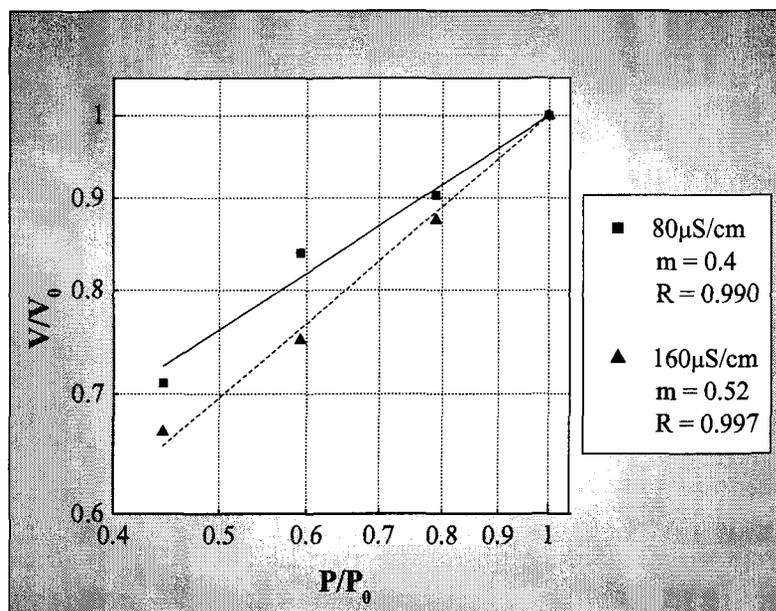
Fig. 4.9 Ratio of flashover voltage vs the ratio of air pressure on log-scales

Table 4.2 Values of exponent *m* for different freezing water

conductivities under AC voltage

σ (μS/cm)	80	250
m	0.40	0.52

The results shown in Table 4.2 demonstrate that exponent *m* was larger for a freezing water conductivity of 250 μS/cm than for 80 μS/cm implying that exponent *m* increased with an increase in water conductivity.

Comparing the above results with those obtained for polluted insulators [146], it was noted that, in both cases, the exponent m increased with an increase in the pollution level (ESDD in pollution tests and freezing water conductivity in icing tests).

4.5 DC FLASHOVER VOLTAGE AT LOW AIR PRESSURE

A series of flashover tests were carried out under both positive and negative DC voltages and under different levels of air pressures to simulate a range in altitude from sea level to 6500 m.

The high voltage was always applied to the top electrode for the ice-covered insulators. The arc always started from this electrode because of the presence of the air gap (refer to Figs. 4.3 and 4.5). Therefore, the DC+ voltage created a positive arc and the DC- voltage led to a negative arc.

Figs. 4.10 and 4.11 illustrate how the minimum flashover voltage, V_{MF}, of ice-covered insulators varied as a function of air pressure, P. These results were obtained using both DC+ and DC- conditions and a freezing water conductivities, σ, of 80 and 250 μS/cm. It was observed that under both DC+ and DC- conditions, the minimum flashover voltage decreased with a decrease in air pressure for both

freezing water conductivities used. The freezing water conductivity influenced V_{MF} such that the higher the conductivity, the lower the value of V_{MF}. For a freezing water conductivity of 80 µS/cm, V_{MF} decreases approximately 22.5 % under DC+ and 18.8 % under DC- conditions when the air pressure was changed from 101.3 kPa to 45 kPa. In contrast, a freezing water conductivity of 250 µS/cm resulted in a V_{MF} decrease of approximately 33.3 % and 28% for DC+ and DC- conditions respectively when the air pressure was changed from 101.3 kPa to 45 kPa.
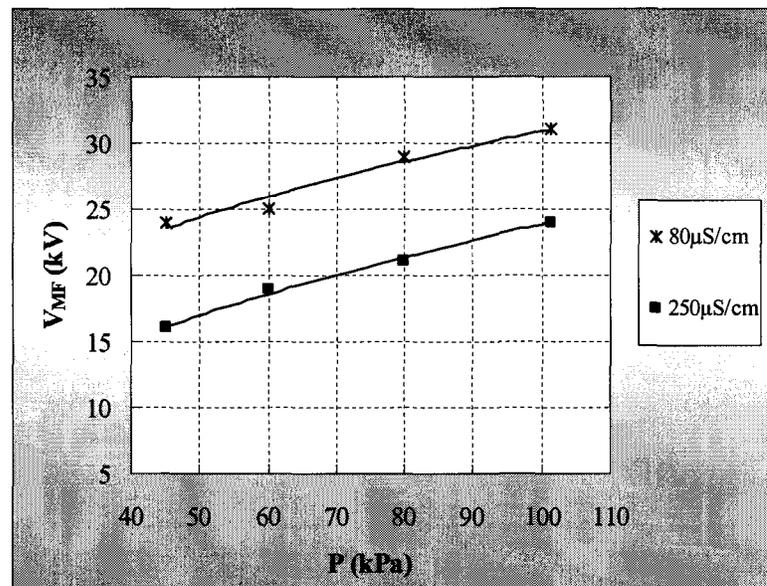
Fig. 4.10 DC+ Minimum flashover voltage of ice-covered short insulator

as a function of air pressure
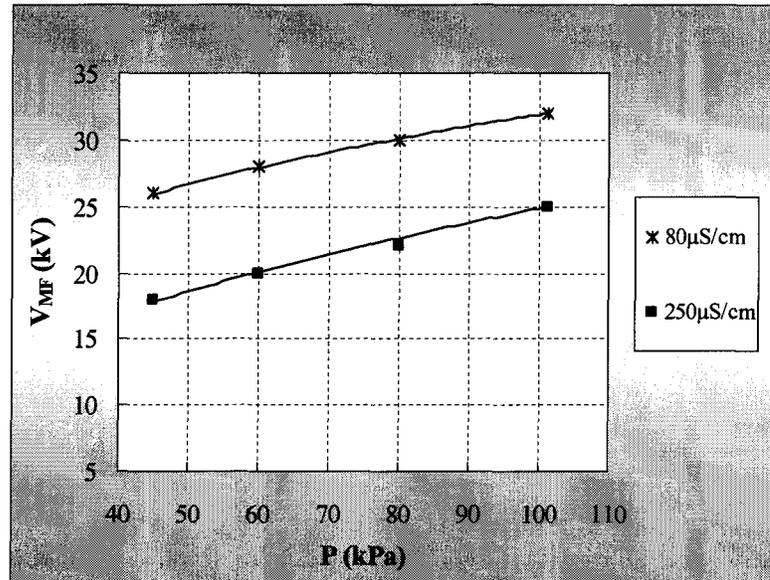
Fig. 4.11 DC- Minimum flashover voltage of ice-covered short insulator

as a function of air pressure

4.6 EXPONENT *m* UNDER DC CONDITIONS

The above test results illustrate the relationship between the ratio of DC minimum flashover voltage, V/V_0, and the ratio of air pressure, P/P_0. This relation was plotted using logarithmic scales as presented in Fig. 4.12. The values for exponent *m* for an ice-covered short post insulator under DC+ and DC- conditions were determined and presented in Table 4.3.
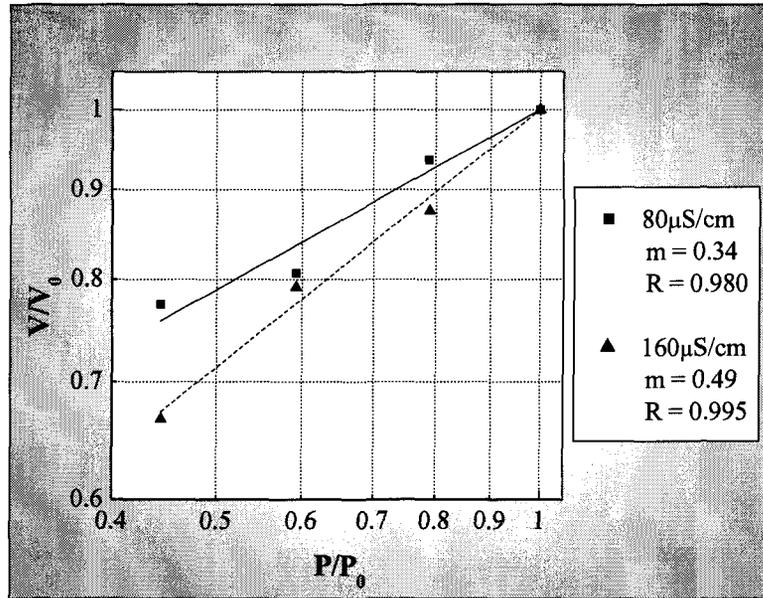
(a) DC+
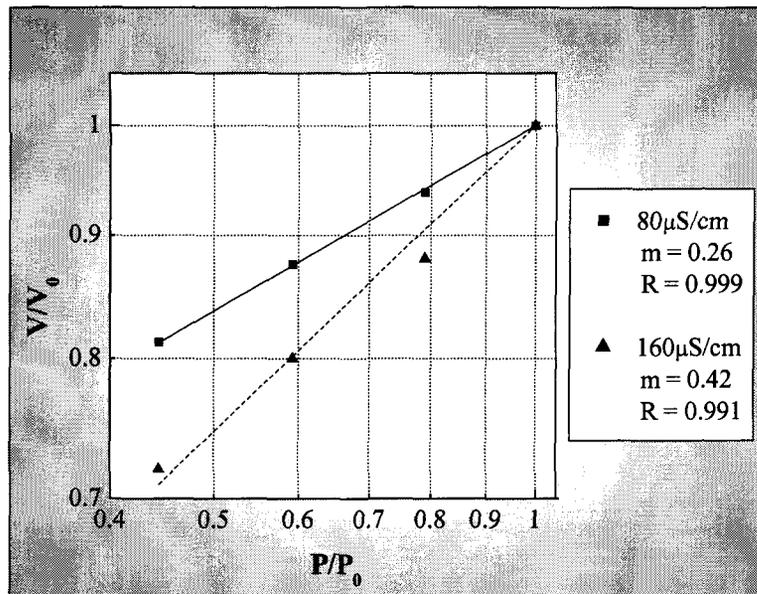
(b) DC-

Fig. 4.12 Relation between the ratio of DC minimum flashover voltage, V/V_0

and the ratio of air pressure, P/P_0 using log-scales

Table 4.3 Values of exponent *m* for an ice-covered short post insulator

under DC voltage

σ (μS/cm)	80	250
Voltage type	*m*	
DC+	0.34	0.49
DC-	0.26	0.42

Under both DC+ and DC- voltages, exponent *m* for the tested insulator increased with an increase in freezing water conductivity. The increase in *m* was approximately 30% for DC+ and 38% for DC- when the freezing water conductivity was increased from 80 to 250μS/cm.

4.7 DISCUSSION

4.7.1 Arc Floating Phenomena

During the flashover test, it was observed that the arc always propagated from the top electrode towards the bottom electrode. Arc propagation can occur in two different ways: along the ice surface or through the air. Fig. 4.13(a) shows an arc propagating through the air, which is called the arc floating phenomena. Fig. 4.13(b) shows an arc propagating along the ice surface. Both situations can occasionally occur within a single arc where part of the arc propagates along the

(a) (b) (c)

Fig. 4.13 Types of Arc propagated

ice surface and the other part goes through the air. This combined arc is illustrated in Fig. 4.13(c). When an arc propagates through the air, the arc length and consequent flashover distance will increases resulting in a higher flashover voltage. In this study, arc floating was frequently observed under high conductivity and DC voltage conditions, particularly under negative DC voltage. This may be due to the fact that the negative DC arc floats more easily [49].

4.7.2 Effects of Voltage Type and Polarity on Flashover Voltage at Low Air Pressure

Fig. 4.14 presents a comparison between the minimum flashover voltages of ice-covered short post insulators obtained under DC and AC voltage conditions for the freezing water conductivities of 80 and 250 μS/cm.

This comparison illustrates that the applied voltage polarity had an obvious influence on the flashover voltage of the insulators tested. V_{MF} was lower under DC+ compared to DC- conditions. When the freezing water conductivity was set to 80 μS/cm. the observed difference between DC+ and DC- voltage conditions was more pronounced when the air pressure was set to 45 kPa compared to when it was set to 101 kPa: the difference between DC+ and DC- voltages was approximately 8% and 3 % for 45 kPa and 101 kPa respectively. This observation implied that the effect of voltage polarity on the minimum flashover voltage of ice-

(a) σ = 80 μS/cm
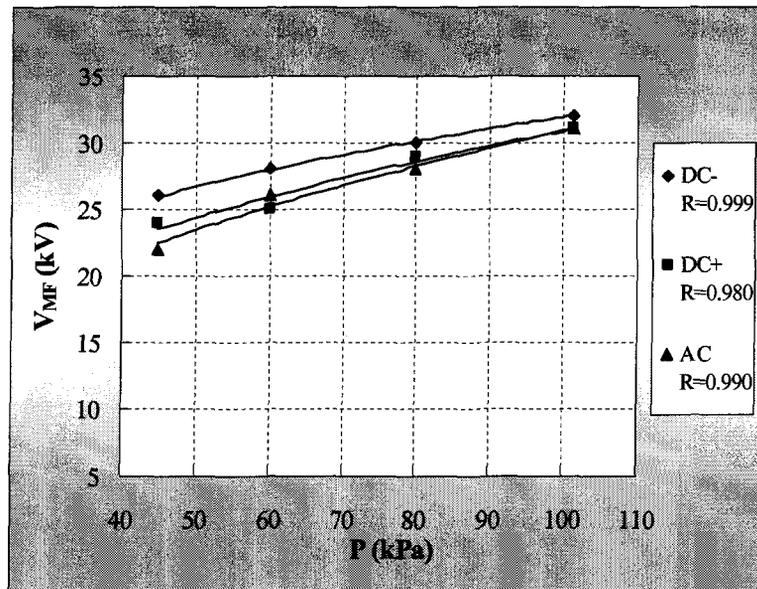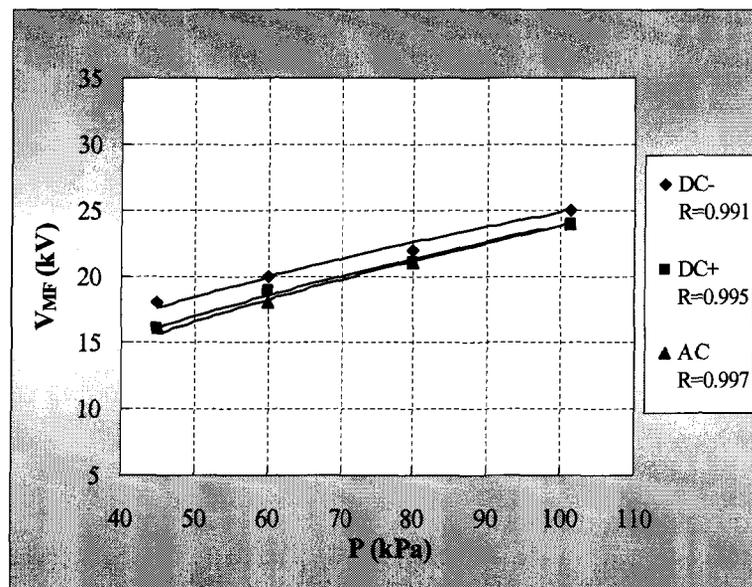
(b) σ = 250 μS/cm

Fig. 4.14 Comparison between V_{MF} of an ice-covered short insulator under DC

and AC conditions for different freezing water conductivities σ

covered insulators was more pronounced at high altitudes than at sea level. A similar conclusion was obtained for a freezing water conductivity of 250 µS/cm where the difference between DC+ and DC- voltages was approximately 11% and 4% for 45 kPa and 101 kPa respectively.

The observed polarity effect on flashover voltage of ice-covered post insulators could be due to the arc floating phenomena. As mentioned above, arc floating can easily occur under negative DC voltage resulting in a higher flashover voltage under DC- than that observed under DC+ conditions.

For freezing water conductivities of both 80 and 250 µS/cm, V_{MF} under AC conditions was considerately lower than that observed under DC- conditions. In contrast, V_{MF} under AC conditions was similar to that observed under DC+ conditions, particularly at 101 kPa.

4.7.3 Effects of Voltage Type and Polarity on Exponent m

The values of exponent m for an ice-covered short post insulator under AC, DC+ and DC- are presented in Table 4.4.

The data presented in Table 4.4 suggest that the applied voltage polarity can influence the value of exponent m for ice-covered short post insulators. For a given conductivity, the value of m was higher under DC+ than under DC-

conditions. These results imply that the effect of high altitude on the critical flashover voltage was larger under DC+ than under DC-.

Table 4.4 Values of exponent m under various conditions

Voltage type $\sigma(\mu S/cm)$	DC+	DC-	AC
	m		
80	0.34	0.26	0.40
250	0.49	0.42	0.53

The above results also suggest that the voltage type can influence the value of exponent m such that the value of m under both DC+ and DC- are clearly lower than that observed under AC conditions. Similar results were reported under pollution conditions [64] [73] [96]. These results indicate that the influence of altitude on the critical flashover voltage of ice-covered short insulators was more pronounced for AC than DC.

Under both DC and AC conditions, the exponent m for the tested insulators increased as the freezing water conductivity was increased. The observed increase in m was approximately 30%, 38% and 25% for DC+, DC- and AC voltage conditions respectively, when the freezing water conductivity was increased from 80 to 250μS/cm. This increase in exponent m could be due to the arc floating phenomenon. When the freezing water conductivity was set to 80 μS/cm, the arc

usually propagated along the ice surface at the standard air pressure. In contrast, when the air pressure was lowered, the arc propagated through the air resulting in a lower percentage decrease in flashover voltage and a consequent lower m value. When the freezing water conductivity was increased to 250 μS/cm due to the larger thermal buoyant force, the arc propagated through the air at both standard and low air pressures leading to a larger percentage decrease in flashover voltage and a larger value of m.

4.8 CONCLUSION

A short post type insulator was used to investigate the AC and DC flashover performance at low air pressure between 45 and 101 kPa. From the results the following conclusions can be drawn:

1). Air pressure had a visible effect on the flashover voltage of post insulators. At low air pressure, the minimum flashover voltage, V_{MF}, was lower under both AC and DC conditions compared to that observed under high air pressure. When the freezing water conductivity, σ, was set to 250 μS/cm, the observed decrease in V_{MF} was 33% under AC, 33% under DC+ and 28% under DC- voltage conditions.

2). Under AC voltage conditions, V_{MF} was observed to be lower than that observed under DC+ and DC-, whereas under DC- voltage conditions, V_{MF} was higher than that observed under DC+. The effect of voltage polarity was more obvious at low air pressure than under standard air pressure.

3). The relationship between the flashover voltage of ice-covered insulators and the air pressure can be expressed as follows:

$$\frac{V}{V_0} = \left(\frac{P}{P_0}\right)^m$$

The exponent m was influenced by the voltage type and polarity as well as the level of freezing water conductivity. For the insulators tested, m increased with an increase in freezing water conductivity. For a given value of conductivity, the value of m under DC- voltage conditions was lower than that observed under DC+. Under both DC- and DC+ voltage conditions, the value of exponent m was lower than that observed under AC conditions.

4). Under high altitude conditions, the arc floating phenomenon was frequently and clearly observed for the test post insulator. It was the main factor contributing to the polarity effect observed with ice-covered post insulators.

CHAPTER 5

FLASHOVER PERFORMANCE OF
A PLANE TRIANGULAR ICE SAMPLE
AT LOW AIR PRESSURE

CHAPTER 5

FLASHOVER PERFORMANCE OF A PLANE TRIANGULAR ICE SAMPLE AT LOW AIR PRESSURE

5.1 INTRODUCTION

The objective of this thesis is to reveal the mechanisms underlying the phenomenon of flashover on ice-covered insulators at low air pressure. Flashovers that occur under these specific conditions are known to be caused by the formation and development of an arc on an ice surface. For this reason, a study on the local arc itself is important and required. However, the ice layer, accordingly the air gap, formed on real insulator string normally has a width. During the flashover process, the initial arc will be randomly established along the air gap. Sometimes, two or more arcs will appear simultaneously. These made it difficult to study the arc characteristics and behavior using real insulators. Therefore, a physical model with a simplified geometry was used in this study; specifically a plane triangular ice sample.

This chapter will present the results obtained from the investigations using such an ice sample at low air pressure. The test sample and experimental conditions will be briefly described. The results will be presented on the minimum flashover voltage of a plane triangular ice sample exposed to varying voltage types (AC and DC), air pressures and freezing water conductivities. Exponent m for a plane triangular ice sample was also calculated under different conditions.

5.2 EXPERIMENTAL CONDITIONS

5.2.1 Plane Triangular Ice Sample

The geometry of a plane triangular ice sample was appropriate because it ensured the formation of a local arc at a predetermined location and, therefore, made possible a detailed study of the arc characteristics further. The base of the mold was a glass plate since the surface properties of glass are similar to the porcelain used in insulators. To form ice sample, water was poured into the triangular glass mold, which was then placed in a cold chamber maintained at a constant -12 °C. Fig. 5.1 depicts the dimensions of the ice sample, which were as follows: a height of 280 mm, a base of 200 mm and a thickness of 15 mm. The first 10 mm of ice on the bottom of the mold was made from distilled water to minimize the component of leakage current at the interface of the ice and triangular glass base. The remaining 5 mm ice layer was made from distilled water adjusted with

sodium chloride to control the level of conductivity. Once the ice sample was completely formed, an air gap with a constant width of 10 mm was made near the top electrode by cutting out a small fragment of ice. This air gap simulated the air gaps naturally created by the heating effect of partial arcs and ice falling during ice accretion on industrial insulators. Fig. 5.2 shows the final physical aspects of a plane triangular ice sample with an air gap.
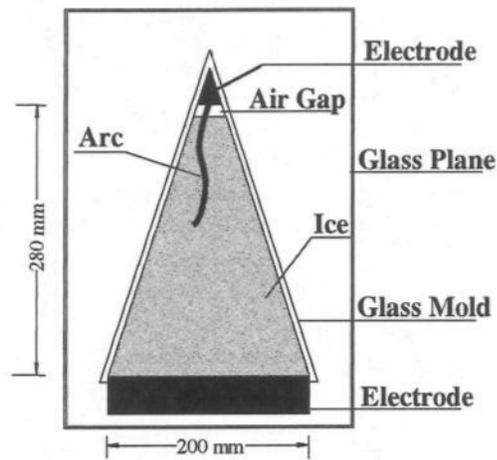
Fig. 5.1 Plane triangular ice sample

Fig. 5.2 Physical aspect of an ice sample

5.2.2 Experimental Set-ups

After the air gap was excised, the ice sample was placed vertically in the same evacuated chamber described in Chapter 4 where the ambient temperature was maintained at a constant 5 °C [147]. A vacuum system was used to adjust the ambient pressure to the desired value. A high voltage was applied to the bottom electrode while the top electrode was connected to ground. Fig. 5.3 shows the ice sample in the evacuated chamber and the test circuit. The methodology used was similar to that described for a short post insulator in the previous chapter.
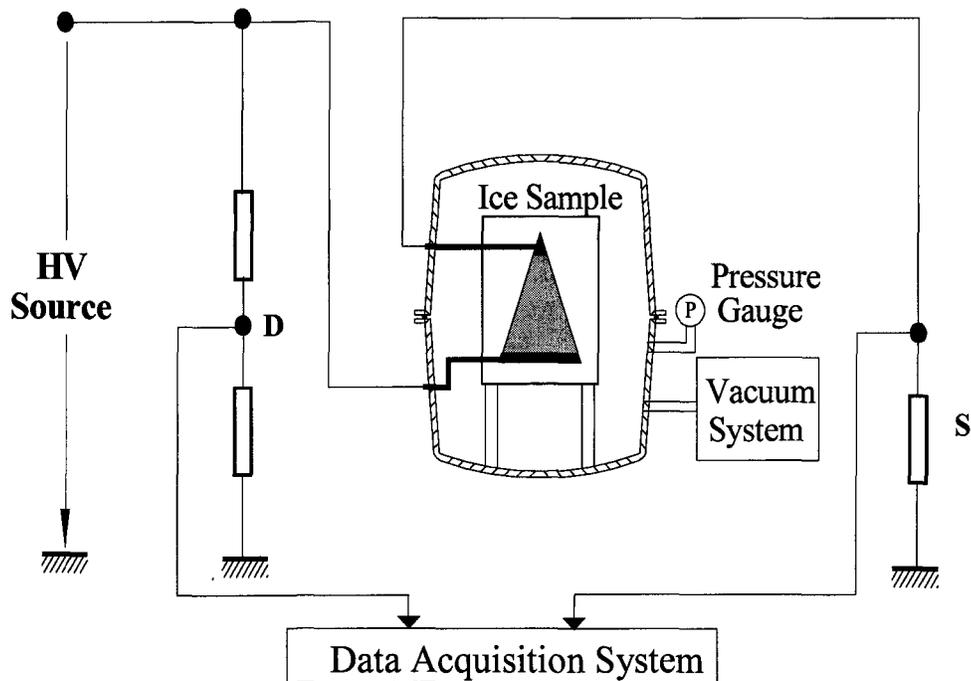
Fig. 5.3 Evacuated chamber and test circuit

D — Voltage divider   S — Current Shunt

5.3 AC FLASHOVER VOLTAGE AT LOW AIR PRESSURE

A number of flashover tests were carried out under varying conditions of freezing water conductivities and air pressure. The levels of conductivity tested in this section were 10, 80, 160, 250 and 400 μS/cm. Air pressure was varied between 101.3 kPa and 30 kPa corresponding to an altitude range of sea level to 9000 m.

Figs 5.4 and 5.5 display the results of V_{MF} measured as a function of ambient pressure under different freezing water conductivities, σ.
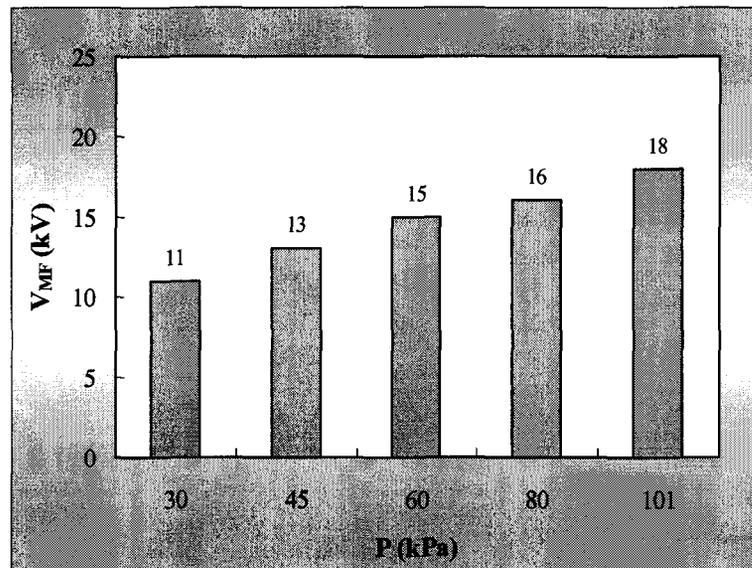
Fig. 5.4 AC minimum flashover voltage of an ice

sample as a function of air pressure (σ = 160 μs/cm)

Fig. 5.4 illustrates that the minimum flashover voltage, V_{MF}, decreased non-linearly with a decrease in air pressure. Fig. 5.5 reveals that the decrease in V_{MF} with a decrease in pressure becomes more pronounced when the conductivity σ was decreased. When the conductivity was set to 10 μS/cm, V_{MF} decreased approximately 41.4% when the pressure was decreased from 101.3 kPa to 30 kPa, corresponding to a climb from sea level to 9000 m. In contrast, when the conductivity was raised to 400 μS/cm, V_{MF} decreased approximately 35.7% when the pressure was decreased from 101.3 kPa to 30 kPa.
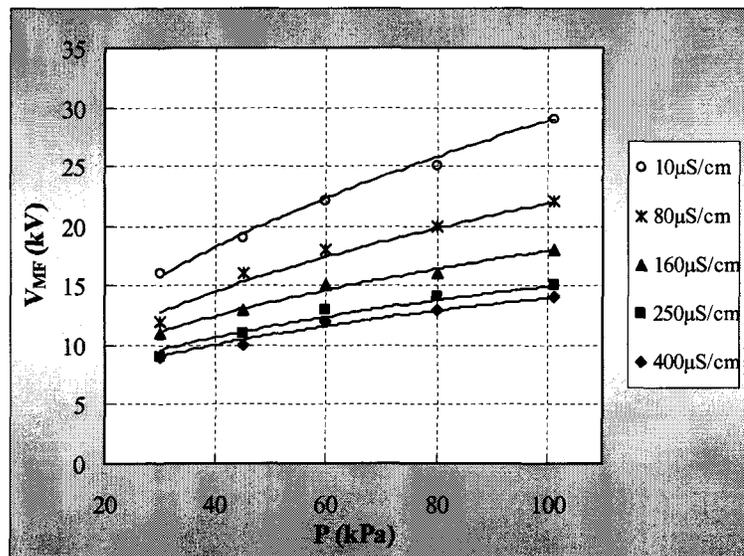
Fig. 5.5 AC minimum flashover voltage of an ice

sample as a function of air pressure

The results presented in Fig. 5.6 show that at a given air pressure, V_{MF} decreased with a decrease in freezing water conductivity, σ. This decrease in V_{MF}

leveled off at a specific saturation value when the conductivity was set to above

250 µS/cm.
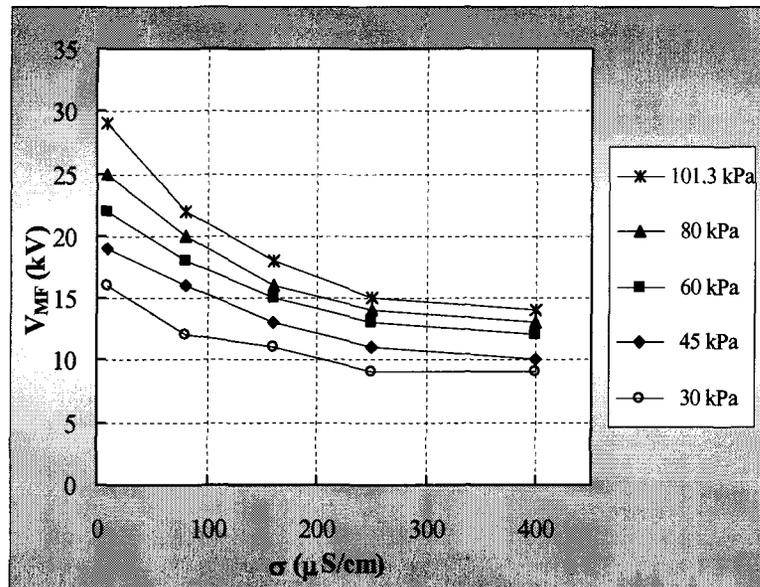
Fig. 5.6 Relationship between the AC minimum flashover voltage

of an ice sample and the conductivity of freezing water

5.4 AC CRITICAL FLASHOVER CURRENT AT LOW AIR PRESSURE

The critical flashover current under AC conditions is defined as the leakage

current peak value in the last half cycle before the final jump. This is indicated in

Fig 5.7 for a typical flashover tests under AC voltage conditions.
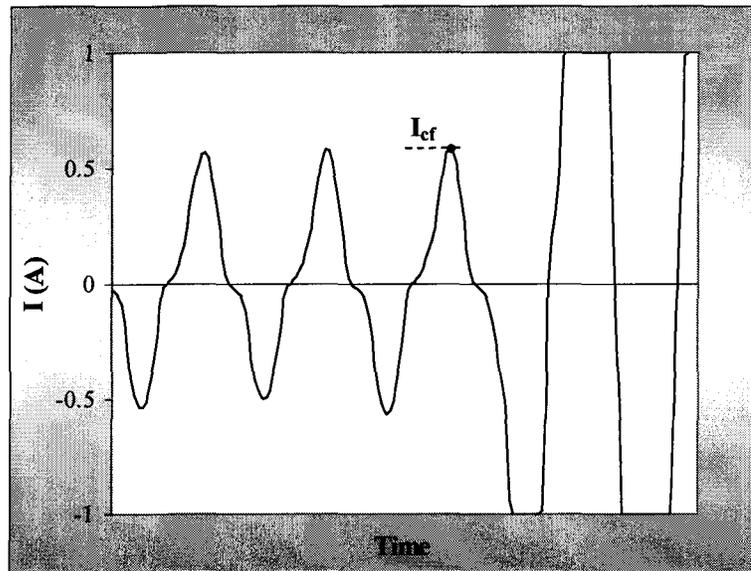
Fig. 5.7 AC critical flashover current I_{cf}

Because the critical flashover current depends on the applied voltage, in our test, it was measured only under the minimum flashover voltage. Additionally, due to the random nature of leakage current, the measured critical flashover current varied for each flashover test, even when all other test conditions were held constant. To minimize this variation, the average critical flashover current, I_{cf}, was calculated for each group of experiments. The values for the average I_{cf}, measured as a function of air pressure under AC conditions, are presented in Fig. 5.8. The standard deviation is in a range from 2.8% to 8.7% for each group of experiments. Under AC conditions, I_{cf} decreased as the pressure was decreased. The observed decrease in I_{cf} with air pressure could be due to the decrease in the V_{MF} of the ice sample. If V_{MF} decreased as the air pressure was decreased then the corresponding critical leakage current I_{cf} will also decrease. The decrease in I_{cf} was

smaller for a freezing water conductivity of 400 µS/cm than that observed for a lower conductivity of 80 µS/cm.
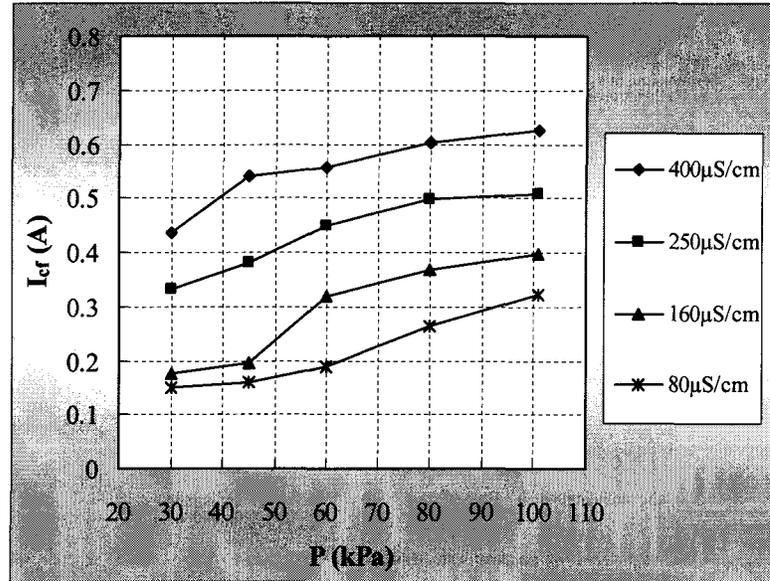
Fig. 5.8 AC critical flashover currents as a function of air pressure,

P, for different freezing water conductivities, σ

5.5 EXPONENT m UNDER AC CONDITIONS

As mentioned above, the influence of high altitude on the critical flashover voltage of ice samples can be evaluated using the exponent m from Equation (4.1).

The values for exponent m were determined by re-plotting the V_{MF} versus pressure data presented in Fig. 5.5 using V/V_0 versus P/P_0 and using the logarithmic scale. Fig. 5.9 depicts the re-plotted logarithmic coordinates. The exponent m was calculated from the log-log slope coefficients derived from Fig. 5.9. The values for exponent m are presented in Table 5.1.
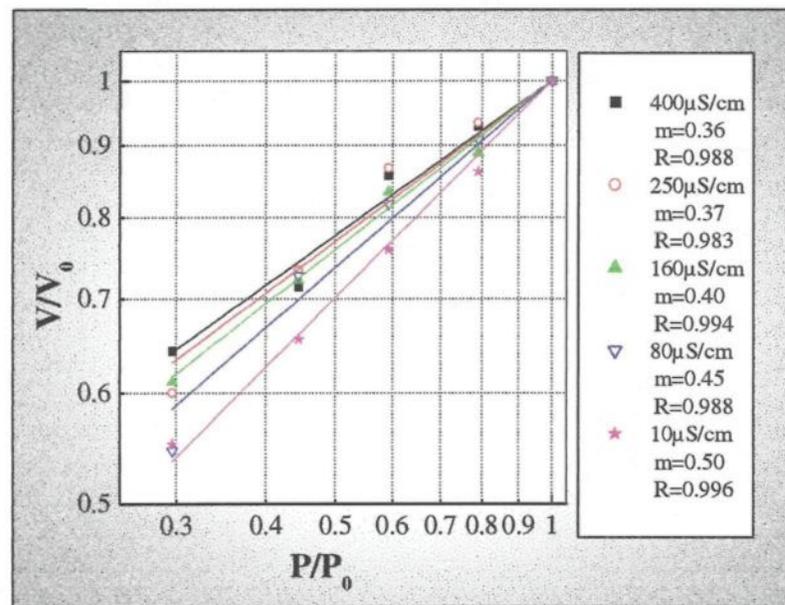
Fig. 5.9 Dependence of AC minimum flashover voltage ratio, V/V_0, on reduced pressure ratio, P/P_0

Table 5.1 Values of m for ice samples under AC voltage and

different freezing water conductivities

σ (μS/cm)	10	80	160	250	400
m	0.50	0.45	0.40	0.37	0.36

The value of m was influenced by the level of freezing water conductivity. As conductivity was increased, m decreased. Comparing the above results with that obtained from a triangular plane glass with a pollution layer (refer to Table 5.2) [48], the value of m for an ice samples was higher than that observed for a polluted samples. This result implied that in mountainous regions, where the pollution is relatively low and the level of ice accretion is high, the effect of high altitude on the critical flashover voltage of ice-covered insulators become larger.

Table 5.2 Value of m for referenced polluted samples [48]

ESDD (mg/cm^2)	0.2
m	0.31

5.6 DC FLASHOVER VOLTAGE AT LOW AIR PRESSURE

Using the triangular ice sample, a series of flashover tests were carried out under DC+ and DC- conditions for air pressure levels of 101, 80, 60, 45 and 30 kPa as well as freezing water conductivities of 80, 160, 250 and 400 μS/cm.

In the experiments presented in this section, the high voltage was always applied to the bottom electrode, (refer to Fig. 5.3), whereas the initial arc always started from the top electrode. Under DC- conditions, the local arc started from the anode and was, therefore, conventionally called the positive arc. Under DC+

conditions, the arc started from the cathode and was called the negative arc. However, the above conventional terms will not be used to allow a comparison of results and to standardize the terminology used in this chapter and introduced in chapter 4, where the high voltage was always applied to the top electrode. Instead, in this Chapter, the terms of DC+ and DC- are redefined as corresponding to the positive and negative arcs.

The results presented in Figs. 5.10 and 5.11 reveal that, under both DC+ and DC- conditions, V_{MF} of an ice sample decreased in a nonlinear manner when the air pressure was decreased. At lower air pressures, V_{MF} decreased at a fast rate. Freezing water conductivity, σ, also had an observable influence on V_{MF}; the higher the conductivity, the lower the V_{MF}. The observed percentage decrease in V_{MF} with a decrease in air pressure became more pronounced as conductivity was decreased. At a freezing water conductivity of 400 µS/cm, the percentage decrease in V_{MF} was approximately 39 % under DC+ and 31 % under DC- conditions when the air pressure was decreased from 101.3 kPa to 30 kPa. In contrast, at a freezing water conductivity of 80 µS/cm, the percentage decrease in V_{MF} was approximately 44 % under DC+ and 38 % under DC- conditions when the air pressure was decreased from 101.3 kPa to 30 kPa.
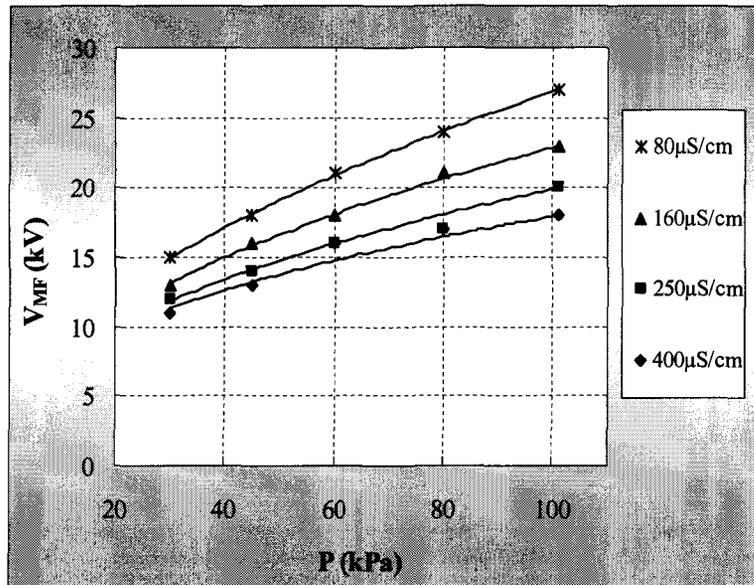
Fig. 5.10 Minimum flashover voltage of an ice sample as a

function of air pressure under DC+ conditions
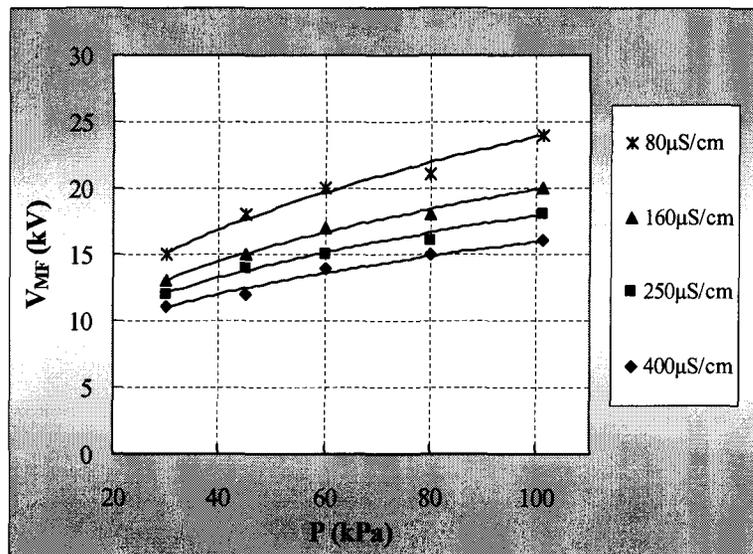
Fig. 5.11 Minimum flashover voltage of an ice sample as a

function of air pressure under DC- conditions

5.7 DC CRITICAL FLASHOVER CURRENT AT LOW AIR PRESSURE

The critical flashover current, I_{cf}, under DC conditions is defined as the intensity of the leakage current before the final jump. The value for critical flashover current is presented in Fig 5.12 for typical flashover tests under DC voltage.
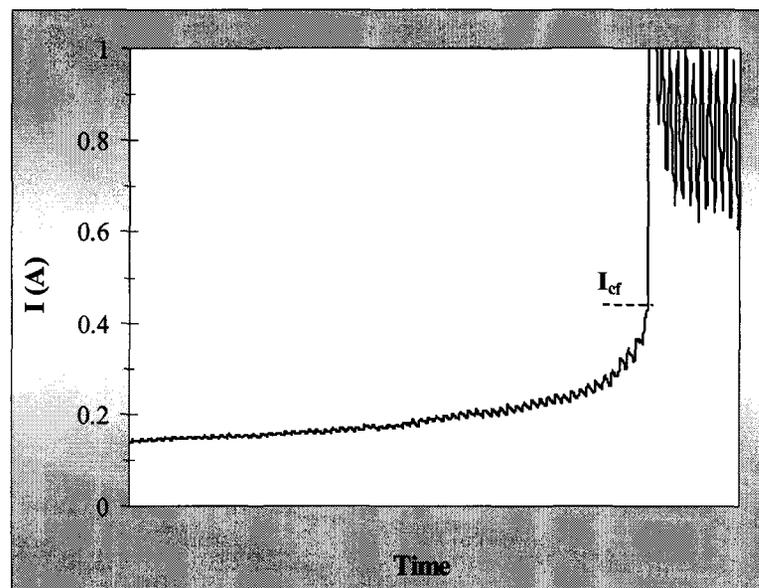
Fig. 5.12 DC critical flashover current I_{cf}

Figs. 5.13 and 5.14 depict how the critical flashover current varied with air pressure. The standard deviation of I_{cf} is between 3.5% to 13.3% for DC+ and between 3% to 11.8% for DC-. Under DC+ and DC- conditions, I_{cf} decreased as the pressure was decreased.
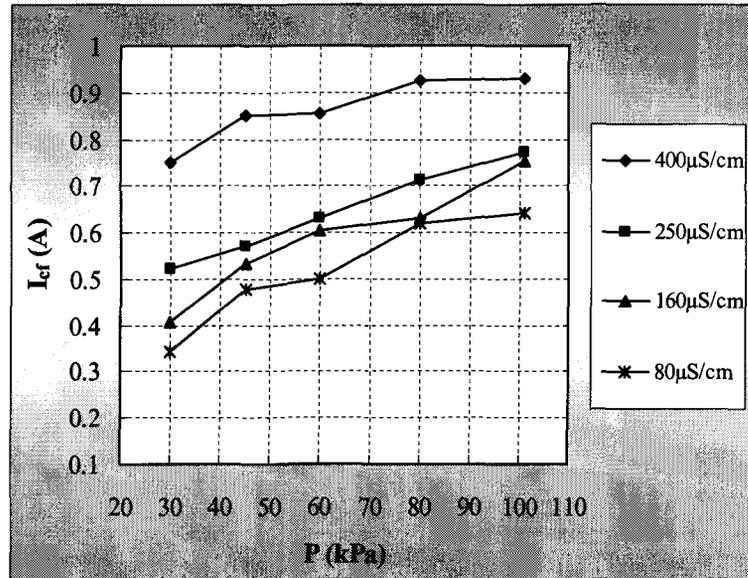
Fig. 5.13 DC+ critical flashover current, I_{cf}, as a function of air pressure,

P, for different freezing water conductivities, σ
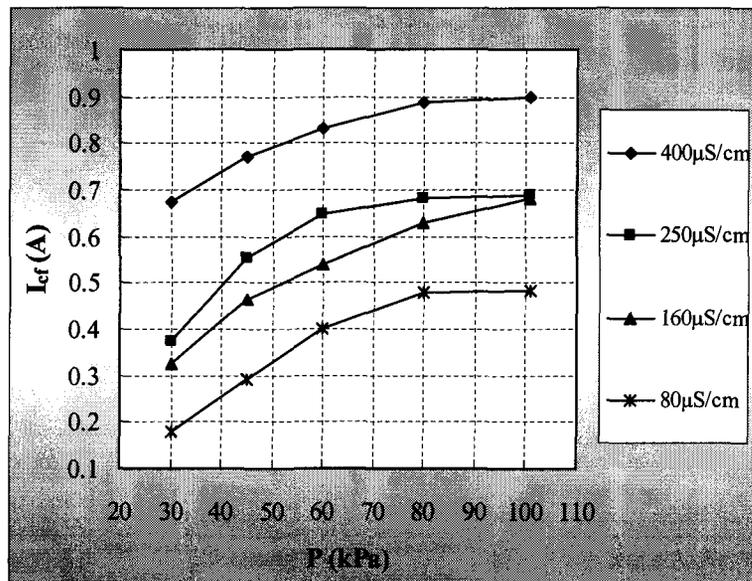
Fig. 5.14 DC- critical flashover current, I_{cf}, as a function of air Pressure,

P, for different freezing water conductivities, σ

5.8 EXPONENT *m* UNDER DC CONDITIONS

The results presented in Figs 5.10 and 5.11 were re-plotted using logarithmic scales as depicted in Fig. 5.15. The values of exponent *m* under DC conditions were calculated from Fig. 5.15 under different conditions and are presented in Table 5.3.

Table 5.3 Values of exponent *m* under DC Conditions and

different freezing water conductivities

σ (µS/cm) Voltage type	80	160	250	400
	m			
DC+	0.49	0.46	0.43	0.38
DC-	0.38	0.35	0.33	0.31

It is clearly shown that under both DC+ and DC- conditions, exponent *m* decreased as freezing water conductivity was increased. The percentage decrease in *m* was approximately 22% under DC+ and 18% under DC- respectively when the freezing water conductivity was increased from 80 to 400µS/cm.
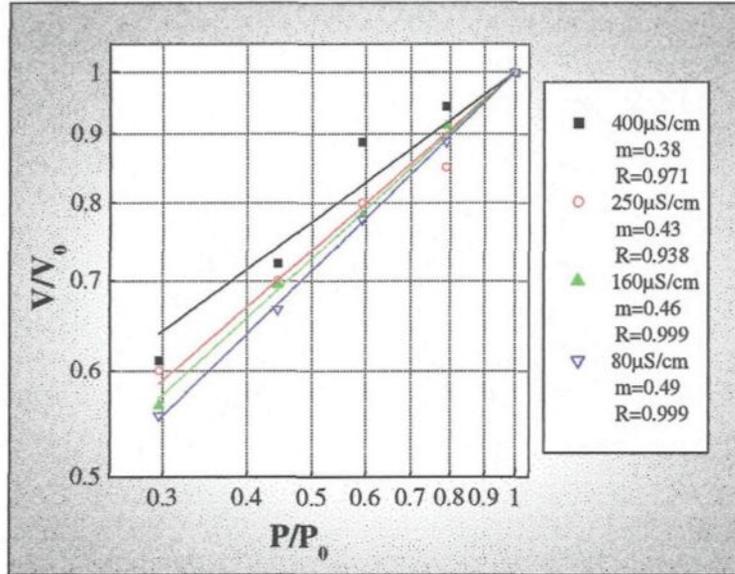
(a) DC+
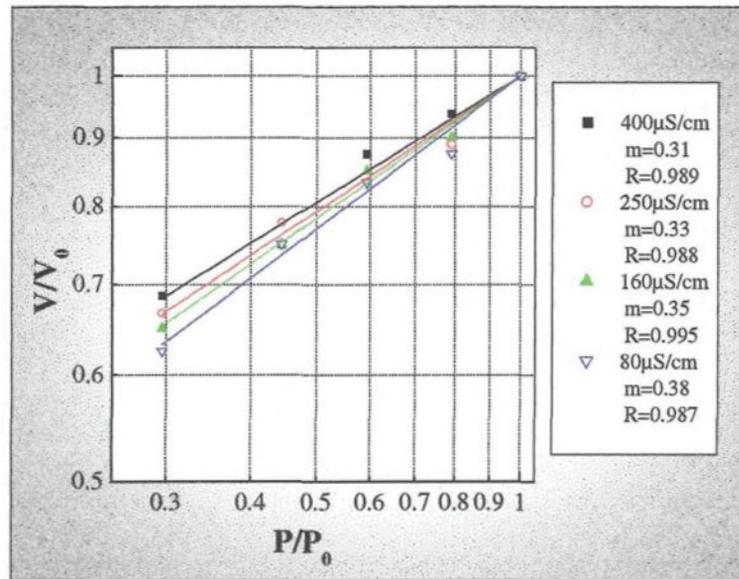
(b) DC-

Fig. 5.15 Dependence of DC minimum flashover voltage ratio,

V/V_0, on the reduced pressure ratio, P/P_0

For the purpose of comparison between the results obtained under icing and pollution conditions, the exponent m was calculated for different equivalent salt deposit densities (ESDD) from the results obtained by **Kawamura et al** [73]. They also used a plane triangular glass sample to investigate the effect of air pressure on the pollution flashover. The results are shown in Table 5.4.

Table 5.4 Values of exponent m for DC- under various ESDD

ESDD (mg/cm^2)	0.067	0.2
m	0.35	0.32

It may be noted that m decreased with an increase in the degree of pollution. This variation manner of m agrees with that obtained in this study.

5.9 DISCUSSION

5.9.1 Effects of Voltage Type and Polarity on Flashover Voltage at Low Air Pressure

The effects of voltage type and polarity on the flashover voltage of an ice sample at low pressure were investigated under both AC and DC voltage conditions.

Fig. 5.16 illustrates the relationship between V_{MF} of an ice sample and air pressure under DC+, DC- and AC conditions. The data is presented in Fig. 5.16a and Fig. 5.16b for the freezing water conductivities of 80 µS/cm and 400 µS/cm, respectively.

V_{MF} was found to decrease as the air pressure was decreased under both DC and AC voltage conditions. Additionally, under a constant air pressure and specific voltage type, (AC, DC- or DC+), V_{MF} was found to be lower for a freezing water conductivity of 400 µS/cm than that observed for 80 µS/cm. Finally, under a given air pressure, the lowest value of V_{MF} was obtained under AC conditions.

The last result was in marked contrast with those obtained by a previous study where the lowest value of V_{MF}, for a short string of IEEE standard insulators covered with artificial ice, was obtained under DC- conditions (**Farzaneh et al.** [21]). The discrepancy could be due to the effects of the insulator shape.

The polarity effect on V_{MF} was found to be the same for both ice and pollution conditions [73]. V_{MF} under DC- was consistently lower than that observed under DC+ conditions for a given air pressure.
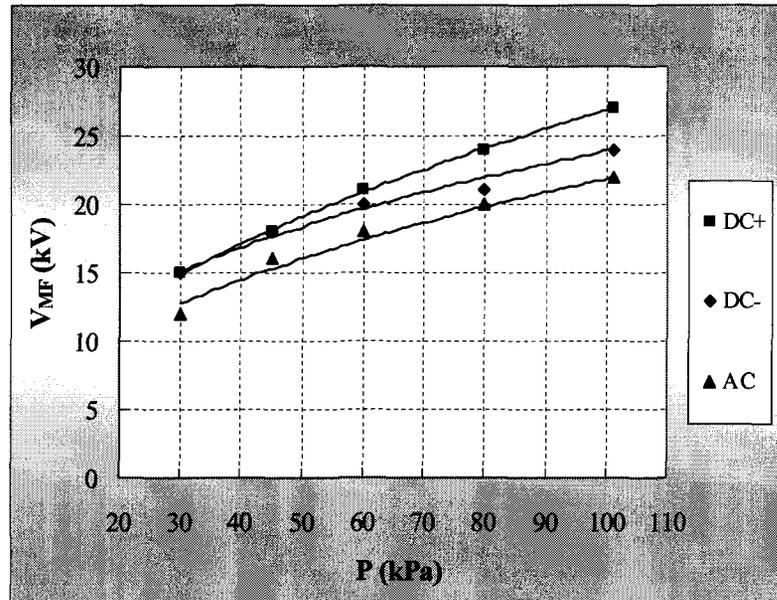
(a) $\sigma = 80\ \mu S/cm$
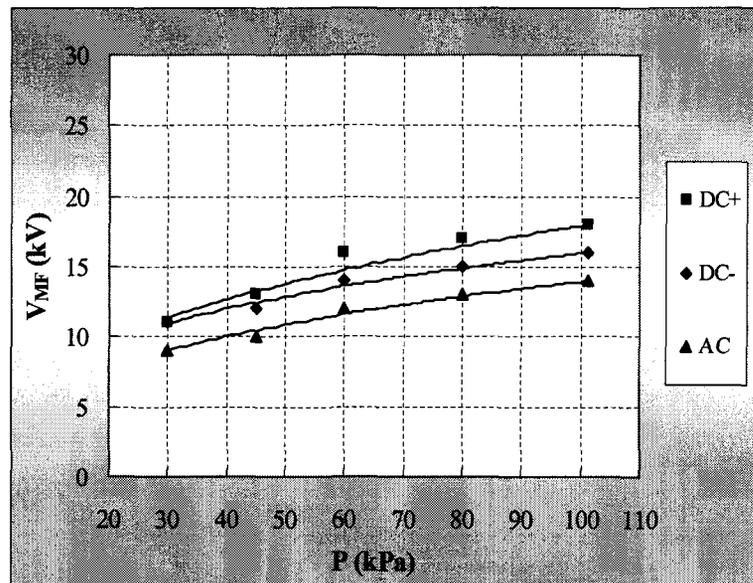
(b) $\sigma = 400\ \mu S/cm$

Fig. 5.16 Minimum flashover voltage, V_{MF}, as a function of air pressure,

P, for different freezing water conductivities σ

5.9.2 Effects of Voltage Type and Polarity on Critical Flashover Current at Low Air Pressure

Fig. 5.17 shows the critical flashover current, I_{cf}, as a function of air pressure under DC+, DC- and AC voltage conditions. The data for the freezing water conductivity of 80 μS/cm and 400 μS/cm is represented in Fig. 5.17a and 5.17b respectively.

I_{cf} was found to be lower under AC than that observed under DC- or DC+ conditions for a given air pressure value. Additionally, the effect of voltage polarity was obvious when the freezing water conductivity was set to 80 μS/cm: I_{cf} was lower under DC- than under DC+ conditions regardless of the air pressure. When the freezing water conductivity was set to 400 μS/cm, voltage polarity had practically no effect on I_{cf}. I_{cf} also decreased as the pressure was decreased under both AC and DC current conditions. Finally, the observed decrease in I_{cf} was smaller for a freezing water conductivity of 400 μS/cm than that observed for a lower conductivity of 80 μS/cm.

5.9.3 Effects of Voltage Type and Polarity on Exponent m

The values for exponent m under AC, DC+ and DC- conditions are given in Fig. 5.18
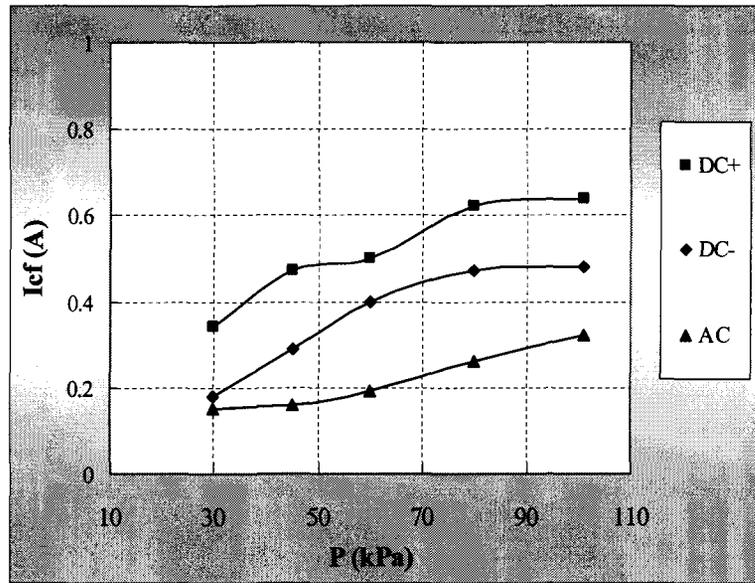
(a) $\sigma = 80\ \mu S/cm$
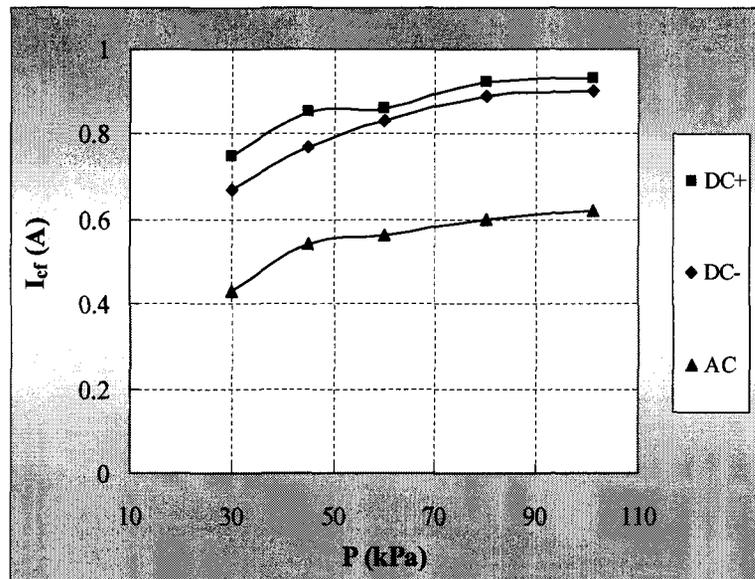
(b) $\sigma = 400\ \mu S/cm$

Fig. 5.17 AC and DC critical flashover currents, I_{cf}, as a function of

air Pressure, P, for different freezing water conductivities, σ

0.8

0.6

0.46 0.47

0.46

0.45

0.39

0.4

0.37

0.38

⊟0.4

0.35

0.34

0.36

0.31

☐ DC-

☒ AC

▣ DC+

0.2

0

80   160   250   400

σ (μS/cm)
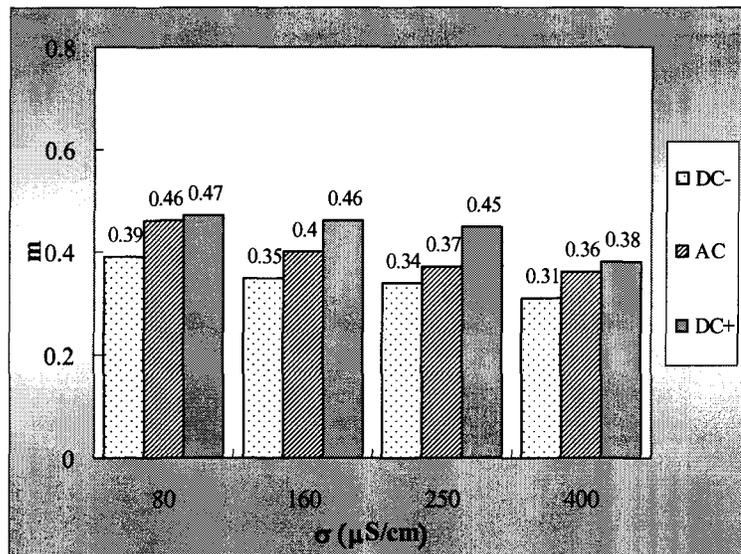
Fig. 5.18 Effects of voltage type and polarity on *m*

Exponent *m* was influenced by the type and polarity of the applied voltage. For a given conductivity, the values of *m* were consistently highest under DC+, and lowest under DC-. The value for *m* under AC fell between the values recorded under DC+ and DC-.conditions

Fig. 5.18 shows that the value of *m* under ice conditions was larger than that observed under pollution conditions, where the exponent *m* was found to be approximately 0.16 under DC+, 0.13 under DC- and 0.30 under AC conditions [48]. A similar triangular sample, albeit polluted at an ESDD of 0.2 mg/cm^2, was utilized for the above pollution data. The above comparison with a polluted insulator suggests that an ice-covered insulator would be more affected by the effects of low air pressure when the level of pollution is less, which is usually the situation in mountainous regions.

5.9.4 Effect of Insulator Profile on Exponent *m*

The values of *m* obtained on the triangular ice sample were compared with those obtained on the short post ice-covered insulator previously presented in Chapter 4. This comparison is represented in Table 5.5.

Table 5.5 Values of exponent *m* under various conditions

Voltage type σ(µS/cm)		DC+	DC-	AC
		m		
Triangular ice sample	80	0.47	0.39	0.46
	250	0.45	0.34	0.37
Ice-covered insulator	80	0.34	0.26	0.40
	250	0.49	0.43	0.53

Under both DC and AC voltages, the exponent *m* for a triangular ice sample decreased with an increase in the freezing water conductivity. In contrast, *m* decreased for a short post insulator with a decrease in freezing water conductivity. This divergent result could be due to the arc floating phenomenon where the arc propagates through the air. Table 5.6 illustrates results on the arc floating phenomena observed from the test using both a triangular ice sample and a short post insulator.

133

Table 5.6 Effects of arc floating on *m*

P (kPa) / σ (µS/cm)	101		45		
80		V-		V-	m-
250		V-		V↑	m↓
80		V-		V↑	m↓
250		V↑		V↑	m-
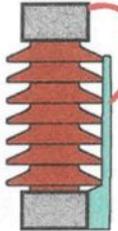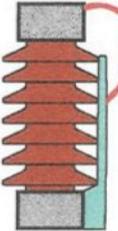
- : normal value   ↑ : relative higher value   ↓ : relative lower value

134

At a lower freezing water conductivity of 80 µS/cm, the arc on a triangular ice sample surface consistently propagated along the ice surface at both standard and low air pressures. In this situation, exponent m had a normal value. When the freezing water conductivity was raised to 250 µS/cm, the arc propagated along the ice surface at standard pressure, whereas it frequently propagated through the air at a lower air pressure of 45 kPa. When an arc floats through the air it follows a longer flashover path. A consequent relative higher flashover voltage at the lower air pressure of 45 kPa lead to a relative lower m value. Hence, for a triangular ice sample, m decreased with an increase in the freezing water conductivity.

Contrary to the observations for a triangular ice sample, at a lower freezing water conductivity of 80 µS/cm, the arc propagated along an ice-covered insulator surface at standard air pressure, whereas it frequently propagated through the air at a lower pressure of 45 kPa, which lead to a relative lower m value. When the freezing water conductivity was set to 250 µS/cm, an arc on an ice-covered insulator surface frequently propagated through the air at both standard and lower air pressures. Consequently, an ice-covered insulator consistently had a relatively higher flashover voltage at both standard and lower air pressures, which lead to normal m values. Therefore, for an ice-covered short post insulator, m increased with an increase in freezing water conductivity. These results prove that insulator profile can influence the value of m.

5.10 CONCLUSION

In this chapter, both AC and DC flashover performance of a plane triangular ice sample were investigated at low air pressure conditions. The following conclusions are summarized from the results:

1). For the plane triangular ice sample subjected to both AC and DC voltage conditions, the air pressure had an observable influence on the minimum flashover voltage, V_{MF}. V_{MF} decreased with a reduction in air pressure. When the freezing water conductivity, σ, was set to 250 μS/cm, the observed decrease in V_{MF}, under an air pressure value set between 101 kPa and 45 kPa, was approximately 27% under AC, 30% under DC+ and 22% under DC- voltage conditions.

2). The voltage type and polarity influenced V_{MF}. The voltage type and polarity had the same effect on V_{MF} at standard pressure as they did at low pressure: for any air pressure value between 101.3 and 30 kPa, the V_{MF} under AC was consistently lower than that observed under DC voltage conditions. The V_{MF} under DC+ was higher than that observed under DC- conditions.

3). The exponent m was influenced by the level of freezing water conductivity, the type and polarity of the applied voltage as well as the insulator profile. For the plane triangular ice sample, m decreased with the increase in freezing water conductivity. For a given freezing water conductivity, m had the highest value under DC+ and the lowest value under DC- conditions. The value of m under AC fell between the values measured under DC+ and DC- conditions.

4). At low air pressure, the critical flashover leakage current, I_{cf}, decreased and it was influenced by the voltage type and polarity. I_{cf} was also lower under AC than under DC voltage conditions for a given air pressure. The effect of voltage polarity was largest when the freezing water conductivity was low. I_{cf} was found to be lower under DC- than under DC+ conditions regardless of the air pressure.

CHAPTER 6

CHARACTERISTICS OF AN ARC
ON AN ICE SURFACE
AT LOW AIR PRESSURE

CHAPTER 6

CHARACTERISTICS OF AN ARC ON AN ICE SURFACE AT LOW AIR PRESSURE

6.1 INTRODUCTION

According to the flashover theory [105] [117], the formation and propagation of a local arc are necessary to the completion of a flashover on an insulator surface. Therefore, the arc characteristics play an important role in the flashover process, particularly an arc's voltage-current characteristics. To understand the mechanisms underlying the flashover phenomenon on an ice-covered insulator at high altitudes, it is necessary to investigate how local arc characteristics vary under low pressure.

The total voltage drop along an arc established between two electrodes, V_{total}, typically has two components: the electrode voltage drop, V_e, and the voltage drop along the arc itself, V_{arc}. V_{total} can be expressed as follows:

$$V_{total} = V_{arc} + V_e \tag{6.1}$$

V_e is a constant and dependent on the electrode material, shape and the environmental conditions. V_{arc} is a function of the arc length, x, and the leakage current through the arc, I. V_{arc} can be expressed as follows:

$$V_{arc} = Ex = AxI^{-n}$$
(6.2)

where E (V/cm) is the average voltage gradient along the arc, and A and n are the arc constants.

A, n, and V_e are referred to as the characteristic parameters of an arc. Together these parameters describe the unique voltage-current characteristics of an arc.

Under high altitude conditions, several researchers have reported that the characteristics of an arc on the polluted surface were influenced by atmospheric pressure, and the values of A, n and V_e were determined in several studies [64] [73] [116] [131].

A few studies on the characteristics of arc on ice surface were conducted by CIGELE [33] [34] and some of these studies ascertained the value for these parameters under standard atmospheric pressure, which corresponded to sea level. There has yet to be a study that examines the effect of low air pressure on the characteristic parameters of an arc on an ice surface.

In this study, the influence of low air pressure or high altitude on the characteristics of an arc on an ice surface was investigated systematically using the plane triangular ice sample. In this chapter, the experimental facilities and methodology used to determine the characteristics of an arc will be introduced. A, n, and V_e for the arcs generated under both AC and DC voltage conditions, (referred to henceforth as an AC arc and a DC arc), will be determined and presented. The effect of air pressure on these parameters will also be examined.

6.2 EXPERIMENTAL FACILITIES AND METHODOLOGY

In previous laboratory experiments, it was observed that occasionally two or more arcs formed simultaneously on the surface of an ice-covered insulator during the flashover process. The apparent random nature of arc formation made it difficult to investigate arc characteristics using real insulators. To avoid the formation of multiple arcs, a plane triangular ice sample was used, which was introduced in Chapter 5. All tests were carried out in the same evacuated chamber presented and described in Chapter 4.

Conventionally, an arc can be classified as either a static or a dynamic arc. The static arc burns along the air gap yet does not propagate along the ice surface. The dynamic arc will first bridge the air gap and then propagate along the ice

surface. Correspondingly, the methods employed to generate these two types of arcs were established by CIGELE [26] [27] [33] [34] and are summarized as follows:

- The method used to generate a static arc:

An air gap was excised, which varied in length for each experiment, and a measuring electrode was installed at the base of the air gap. Voltage was applied and increased until an air gap breakdown occurred. A steady static arc was then established across the air gap, which did not extend along the ice surface.

- The method for used to generate a dynamic arc:

An air gap with a constant length was excised and the measuring electrode was repositioned for each experiment. The voltage was applied and increased until flashover occurred. A local dynamic arc was established, which bridged the air gap and then propagated along the ice surface. When it reached the measuring electrode, it did not stop but continued propagating towards the HV electrode.

During the flashover process observed on ice-covered insulators, local arcs will often bridge the air gap and propagate along the ice surface. Therefore, arcs

generated during the flashover process are likely to be dynamic arcs. For this study, the method for measuring the characteristics of the dynamic arcs was employed and described in detail as follows:

- After the ice sample was formed, a 1 cm wide air gap was excised near the top electrode. A measuring electrode was installed on the ice surface at a predetermined position as depicted in Fig. 6.1. The ice sample was then placed vertically in an evacuated chamber in a climate room where the temperature was maintained at +5°C. A vacuum system was used to decrease the air pressure in the chamber to a desired value. High voltage was applied to the bottom electrode, as illustrated in Fig. 6.2, and was increased at a constant rate of approximate 3.9 kV/s until flashover occurred.
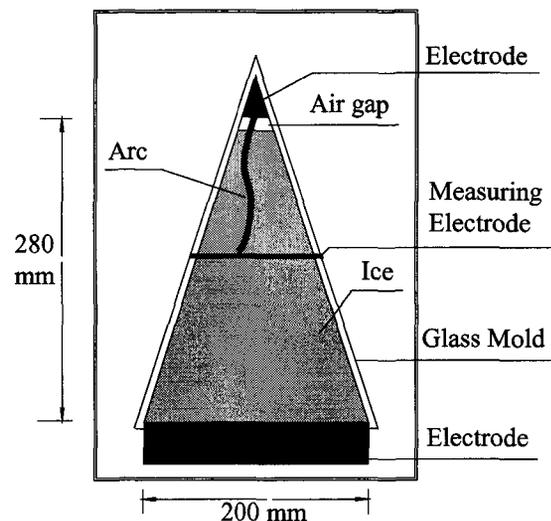
Fig. 6.1 Physical ice model
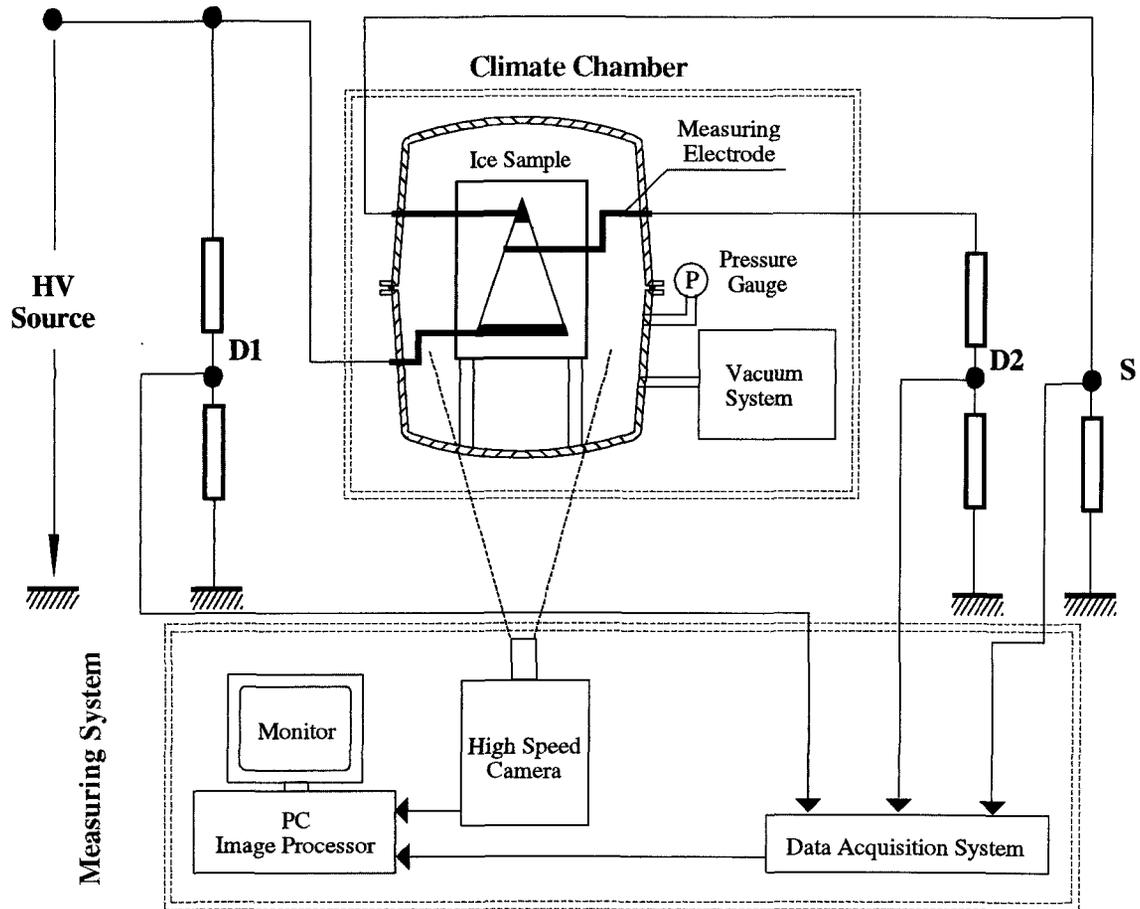
Fig. 6.2 Schematic diagrams of the evacuated chamber and test circuit

D1, D2 — Voltage divider   S — Current Shunt

– Fig. 6.3 portrays the high-speed camera, which was a Kodak Ektapro EM Motion Analyzer, Model1012 and had a maximum record rate of 12000 frames per second. This camera was employed to record the propagation of an arc and to determine the moment when the arc reached the measuring electrode. Since the arc propagation velocity on an ice surface was relatively slow, a recording rate of 1000 frames per second and an exposure time of 1 ms per frame were used. A data acquisition system, (DAS), permitted the measurement of the applied voltage, V, the measuring electrode voltage, V_m, and the leakage current, I. These quantities were recorded simultaneously and displayed on the arc propagation images recorded by the high-speed camera as presented in Fig. 6.4.

– When the arc arrived at the measuring electrode, V_m represented the total voltage along the arc, V_{total}. It was straightforward to observe the moment when the arc arrived at the measuring electrode by analyzing the image recorded by the high-speed camera and the waveforms recorded by the DAS. Fig. 6.4 depicts a typical image at the moment of arc arrival.

Fig. 6.3 High speed camera
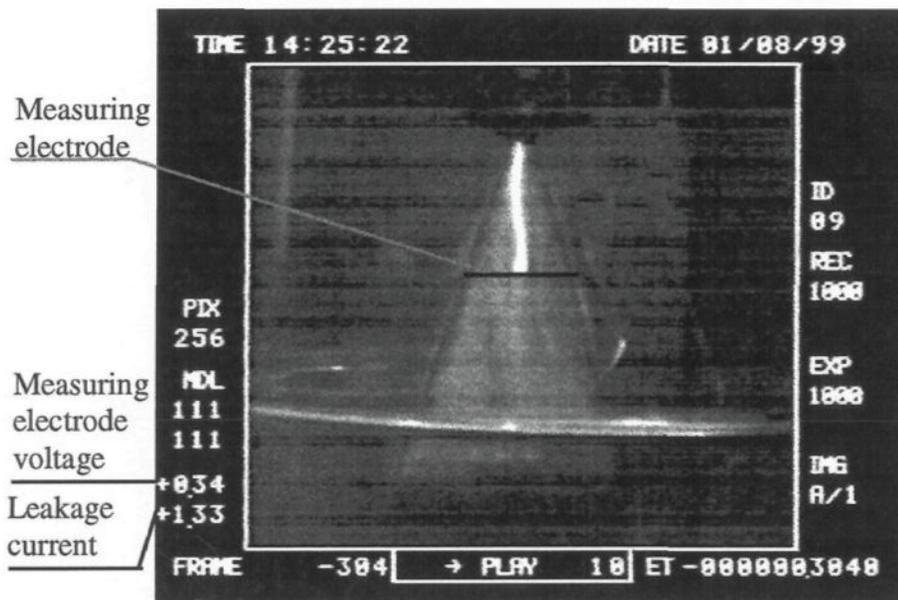
Fig. 6.4 Image of an arc at the moment of contact with the measuring electrode

– Fig. 6.5(a) shows the typical waveforms for V, V_m, and I obtained under AC conditions. For each cycle, V_m increased with an increase in V. When V increased to a certain value, referred to as point P_1, the air gap breakdown occurred and V_m increased relatively slowly. When the arc reached the measuring electrode, referred to as point P_2, V_m dropped suddenly. V_m at this moment corresponded to the voltage across the arc, V_{total}. In the present study, the difference between the voltage drop at metallic measuring electrode and that at ice layer was ignored.

– Fig. 6.5(b) shows the waveforms for V, V_m, and I obtained under DC conditions. As V was increased, V_m increased. When V reached a specific value, referred to as point t_0, the local arc extended and reached the measuring electrode and V_m dropped suddenly. At point t_0, V_m corresponds to the total voltage across the arc, V_{total}.

– Each ice sample was used once for a single flashover test. The measuring electrode was adjusted to different positions to measure the voltage along the arc as a function of arc length. In this study, the distance between the measuring electrode and the top electrode was adjusted from 1 to 15 cm, which corresponded to an arc length increase from 1 to 15 cm.
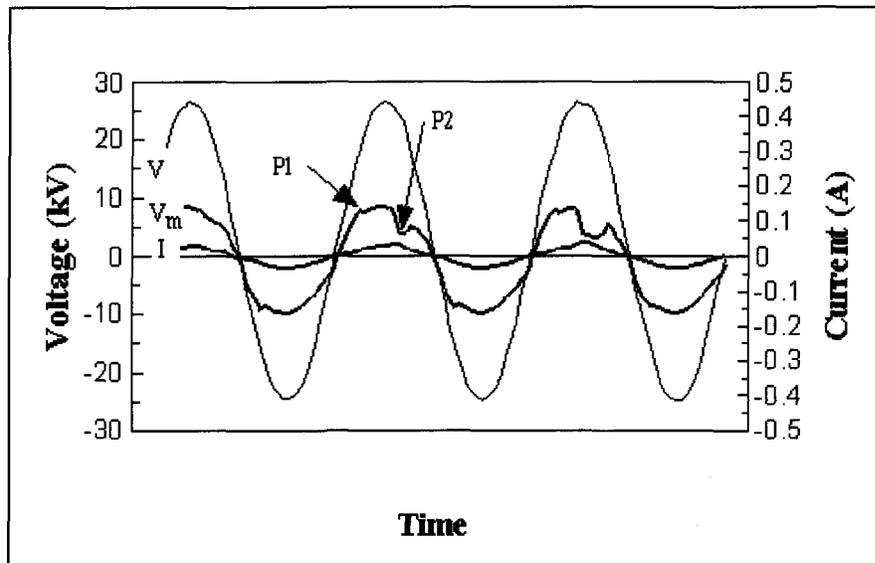
(a) AC
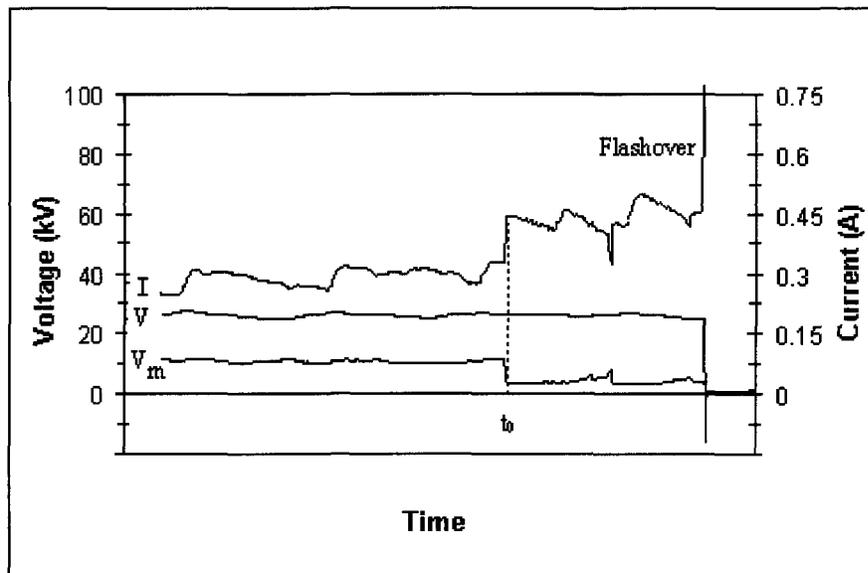
(b) DC

Fig. 6.5 Typical waveforms

V: Applied voltage; *V*$_m$: Measuring electrode voltage; *I*: Current

6.3 EFFECT OF AIR PRESSURE ON AC ARC CHARACTERISTICS

6.3.1 Electrode voltage drop

In previous studies of CIGELE [33], the magnitude of the electrode voltage drop, V_e, was included in the arc constant A in order to simplify the mathematical model. In this study, V_e was determined separately from A in order to investigate the effects of low air pressure on the arc parameters and to compare them with those under DC voltages.

To determine V_e, the arc length was varied in a series of experiments where the air pressure was established at one of four values: 101, 80, 60, or 45 kPa, corresponding to the altitudes of sea level, 2000, 4000, and 6500 m, respectively. The freezing water conductivity was adjusted in a range of 80 and 160 μS/cm to obtain different leakage current values. From these experiments, the total voltage drop along arc, V_{total} were determined, and the results are displayed in Figs. 6.6(a), 6.6(b), 6.6(c) and 6.6(d), respectively. Within these figures, the leakage current, I, on the horizontal axis represents the peak value for the measured leakage current.
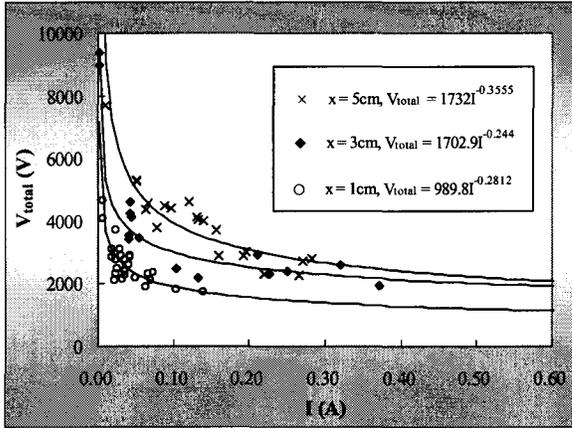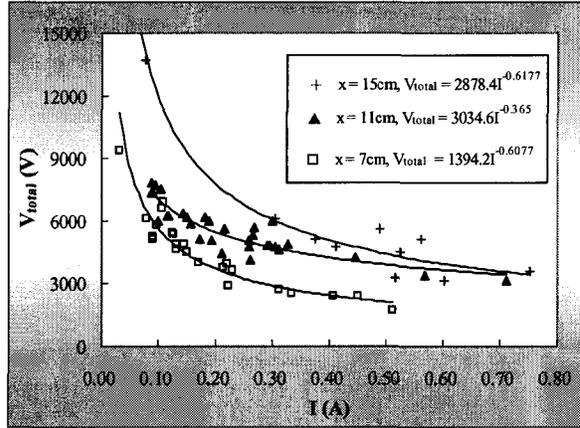
$x \leq 5$ cm $x \geq 7$ cm

(a) at standard pressure (101 kPa)
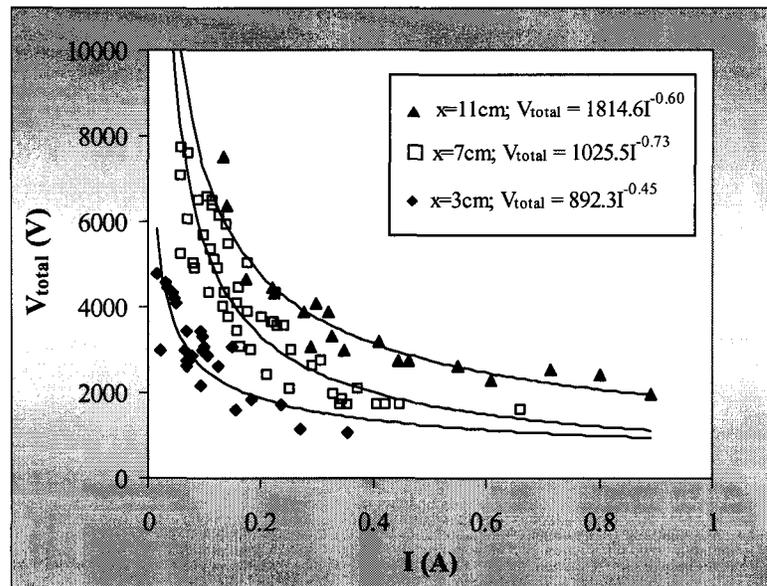
(b) at pressure of 80 kPa
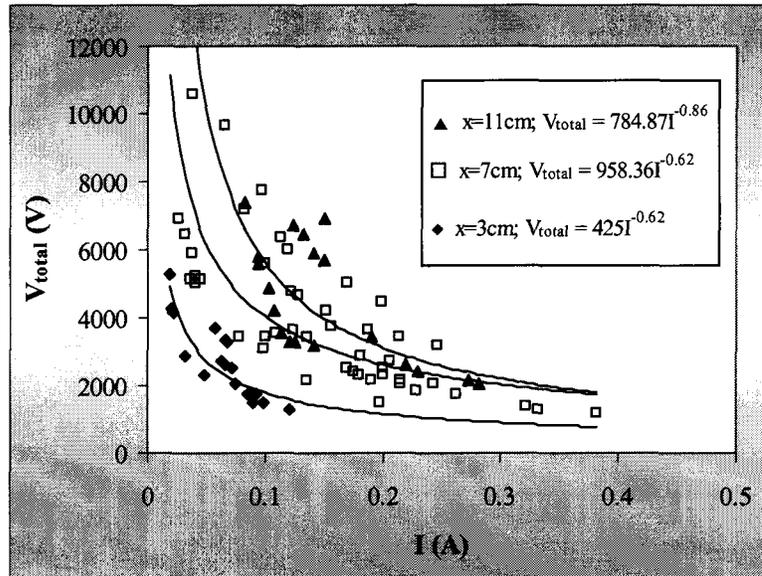
(c) at pressure of 60 kPa
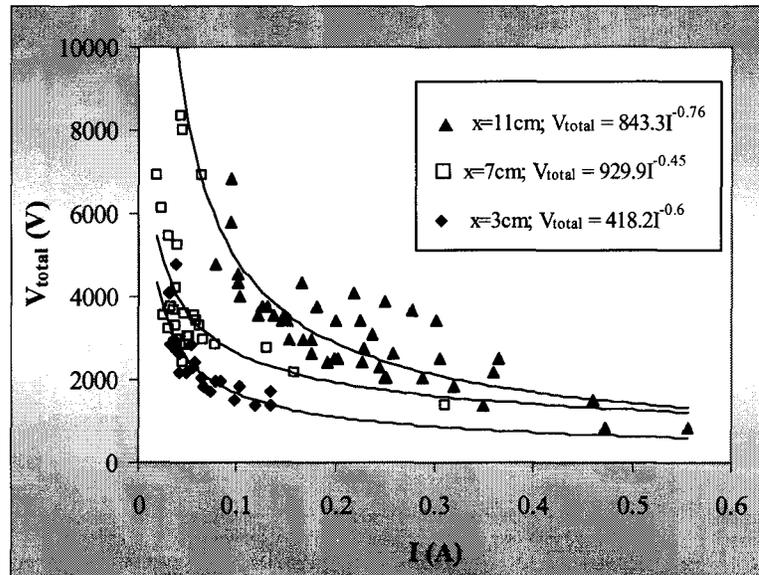
(d) at pressure of 45 kPa

Fig. 6.6 V_{total} as a function of I at different air pressures under AC condition

Regression analysis was applied to the above results to determine the relationship between the total voltage drop along arc, V_{total}, and the leakage current, I, at different arc lengths and air pressures. The result of this analysis is also displayed in Fig. 6.6. From the relationship established from the regression analysis, the value for V_{total} for a given value of arc length, x, the leakage current, I, and air pressure, P, was calculated and plotted in Fig. 6.7. For a given value of I, there was a positive linear relationship between V_{total} and x. When x tended towards 0, V_{total} tended towards a value corresponding to V_e. Due to its randomicity, V_e has different values for different I. The average value was calculated to be the arc electrode voltage drop in the present study. For example, when the air pressure was set to 60 kPa, V_e was equal to 482 V.

The magnitude of V_e under different air pressures is presented in Fig. 6.8. It may be noted that V_e decreased with a decrease in P. Using the regression analysis, the relationship between V_e and air pressure can be approximately expressed as follows:

$$V_e = 931\left(\frac{P}{P_0}\right)^{1.22}, \quad R=0.992 \tag{6.3}$$

where P_0 and P are the air pressures at sea level and high altitude, respectively; R is the correlation coefficient.
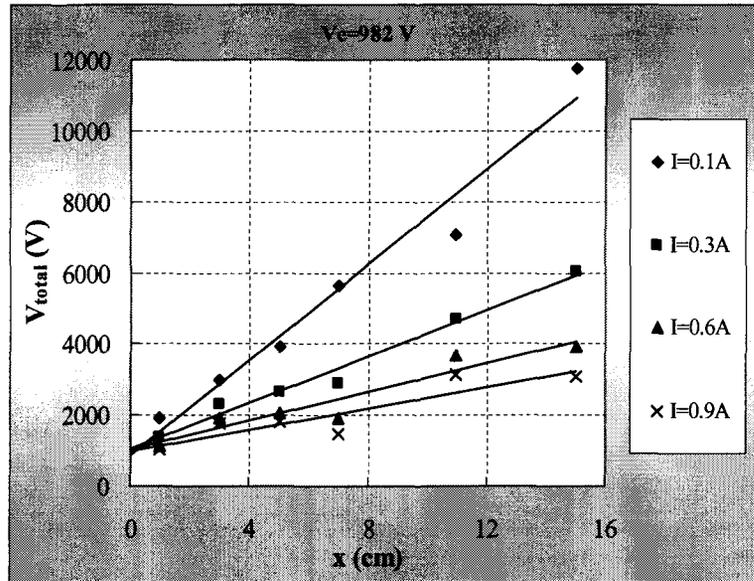
(a) at 101 kPa
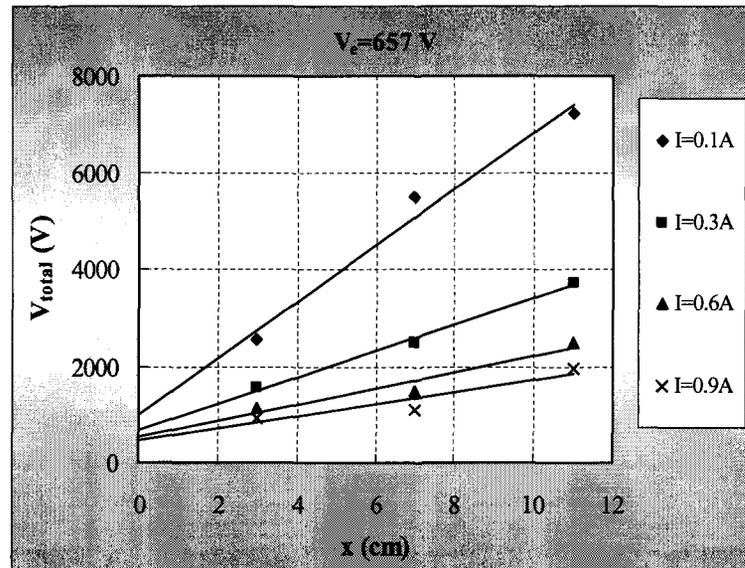
(b) at 80 kPa
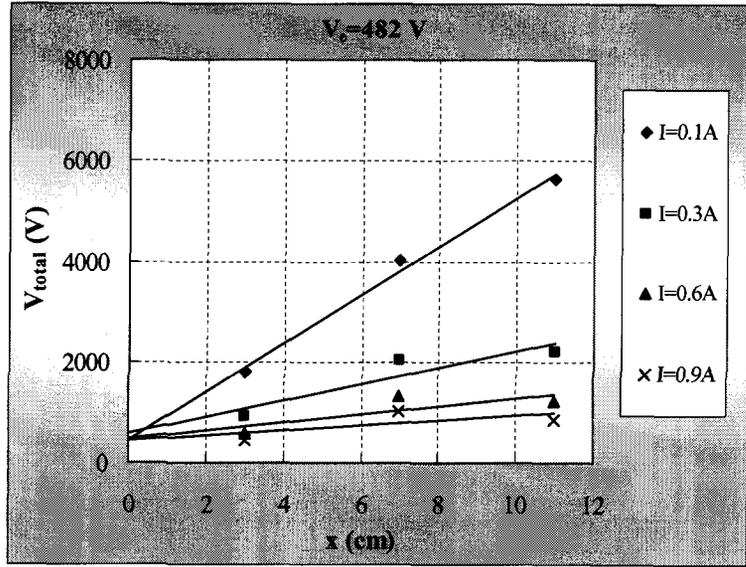
(c) at 60 kPa
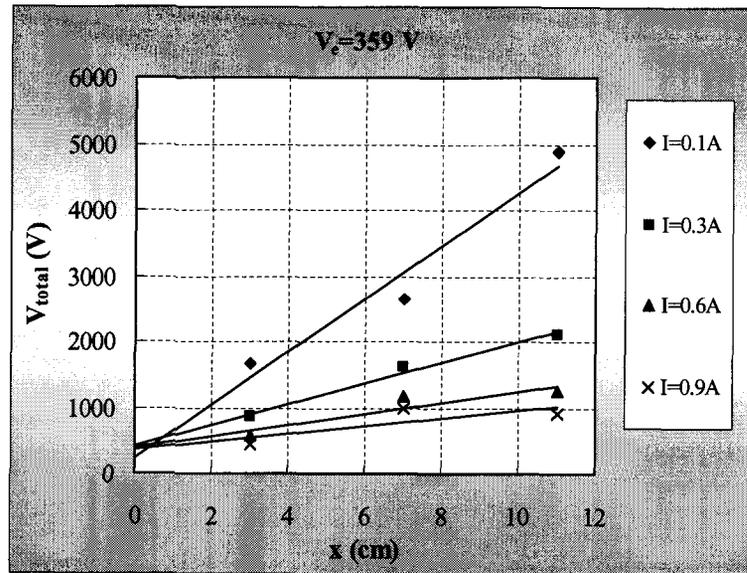
(d) at 45 kPa

Fig. 6.7 Relation between the total voltage drop along an arc and arc length
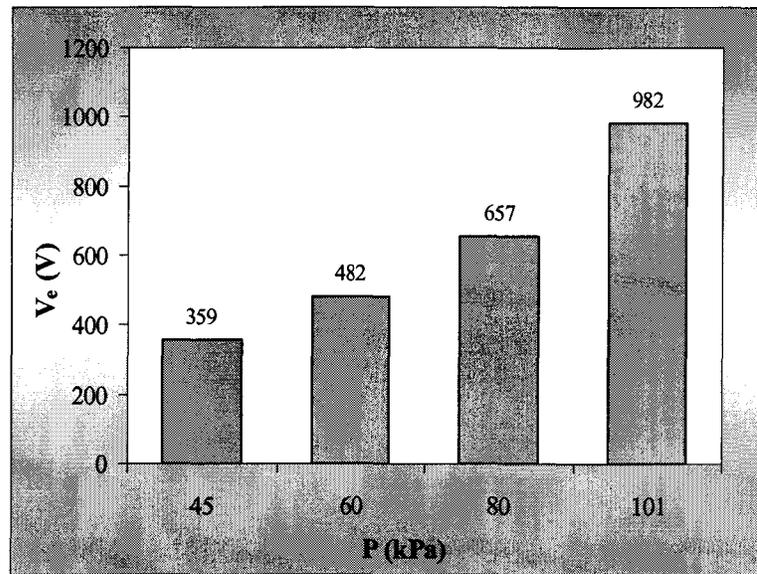
Fig. 6.8 Values of electrode voltage drop under AC conditions

6.3.2 Arc Constant *n*

Once the electrode voltage drop, V_e, was determined, the voltage gradient along the arc, E, was obtained:

$$E = (V_{total} - V_e)/x = AI^{-n}$$
(6.4)

Fig. 6.9 illustrates the E-I characteristics of an AC arc when the air pressure was maintained at 80 kPa. Regression analysis was applied to determine the arc constants A and n. In this case, n was 0.76.
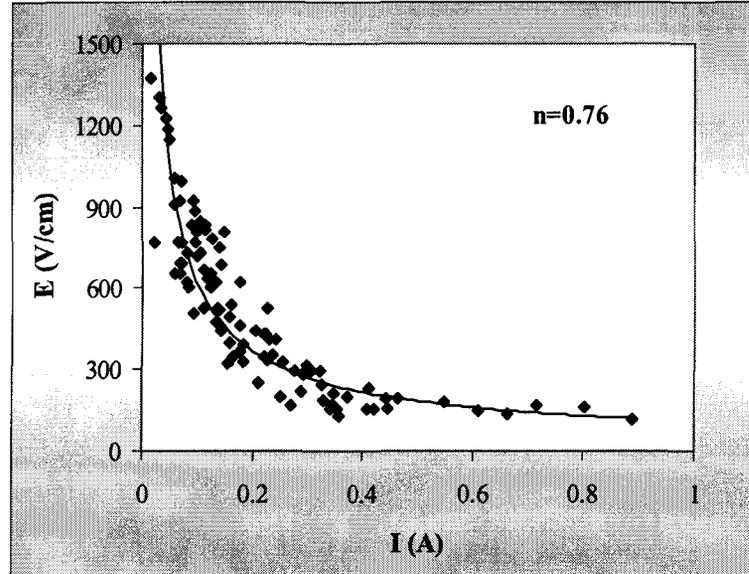
Fig. 6.9 E-I characteristics of AC arc (P = 80 kPa)

At different air pressures, the values for the arc constant n were determined, and they are listed in Table 6.1. The effect of air pressure on the constant n was not apparent. Therefore, the mean value for n, which is equal to 0.7 and the standard deviation is 7.94%, was used for all pressure conditions.

Table 6.1 Values for the constant n of an AC arc

Pressure (kPa)	n
101	0.65
80	0.76
60	0.74
45	0.66
Mean value	0.7

6.3.3 Arc constant A

Knowing the mean value for n permitted the determination of the other arc constant A. Regression analysis was applied to the above results to determine the arc constant A under different pressures. The values for A are displayed in Fig. 6.10.
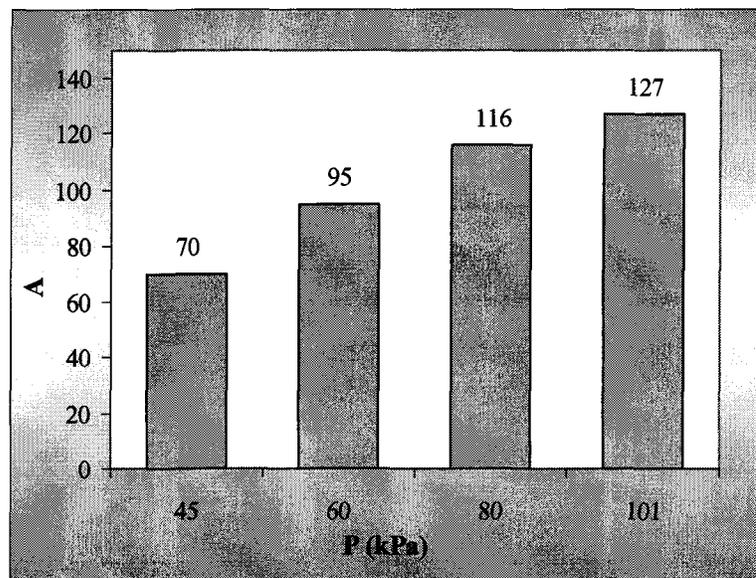
Fig. 6.10 Values for constant A of an AC arc

From the results, the value for A was substantially influenced by air pressure. The lower the air pressure, the smaller the value for A. The relationship between A and air pressure was nonlinear and can be approximately expressed as follows:

$$A = 133\left(\frac{P}{P_0}\right)^{0.74}, \qquad R=0.981 \qquad (6.5)$$

where P_0 and P are the air pressures at sea level and high altitude, respectively.

6.3.4 Arc E-I Characteristics

Using the values for A and n obtained above, the E-I characteristic curve of an AC arc at different air pressures was plotted as depicted in Fig. 6.11. E decreased with a decrease in air pressure because of the decrease in the arc constant A. The rate of decrease in E was more pronounced at lower air pressures.
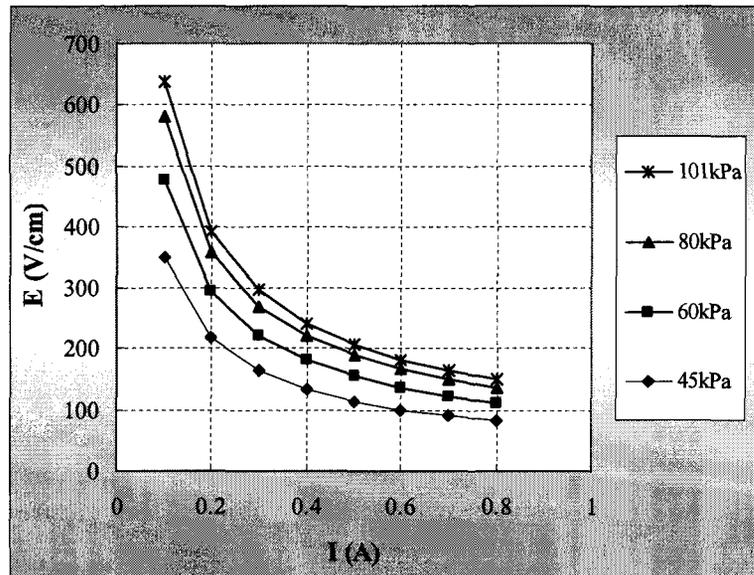
Fig. 6.11 E-I characteristics at different air pressures

From Equations 6.4 and 6.5, the E-I characteristics of an AC arc on an ice surface can be expressed by the following:

$$E = 133\left(\frac{P}{P_0}\right)^{0.74} I^{-0.7} \qquad (6.6)$$

Thus, combining the Equations 6.1, 6.2, 6.3 and 6.4, the total voltage drop along an AC arc can be approximately expressed as follows:

$$V_{total} = 931\left(\frac{P}{P_0}\right)^{1.22} + 133\left(\frac{P}{P_0}\right)^{0.74} x I^{-0.7} \qquad (6.7)$$

6.4 EFFECT OF AIR PRESSURE ON DC ARC CHARACTERISTICS

6.4.1 Electrode Voltage Drop

Under DC conditions, the local arc consistently started from the grounded top electrode and propagated towards the HV bottom electrode. For this reason, a negative arc refers to positive applied voltage (DC+) and a positive arc refers to negative applied voltage (DC-).

The total voltage along an arc, V_{total}, was determined under DC+ and DC-voltage conditions using the same method used for AC conditions. The results for V_{total} for positive and negative arcs are presented in Figs. 6.12 and 6.13, respectively.
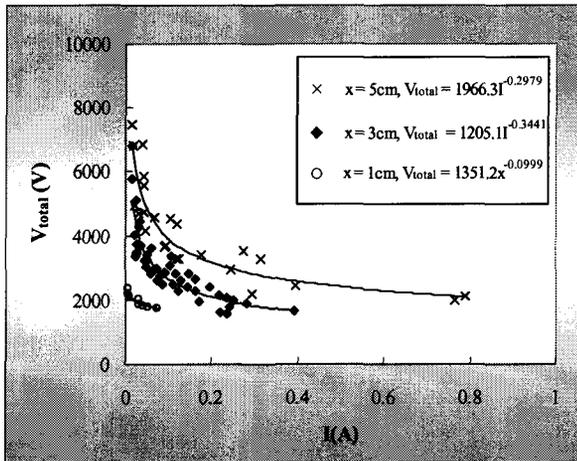
$x \leq 5$ cm $\qquad\qquad\qquad x \geq 7$ cm
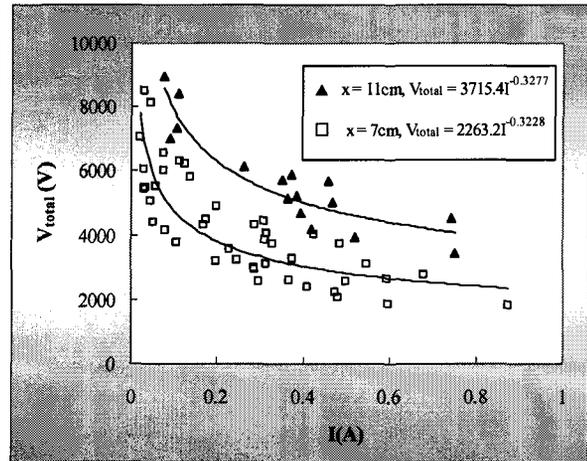
(a) at the standard pressure (101 kPa)
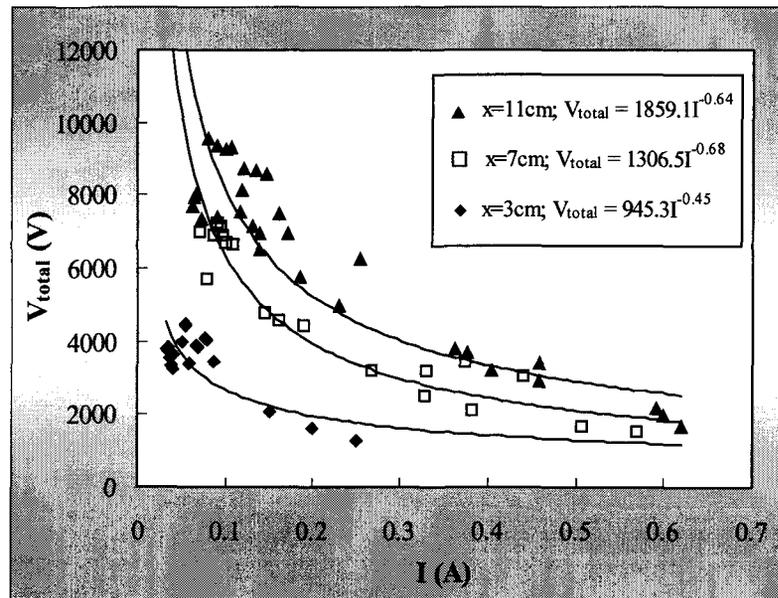
(b) at the pressure of 80 kPa
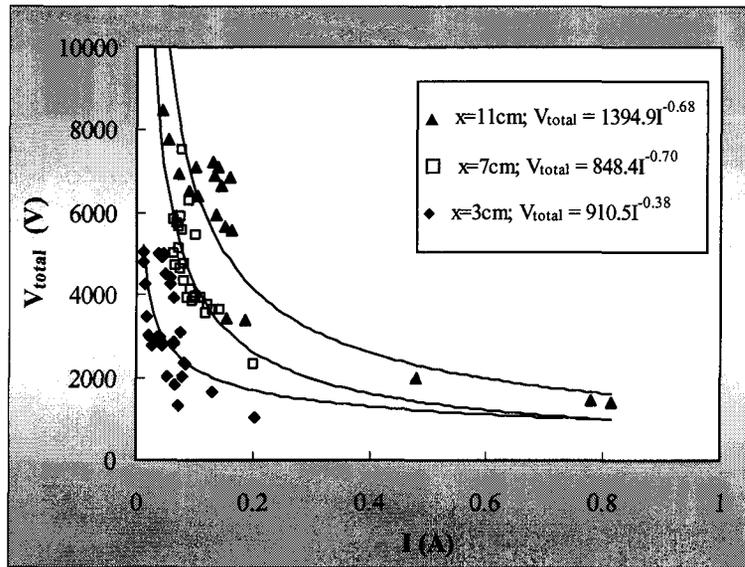
(c) at the pressure of 60 kPa
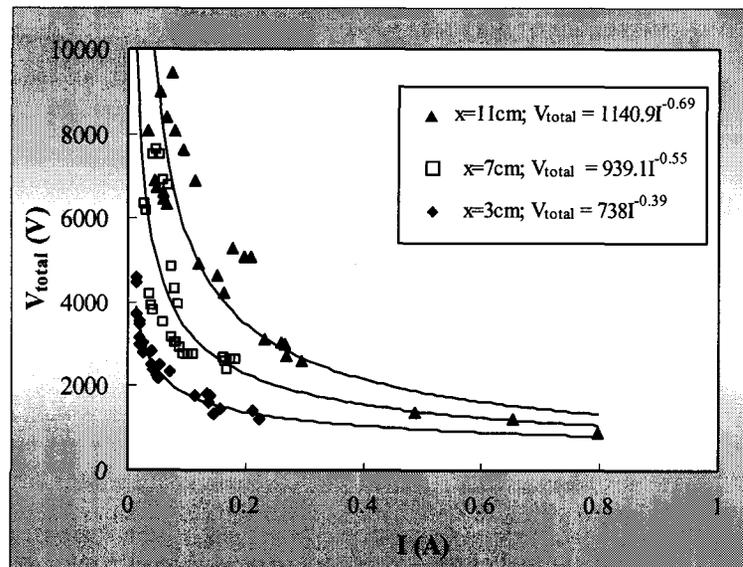
(d) at the pressure of 45 kPa

Fig. 6.12 V_{total} as a function of I at different air pressures for a positive arc
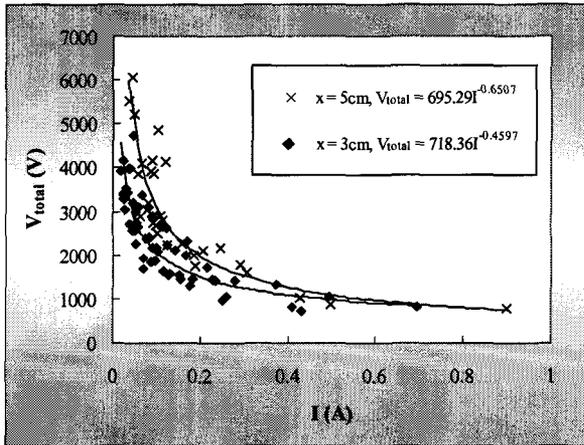
$x \leq 5$ cm $x \geq 7$ cm
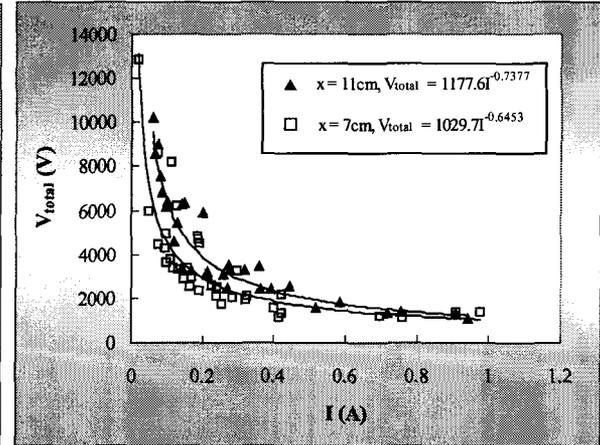
(a) at the standard pressure (101 kPa)
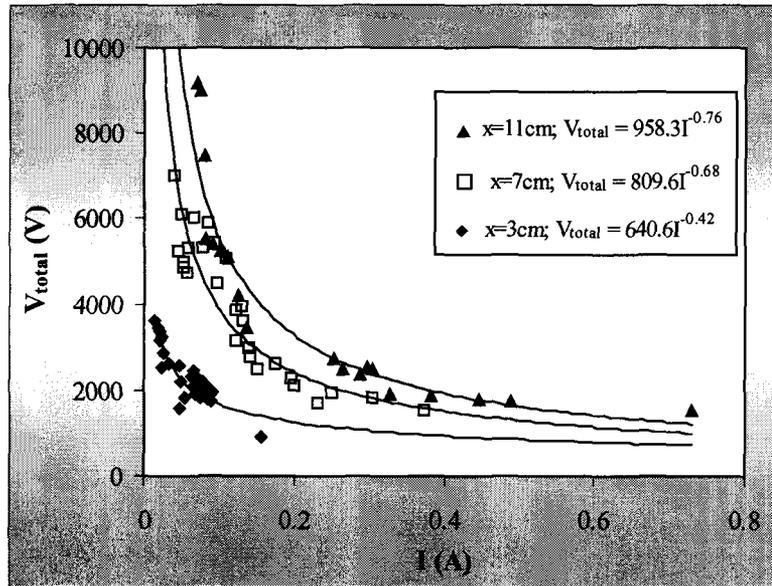
(b) at the pressure of 80 kPa
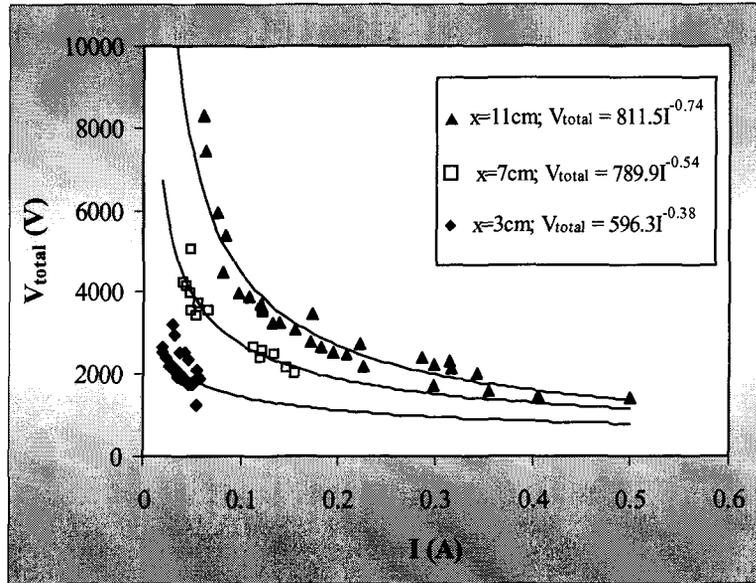
(c) at the pressure of 60 kPa
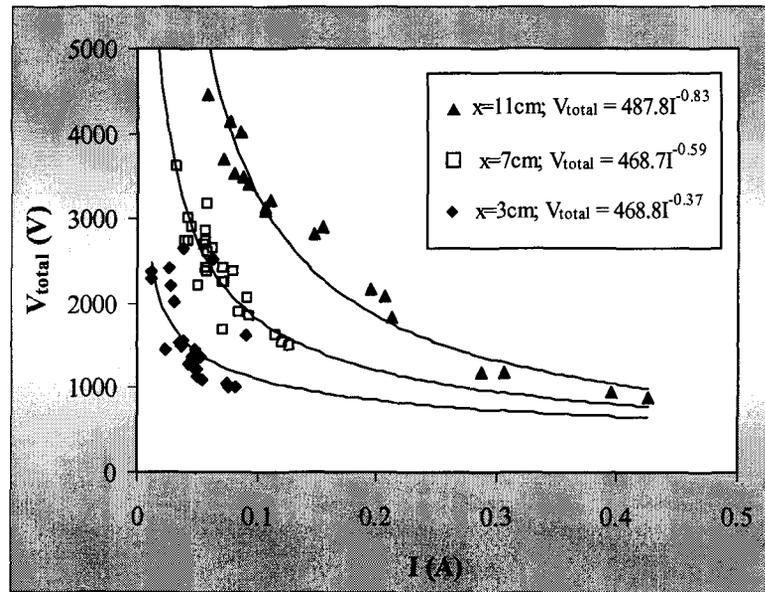
(d) at the pressure of 45 kPa

Fig. 6.13 V_{total} as a function of I at different air pressures for a negative arc

From the relations obtained from Figs. 6.12 and 6.13, the value for V_{total} for a given value of arc length, x, leakage current, I, and air pressure, P, was determined. The values calculated for V_{total} and the corresponding graphs are displayed in Fig. 6.14 for a positive arc and Fig. 6.15 for a negative arc.

From Figs. 6.14 and 6.15, the electrode voltage drop, V_e was determined. The values for V_e are shown in Fig. 6.16. For both positive and negative arcs, V_e decreased with a decrease in P. The relationship between V_e and P can be approximately expressed as follows:

$$V_e = 817\left(\frac{P}{P_0}\right)^{0.54}, \qquad R=0.991 \qquad \text{for a positive arc} \qquad (6.8)$$

$$V_e = 539\left(\frac{P}{P_0}\right)^{0.31}, \qquad R=0.929 \qquad \text{for a negative arc} \qquad (6.9)$$

where P_0 and P are the air pressures at sea level and high altitude, respectively.

6.4.2 Arc Constant n

Once the electrode voltage drop was determined, the voltage gradient along the arc, E, was obtained. Fig. 6.17 displays the results for both positive and negative arcs under an air pressure set to 80 kPa. Regression analysis was applied to the results to calculate the arc constant n. Under an air pressure of 80 kPa, n was determined to be 0.72 for a positive arc and 0.68 for a negative arc.
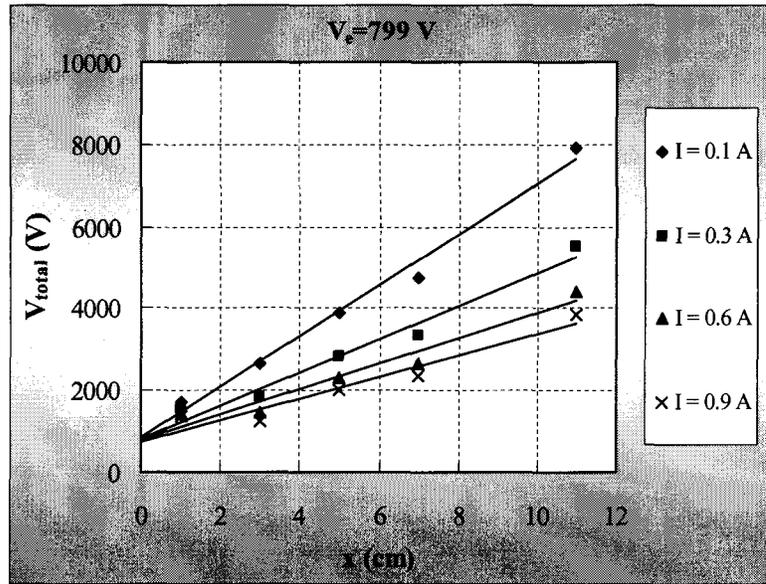
(a) at 101 kPa
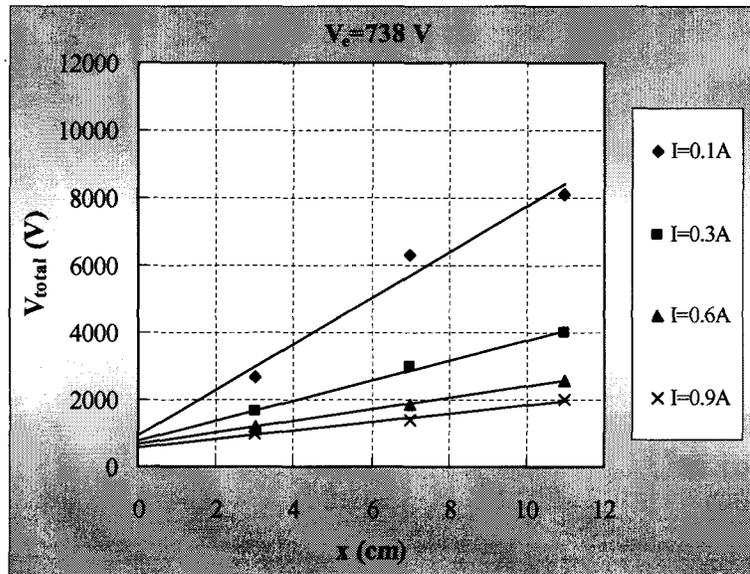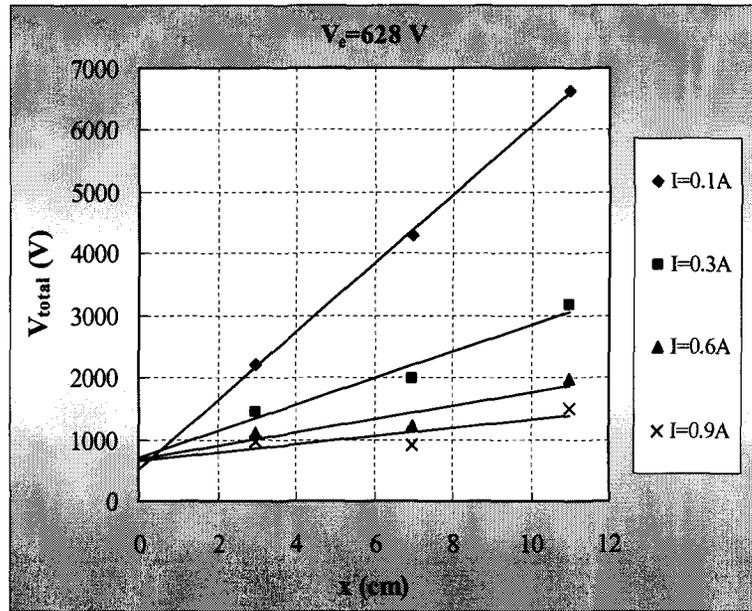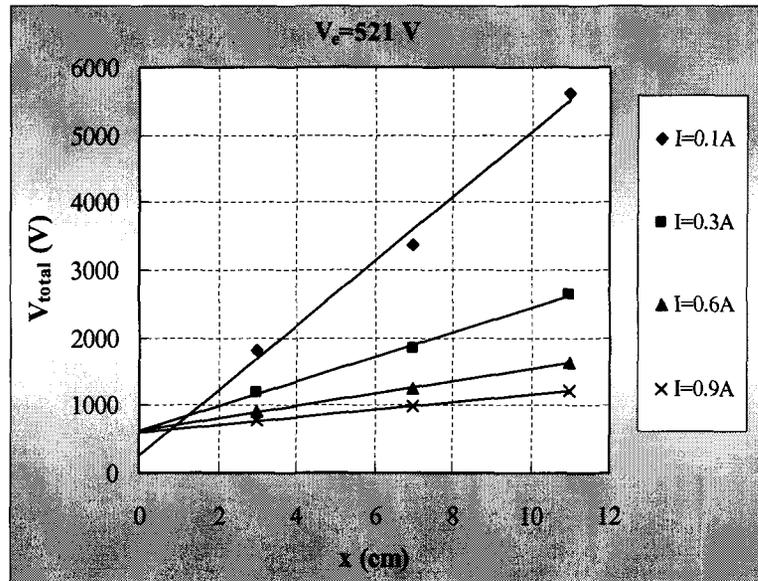
(b) at 80 kPa

(c) at 60 kPa

(d) at 45 kPa

Fig. 6.14 Relation between the total voltage drop along an arc and

arc length for a positive arc
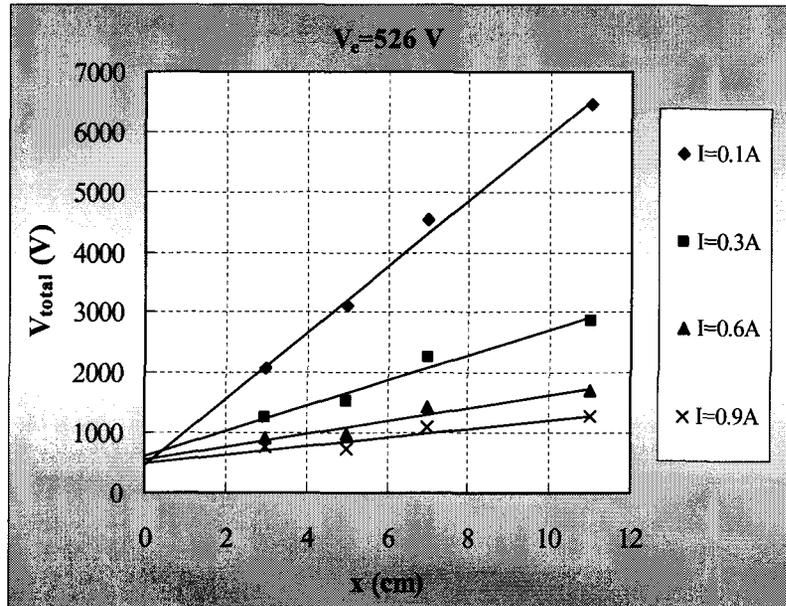
(a) at 101 kPa
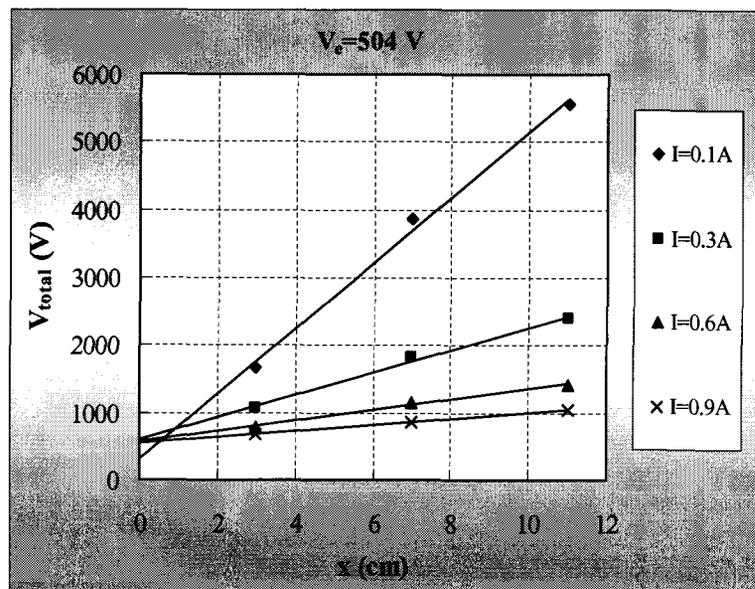
(b)   at 80 kPa
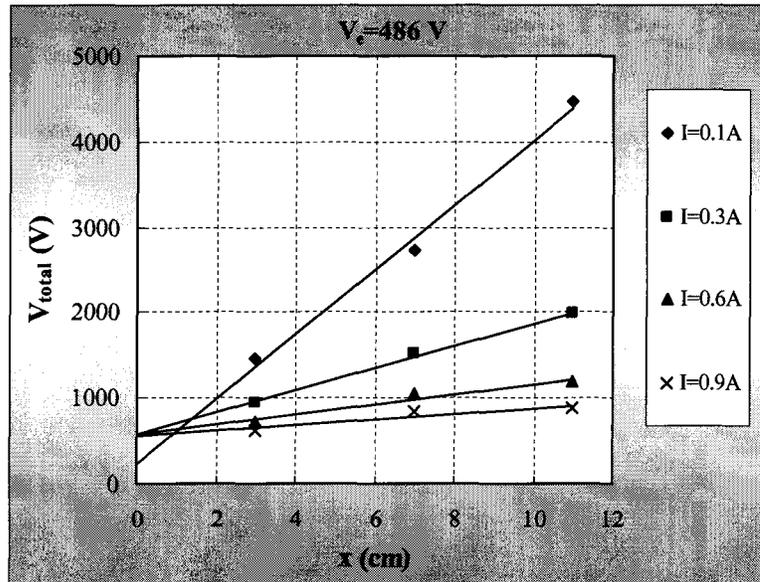
(c)   at 60 kPa
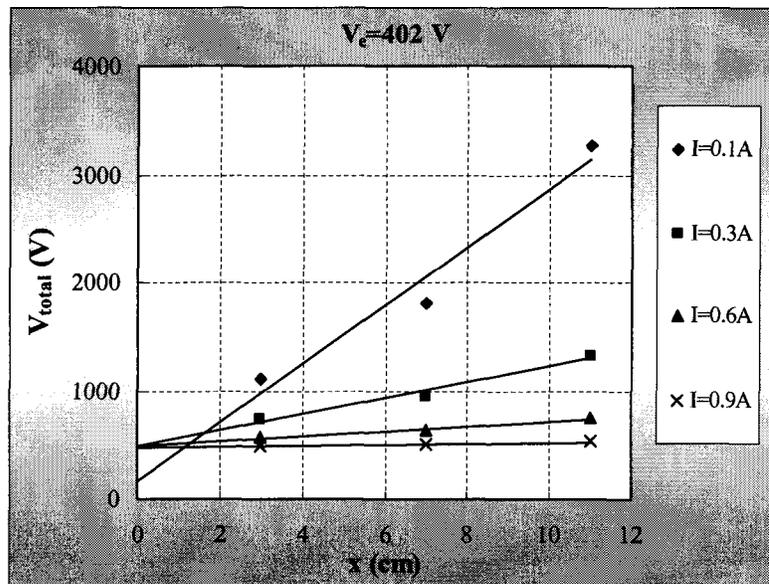
(d)   at 45 kPa

Fig. 6.15 Relation between the total voltage drop along an

arc and arc length for a negative arc
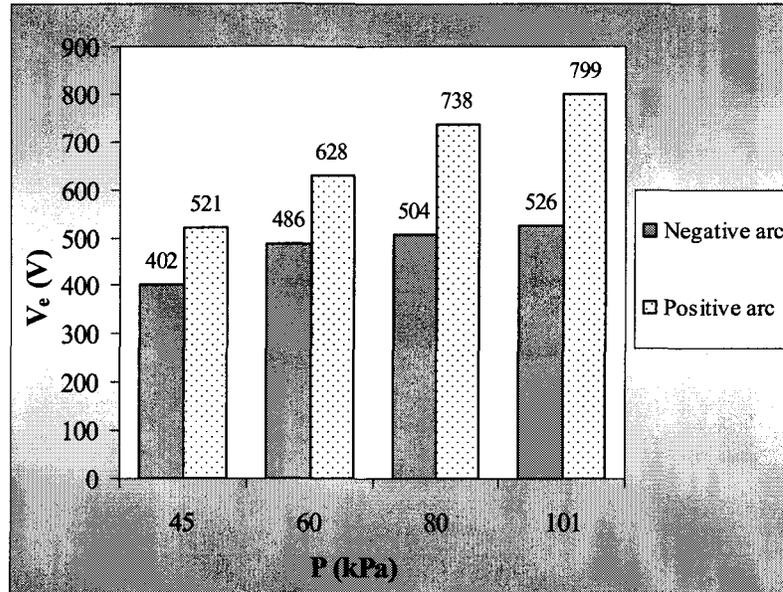
Fig. 6.16 Values for electrode voltage drop

Similar analysis method was applied to the results obtained under different air pressures and arc polarity in order to calculate the value for the arc constant n. The results of this analysis are presented in Table 6.2. The effect of air pressure on the constant n was not apparent. Therefore, the mean value for n, which was approximately 0.61 with a standard deviation of 18.8% for a positive arc and 0.69 with a standard deviation of 7.94% for a negative arc, was used for all pressure conditions.
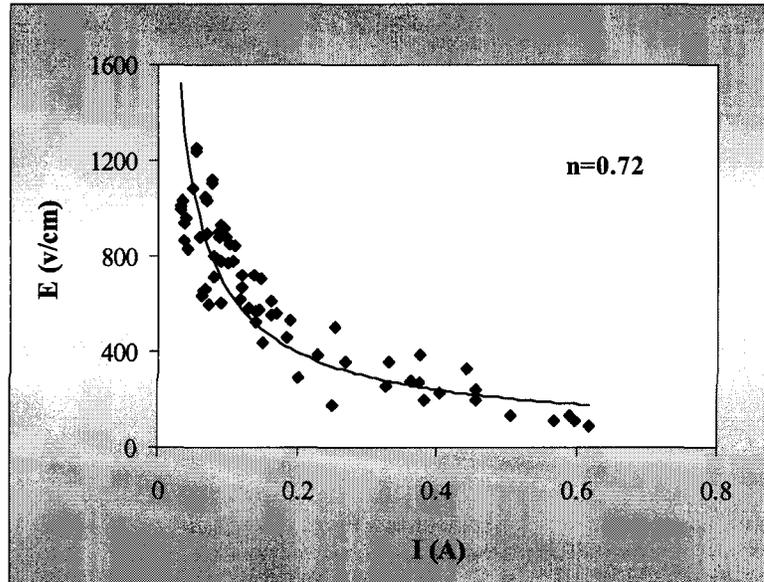
(a) Positive arc
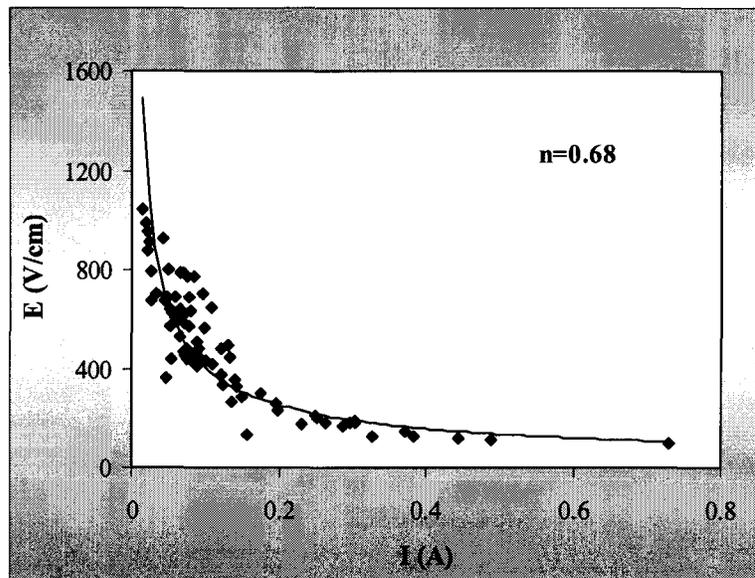
(b) Negative arc

Fig. 6.17 E as a function of I for DC arcs (P = 80 kPa)

Table 6.2 Values of the arc constant n

Pressure (kPa)	n	
	Positive arc	Negative arc
101	0.45	0.77
80	0.72	0.68
60	0.64	0.65
45	0.64	0.66
Mean value	**0.61**	**0.69**

6.4.3 Arc Constant A

Knowing the mean value for n permitted the calculation of the other arc constant A. Regression analysis was applied to the above results to determine the best-fit line allowing the calculation of the value for A. The value for A at different air pressures and arc polarities is presented in Fig. 6.18. It was noticeably influenced by air pressure. The lower the air pressure, the smaller the value for A. The relationship between A and air pressure was nonlinear and can be approximately expressed as follows:

$$A = 178\left(\frac{P}{P_0}\right)^{0.75}, \quad R=0.981 \quad \text{for a positive arc} \qquad (6.10)$$

$$A = 103\left(\frac{P}{P_0}\right)^{1.14}, \quad R=0.997 \quad \text{for a negative arc} \qquad (6.11)$$

where P_0 and P are the *air* pressures at sea level and high altitude, respectively.
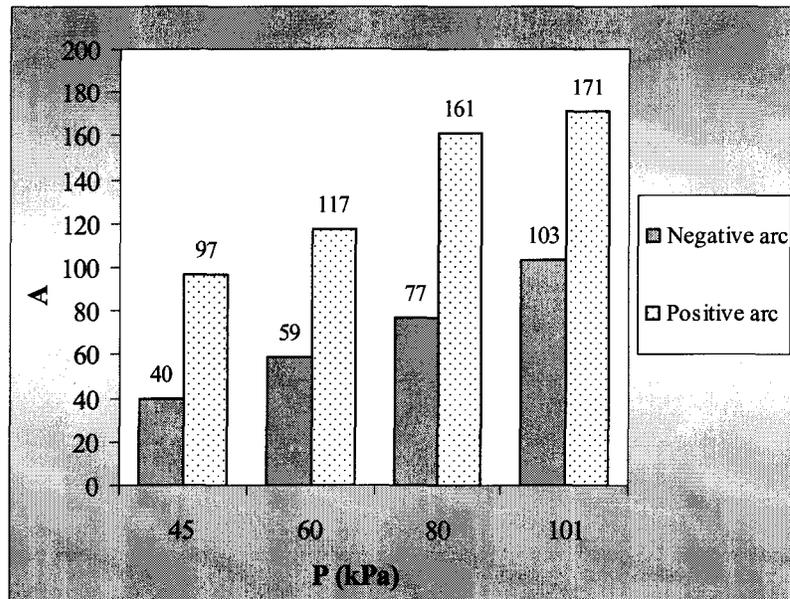
Fig. 6.18 Values for the constant *A*

6.4.4 Arc E-I Characteristics

Using the values for *A* and *n* obtained above, the E-I characteristic curves of arcs generated under DC voltage conditions, (DC arcs), at different pressures and voltage polarities were plotted as shown in Fig. 6.19.

For both positive and negative arcs, *E* decreased with a decrease in air pressure because of the decrease in the arc constant *A*. The rate of decrease in *E* was more pronounced under lower air pressures. This observation could explain why the flashover voltage of an ice-covered insulator was observed to decrease with an increase in altitude.
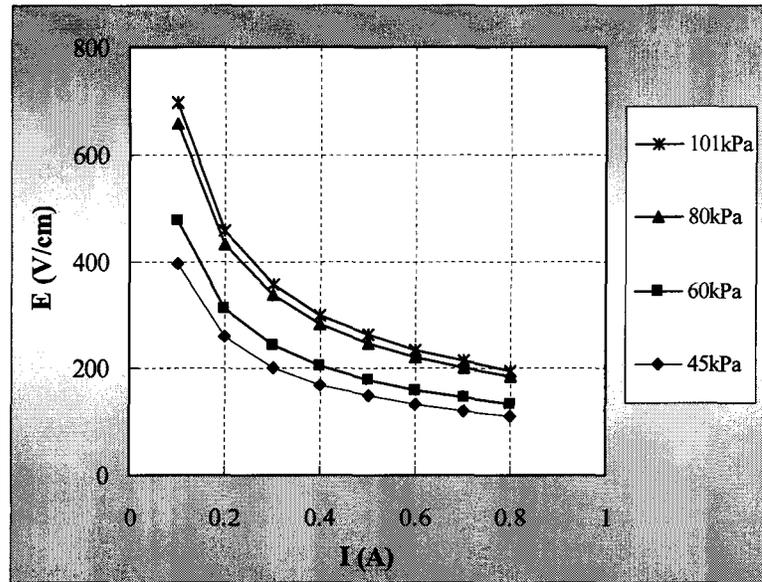
(a) Positive arc
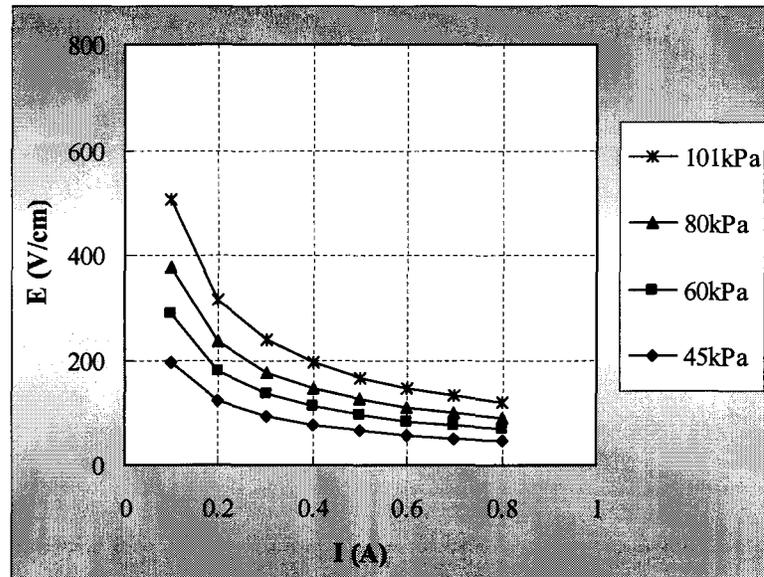
(b) Negative arc

Fig. 6.19 E-I characteristics of DC arcs at different air pressures

From Equations 6.4, 6.10 and 6.11, the E-I characteristics of DC arcs on an ice surface under low air pressure conditions can be expressed as follows:

$$E = 178\left(\frac{P}{P_0}\right)^{0.75} I^{-0.61} \quad \text{for a positive arc} \quad (6.12)$$

$$E = 103\left(\frac{P}{P_0}\right)^{1.14} I^{-0.69} \quad \text{for a negative arc} \quad (6.13)$$

Hence, combining the Equations 6.2, 6.3, 6.8, 6.9, 6.10 and 6.11, the total voltage drop along a DC arc can be approximately expressed as follows:

$$V_{total} = 817\left(\frac{P}{P_0}\right)^{0.54} + 178\left(\frac{P}{P_0}\right)^{0.75} xI^{-0.61} \quad \text{for positive arc} \quad (6.14)$$

$$V_{total} = 539\left(\frac{P}{P_0}\right)^{0.31} + 103\left(\frac{P}{P_0}\right)^{1.14} xI^{-0.69} \quad \text{for negative arc} \quad (6.15)$$

6.5. DISCUSSION

6.5.1 Effects of Applied Voltage Type and Polarity on the Electrode Voltage Drop, V_e

Fig. 6.20 shows the values for the electrode voltage drop, V_e, under different pressure conditions and voltage types. Under standard air pressure, V_e under AC conditions was higher than that observed under DC conditions. In contrast, under

an air pressure less than 60 kPa, V_e under AC conditions was lower than that observed under DC conditions.
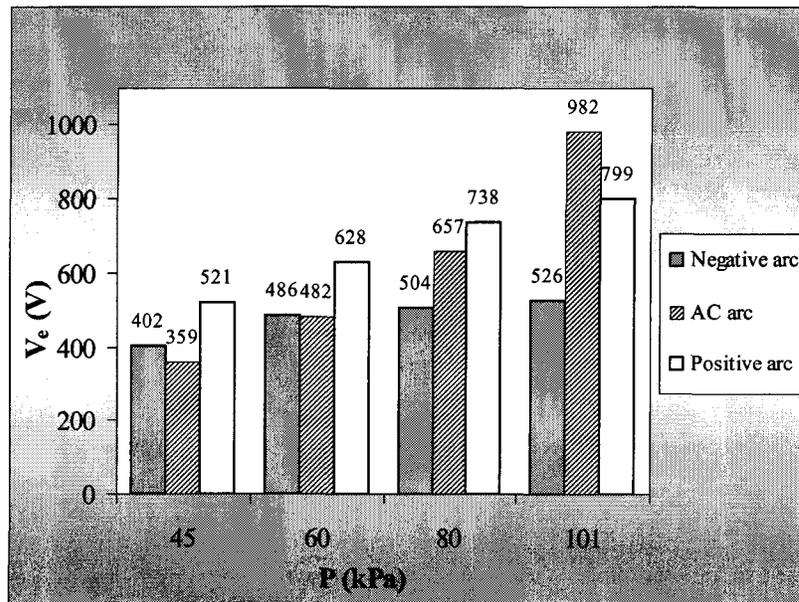
Fig. 6.20 Values for the electrode voltage drop under AC and DC conditions

Voltage polarity also had a marked effect on V_e. For a given pressure, V_e for a positive arc was consistently greater than that observed for a negative arc. A similar result was obtained in previous studies where other ice samples were examined under standard air pressure [10]. The magnitude difference in the value obtained for V_e between positive and negative arcs became less apparent when air pressure was decreased. Comparing the results obtained in this study with those obtained from studies of polluted surfaces, the value for V_e in ice conditions was lower than that observed in pollution conditions under standard air pressure [140].

6.5.2 Effects of Applied Voltage Type and Polarity on the Arc Constant *n*

Table 6.3 gives the mean values for the arc constant *n* under AC and DC conditions. The values for *n* obtained under pollution conditions [6] [55] [64] [73] [148] are also presented in Table 6.3 to allow for a comparison of results. Under ice conditions, the value for *n* for an AC arc was higher than that observed for either a positive or a negative arc. The value for *n* for a negative arc was higher than that observed for a positive arc.

Table 6.3 Mean value for the arc constant *n* for AC and DC

voltages under ice and pollution conditions

Mean value of *n* / Voltage Type	Ice	Pollution
AC Arc	0.7	0.67 [148], 0.7 [6]
Positive Arc	0.61	0.52 [55], 0.8 [64]
Negative Arc	0.69	0.52 [55], 0.75 [73], 0.8 [64]

From Table 6.3, the value for *n* for an AC arc was determined to be between 0.67-0.7 under pollution conditions. This value for *n* was just under the value determined under ice conditions in this study, where *n* was found to be 0.7. For a DC arc, the value for *n* under pollution conditions varied between researchers. However, in this study the value for *n* for a DC arc under ice conditions lay within

the values calculated for n under pollution conditions. These comparisons imply that ice could be treated as a type of pollution.

6.5.3 Effects of Applied Voltage Type and Polarity on the Arc Constant A

Fig. 6.21 shows the value for A under different voltage types and polarities. At a given pressure, the magnitude of A was highest for a positive arc and lowest for a negative arc. The magnitude of A for an AC arc fell between those measured for a positive arc and a negative arc.
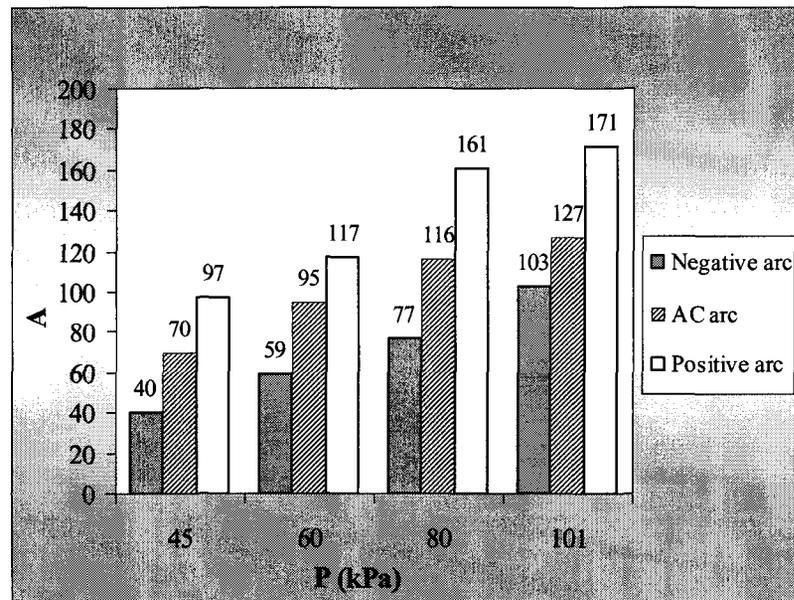
Fig. 6.21 Values of A for AC and DC arcs at different pressures

Comparing Fig. 6.21 with Table 3.10, the constant A for DC arcs varied in the same manner under both pollution and icing conditions: the constant A decreased with a decrease in air pressure.

In this study, the electrode voltage drop, V_e, was calculated separately from the constant A. This lead to a smaller value for A than that calculated in a previous study by CIGELE [34], where V_e was included in the determination of A. If V_e is included in the calculation of A, then the value for A under ice conditions will be higher than that obtained under pollution conditions as illustrated in Table 3.10.

For DC arcs, even calculating V_e separately from the arc constant A, the value for A under ice conditions is obviously higher than that obtained under pollution conditions. Comparing Fig. 6.21 with Table 3.9, the rate of decrease in A with pressure was higher under ice conditions than under pollution conditions. In summary, air pressure had a larger effect on the arc constant A under ice conditions than under pollution conditions.

6.5.4 Effects of Applied Voltage Type and Polarity on the Arc E-I Characteristics

The arc E-I characteristics under AC and DC voltages are plotted in Figs. 6.22(a), (b), (c) and (d) for the pressures 101, 80, 60 and 45 kPa, respectively.
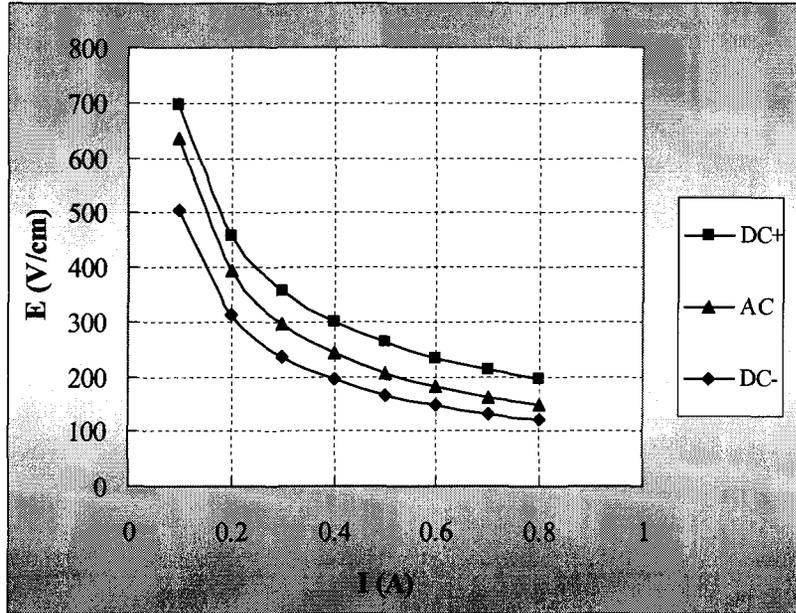
(a) at standard pressure (101 kPa)
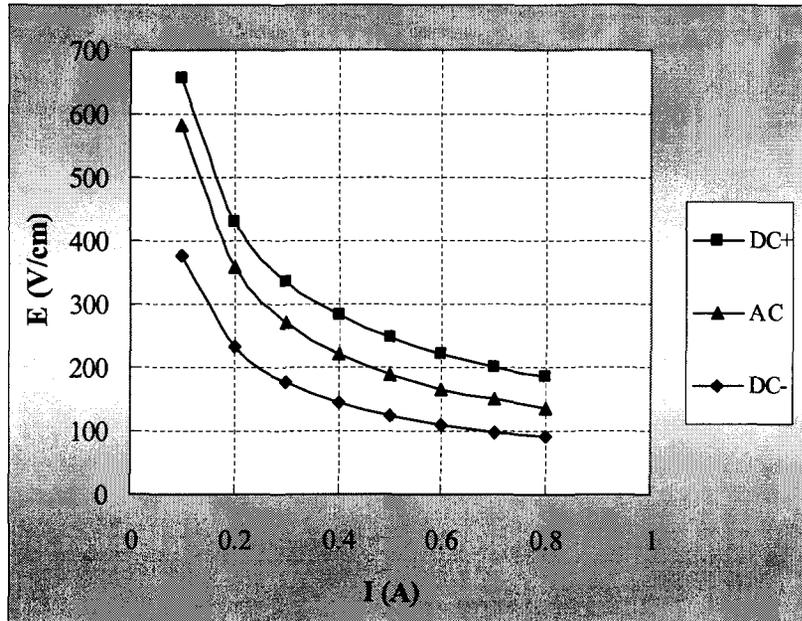
(b) at the pressure of 80 kPa
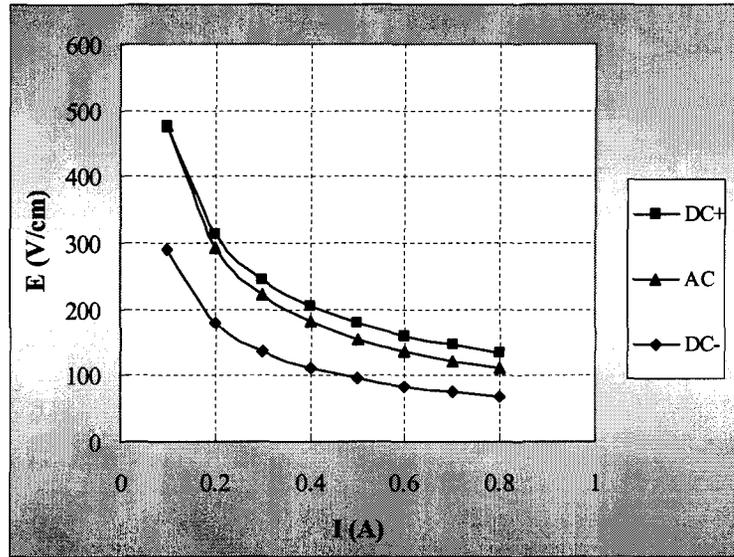
(c) at the pressure of 60 kPa

(d)
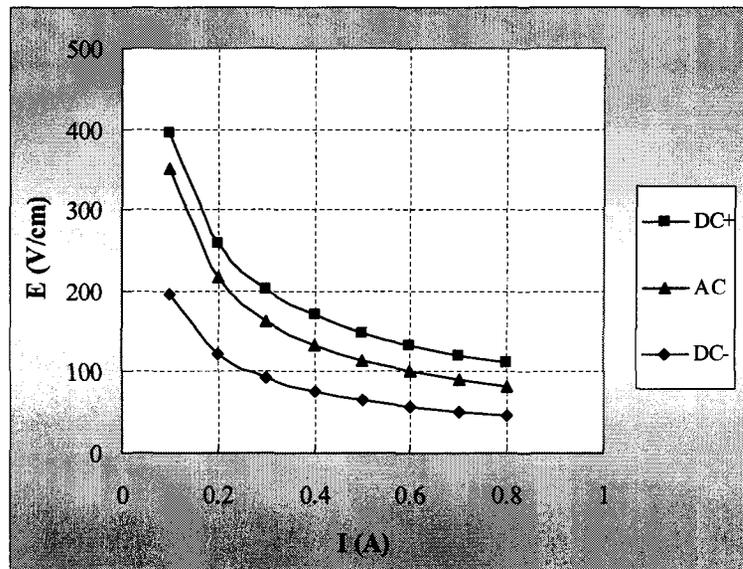
(e) at the pressure of 45 kPa

Fig. 6.22 Arc E-I characteristics under different voltage types and polarities

From Figs. 6.22(a-d), at a given air pressure, the E-I curve for a positive arc was consistently higher than that observed for a negative arc. The E-I curve for an AC arc fell between the E-I curves obtained for a positive arc and a negative arc. These results illustrate that voltage type and polarity have a noticeable effect on the E-I characteristics of an arc.

In order to compare our results with those obtained under pollution conditions [6] [64], the electrode voltage drop, V_e, was included in the calculation of the arc constant A. The E-I characteristics curves for AC and DC arcs under both the icing (our test results) and pollution conditions are plotted in Figs. 6.23 and 6.24.
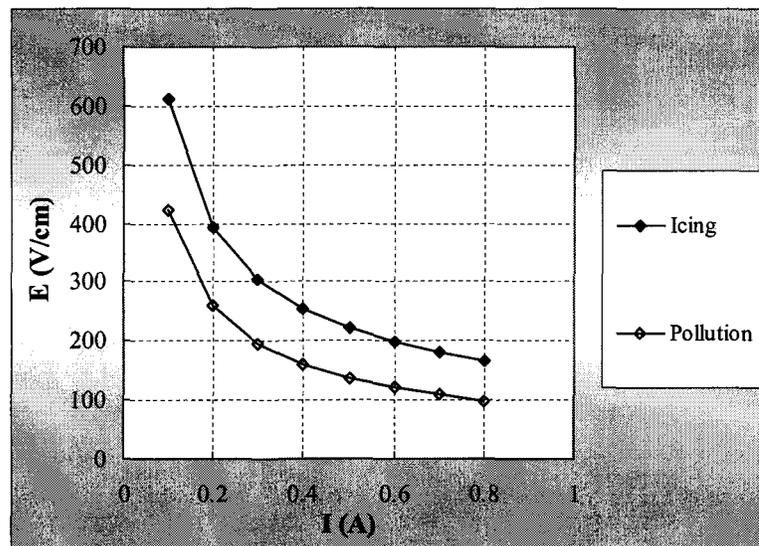
Fig. 6.23 E-I characteristics of AC arc at the pressure of 70 kPa

under icing and pollution conditions [6]
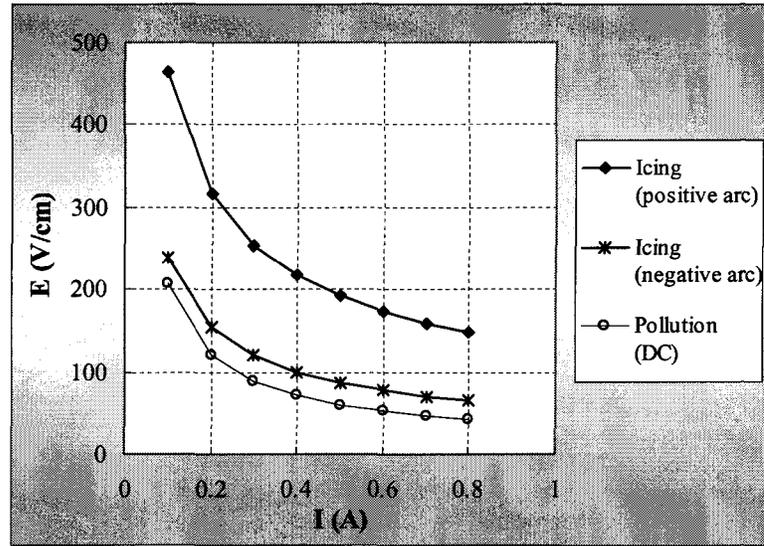
Fig. 6.24 E-I characteristics of DC arcs at the pressure of 40 kPa

under icing and pollution conditions [64]

From these figures, the E-I curves for both AC and DC arcs were higher under icing conditions than those obtained under pollution conditions. These results were primarily due to the higher value for the arc constant A under icing conditions than that calculated under pollution conditions. During the flashover process on an ice surface, the local arc will produce a considerable amount of water vapour, which will influence the arc characteristics. Some researchers have investigated the effect of water vapour on the E-I characteristics of an AC arc at standard air pressure [2] [20] [81] [114], which can be stated as follows [114]:

$$E = 63I^{-0.63} \qquad \text{in dry air} \qquad (6.10)$$

$$E = 530I^{-0.24} \qquad \text{in water vapour} \qquad (6.11)$$

Water vapour clearly had a substantial effect on the value for *A* when compared to the value for *A* calculated in dry air.

6.6 CONCLUSIONS

In this chapter, the voltage-current characteristics of both AC and DC arcs on an ice surface were investigated at low air pressure. The arc characteristic parameters, such as the electrode voltage drop, V_e, and the arc constants *A* and *n*, were determined. The principal conclusions are summarized as follows:

1). For both AC and DC arcs, V_e and the constant *A* were substantially influenced by air pressure. V_e and *A* decreased with a decrease in air pressure. The effect of air pressure on the constant *n* was not evident. Therefore, a mean value for *n* was used for all pressure levels. The mean values calculated for *n* were 0.7, 0.61 and 0.69 for an AC arc, a positive arc and a negative arc, respectively.

2). The E-I characteristics for both AC and DC arcs on an ice surface as a function of air pressure can be expressed as follows:

$$E = 133\left(\frac{P}{P_0}\right)^{0.74} I^{-0.7} \qquad \text{for an AC arc}$$

$$E = 178\left(\frac{P}{P_0}\right)^{0.75} I^{-0.61} \qquad \text{for a positive arc}$$

$$E = 103\left(\frac{P}{P_0}\right)^{1.14} I^{-0.69} \qquad \text{for a negative arc}$$

3). The constants V_e and A were found to be higher for a positive arc than those calculated for a negative arc. This observation suggests that a positive arc on a plane triangular ice sample will have a higher flashover voltage than a negative arc.

4). Due to the decrease in V_e and A at low air pressure, the voltage-current curves of a local arc on an ice surfaces lowered with a decrease in air pressure. This result explains why the flashover voltage of an ice-covered insulator decreased at low air pressure.

CHAPTER 7

BEHAVIOR OF AN ARC
ON AN ICE SURFACE
AT LOW AIR PRESSURE

CHAPTER 7

BEHAVIOR OF AN ARC ON AN ICE SURFACE AT LOW AIR PRESSURE

7.1 INTRODUCTION

The flashover on a polluted insulator at standard [19] [68] [140] or low air pressure [44] [55] [64] has been studied for many years. It is generally accepted that the process of pollution flashover at low air pressure would be similar to that observed under standard air pressure. There are some differences, however; the fundamental behavior of an arc on a polluted surface, which includes the arc radius and the arc propagation velocity, can be affected by air pressure [55] [64]. Under ice conditions, the flashover on an insulator and the fundamental characteristics of an arc have recently been studied under standard air pressure [12] [27] [34] [144]. To the best of our knowledge, there has yet to be a study of the behavior of an arc on an ice surface at low air pressure.

In this chapter, the behavior of both AC and DC arcs on an ice surface at low air pressure will be presented. The arc propagation velocity on an ice surface

at low air pressure will be measured and the effects of low air pressure on arc propagation will be investigated using a plane triangular ice sample. The root radius of DC and AC arcs will also be investigated at low air pressure. Finally, how the type and polarity of the applied voltage affect the behavior of an arc will be analyzed.

7.2 EXPERIMENTAL FACILITIES

The simultaneous appearance of more than one local arc on an ice surface made it difficult to exactly measure the arc parameters. Therefore, a plane triangular ice sample was used, which was introduced in Chapter 5.

The ice sample was placed vertically in an evacuated chamber located in a climate room. The temperature was maintained at +5 °C to ensure the slight melting of the ice surface and the generation of a water film. When a water film was formed on ice surface, the vacuum system was used to lower the air pressure in the chamber to a desired value. A high voltage was then applied to the bottom electrode and increased at a constant rate until 1 kV above the critical flashover voltage of an ice sample was attained. This voltage ensures to flashover occur. The test circuit is illustrated in Fig. 7.1.
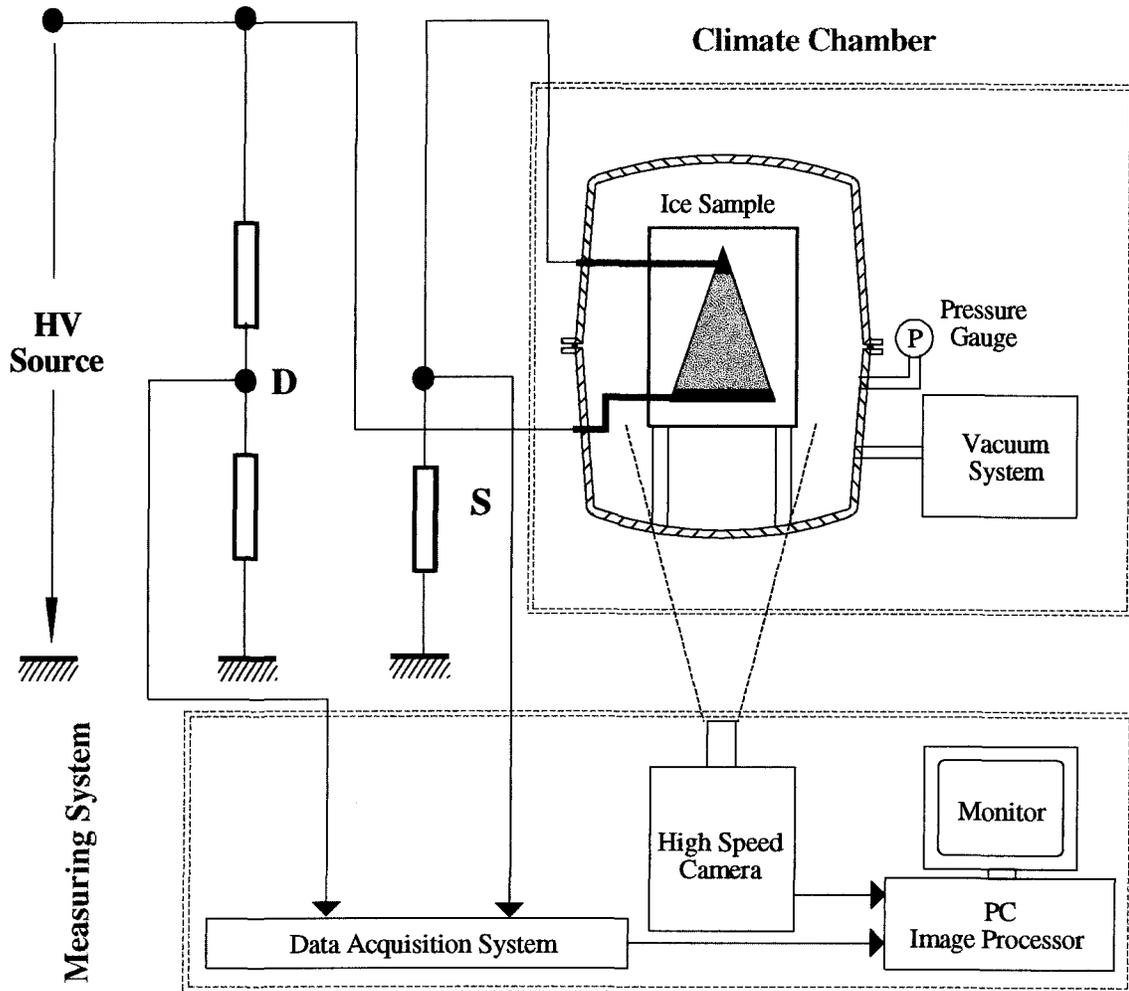
Fig. 7.1 Test Circuit

D — Voltage divider   S — Current Shunt

A high-speed photographic system was employed to record the progression of arc propagation during the flashover process. This photographic system included a high-speed camera and a data acquisition system (DAS). In this study, the recording rate of 1000 frames per second and a single frame exposure time of 1 ms were used. The applied voltage and the leakage current were recorded by the DAS and displayed simultaneously on a monitor along with an image of the arc propagation process.

From each photo recorded by the high-speed camera, the arc length, radius and time were examined. From this data, the arc propagation velocity was calculated and the arc root radius subsequently determined.

7.3 EFFECTS OF AIR PRESSURE ON AN ARC PROPAGATION ON AN ICE SURFACE

On an ice-covered insulator, arc propagation was a critical and necessary stage for a flashover. Therefore, the study of arc propagation is important and necessary to reveal the mechanisms underlying a flashover on an ice-covered insulator. A series of experiments investigating arc propagation were carried out under low pressure using both AC and DC voltage conditions.

7.3.1 Propagation of a Positive Arc

As presented in Fig. 7.1, when a negative high voltage was applied to the bottom electrode of an ice sample, due to the geometry of the ice sample and the position of the air gap, the arc consistently started from the top electrode or anode, and propagated towards the bottom electrode, or cathode. When the arc propagated from the anode towards the cathode, the arc was called a positive arc.

In describing the arc propagation process, the most important parameter was the change in arc length with time, or more precisely, the arc propagation velocity [45] [64] [83] [120]. Figure 7.2 depicts a series of images of an arc at different moments during the propagation of a positive arc on the ice surface at a low pressure of 45 kPa. For this experiment, the applied voltage was set to -20 kV and the freezing water conductivity was set to 80 μS/cm. These images permitted the determination of the arc length at a specific time, t, and, consequently, the arc propagation velocity.

t = 0 s　　　　　t = 0.328 s　　　　　t = 0.821 s　　　　　t = 1.529 s

t = 2.8 s　　　　　t = 2.811 s　　　　　t = 2.812 s　　　　　t = 2.813 s
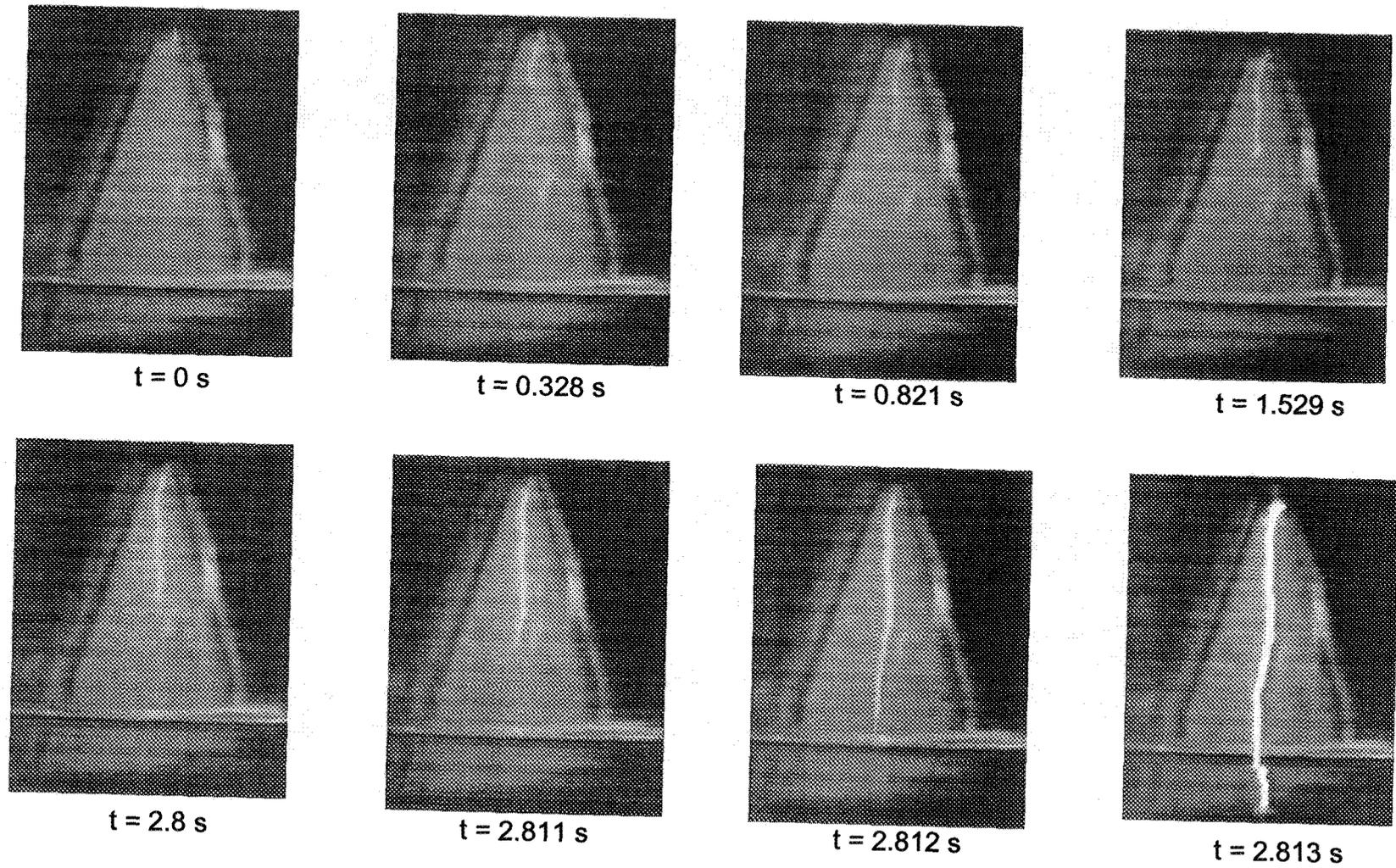
Fig. 7.2 Positive arc propagation process on an ice surface (P = 45 kPa)

When t was equal to 0 s, a violet arc was established with an initial length of approximately 1 cm, which corresponded to the air gap length. When t was equal to 0.328 s, 0.821 s and 1.592 s, the arc extended to a length of approximately 5 cm, 7.5 cm and 9 cm, respectively. When t was equal to 2.8 s, the arc reached a length of approximately 12 cm. After this point, the arc developed more quickly. When t was equal to 2.811 s, the arc was approximately 14 cm long and when t was equal to 2.812 s, it was approximately 21 cm long. When the arc reached the bottom electrode, the flashover was completed and t was equal to 2.813 s.

The change in the length of a positive arc with time is plotted in Fig. 7.3. The arc length, L_{arc}, was expressed as a percentage of the maximum length of the arc, L, which was equal to the height of the ice sample (280 mm).
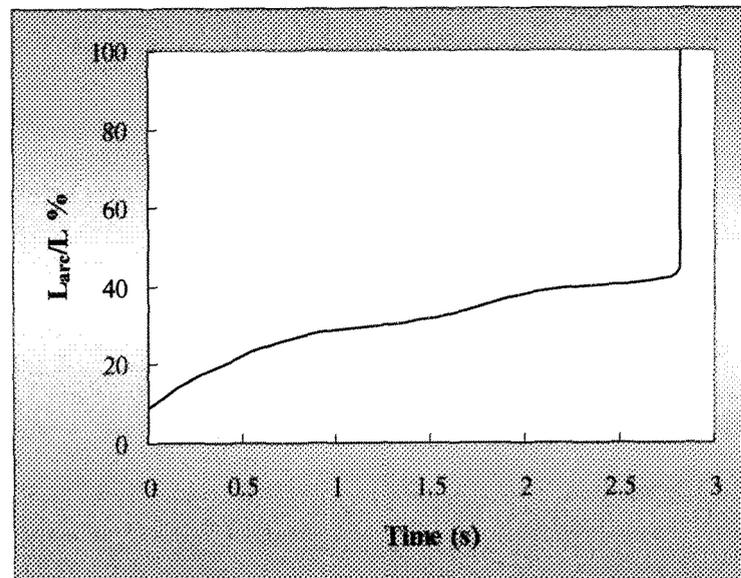
Fig. 7.3 Change in the length of a positive arc on an ice surface as

a function of time at low air pressure of 45 kPa

Fig. 7.4 depicts the change in the length of a positive arc with time at different air pressures. At various levels of air pressure, the propagation of a positive arc on an ice surface was divided into two stages. The first stage began at the moment when a violet arc was established, ($t = 0$), with an initial length of 5% of L, which corresponded to the length of the air gap. The first stage ended when the arc length reached approximately 45% of L. Arc propagation was relatively slow during this initial stage. For example, the average arc velocity during the first stage was calculated to be approximately 0.034 m/s in Fig. 7.3. The second stage corresponded to an arc length between 45% and 100% of L. In this stage, the arc propagation velocity dramatically increased. Maximum velocity was obtained just before the flashover occurred. For example, during the second stage, the average arc propagation velocity was approximately 12 m/s and the maximum velocity attained was approximately 70 m/s in Fig. 7.3.

The average propagation velocity of a positive arc at different air pressures was determined and is listed in Table 7.1. During the first stage, air pressure did not have any notable effect on the arc propagation velocity when the air pressure was higher than 60 kPa. The average propagation velocity ranged from 0.04 to 0.25 m/s during the initial stage. When the air pressure was set to 45 kPa, a lower arc propagation velocity was measured, which implied that a relatively low air pressure was able to decrease the arc propagation velocity during the first stage. During the second stage, the air pressure did affect the arc propagation velocity:

the lower the air pressure, the lower the arc propagation velocity. The maximum velocity attained by a propagating arc was also influenced by air pressure. The maximum velocity decreased with a decrease in air pressure.
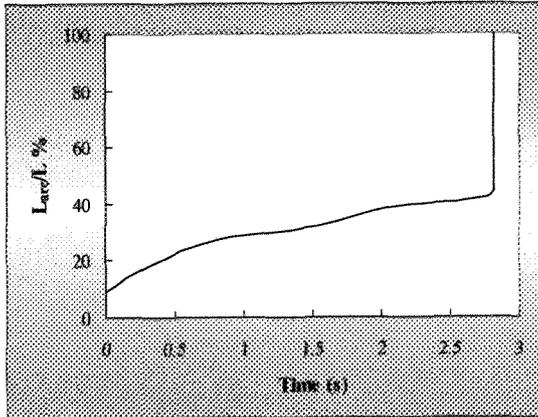
(a) P = 45 kPa
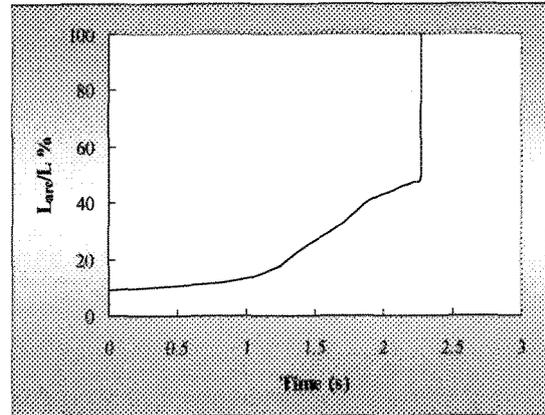
(b) P = 60 kPa
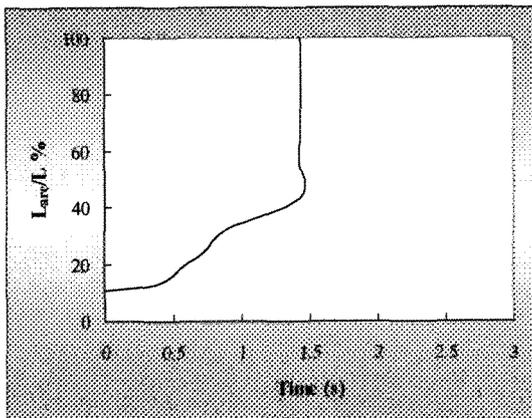
(c) P = 80 kPa
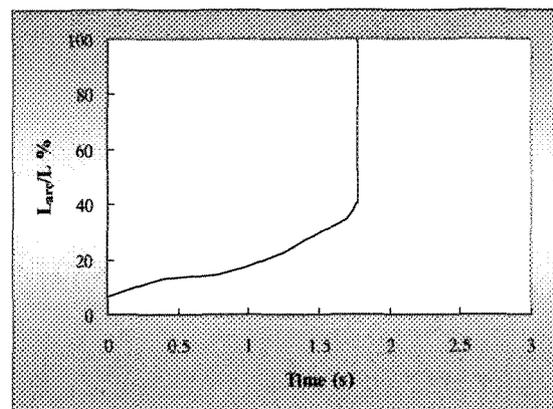
(d) P = 101 kPa

Fig. 7.4 Change of the length of a positive arc on an ice surface as

a function of time at different air pressures

Table 7.1 Effect of air pressure on the propagation velocity of a positive arc

Air Pressure (kPa)	Velocity of Arc (m/s)		
	First Stage	Second Stage	Maximum
101	0.05 – 0.25 [144]	20 – 50 [144]	100 [144]
80	0.04 – 0.15	5.6 – 40	91
60	0.05 – 0.12	4.5 – 22	83
45	0.03 – 0.06	4 – 14	70

7.3.2 Propagation of a Negative Arcs

A negative arc corresponded to DC+ applied voltage as described in Fig. 7.1. Figure 7.5 illustrates a typical negative arc propagation process on an ice surface at a pressure of 60 kPa. For this experiment, the applied voltage was set to +22kV and the freezing water conductivity was set to 80 µS/cm.

When t was equal to 0 s, a violet arc was established with an initial length of approximately 1 cm, which corresponded to the length of the air gap. The arc propagated slowly: when t was equal to 0.6 s, the arc length was approximately 5 cm. At this moment, the arc became slightly brighter. When t was equal to 0.75 s, 0.86s and 0.905 s, the arc length was approximately 7 cm, 9cm and 12 cm, respectively. After this point, the arc developed more quickly. When t was equal to 0.933 s, the arc reached the bottom electrode and a flashover occurred.
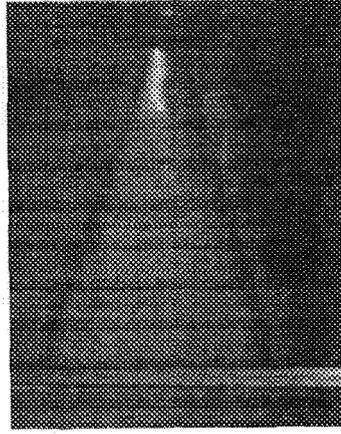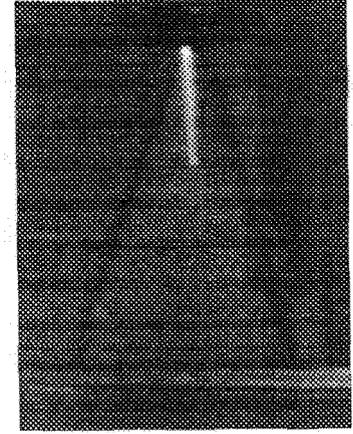
t = 0 s　　　　　　t = 0.597 s　　　　　　t = 0.754 s　　　　　　t = 0.861 s
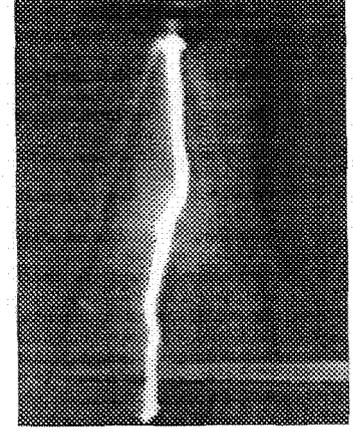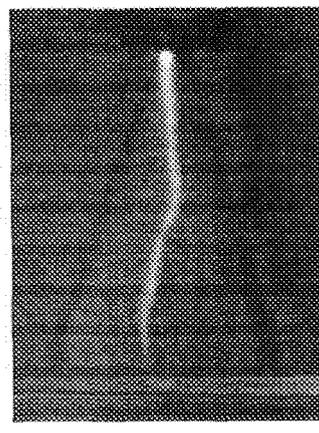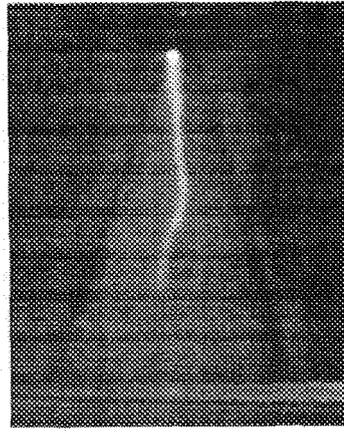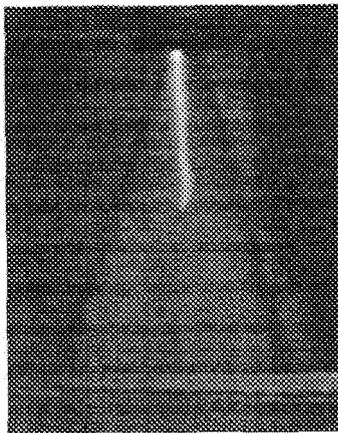
Fig. 7.5 Negative arc propagation process on an ice surface (P = 60 kPa)

The results from this experiment, where the length of a negative arc varied with time, are displayed in Fig. 7.6. The arc length, L_{arc}, was expressed as a percentage of the maximum length of an arc, L, which was equal to the height of the ice sample (280 mm).
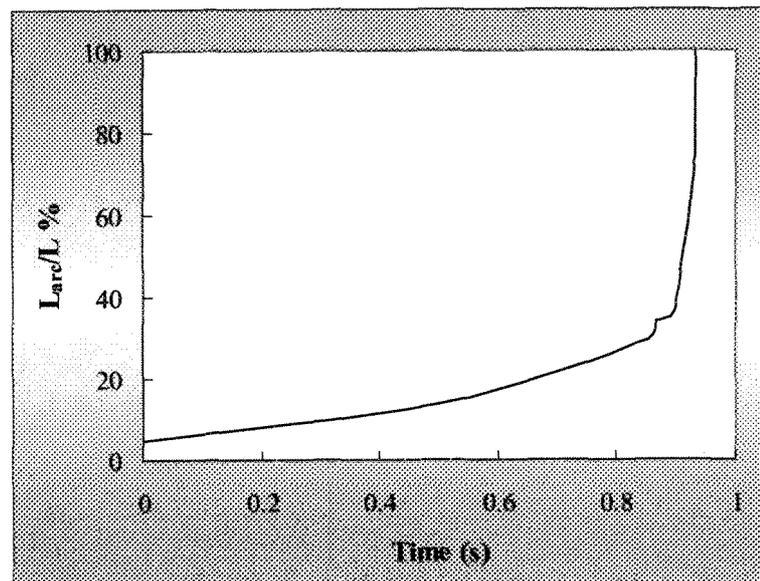
Fig. 7.6 Change in the length of a negative arc on an ice surface

as a function of time at low air pressure of 60 kPa

The negative arc propagation process was recorded and analyzed under different air pressures. The change in arc length as a function of time under different air pressures is shown in Fig. 7.7. The propagation of negative arc on an ice surface was also divided into two stages. The first stage began the moment a

violet arc was established with an initial length of 5% of L, which corresponded to the length of the air gap. The first stage ended when the arc length reached approximately 40% of L. The arc propagation velocity developed relatively slowly in this initial stage: for example, the average arc propagation velocity was approximately 0.09 m/s in Fig. 7.6. During the second stage, the arc propagation velocity dramatically increased until a flashover occurred. Maximum velocity was attained immediately before flashover occurred. For example, the average arc propagation velocity was approximately 5 m/s and the maximum velocity attained was approximately 51 m/s in Fig. 7.6.

The propagation velocity of a negative arc at different air pressures was determined and presented in Table 7.2.

Table 7.2 Propagation velocity of a negative arc at different air pressures

Air Pressure (kPa)	Velocity of Arc (m/s)		
	First Stage	Second Stage	Maximum
101	0.05 – 0.3 [144]	35 – 60 [144]	100 [144]
80	0.05 – 0.25	5 – 37	67
60	0.05 – 0.3	4 – 21	51
45	0.05 – 0.15	4 – 12	38
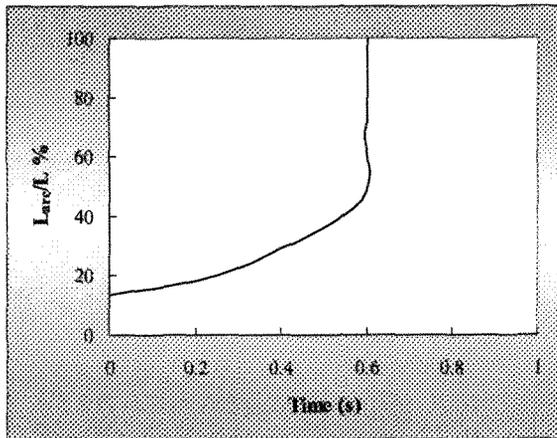
(a) P = 45 kPa
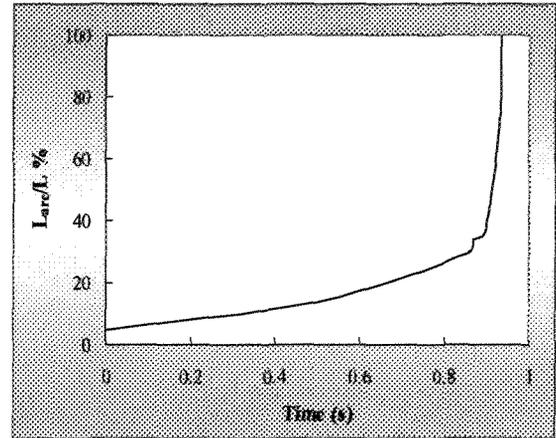
(b) P = 60 kPa
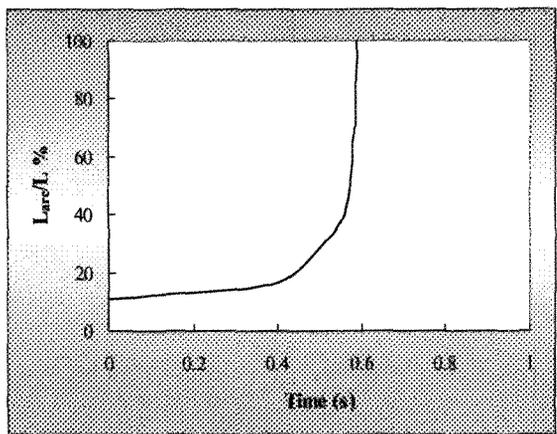
(c) P = 80 kPa
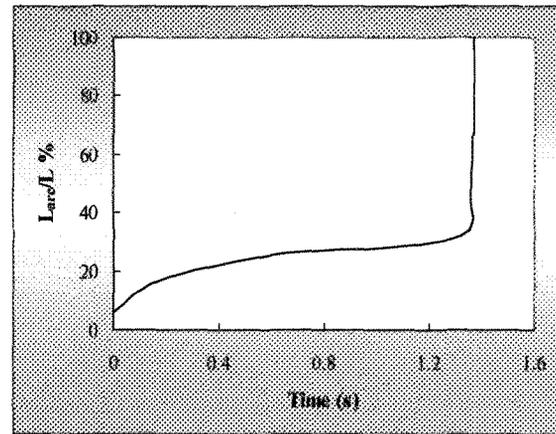
(d) P = 101 kPa

Fig. 7.7 Change in the length of a negative arc on an ice surface

as a function of time at different air pressures

As observed with a positive arc, the propagation velocity during the first

stage of a negative arc at air pressures between 101 and 60 kPa was consistently

between 0.05 and 0.3 m/s and, therefore, was not notably influenced by air pressure. However, when the air pressure was set to 45 kPa, the propagation velocity had a lower value than that measured under pressures set above 60 kPa.

During the second stage, the arc propagation velocity was influenced by air pressure. As the air pressure was decreased, the arc propagation velocity decreased. The air pressure also had an affect on the maximum propagation velocity of a negative arc. The lower the air pressure, the smaller the maximum propagation velocity of a negative arc on an ice surface.

7.3.3 Propagation of an AC Arcs

The propagation process of an AC arc on an ice surface was investigated at different air pressures using the same methodology employed for a DC arc.

Under AC conditions, the local arc extinguished and reignited according to the cycle of the applied voltage. Fig. 7.8 illustrates the aspect of an arc at different moments within a half cycle of the applied voltage. Fig. 7.9 presents the change in the arc length, L_{arc}, during 2 cycles of the applied voltage. Figs. 7.8 and 7.9 show that the change in L_{arc} during a half cycle of the applied voltage was divided into three steps. Initially the arc reignited and its length increased as the voltage was increased. Then, L_{arc} tended to maintain a specific length with practically no

change for a period of time. During this period, the arc diameter initially increased then decreased as the applied voltage passed through its peak value. Finally, the arc length decreased to zero as the applied voltage passed through zero. The change in the arc length was not synchronous with the applied voltage, as the reignition of the arc did not coincide with the zero point of the applied voltage. Likewise, the maximum length of the arc, L_M, was not reached at the same time as the peak value of the applied voltage. There was a time delay of approximately 1 to 2 ms between reaching L_M and the applied voltage peak value. The time delay was due to the thermal inertia of the arc. Although L_{arc} varied throughout a half cycle of the applied voltage, L_{arc} consistently reached the maximum value L_M.

Fig. 7.9 shows that L_M varied according to the cycle of the applied voltage. If the applied voltage was high enough, L_M increased and eventually resulted in a flashover. Therefore, the value for L_M during a half cycle was a reference parameter that characterized the propagation of an AC arc during a flashover on an ice sample. In this study, the propagation velocity of an AC arc was defined as the rate of increase of L_M.

Fig. 7.10 depicts the recorded propagation process of an AC arc on an ice surface at a pressure of 60 kPa. Each picture portrays the moment when the arc length reached its maximum value within each half cycle. The applied voltage was 20 kV$_{rms}$ and the freezing water conductivity was set to 80 µS/cm.
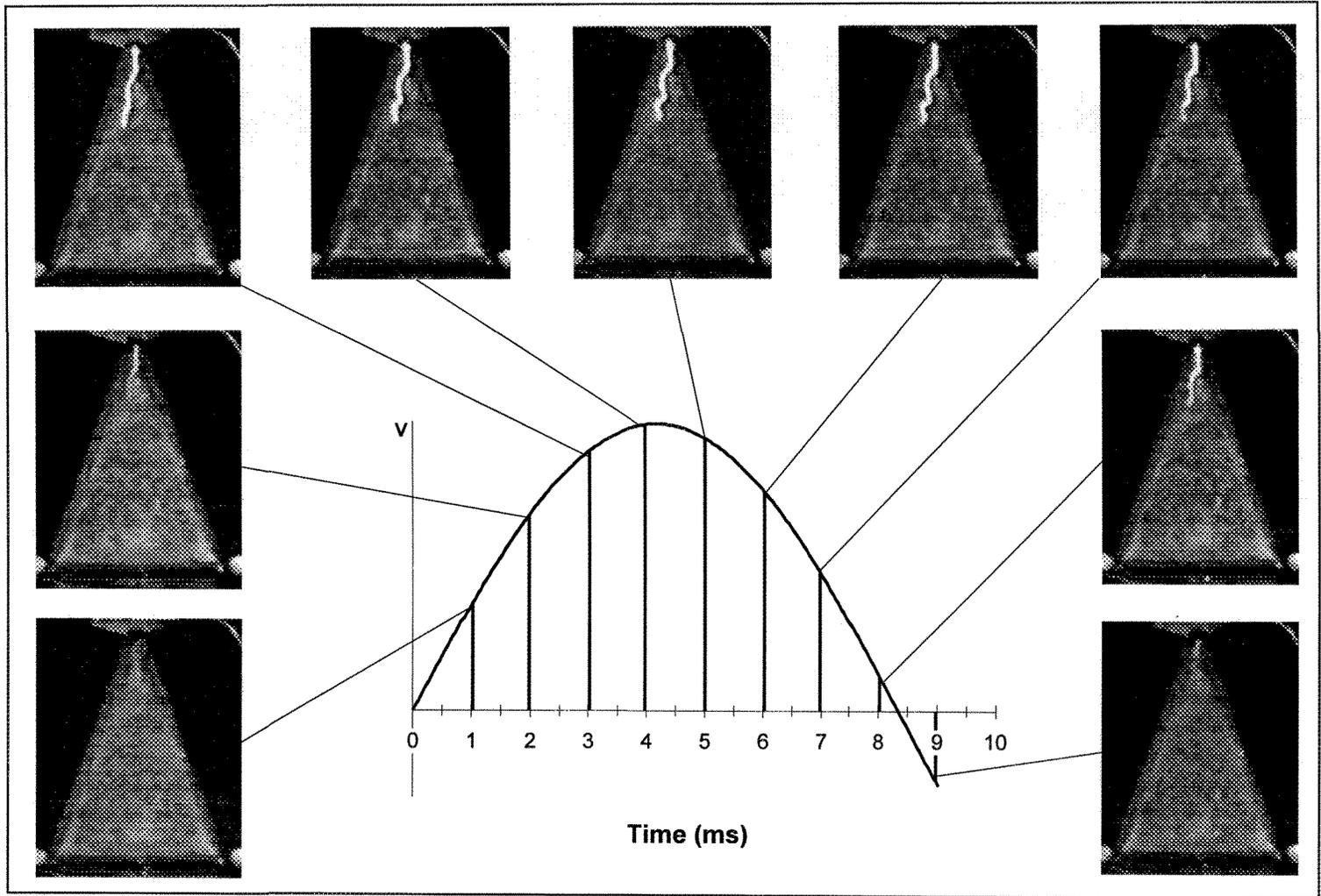
Fig. 7.8 Arc aspect at different moments duing a half cycle of applied voltage
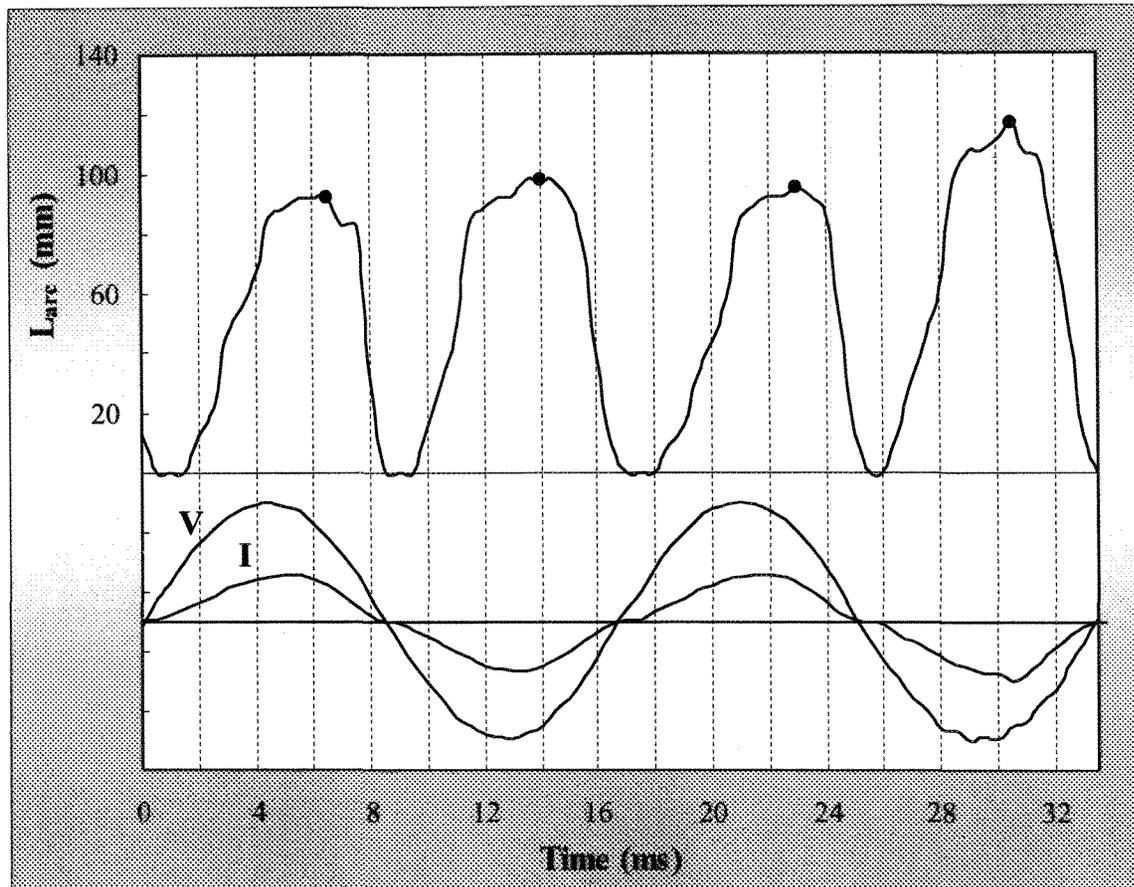
Fig. 7.9 Change in the arc length during 2 cycles of applied voltage
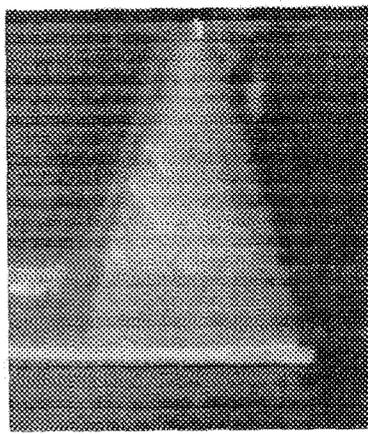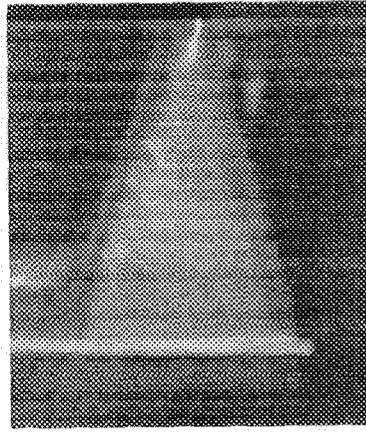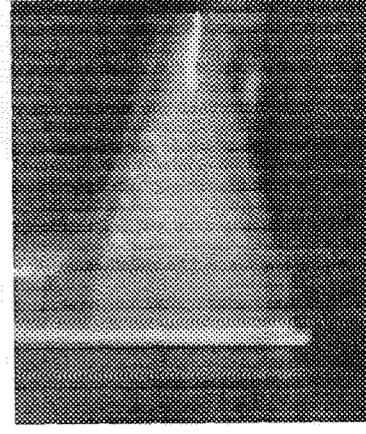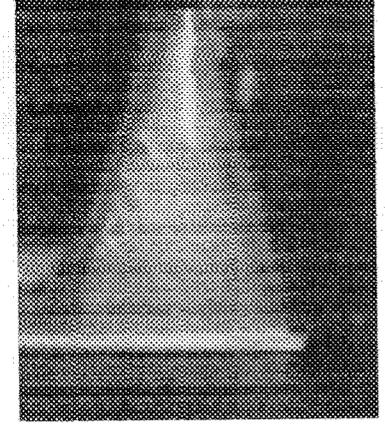
t = 0 s   t = 0.45 s   t = 0.833 s   t = 1.4 s
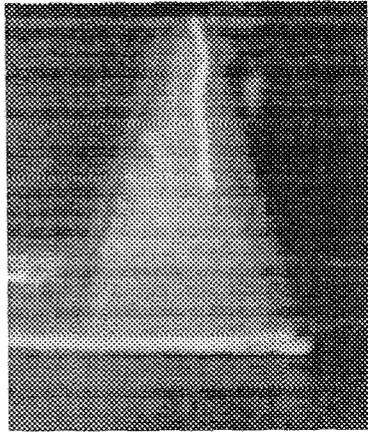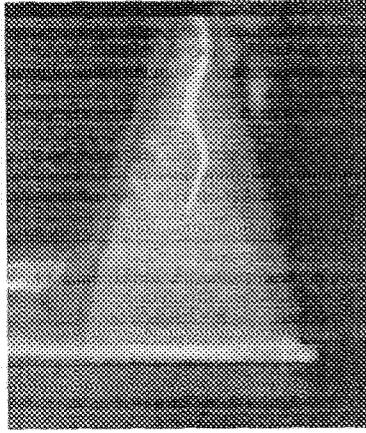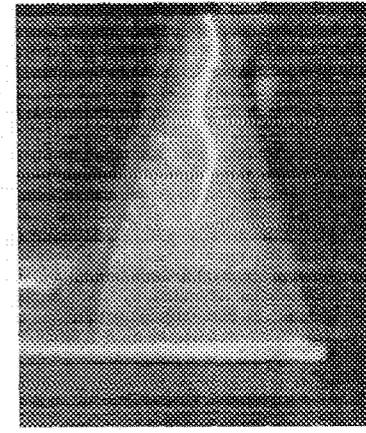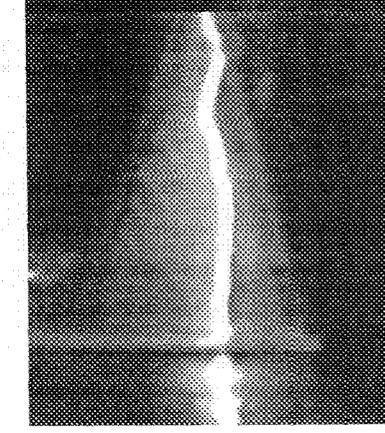
t = 1.784 s   t = 1.8 s   t = 1.808 s   t = 1.817 s

Fig. 7.10 AC arc propagation process on an ice surface ($P = 60$ kPa)

When t was equal to 0 s, an arc was established with an initial length of approximately 1 cm as shown in Fig. 7.10. The arc propagated slowly and, when t was equal to 0.45 s, the arc length was approximately 3 cm and the arc became visibly brighter. When t was equal to 1.784 s, the arc reached approximately 11 cm at which point the arc developed more quickly. When t was equal to 1.8 and 1.808 s, the arc reached a length of approximately 12 cm and 13 cm, respectively. Flashover occurred when t was equal to 1.817 s.

The relationship between the change in L_M and the propagation time is depicted in Fig. 7.11, where L_M is expressed as a percentage of the maximum length of the arc, L. The maximum length was equal to the height of the ice sample, which was 280 mm.

As noted for a DC arc, the propagation process of an AC arc was completed in two stages, which are shown in Fig. 7.11. During the first stage, the arc extended relatively slowly. The calculated arc propagation velocity at this initial stage was 0.05 m/s. During the second stage, the arc propagation velocity dramatically increased to a relatively larger value until flashover was completed. The average arc velocity during the second stage was approximately 5 m/s.
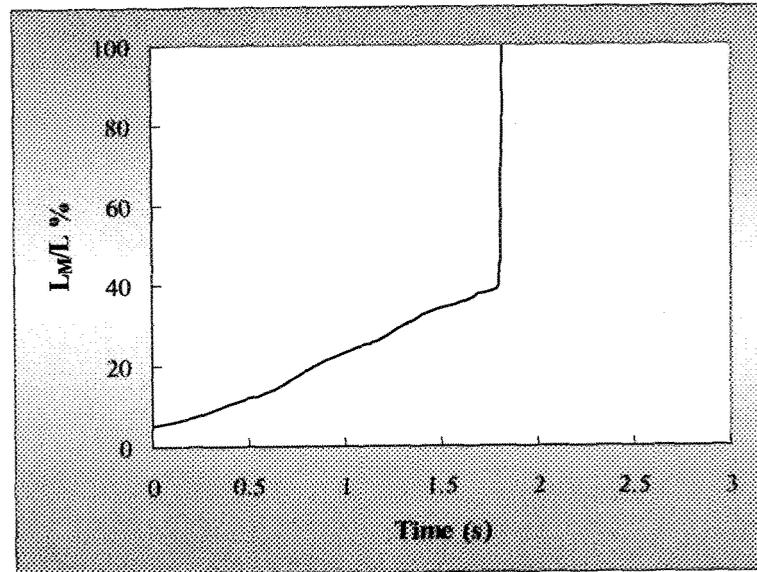
Fig. 7.11 Change in the length of an AC arc on an ice surface

as a function of time (P = 60 kPa)

If the maximum arc length, L_M, during the half cycle was used to calculate the maximum velocity, the maximum velocity was approximately 17 m/s for the above example. However, because the arc was extinguished when the applied voltage passed the zero point, the actual maximum velocity was much higher than this value. Fig. 7.12 illustrates the difference between the change in L_M and the change in the actual arc length, L_{arc}, with time immediately before flashover. The change in L_{arc} with time was considerably faster than that observed for L_M. The corresponding maximum velocity was approximately 170 m/s. Therefore, for this

study, the maximum propagation velocity of an AC arc was defined as the change in L_{arc} with time immediately before flashover occurred.
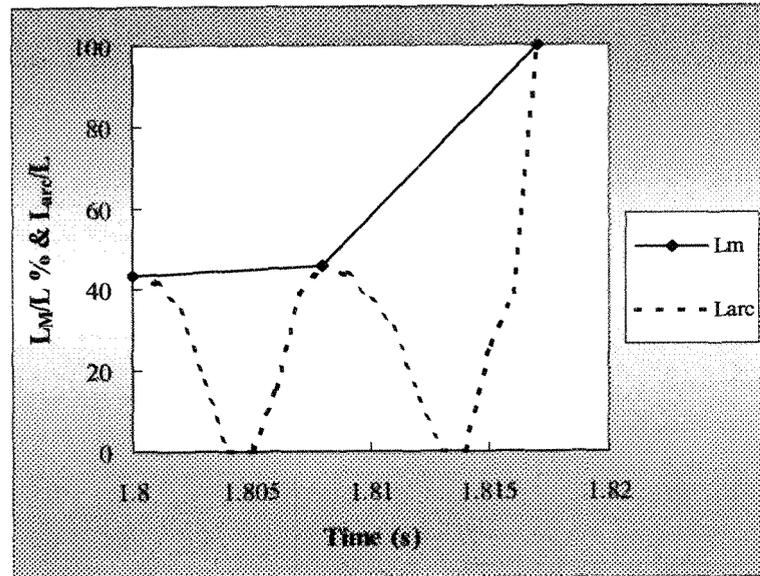
Fig. 7.12 Difference between the change in L_M and the change in L_{arc} with time, one cycle immediately before flashover

The propagation process of an AC arc was investigated at different air pressures and some typical results are illustrated in Fig. 7.13. The propagation velocity of an AC arc on an ice surface at different air pressures are calculated and presented in Table 7.3.
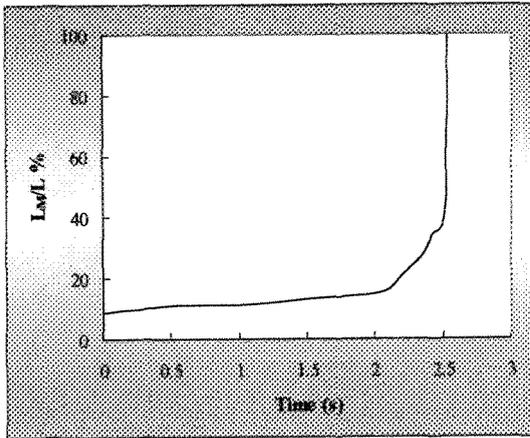
(a) $P = 45$ kPa
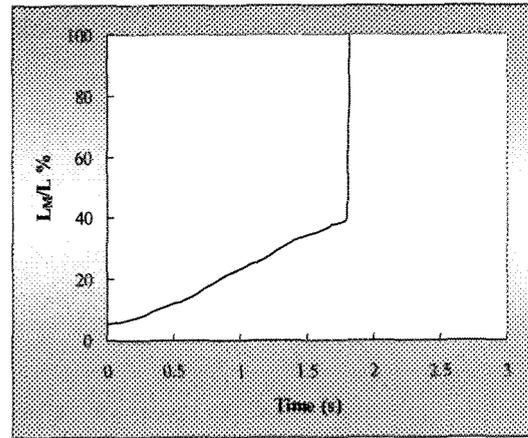
(b) $P = 60$ kPa
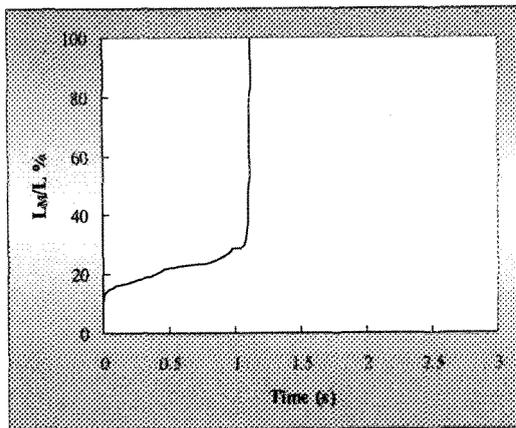
(c) $P = 80$ kPa
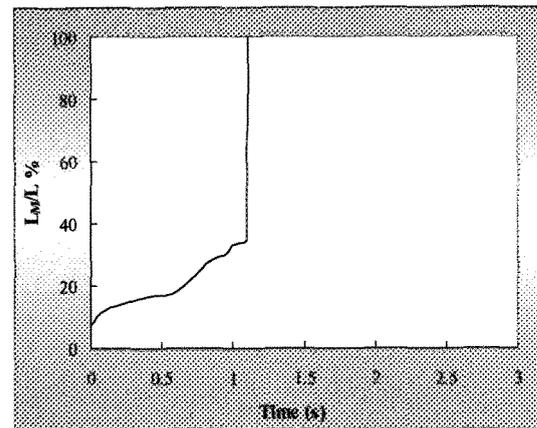
(d) $P = 101$ kPa

Fig. 7.13 Change in the length of an AC arcs on an ice surface as

a function of time at different air pressures

Table 7.3 AC arc propagation velocity at different air pressures

| Air Pressure (kPa)	Velocity of Arc (m/s)		
	First Stage	Second Stage	Maximum
101	0.04 – 0.15 [144]	16 – 30 [144]	440 [144]
80	0.04 – 0.13	4.3 – 26	187
60	0.05 – 0.1	4 - 19	170
45	0.02 – 0.06	1.1 – 14	140

Air pressure did not have a notable effect on the propagation velocity of an AC arc on an ice surface during the first stage when the air pressure was set to above 60 kPa. The average velocity of an AC arc during the first stage was between 0.04 and 0.15 m/s. When the pressure was set to 45 kPa, the propagation velocity was approximately half of that calculated for air pressures above 60 kPa.

During the second stage, the air pressure had a slight influence on the arc propagation velocity: with a decrease in air pressure, the arc propagation velocity decreased.

Air pressure had an appreciable effect on the maximum AC arc propagation velocity; the lower the air pressure, the lower the maximum AC arc propagation velocity on an ice surface.

7.4 EFFECTS OF AIR PRESSURE ON THE RADIUS OF AN ARC ON AN ICE SURFACE

The results from the high-speed photography illustrated that the diameter of an arc was inconstant along the arc column. A previous study at CIGELE [144] showed that the arc radius at the arc root was the most critical in the calculation of the flashover voltage of an ice-covered insulator. Therefore, the arc root radius was investigated in this study.

Generally, the arc root was influenced by environmental conditions such as temperature, humidity and air pressure [117] [144]. For a given environmental condition, particularly the air pressure, the arc root radius was a function of the leakage current. The relationship between the arc root radius and the leakage current can be expressed by the following equation [27] [34] [117] [140]:

$$r = \sqrt{\frac{I}{\pi \cdot J}} \tag{7.1}$$

where r is the arc root radius, I is the leakage current, and J represents the average current density in an arc root. J is the average current density at the arc root for a given air pressure. From the images recorded by the high-speed camera during the arc propagation process, the arc radius and the corresponding leakage current, as well as the consequent average current density J, can be determined [27] [34] [147].

Using the and could be determined from the images recorded by the high-speed camera during the arc propagation process [27] [34] [147]. The value for J was influenced by the environmental conditions such as temperature, humidity and air pressure [117].

7.4.1 Arc Appearance at Low Air Pressure

The appearance of an arc at low air pressure was different from that observed at the standard air pressure. Fig. 7.14 depicts two negative arcs generated at an air pressure of 101.3 kPa and 45 kPa, respectively. The arc generated under standard air pressure had a relatively uniform bright column with a diameter of ~1.6 cm, which implied that the current density in the column was also uniform. In contrast, the arc generated at low air pressure had a relatively bright core with a diameter of ~0.3 cm and a dim outer layer with a diameter of ~1.6 cm. This suggested that, under low air pressure, the current through the column was non-uniform. In other words, the current density was higher in the center of the column than the current density in the dim outer layer.

Only the bright core of the arc was visible on the monitor because of the limited sensitivity of the high-speed camera, particularly when the leakage current was small. However, the majority of the leakage current was concentrated in the bright core of the arc. For this study, the arc radius was defined as the radius of the

bright arc core. Under standard air pressure, the bright arc core constituted the entire arc.

(a) 101 kPa   (b) 45 kPa
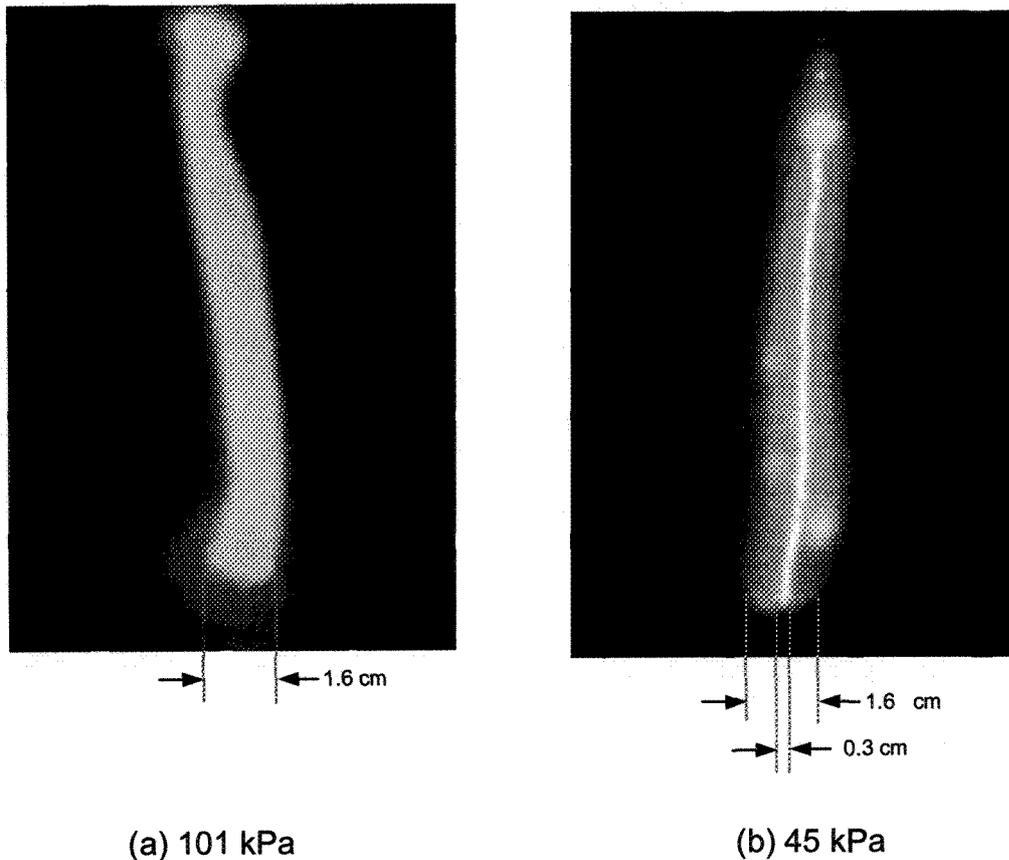
Fig. 7.14 Appearance of negative arcs on an ice surface at different air pressures

7.4.2 DC Arc Radius

The magnitude of the leakage current was varied by adjusting the conductivity of the water used to form the ice samples. Regression analysis was applied to determine the relationship between the arc root radius and the leakage current for both a positive and negative arc under an air pressure that was varied

between 101 kPa and 45 kPa. Figs. 7.15 and 7.16 illustrate the results for a positive and negative arc, respectively. As the leakage current was increased, the arc root radius increased.
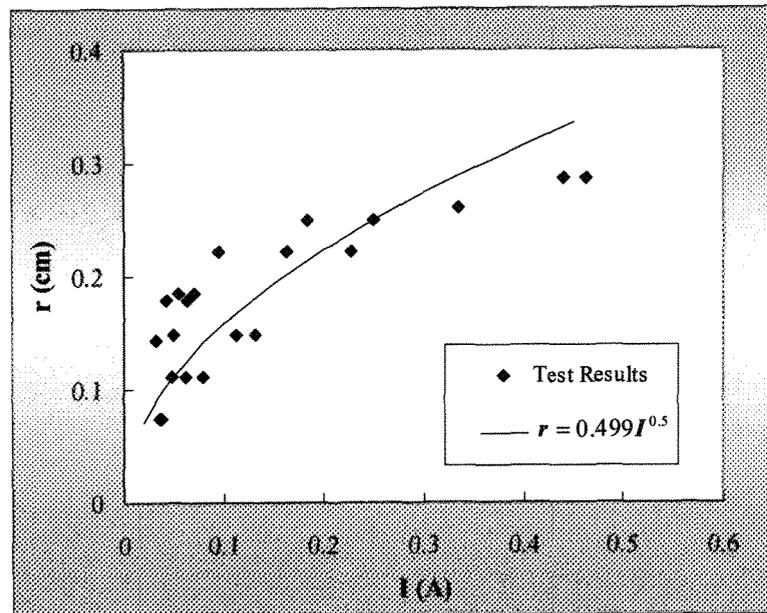
(a) P = 45 kPa
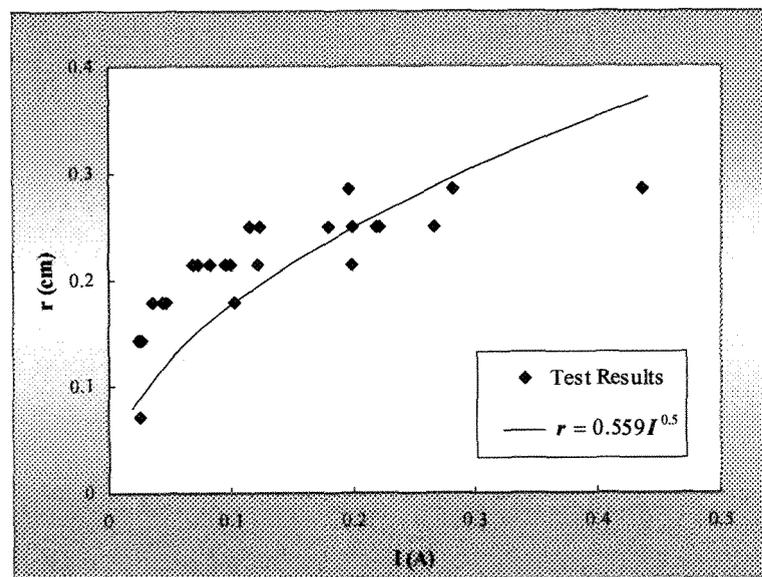
(b) P = 60 kPa
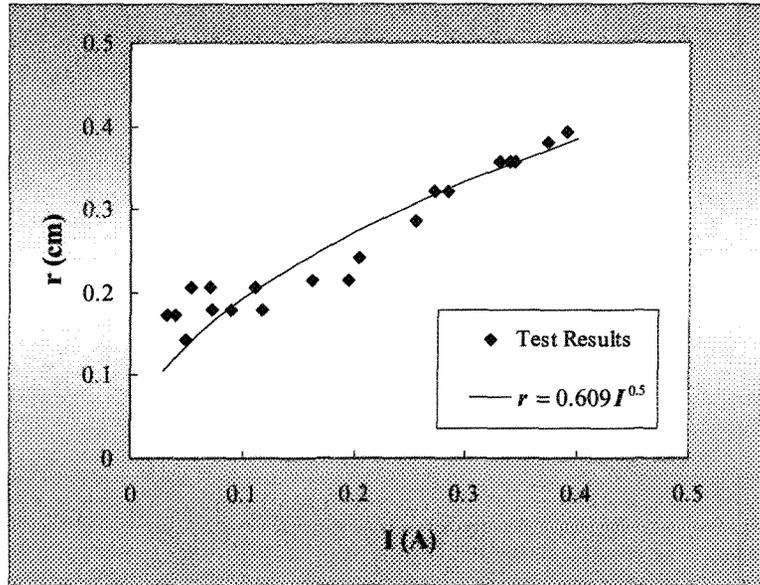
(c) P = 80 kPa
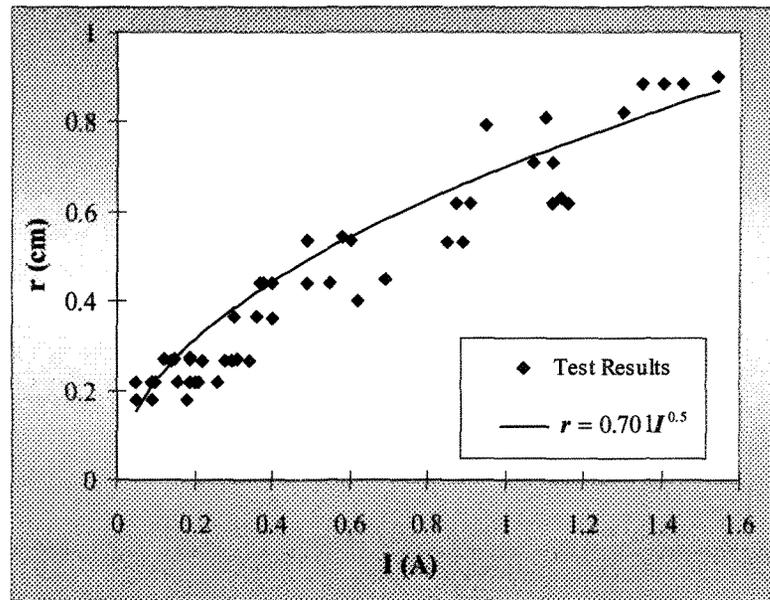
(d) P = 101 kPa

Fig. 7.15 Radius of a positive arc as a function of the leakage

current at different air pressures
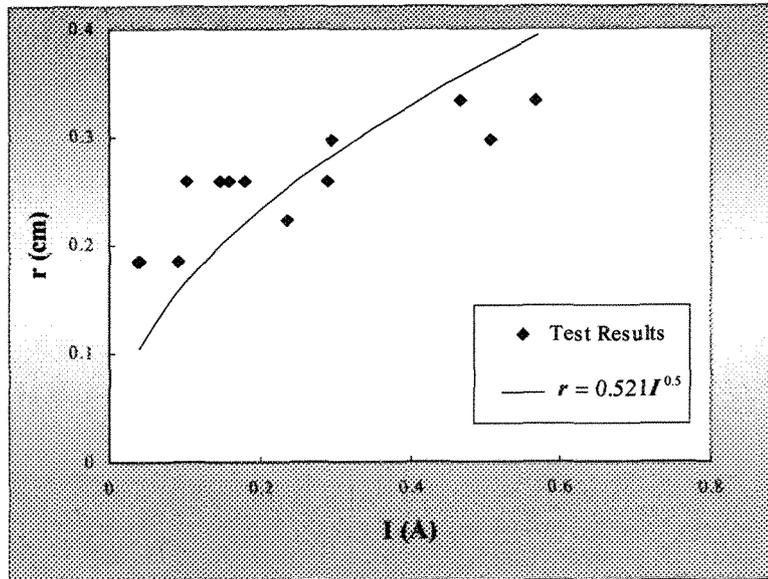
(a) $P = 45$ kPa
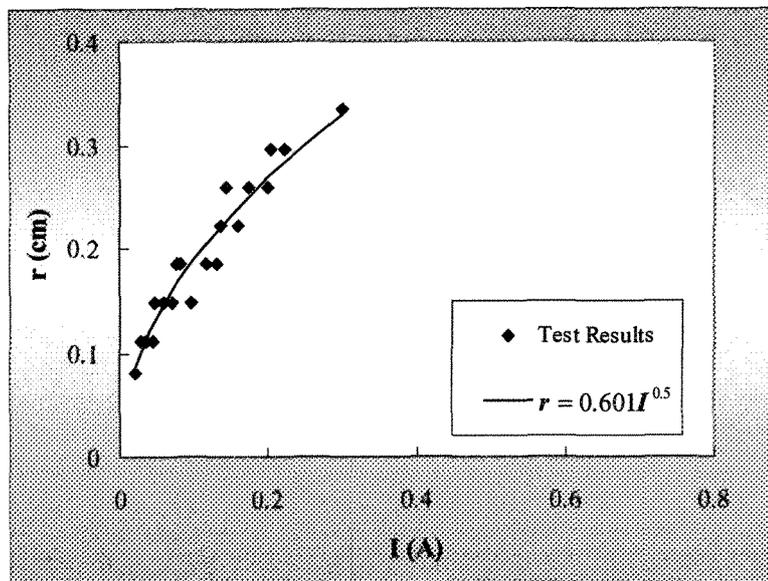
(b) $P = 60$ kPa
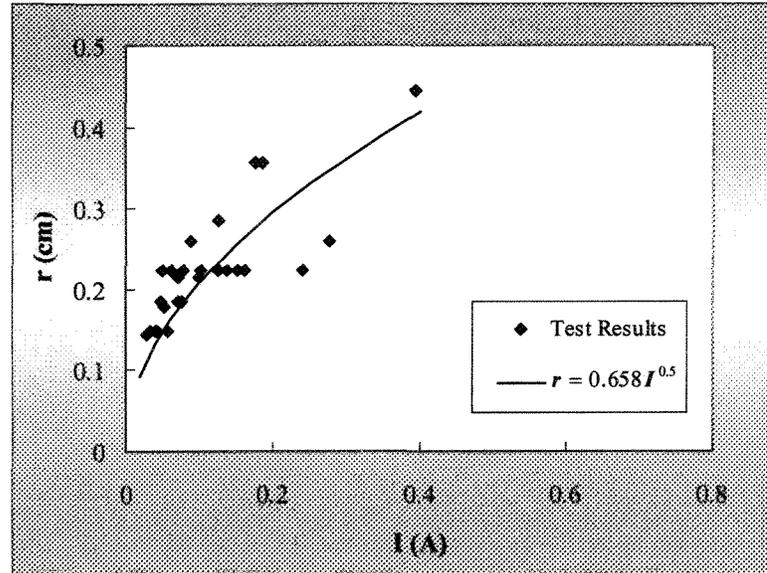
(c) P = 80 kPa
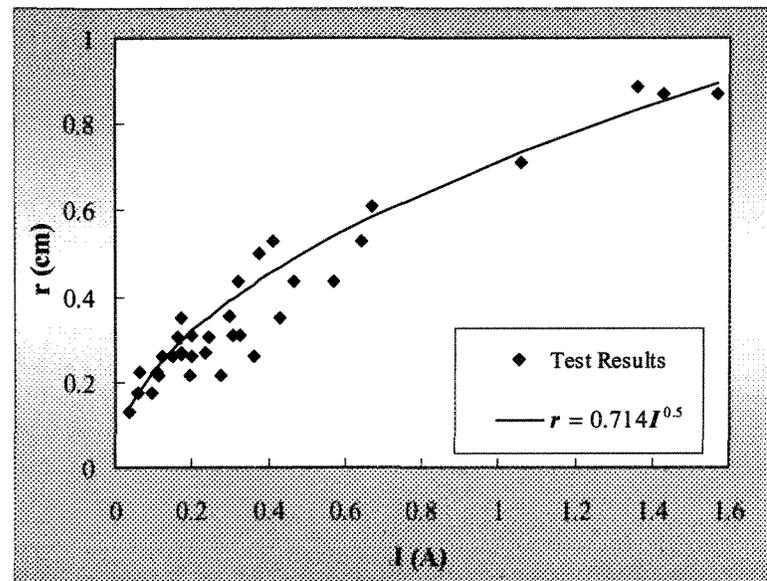
(d) P = 101 kPa

Fig. 7.16 Radius of a negative arc as a function of the leakage

current at different air pressures

From the equations derived from the above regression analysis, the current density in an arc root, J, was determined at different air pressures, for both a negative and positive arc. These results are presented in Table 7.4.

Table 7.4 Values for the constant J for DC arcs at various air pressures

Air Pressure (kPa)	Positive Arc		Negative Arc	
	r (cm)	J (A/cm²)	r (cm)	J (A/cm²)
101	$r = \sqrt{\dfrac{I}{\pi \cdot 0.648}}$	0.648	$r = \sqrt{\dfrac{I}{\pi \cdot 0.624}}$	0.624
80	$r = \sqrt{\dfrac{I}{\pi \cdot 0.858}}$	0.858	$r = \sqrt{\dfrac{I}{\pi \cdot 0.736}}$	0.736
60	$r = \sqrt{\dfrac{I}{\pi \cdot 1.017}}$	1.017	$r = \sqrt{\dfrac{I}{\pi \cdot 0.882}}$	0.882
45	$r = \sqrt{\dfrac{I}{\pi \cdot 1.279}}$	1.279	$r = \sqrt{\dfrac{I}{\pi \cdot 1.174}}$	1.174

Table 7.4 shows that J increased with a decrease in air pressure. When placed in the context of Equation 7.1, these results implied that the arc root radius decreased as air pressure was decreased for a given leakage current value. The polarity of the applied voltage slightly affected the value for J. The value for J for a positive arc was somewhat greater than that measured for a negative arc. Therefore, the arc root radius of a positive arc was slightly smaller than the radius of a negative arc.

Table 7.4 depicts the relation between the current density in an arc root, J (A/cm^2), and the air pressure, P. This relation can be expressed as follows:

$$J = 0.67 \left(\frac{P}{P_0} \right)^{-0.81}, \quad R=0.990 \quad \text{for a positive arc} \quad (7.2)$$

$$J = 0.62 \left(\frac{P}{P_0} \right)^{-0.78}, \quad R=0.995 \quad \text{for a negative arc} \quad (7.3)$$

7.4.3 AC Arc Radius

Under AC voltage, the arc root radius cycled with the leakage current during a half cycle of the applied voltage as illustrated in Fig. 7.8. The arc root radius reached its peak value when leakage current reached its peak value, I_m. The relationship between the peak value of the arc root radius and the leakage current was essential to the modeling of the flashover process on an ice-covered insulator [143]. Therefore, the effects of air pressure on this relationship were investigated.

Regression analysis was applied to the results to determine the relationship between the arc root radius, r, and the leakage current peak value, I_m, at different air pressures. The results of this analysis are presented in Fig. 7.17. The current density in an AC arc root, J, was also determined at different air pressures and presented in Table 7.5.

Table 7.5 Values of J for an AC arc at various air pressures

Air pressure (kPa)	r (cm)	J (A/cm^2)
101	$r = \sqrt{\dfrac{I_m}{\pi \cdot 0.875}}$	0.875
80	$r = \sqrt{\dfrac{I_m}{\pi \cdot 0.958}}$	0.958
60	$r = \sqrt{\dfrac{I_m}{\pi \cdot 1.104}}$	1.104
45	$r = \sqrt{\dfrac{I_m}{\pi \cdot 1.308}}$	1.308

For an AC arc, J increased as the air pressure decreased as depicted in Table 7.5. Correspondingly, the AC arc root radius decreased with a decrease in air pressure for a given leakage current value. The relation between the current density in an AC arc root, J (A/cm^2), and the air pressure, P, can be expressed as follows:

$$J = 0.86 \left(\frac{P}{P_0} \right)^{-0.5} , \quad R=0.995 \quad \text{for an AC arc} \quad (7.4)$$
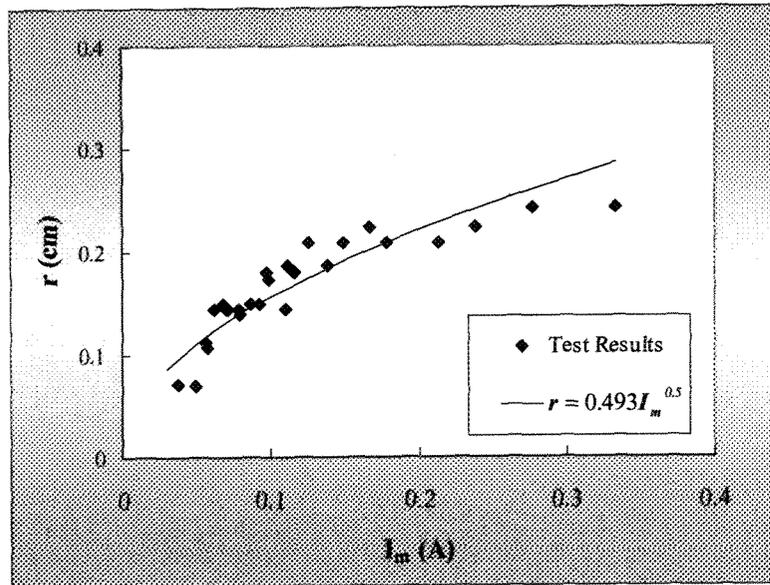
(a) P = 45 kPa
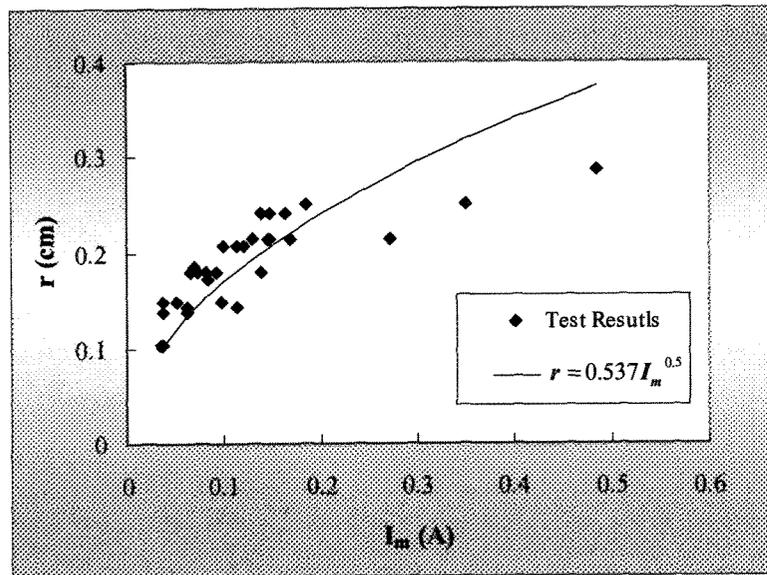
(b) P = 60 kPa
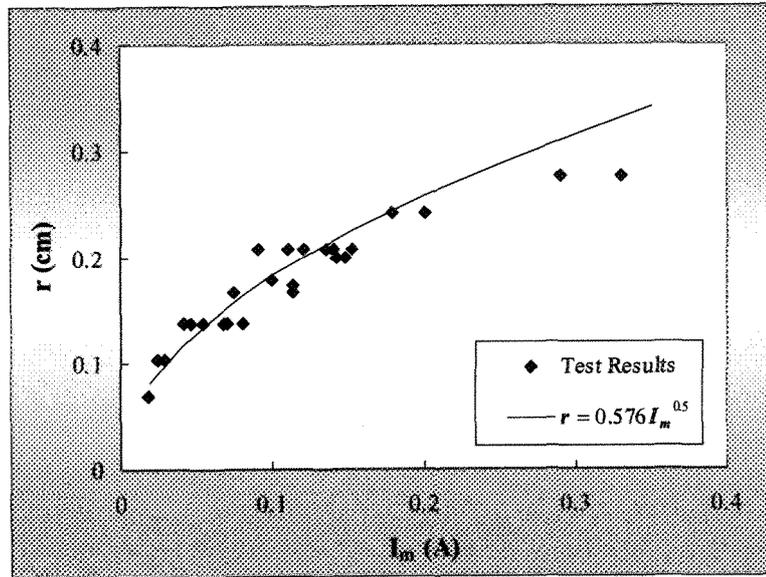
(c) P = 80 kPa
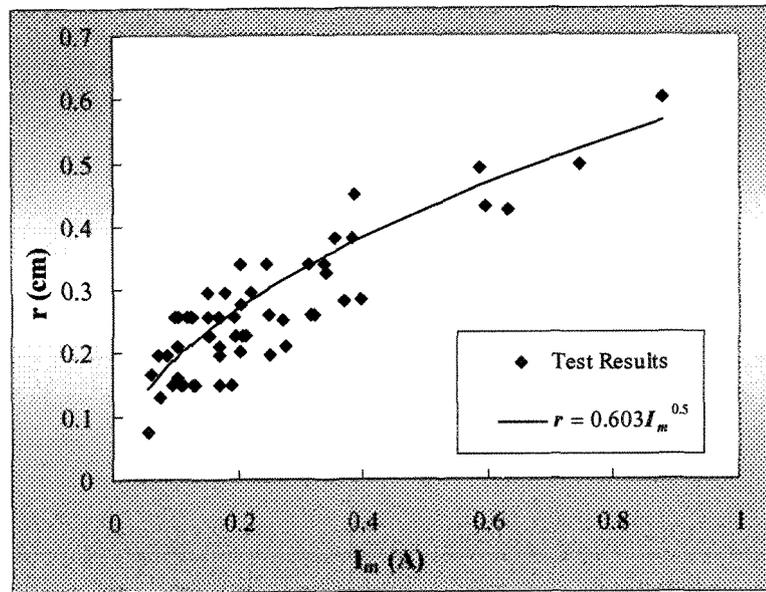
(d) P = 101 kPa

Fig. 7.17 AC arc root radius as a function of the leakage current at

different air pressures

7.5 DISCUSSION

7.5.1 Influence of the Applied Voltage Level on the Arc Propagation Velocity

The arc propagation velocity depended on many factors such as the environmental conditions and the applied voltage level. For an ice-covered insulator, the flashover process could have continued for several seconds or minutes [147] if the applied voltage was maintained at the critical flashover voltage. However, the high-speed camera used in this study had a maximum recording time limit of 3.2 s. In order to record a complete flashover process on a triangular ice sample, the applied voltage was raised 1 kV above the critical flashover voltage. Since the critical flashover voltage of an ice sample decreased with a decrease in air pressure [85], the applied voltage was also decreased according to the air pressure level used.

7.5.2 Effects of Voltage Type and Polarity on the Arc Propagation Velocity

The propagation velocities for an AC and DC arcs are presented in Table 7.6. During the first stage, there was practically no notable difference between the propagation velocities of a negative and positive arc for a given pressure. During the second stage, the polarity of the applied voltage did not have a perceptible effect on the arc propagation velocity. However, the maximum velocity of a positive arc was higher than that measured for a negative arc at a given air pressure as

shown in Fig 7.18. Furthermore, a decrease in the air pressure leads to an increase in the spread between the maximum velocities of a positive and a negative arc.

Table 7.6 Comparison between the propagation velocities of an AC and a DC arcs

Air Pressure (kPa)		Arc Velocity (m/s)			Applied Voltage (kV)
		First Stage	Second Stage	Maximum	
Positive Arc	101	0.05 – 0.25	20 – 50	100	-28
	80	0.04 – 0.15	5.6 – 40	91	-25
	60	0.05 – 0.12	4.5 – 22	83	-22
	45	0.03 – 0.06	4 – 14	70	-19
Negative Arc	101	0.05 – 0.3	35 – 60	100	+25
	80	0.05 – 0.25	5 – 37	67	+22
	60	0.05 – 0.3	4 – 21	51	+21
	45	0.05 – 0.15	4.2 – 12	38	+19
AC Arc	101	0.04 – 0.15	16 - 30	440	23
	80	0.04 – 0.13	4.3 - 26	187	21
	60	0.05 – 0.1	4 - 19	170	19
	45	0.02 – 0.06	1.1 – 14	140	17
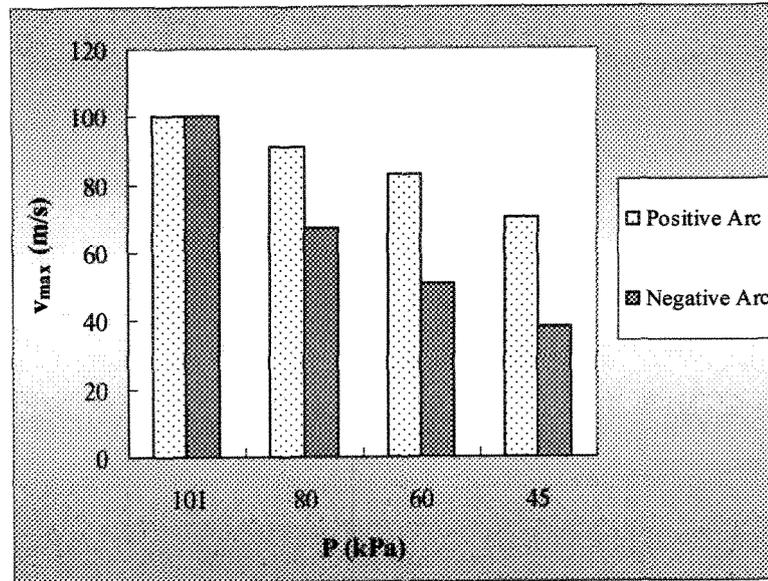
Fig. 7.18 Maximum arc propagation velocity, v_{max}, of DC arcs at

different air pressures

The type of voltage did not appreciably affect the arc propagation velocity

during the first stage. During the second stage, the propagation velocity of an AC

arc was slightly slower than that measured for a DC positive and negative arc. This

observed decrease in propagation velocity for an AC arc was likely due to the fact

that an AC arc burned less steadily than a DC arc. However, the maximum

instantaneous velocity of an AC arc before flashover was higher than that observed

for a DC arc for a given value of air pressure. When the air pressure was set to

80 kPa, the maximum propagation velocity for an AC arc was 187 m/s whereas a

positive and negative arc had a maximum propagation velocity of 91 and 67m/s,

respectively. This was because an AC arc extinguished when the applied voltage passed zero.

For a given voltage type, the maximum arc propagation velocity was noticeably influenced by air pressure; the lower the air pressure, the lower the maximum velocity at a lower applied voltage. In other words, under low air pressure and low applied voltage, the arc propagated more slowly yet was still able to complete the flashover process. This observation could partly explain why the flashover voltage of an ice-covered insulator decreased under a reduced air pressure.

7.5.3 Effects of Voltage Type on Arc Radius

The values for the current density in an arc root, J, for an AC and DC arc under low air pressure are presented in Fig. 7.19. For a given value of air pressure, the constant J of an AC arc was consistently greater than that measured for a DC positive and negative arc. In effect, an AC arc radius was smaller than the arc radius of a DC arc for a given leakage current under both standard and low air pressure. The observed smaller radius was likely due to the cyclical extinction and re-ignition of an AC arc.
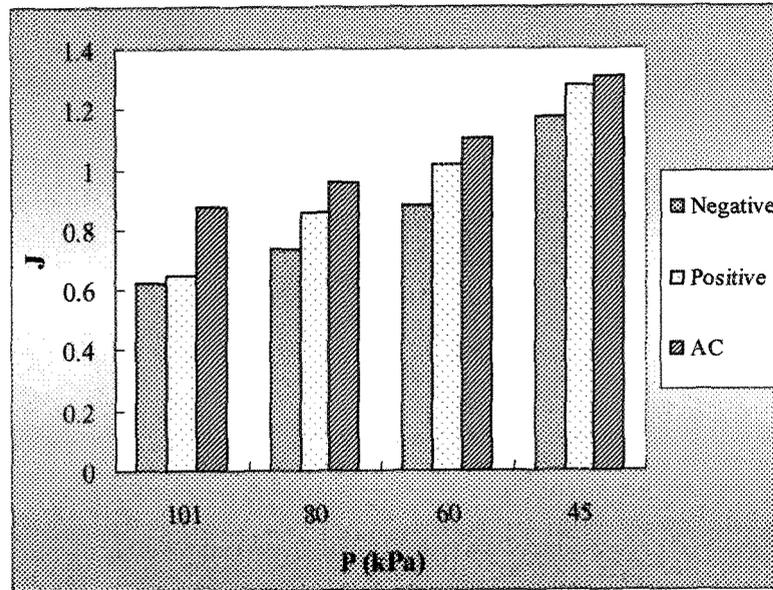
Fig. 7.19 Effect of the applied voltage type on the current density

in an arc root, J, at different air pressures

The arc root radius affected the residual resistance of an ice layer according to the mathematical model developed by CIGELE [27] [34], which was used to predict the flashover voltage of an ice-covered insulator at standard pressure. Consequently, the calculated flashover voltage of an ice-covered insulator will also be affected by the arc root radius. In this mathematical model, the current density in the arc root was assumed to be uniformly distributed. This has since been proven true for standard air pressure. However, the distribution of the current through the arc root was non-uniform at low air pressure. Therefore, the mathematical model needs to be modified before it can be applied to an ice-covered insulator at low air pressure.

7.6 CONCLUSION

A series of experiments were carried out to investigate the effects of low air pressure on the behavior of an AC and a DC arc. The results obtained in this investigation lead to the following conclusions:

1). At standard and low air pressures, the propagation process for both an AC and a DC arc was divided into two stages. The first stage was marked by a relatively low arc propagation velocity whereas the second stage had a substantially higher arc propagation velocity. The maximum propagation velocity was attained immediately before flashover occurred.

2). The type and polarity of the applied voltage had no notable influence on the arc propagation velocity during the first stage. During this initial stage, the arc propagation velocity did not vary greatly when the pressure was varied between 101 kPa and 60 kPa. When the pressure was set to below 60 kPa, the arc propagation velocity occasionally decreased.

3). During the second stage, a low air pressure lead to a decrease in the arc propagation velocity for both an AC and a DC arc. For a given value of air pressure, the propagation velocity of an AC arc was slightly slower than that observed for a positive and negative arc. However, the polarity of the

applied voltage had no appreciable affect on the arc propagation velocity during the second stage.

4). As the air pressure was decreased, the maximum propagation velocities for both an AC and a DC arc decreased. The maximum propagation velocity for a negative arc was lower than that observed for a positive arc. For a given value of air pressure, the maximum propagation velocity of an AC arc was consistently higher than that of both a positive and a negative arc.

5). The arc appearance at low air pressure was different from that observed at standard air pressure. At standard air pressure, the arc had a relatively uniform bright column. At low air pressure, the arc had a bright core and a dim outer layer, which suggested that the current density in the column was non-uniform.

6). With a decrease in air pressure, the current density in an arc root increased. For a given value of leakage current, the radius of the bright core of an arc decreased with a decrease in air pressure under both AC and DC voltage conditions. The applied voltage polarity had a slight effect on the arc radius. The arc radius under AC voltage was somewhat smaller than that observed under DC voltage conditions.

CHAPTER 8

PROCESS AND MECHANISM OF FLASHOVER ON AN ICE SURFACE AT LOW AIR PRESSURE

CHAPTER 8

PROCESS AND MECHANISM OF FLASHOVER ON AN ICE SURFACE AT LOW AIR PRESSURE

8.1 Introduction

Understanding the mechanisms underlying flashover is an important step in reducing and perhaps avoiding flashover faults in power systems. Research into the processes and mechanisms underlying the flashover phenomenon in ice conditions has only recently begun. Current results [17] [25] [26] [29] [34] [145] have shown that ice accretion on insulator strings was non-uniform and that there exists regions on an insulator where there is no ice. These ice-free regions are referred to as air gaps. It was also shown that a water film on the ice surface was necessary for a flashover. This water film resulted from wet ice accretion, condensation, the heating effect of the leakage current, local arcs or, as is often the case, a simple rise in ambient temperature. The conductivity of the water film was found to be quite high because of two possible causes: the rejection of impurities from the solid part toward the liquid part of water drops during solidification; and the pollution of water and ice surface by the products of the

corona discharge [29]. The high conductivity of the water film ensured that the majority of the voltage dropped across the air gaps. If the electrical stress across an air gap was high enough, then several violet colored arcs appeared. Under sufficient electrical stress, these violet arcs will propagate along the ice surface and will eventually form a white arc. When a white arc reaches a specific length, flashover will suddenly occur [29].

This chapter will discuss the flashover process and mechanism under ice conditions and low air pressure. An explanation for the observed decrease in flashover voltage under high altitude conditions will also be presented and discussed.

8.2 FLASHOVER PROCESS ON ICE-COVERED INSULATORS AT LOW AIR PRESSURE

The flashover on an ice surface at low air pressure is a complex process. In order to investigate in detail the flashover process, a series of flashover tests were carried out on a short post insulator covered with ice as presented in Chapter 4. By means of a video camera, the flashover process was recorded and studied in detail.

8.2.1 DC Conditions

The incidence of flashover was random. However, a common process was ascertained and general rules governing the flashover process were established from a large series of experiments conducted under both DC+ and DC- voltage conditions.

Figure 8.1 depicts a typical DC flashover process on an ice-covered insulator at low air pressure. The flashover process was roughly divided into several steps as follows:

— A few minutes after DC voltage application, a very thin water film appeared on the ice surface due to the environmental temperature of 5 °C. The high conductivity of the water film resulted in a voltage drop across the air gap, which was considerably higher than that measured across the ice layer. An initial violet arc appeared across the air gap near the top electrode as shown in Fig. 8.1(a). The start position of this initial arc was random and the arc was able to move laterally along the air gap. Occasionally, two or more arcs appeared simultaneously as illustrated in Fig. 8.1(b). Due to the heating effect of these arcs, the ice near the arc foot melted, increasing the length of the local air gap.

- As the air gap elongated, the arc length increased. If the applied voltage was high enough, the arc propagated across the air gap and extended along the ice surface as depicted in Fig. 8.1 (c). During this period, arc development was exceptionally slow.

- As the arc length increased, ice surrounding the arc root melted. The arc became thicker and brighter and its color changed to white as shown in Fig. 8.1 (d). The white arc was more active and was able to curve along the ice surface as illustrated in Fig. 8.1 (e). Occasionally, part of the arc gradually left the ice surface and floated in the air as shown in Fig. 8.1 (f). Under standard pressure, this arc floating phenomenon rarely appeared, whereas under low pressures this phenomenon was frequently observed.

- The white arc developed quickly and, when it reached a specific length depicted in Fig. 8.1 (g), the flashover suddenly occurred. Finally, the arc reached the bottom electrode as shown in Fig. 8.1 (h).

8.2.2 AC Conditions

The AC flashover process on an ice surface at low pressures was slightly different than the DC flashover process. Under DC conditions, if the applied voltage was high enough, then the arc consistently extended forward until the flashover took place. In contrast, under AC conditions the arc length fluctuated as
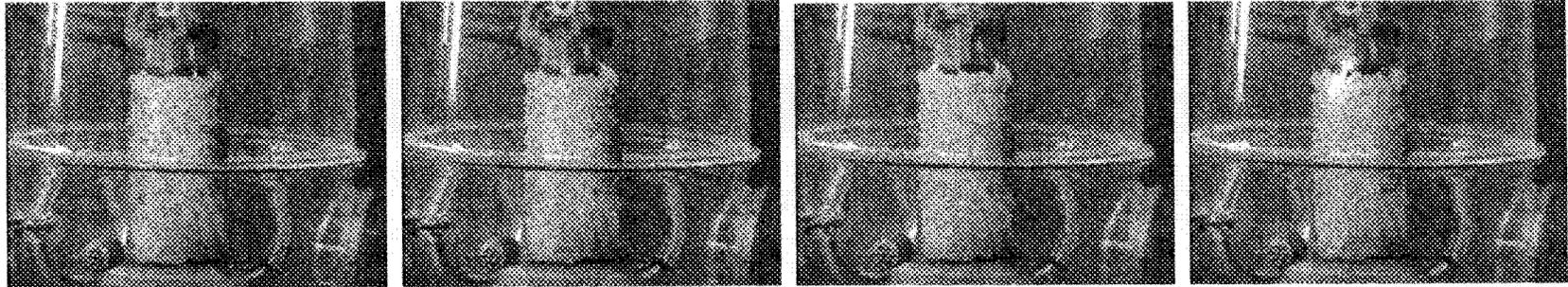
(a) (b) (c) (d)

(e) (f) (g) (h)

Fig. 8.1 DC flashover process on an ice surface at low air pressure

the AC applied voltage cycled. As the AC applied voltage decreased from its peak value towards zero, the arc length shortened from its maximum length towards extinction. When the AC applied voltage passed the zero point and increased to another polar peak value, the arc developed in one of two directions. If the applied voltage was not high enough to result in arc reignition, the flashover failed to take place. If the applied voltage was high enough to produce arc reignition, the arc was rebuilt and the arc length increased to its maximum value as the applied voltage increased to its peak value. Under specific conditions, the peak arc lengths in each half cycle extended until a flashover occurred and the arc reached the bottom electrode.

8.3 ANALYSIS OF A FLASHOVER PHENOMENA ON AN ICE SURFACE AT LOW AIR PRESSURE

8.3.1 Physical Mechanism Underlying a Flashover

The observations of the flashover process described in Section 8.2 revealed that there was no essential difference between the flashover process of an ice-covered insulator under standard and low air pressure. As discussed in Chapter 7, the arc propagation velocity under both standard and low air pressure was of the same order of magnitude. Therefore, the flashover on an ice surface under both low and standard air pressure had a similar physical mechanism.

In an attempt to theoretically analyze the flashover process, the sequence of events necessary for flashover on an ice surface were divided into four successive stages as listed below:

1). The accumulation of ice and formation of air gaps

2). The appearance of water film

3). The establishment of a local arc across the air gap

4). The propagation of an arc along an ice surface, bridging the insulator

The physical processes involved in stage 4 are as yet poorly understood. Therefore, the propagation of an arc along an ice surface will be the main topic discussed in this section.

As mentioned in the preceding chapters, ice deposited on an insulator string can be referred to as a special type of pollution. Therefore, listed below are the three major hypotheses currently on the mechanisms underlying pollution flashover which may be used for analyzing the flashover on an ice surface.

  − The external force "pulling" theory [108] [114]:

   External forces, particularly the electrostatic force, "drags" the arc over the ice surface, resulting in a flashover

- The electrical breakdown theory [67]:

  A high local electric field at the arc root accelerates the electrons such that their impact results in the ionization of the air in front of the arc root. This ionization, results in arc extension and eventually a flashover

- The thermal breakdown theory [84] [139] [146]:

  A high temperature at the arc root results in the ionization of air, which elongates the arc and results in a flashover

To test the electrostatic force pulling theory, it was necessary to estimate the order of magnitude of the electrostatic force. For a typical arc on an ice surface under standard air pressure, the arc root radius was about 0.4 cm for a leakage current of 0.4 A. Referring to the pollution condition, an electric field of 5.3 kV/cm was used [67]. The electrostatic force can be calculated by the following relation:

$$F = \frac{1}{2}\varepsilon_0 E^2 r^2 \cong 2 \times 10^{-5} \text{ N}$$

where F is the electrostatic force in Newton, E is the electric field strength in kV/cm, r is the arc root radius in cm and ε_0 is the permittivity of air, which is equal to $8.854e^{-12}$ F/m.

Jolly (refer to the discussion of [114]) and **Obenaus** [106] noted that, while the electrostatic force was able to deflect an arc, the force was too weak to elongate the arc over an electrolyte. A force of this magnitude resulted in the

propagation velocity of an arc at a mere few centimeters per second [67] [103]. As discussed in Chapter 7, the arc propagation velocity reached a few tens even hundred meters per second. Therefore, it was not possible that such a high propagation velocity was the result of feeble electrostatic forces pulling on the arc. Hence, the electrostatic force was not likely to be a main factor contributing to a flashover on an ice surface.

To the best of our knowledge, there is no available study on the electric field strength at the root of arc on ice surface. A few researchers calculated the electric stress at the root of arc on a polluted surface. Before the arc length reached 90% of the leakage distance, the electric field strength was found to be considerably lower than that required for the electric breakdown of air [84] [146]. The results in Chapter 7 illustrated that if the applied voltage was raised 1 kV higher than the critical flashover voltage of an ice sample, then the arc propagation velocity in the first and second stages, before the final jump, was less than 60 m/s. This velocity was considerably lower than the magnitude of a few hundred meters per second, which was the lower limit for the arc propagation velocity caused by the ionization of air in the front of an arc root under a high local electric field [67]. Therefore, arc movement in the first stage and in the majority of the second stage was not due to the electrical breakdown of the air in front of the arc root. In the final moment of flashover, the applied field strength became exceptionally high. At the same time, the arc propagation velocity rose quickly and reached a velocity of hundreds of

meters per second. Only at this moment, the electric breakdown might contribute to arc propagation.

In this study, the plane triangular ice sample was used to study the physical basis underlying arc propagation in the first and second stages. The time to flashover was recorded, which encompassed the period from the point of application of the minimum flashover voltage to the occurrence of a flashover. Table 8.1 depicts the results under different conditions of air pressure, P, conductivity of freezing water, σ, and type of applied voltage, AC or DC.

Despite the variation in test conditions, the time to flashover was consistently within a few tens of seconds. It has been stated that a flashover time of this order implied that thermal ionization processes played an important role in generating a flashover [66]. Thermal ionization is the ionization of gas atoms or molecules in response to thermal energy. Within high temperature gases, there exist the following possible routes that lead to ionization [102]:

- Ionization by mutual collision of gas atoms. High temperatures will increase both the velocity and kinetic energies of gas atoms, leading to ionization.

- Photoionization caused by the thermal emission of the hot gases

- Ionization by collision with high-energy electrons produced by either of the above two processes

Table 8.1 Time to flashover under different conditions

P (kPa)	Average Time (s)											
	AC Arc				Negative Arc				Positive Arc			
	σ=80	σ=160	σ=250	σ=400	σ=80	σ=160	σ=250	σ=400	σ=80	σ=160	σ=250	σ=400
101	12.6	11.6	10.8	6.4	16	15.2	12.1	9.8	14.6	13.6	11.1	9.2
80	13.5	13.1	11.9	7.2	18.7	16.6	14.6	11.7	15.0	14.4	14.4	10.6
60	14.4	14.1	13.3	9.9	22.8	21.8	16.6	12.4	18.0	16.4	15.4	12.1
45	16.1	15.0	14.8	10.5	26.1	25.4	17.8	13.7	23.1	18.3	17.3	12.5
30	20.9	18.5	16.6	11.6	29.4	25.9	21.4	15.7	28.9	23.6	20.5	15.3

From the above, it was inferred that the thermal ionization of the air in front of an arc root contributed to arc movement in the first stage and in the majority of the second stage. In these two stages, the arc had a propagation velocity of less than a few tens of meters per second. The electrostatic force had an auxiliary effect on impelling arc propagation. After the arc reached its critical length, the electrical field strength in front of the arc root rose rapidly. This resulted in a positive feedback: the rapid rise in the electrical field increases the number of collision ionization in gas and the later leaded to a further increase in electrical field strength. When the electrical field strength reached the critical breakdown field strength of air, the electrical breakdown occurred and the arc propagation velocity reached a magnitude of a few hundred meters per second. At this point, the final jump of the flashover was completed.

8.3.2 Mechanism Underlying the Observed Decrease in Flashover Voltage of Ice-covered Insulators at Low Air Pressure

It was observed that the flashover voltage of an ice-covered insulator decreased with a decrease in the air pressure. However, the mechanism that leads to this decrease is currently not well understood. The experimental and observational results from this study lead to four deductions concerning the observed decrease in flashover voltage.

8.3.2.1 Decrease in the arc E-I characteristics at low air pressure

Deduction one: A Decrease in the voltage gradient-current, E-I, characteristics of an arc was one of the main factors that lead to a decrease in the flashover voltage of an ice-covered insulator at low air pressure.

In Chapter 6, it was noted that the arc E-I characteristics decreased with a decrease in air pressure. Because an arc was a thermal as well as an electrical phenomenon, the thermal conditions surrounding an arc influenced its electrical properties. Some possible factors affecting the voltage gradient along an arc column are discussed as follows:

1). Water vapour

An arc at low air pressure was observed to be darker than that observed at standard air pressure. This color phenomenon indicated that the current through an arc at low air pressure was less than the current through an arc at standard air pressure. A lower current at low pressure compared to that observed at standard pressure was measured and noted in Chapter 5 (Figs. 5.8, 5.13c and 5.14). Therefore, at low air pressure, a smaller current resulted in a smaller heating effect. As a result, less water vapour was produced during the arc propagation process at low air pressure compared to the water vapour produced at standard pressure.

Several researchers have studied the effects of dry and water saturated air on the E-I characteristics of an arc, which is the relation between the voltage gradient along an arc and the current through an arc. Thus far, all studies have shown that the amount of water vapour in the air substantially affects the E-I characteristics of an arc [50] [114].

Alston et al [2] measured the E-I characteristics of an arc burning in dry air and determined the relation to be as follows:

$$E = 63I^{-0.76} \tag{8.1}$$

Rahal et al [114] determined the relation between E and I of an arc in water saturated air, steam, to be as follows:

$$E = 530I^{-0.24} \tag{8.2}$$

Hamptom [50] investigated the E-I characteristics of arc in dry and in water saturated air and concluded that water vapour elevated the E-I characteristics of arc.

For a steady-state free burning arc in either dry or water saturated air, the majority of the electrical dissipation heated the surrounding gases [133]. The temperature of an arc core was approximately 3500 °K for an arc propagating through water saturated air. This high temperature was able to dissociate 20% of the water vapour into hydrogen [2], which altered the thermal conductivity of the surrounding air. Fig 8.2 illustrates the thermal conductivities of hydrogen, water

vapour and air for different temperatures at standard air pressure [4] [59]. At high temperatures, the thermal conductivities of water vapour and hydrogen were consistently much higher than that observed for air. Furthermore, the differences between the conductivities of water vapour or hydrogen and the conductivity of air tended to increase with an increase in temperature. Concurrently, the high thermal conductivities of the gases surrounding an arc also increased heat dissipation, which strengthened the de-ionization process in an arc column and, consequently, lead to a higher voltage gradient along an arc column. In conclusion, water saturated air elevated the E-I characteristics of an arc when compared to the effects of dry air.
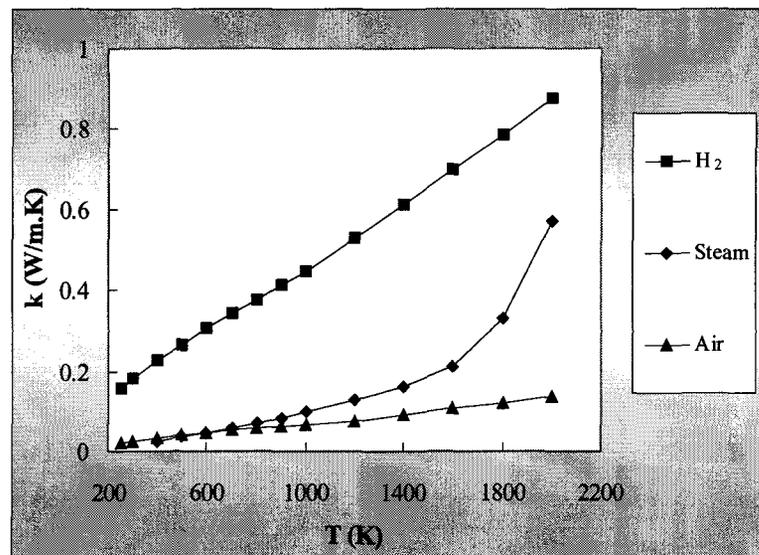
Fig. 8.2Thermal conductivities, k, of gases under different temperatures

The temperature of an arc on an ice surface and the temperature of the immediate area surrounding an arc were not precisely measured up until now. However, as mentioned above, less water vapour was produced during arc propagation at low air pressure compared to the amount produced at standard air pressure. This leads to a decrease in the E-I characteristics and, consequently, a lower flashover voltage.

In Chapter 5 it was noted that the voltage type and polarity influenced the critical flashover leakage current, I_{cf}. For a triangular ice sample, I_{cf} was lower under AC than under DC voltage conditions for a given value of air pressure. This implied that the energy dissipation under AC voltage was less than that observed under DC voltage. Therefore, the water vapour produced during arc propagation · under AC was less than that produced under DC, which resulted in a lower flashover voltage under AC than that observed under DC. For the same reasons, the flashover voltage under DC- was observed to be less than that observed under DC+ voltage conditions.

2). Propagation velocity

A higher arc propagation velocity leads to a stronger cooling effect on the arc, which resulted in a stronger de-ionization process in the arc column and, consequently, a higher voltage gradient along the arc column [136]. At low air pressure, the arc propagation velocity in the second stage was lower, particularly

during the final jump. Therefore, the voltage gradient along an arc column was lower, which resulted in a lower flashover voltage.

3). Na atoms

The high temperatures found within an arc could have disintegrated the salt (NaCl) on a polluted ice surface into Na atoms. These Na atoms would have been transported into the arc column and would have affected the arc characteristics. Because of the low ionization potential of Na (5.14 eV), even a few ppm of Na atoms in the arc could have substantially increased the electrical conductivity of the arc column plasma and consequently decreased the arc E-I characteristics and the flashover voltage.

Ishii et al [64] measured the density of Na in an arc on a polluted surface at standard air pressure and at a low air pressure of 40 kPa. The Na density was determined to be only a few ppm at standard air pressure and a few tens of ppm at 40 kPa of pressure. This observation implied that the increase in the density of Na in an arc at low pressure likely contributed to the observed decrease in the flashover voltage of an ice-covered insulator at low pressure.

8.3.3.2 Increase in the current density in an arc core root at low air pressure

Deduction two: An increase in the current density in an arc core root was one of factors that lead to a decrease in the flashover voltage of an ice-covered insulator at low air pressure.

In Chapter 7 it was noted that the current density in the arc core root increased with a decrease in air pressure. Due to the larger current density, the temperature could have increased in the area immediately surrounding the arc core root. This higher temperature could have assisted the thermal ionization process. From this extrapolation, it was deduced that there was a stronger ionization surrounding the arc root, which lead to a decrease in the flashover voltage of an ice-covered insulator at low air pressure.

8.3.2.3 Decrease in the electrode voltage drop at low air pressure

Deduction three: A decrease in the electrode voltage drop was one of the factors that lead to a decrease in the flashover voltage of an ice-covered insulator at low air pressure.

In Chapter 6 it was demonstrated that a decrease in air pressure resulted in a decrease in the electrode voltage drop under both AC and DC voltage

conditions. Since the electrode voltage drop was a component of the total voltage drop along the arc, the observed decrease in the electrode voltage drop resulted in a decrease in the flashover voltage of an ice-covered insulator.

8.3.2.4 Arc floating at low air pressure

Deduction four: Arc floating influenced the flashover voltage of an ice-covered insulator at low air pressure.

In Chapter 7 it was noted that low air pressure resulted in a decrease in the arc propagation velocity in the second stage as well as the maximum propagation velocity. A lower arc propagation velocity could have resulted in the detachment of the arc from the ice surface by thermal buoyant forces. Thus, at low air pressure, the detachment of an arc from the ice surface would have resulted in a stronger arc floating phenomenon. In corroboration of this deduction, results presented in Chapter 5 showed that the arc floating phenomenon was observed more frequently at low air pressure than at standard pressure.

The effect of arc floating on the flashover voltage of an ice-covered insulator was complex;

1). The larger the distance between the arc and the ice surface, the smaller the cooling effect of the ice surface on the arc, This cooling effect is termed the cooling wall effect.

2). The larger the distance between the arc and the ice surface, the smaller the effect of water vapour on the arc.

3). The arc floating also lead to a longer arc length and a longer flashover distance.

4). The larger distance between the arc and the ice surface would have hindered the transportation of Na atoms from the polluted ice surface to the arc column.

The first two outcomes could have caused a lower voltage gradient along the arc column and, consequently, a decreased flashover voltage under low air pressure. However, the last two outcomes resulted in an increase in flashover voltage. The overall outcome on the flashover voltage depended on the above four cumulative effects of arc floating. According to the test results, the synthetic effect of arc floating slightly increased the flashover voltage of an ice-covered insulator. This is opposite to that observed under pollution conditions, where the arc bridged between the ribs of an insulator hence shortening the flashover distance.

CHAPTER 9

GENERAL CONCLUSIONS

CHAPTER 9

GENERAL CONCLUSIONS

9.1 GENERAL CONCLUSIONS

In this thesis, the flashover phenomenon on an ice surface at standard and low air pressures was systematically studied for the first time using both a real short post insulator covered with ice and a physical ice model with a simplified geometry. The work presented in this thesis can be roughly divided into four components as follows:

- Flashover performance

- Arc characteristics

- Arc behavior

- Flashover mechanisms

Based on the experimental results and the subsequent theoretical analyses presented in previous chapters, the general conclusions are summarized as follows:

1. Flashover performance

1.1). For both the plane triangular ice sample and real short post insulator the ambient air pressure had a substantial influence on the minimum flashover voltage, V_{MF}, under AC and DC voltage conditions. V_{MF} decreased with a reduction in air pressure.

1.2). The relationship between the observed decrease in flashover voltage and decrease in air pressure can be expressed as follows:

$$\frac{V}{V_0} = \left(\frac{P}{P_0}\right)^m \tag{9.1}$$

The exponent m represents the influence of air pressure on the flashover voltage. The value for m was influenced by the level of freezing water conductivity, voltage type and polarity, and the insulator profile.

For the triangular ice sample the value for m was consistently highest under DC+ and lowest under DC- voltage conditions, for a given freezing water conductivity. The value for m under AC conditions fell between those values calculated under DC+ and DC- voltage conditions. For a real short post insulator, the value for m was higher under AC than that measured under DC voltage conditions.

1.3). At low air pressures, the critical flashover leakage current, I_{cf}, was smaller than that observed at the standard air pressure. I_{cf} was also influenced by both the voltage type and polarity.

1.4). The arc floating phenomenon was observed frequently under high altitude conditions. It appearances more frequently under DC, particularly under DC- voltage for an post type insulator covered with ice. The arc floating was one of the main factors contributing to the observed polarity effect on the flashover voltage of an ice-covered post insulator.

2. Arc characteristics

2.1). The voltage-current, V-I, characteristics of an arc can be expressed by the following equation:

$$V_{total} = V_e + V_{arc} = V_e + AxI^{-n} \qquad (9.2)$$

The arc characteristics were characterized by the electrode voltage drop V_e and the arc constants A and n.

Under both AC and DC voltages, V_e and A decreased with a decrease in air pressure. The value for V_e and A at different air pressure can be approximately calculated by the following equation:

For V_e (volt):

$$V_e = 931\left(\frac{P}{P_0}\right)^{1.22} \quad \text{(rms volt)... for AC arc} \qquad (9.3)$$

$$V_e = 817\left(\frac{P}{P_0}\right)^{0.54} \quad \text{(volt)} \quad \text{for a positive arc} \qquad (9.4)$$

$$V_e = 539\left(\frac{P}{P_0}\right)^{0.31} \quad \text{(volt)} \quad \text{for a negative arc} \qquad (9.5)$$

For A:

$$A = 133\left(\frac{P}{P_0}\right)^{0.74} \quad \text{for AC arc} \qquad (9.6)$$

$$A = 178\left(\frac{P}{P_0}\right)^{0.75} \quad \text{for a positive arc} \qquad (9.7)$$

$$A = 103\left(\frac{P}{P_0}\right)^{1.14} \quad \text{for a negative arc} \qquad (9.8)$$

The effect of air pressure on the arc constant n was not evident; therefore, the mean value for n for AC, DC positive and DC negative arcs was calculated to be 0.7, 0.61 and 0.69 respectively. The mean value for n was used for all air pressure levels tested, which ranged between 101 kPa and 45 kPa.

2.2). Air pressure had a considerable effect on the V-I characteristics of an arc on an ice surface under both AC and DC voltages. The observed decrease in V_e and A lead to a decrease in the arc V-I characteristics

at low air pressure. In general, the V-I characteristics of an arc on an ice surface can be expressed as a function of the air pressure as follows:

$$V_{total} = 931\left(\frac{P}{P_0}\right)^{1.22} + 133\left(\frac{P}{P_0}\right)^{0.74} xI^{-0.7} \quad \text{for AC arc} \quad (9.9)$$

$$V_{total} = 817\left(\frac{P}{P_0}\right)^{0.54} + 178\left(\frac{P}{P_0}\right)^{0.75} xI^{-0.61} \quad \text{for positive arc} \quad (9.10)$$

$$V_{total} = 539\left(\frac{P}{P_0}\right)^{0.31} + 103\left(\frac{P}{P_0}\right)^{1.14} xI^{-0.69} \quad \text{for negative arc} \quad (9.11)$$

2.3). The difference between the values for V_e and A was also a factor contributing to the observed polarity effect on the flashover voltage of an ice-covered insulator. The flashover voltage of a plane triangular ice sample was higher for a positive arc than that observed for a negative arc and this polarity effect was due to the higher values of V_e and A for a positive arc compared to a negative arc.

3. Arc behavior

3.1). At both the standard and the low air pressures, the propagation process for both AC and DC arcs was divided into the two following stages:

–   First stage: the arc had a relatively low propagation velocity and the arc length was usually shorter than 40% of the total insulator length.

–   Second stage: the arc became brighter and had a much higher propagation velocity than that observed in the first stage. The maximum propagation velocity was reached at the moment just before flashover.

3.2).   In the first stage, the arc propagation velocity was not notably influenced by the type and polarity of the applied voltage. During this initial stage, the arc propagation velocity did not vary greatly when the pressure was varied between 101 kPa and 60 kPa. The average arc propagation velocity was approximately a few cm/s to tens of cm/s. When the pressure was set to below 60 kPa, the arc propagation velocity occasionally decreased.

3.3).   In the second stage, the average arc propagation velocity was a few m/s to tens of m/s. Air pressure appeared to have a small effect on the arc propagation velocity: a decrease in air pressure resulted in a decrease in the arc propagation velocity for both AC and DC arcs.

Under a given air pressure, the propagation velocity of an AC arc was slightly slower than the velocities measured for both positive and negative arcs. In the second stage, the polarity of the applied voltage had no notable influence on the arc propagation velocity.

3.4). The maximum propagation velocity of an arc on an ice surface varied from a few tens to hundreds of m/s. As the air pressure was decreased from 101 kPa to 45 kPa, the maximum propagation velocity of an arc decreased approximately 68% for an AC arc, 30% for a positive arc and 63% for a negative arc.

Under a given air pressure, the maximum propagation velocity for a positive arc was lower than that measured for an AC arc but higher than that measured for a negative arc.

3.5). The appearance of an arc at low air pressures was different from that observed at standard air pressure. At standard air pressure, the arc appeared as a relatively uniform bright column. In contrast, at low pressure, the arc column had a bright core and a relatively dim outer layer, which suggested that the current density in the column was non-uniform.

3.6). The relationship between the arc root radius and the leakage current can be expressed by:

$$r = \sqrt{\frac{I}{\pi \cdot J}}$$ (9.12)

With a decrease in air pressure, the current density in the arc root, J, increased. The value for J at different air pressure can be approximately calculated by the following equation:

$$J = 0.86\left(\frac{P}{P_0}\right)^{-0.5}$$ for AC arc (9.13)

$$J = 0.67\left(\frac{P}{P_0}\right)^{-0.81}$$ for positive arc (9.14)

$$J = 0.62\left(\frac{P}{P_0}\right)^{-0.78}$$ for negative arc (9.15)

For a given value of leakage current, the radius of the bright arc core decreased as the air pressure was decreased for both an AC and DC arc. The applied voltage polarity had a slight effect on the arc radius. The arc root radius under AC voltage was somewhat smaller than that observed under DC voltage.

4. Flashover mechanisms

4.1). The flashover process of an ice-covered insulator was divided into the following stages:

–   The accumulation of ice and formation of air gap

–   The appearance of water film

–   The establishment of local arc along the air gap

■   A violet arc first appeared

■   The arc moved laterally occasionally along the air gap.

■   Two or more arcs occasionally appeared simultaneously

–   The propagation of an arc on an ice surface, and

bridging of the insulator

■   The arc propagated along the ice surface

■   The color of the arc changed to white

■   The arc occasionally curved along the ice surface

■   Part of arc occasionally left the ice surface and floated in

the air

■   The flashover occurred suddenly

4.2). Physical mechanism underlying a flashover on an ice surface:

During the first stage, and for the majority of the second stage, of

arc propagation on an ice surface, thermal ionization of the air in

front of an arc root led to arc movement. Electrostatic force had

an auxiliary effect on impelling arc propagation. After the arc

reached its critical length, the electric field in front of an arc root

rose rapidly. The subsequent rise in electric field permitted a positive feedback effect on collision ionization. When the electric field strength rose higher than the critical air breakdown field, the electrical breakdown appears which results in the final jump of flashover

4.3). Four main factors thought to cause the decrease in the flashover voltage of an ice-covered insulator at low air pressure are summarized below:

- A decrease in the voltage gradient-current, E-I, characteristics of an arc was one of main factors that lead to a decrease in the flashover voltage of an ice-covered insulator at low air pressure. This decrease in the arc E-I characteristics was mainly due to the effect of water vapour, the arc propagation velocity and the transportation of Na atoms into the arc column.

- An increase in the current density in arc core root was another factor that leads to a decrease in the flashover voltage of an ice-covered insulator at low air pressure.

- A decrease in the electrode voltage drop was also a factor that leads to a decrease in the flashover voltage of an ice-covered insulator at low air pressure.

–   Finally, the effect of the arc floating phenomenon could have slightly increased the flashover voltage of an ice-covered insulator at low air pressure.

9.2 RECOMMENDATIONS

To the best of our knowledge, this is the first time the mechanisms underlying flashover on an ice surface at low air pressure was systematically investigated. The results and conclusions of this study will contribute to the understanding of flashover phenomena observed on insulators covered with ice under low air pressure conditions and preventing such phenomena in power systems. However, due to the limit of time for this PhD project, several aspects still remain unexplained. Three main areas for future research are identified below:

1.   In the present study, the V-I characteristics of an AC and a DC arc on an ice surface as well as the electrode voltage drop were determined at low air pressure as presented in Chapter 6. Meanwhile, the arc root radius at low air pressure was also investigated as presented in Section 7.4. However, in order to develop a mathematical model that predicts the AC flashover voltage of an ice-covered insulator at low air pressure, the arc reignition conditions must be determined.

2. A number of mechanisms and deductions were proposed concerning the flashover on an ice surface at low air pressure as presented in Chapter 8. From these deductions, it was noted that the electrical field and temperature surrounding an arc likely played an important role in the flashover mechanism. To completely reveal and understand the flashover mechanism for an ice-covered insulator at low air pressure, the electrical field and temperature distributions surrounding an arc must be measured.

3. All of the experiments conducted in this study were carried out in a small cylindrical evacuated chamber introduced in Section 4.2.2. Due to the limitation of its dimensions, only small ice samples and short post insulators were tested. In high voltage power networks, the dimensions of an insulator are much larger than the samples tested in this study. Therefore, in order to verify the results obtained in this study and validate the mathematical model, a larger evacuated chamber will be required to test full-size industrial high voltage insulators.

4. Some other parameters such as the environmental relative humidity and the number and position of air gaps may also influence the flashover voltage and mechanism of ice-covered insulators at normal or reduced air pressure. They also need to be studied further.

REFERENCES

REFERENCES

[1]   Al-Baghdadi, A., "The Mechanism of Flashover on Polluted Insulators", *Thesis of PhD*, University of Manchester, USA, pp. 67, 1970.

[2]   Alston, L. L. and Zoledziowski, S., "Growth of discharges on polluted insulation", *Proceedings of IEE*, Vol. 110, No. 7, pp. 1260-1266, July 1963.

[3]   Anibal de la O L. and Jorge Glez. De la Vega, "Performance of AC insulators under Low Pressure Fog Chamber tests", *Proceedings of 7th International Symposium on High Voltage Engineering*, Dresden, German, Paper No. 44.19, August 1991.

[4]   Bejan, A., "Heat Transfer", *John Wiley & Sons, Inc.,* 1993.

[5]   Bergman, V. I. and Kolobova, O. I., "Some results of an Investigation of the Dielectric Strength of Contaminated Line Insulation in Reduced Air-pressure Conditions", *Elektrotekhnika*, Vol. 54, No. 2, pp. 54 –56, 1983.

[6]   Bergman, V. I. and Shamsiev, A. S., "Parameters of Electric Arc Discharge in Condition of Low Gas Pressure", *Izvestia Visshikh Uchebnikh Zavedenii, Energetika*, Vol. 21, No. 8, pp. 29 –34, 1978.

[7]   Boyer, A. E. and Meale, J. R., "Insulation Flashover under Icing Conditions on the Ontario-Hydro 500 kV Transmission Line System," *Proceedings of CEA Spring Meeting*, Montreal, Canada, March 1988.

[8]   Brown, S. D., "Introduction to electrical discharges in gases", *John Wiley & Sons, Inc.*, 1966.

[9]   Bueckert, D., "Ice Storm Damage Tallied", *Report of Cnews on Ice Storm '98*, December 15, 1998.

[10]   Bui, H. T., Phan, L. C., Huraux, C. and Pissolato, J., "HVDC Flashover on the Surface of Conductive Ice", *IEEE International symposium on Electrical Insulation*, Montreal, Canada, Paper No. 84CH1964-6, pp. 85-88, 1984.

[11]   Charneski, M. D., Gaibrois, G. L. and Whitney, B. F., " Flashover Tests on Artificially Iced Insulators," *IEEE Transactions on Power Apparatus & Systems*, Vol. PAS-101, No. 8, pp. 2429-2433, 1982.

[12]   Chen, X., "Modeling of Electrical Arc on Polluted Ice Surface", *Thesis of PhD*, University of Montreal, Canada, 2000.

[13]   Cheng, T. C., Wu, C. Y. and Nour, H., " DC Interfacial Breakdown on Contaminated Electrolytic Surfaces", *IEEE Transactions on Electrical Insulation*, Vol. EI-19, No. 6, pp. 536-542, December 1984.

[14]   Cherney, E. A., "Flashover Performance of Artificially Contaminated and Iced Long-rod Transmission Line Insulators", *IEEE Transactions on Power Apparatus and Systems*, Vol. PAS-99, No. 1, pp. 46-52, February 1980.

[15]   Cherney, E. A., Beausejour, Y., Cheng, T. C., Lloyd, K. J., Marrone, G., Moran, J. H., Naiyo, K., Pargamin, L., Reynaert, E., Sakich, J. D. and Sarkinen, C. F., "The AC Clean-fog Test for Contaminated Insulators", *IEEE Transactions on Power Apparatus and Systems*, Vol. PAS-102, No. 3, pp. 604-613, March 1983.

[16]   Chisholm, W. A., Ringler, K. G., Erven, C. C., Green, M. A., Melo, O., Tam, Y., Nigol, O., Kuffel, J., Boyer, A., Pavasars, I. K., Macedo, F. X., Sabiston,

J. K. and Caputo, R. B., "The Cold-Fog Test", *Proceedings of IEEE/PES Winter Meeting*, Baltimore, USA, Paper No. 96 WM 099-2 PWRD, 1996.

[17]   CIGRE Task Force 33.04.09, "Influence of Ice and Snow on the Flashover Performance of outdoor insulators Part I: Effects of Ice", *ÉLECTRA*, No. 187, pp. 90-111, December 1999.

[18]   Claverie, P. and Porcheron, Y., "How to Choose Insulators for Polluted Areas", *IEEE Transactions on Power Apparatus and Systems*, Vol. PAS-92, No. 3, pp. 1121-1131, 1973.

[19]   Claverie, P., "Predetermination of the Behavior of Polluted Insulators", *IEEE Transactions on Power Apparatus and Systems*, Vol. PAS-90, pp. 1902-1908, 1971.

[20]   Engel, A. V., "Ionized Gases", *Oxford*, 1965.

[21]   Farzaneh, M. and Drapeau, J. F., "AC Flashover Performance of Insulators Covered with Artificial Ice," *IEEE Transactions on Power Delivery*, Vol. 10, No 2, pp 1038-1051, April 1995.

[22]   Farzaneh, M. and Kiernicki, J., "Flashover Performance of ice-covered Insulators", *Canadian Journal of Electrical and Computer Engineering*, Vol. 22, No. 3, pp. 95 - 109, July 1997.

[23]   Farzaneh, M. and Kiernicki, J., "Flashover Performance of IEEE Standard Insulators under Ice Conditions", *IEEE Transactions on Power Delivery*, Vol. 12, No. 4, pp. 1602-1613, October 1997.

[24]   Farzaneh, M. and Kiernicki, J., "Flashover Problems Caused by Ice Build-up on Insulators", *IEEE Transactions on Electrical Insulation*, Vol. EI-11, No. 2, pp. 5-17, March/April 1995.

[25] Farzaneh, M. and Zhang, J., " Behavior of DC Arc Discharge on Ice Surfaces", *Proceedings of 8th International Workshop on the Atmospheric Icing of Structures*, Iceland, pp. 193-197, 1998.

[26] Farzaneh, M. and Zhang, J., "Modeling of DC Arc Discharge on Ice Surfaces", *IEE Proceedings Generation, Transmission and Distribution*, Vol. 147, No. 2, pp. 81-86, 2000.

[27] Farzaneh, M., "Effect of Ice Thickness and Voltage Polarity on the Flashover Voltage on Ice Covered High Voltage Insulators", *Proceedings of 7th International Symposium on High Voltage Engineering*, Dresden, Germany, Vol. 4, Paper No. 43.10, pp.203-206, 1991.

[28] Farzaneh, M., "Ice Accretions on High-Voltage Conductors and Insulators and related phenomena", *Philosophical Transactions of the Royal Society*, Vol. 358, No. 1776, pp. 297-3005, November 2000.

[29] Farzaneh, M., Fofana, I. Tavakoli, C. and Beroual, A., "A Mathematical Model of Arc Development on Ice Surfaces under DC Voltage", *Proceedings of IASTED International Conferences on Power and Energy Systems*, Rhodes, Greece, Paper No. 337-070, July 2001.

[30] Farzaneh, M., Kiernicki, J. and Dallaire, M. A., "AC and DC Flashover Performance of Ice-covered Insulators during a De-Icing Period", *Proceedings of 5th International Workshop on the Atmospheric Icing of Structures*, Tokyo, Japan, Paper No. B-48, pp. 1-4, 1990.

[31] Farzaneh, M., Kiernicki, J., Chaarani, R., Drapeaum, J. F. and Martin, R., "Influence of Wet-grown Ice on the AC Flashover Performance of Ice Covered Insulators", *Proceedings of 9th International Symposium on High Voltage Engineering*, Austria, Paper No. 3176, pp.1-4, 1995.

[32] Farzaneh, M., Zhang, J. and Chen, X., " DC characteristics of Local Arc on Ice Surface", *Atmospheric Research*, Vol. 46, pp.49-56, 1998.

[33] Farzaneh, M., Zhang, J. and Chen, X., " Modeling of the AC Arc Discharge on Ice Surfaces", *IEEE Transactions on Power Delivery*, Vol. 12, No. 1, pp.325-338, 1997.

[34] Farzaneh, M., Zhang, J., Brettschneider, S. and Miri, A. M., "DC Flashover Performance of Ice-Covered Insulators", *Proceedings of 10th International Symposium on High Voltage Engineering*, Montreal, Canada, Vol. 3, pp. 77-80, 1997.

[35] Fikke, S. M., "Possible Effects of Contaminated Ice on Insulator Strength", *Proceedings of 5th International Workshop on the Atmospheric Icing of Structures*, Tokyo, Japan, Paper No. B4-2-(1), 1990.

[36] Fikke, S. M., Hanssen, J. E. and Rolfseng, L., "Long Range Transported Pollution and Conductivity on Atmospheric Ice on Insulators", *IEEE Transactions on Power Delivery*, Vol. 8, No. 3, pp. 13411-1321, July 1993.

[37] Fofana, I., Farzaneh, M. and Tavakoli, C. "Modelling Arc Propagation Velocity on Ice-covered Surfaces", *Proceedings of 10th International Workshop on Atmospheric Icing of Structures*, Brno, Czech Republic, pp.1-6, June 2002.

[38] Fofana, I., Farzaneh, M., Tavakoli, C. and Beroual, A., "Dynamic modelling of flashover process on Insulator under Atmospheric Icing conditions", *Proceedings of 2001 IEEE Conference on Electrical Insulation and Dielectric Phenomena*, pp. 605-608, Kitchener, Canada, October 2001.

[39] Forest, J. S., "The Performance of High Voltage Insulators in Polluted Atmospheres", *Proceedings of IEEE Winter Meeting*, New York, 1969.

[40]   Frischmann, W., "Contatimation Flashover and Arc Root Motion", *Dtsch. Elektrotechnik,* Vol. 11, pp. 290-295, 1957.

[41]   Fryxell, J. and Schei, A., "Influence of High Altitudes on the Flashover Voltage of Insulators", *Elteknik,* Vol. 9, No. 1, pp. 1-3, 1966.

[42]   Fujimura, T., Naito, K., and Suzuki, Y., "DC Flashover Voltage Characteristics of Contaminated Insulators", *IEEE Transactions on Electrical Insulation,* Vol. EI-16, No. 3, pp. 189-197, June 1981.

[43]   Fujimura, T., Naito, K., Hasegawa, Y. and Kawaguchi, T., " Performance of Insulators Covered with Snow or Ice", *IEEE Transactions on Power Apparatus & Systems,* Vol. PAS-98, No. 5 pp. 1621-1631, Sept. 1979.

[44]   Fujishima, T., Takenouchi, O., Fujimoto, A., Yamashita, T. and Matsuo, H., "The Relation between the Photo-emission intensity and the Propagation Velocity of a Local Discharge on an Electrolytic Solution under low Pressure Air", *Proceedings of 9th International Symposium on High Voltage Engineering,* Austria, Paper No. 3213, 1995.

[45]   Ghosh, P. S. and Chatterjee, N., "Arc Propagation over Electrolytic Surfaces under Power Frequency Voltage", *IEEE Transactions on Dielectrics and Electrical Insulation,* Vol. 3, No. 4, pp. 529-536, 1996.

[46]   Gou, R., " Influence of Pressure on AC-flashover Voltage and Pre-flashover current of Contaminated Insulators", *Proceedings of 7th International Symposium on High Voltage Engineering,* Dresden, German, Paper No. 43.06, 1991.

[47]   Gu, L., Sun, C., Xie, J. and Zhang, J., "AC Flashover Charcateristics opf EHV Line Insulators for High Altitude Contamination Regions", *Proceedings of 2nd ICPADM,* Beijing, China, 1988.

[48] Guan, Z. and Huang, C., "Discharge Performance of Different Models at Low Pressure Air", *Proceedings of 4th International Conference on Properties and Applications of Dielectric Materials*, Brisbane Australia, Paper No. 5102, pp. 463-466, July 1994.

[49] Guan, Z., Warren, L., Bagdahdi, A. A. J. and Goulsbra, D. R., "The Polarity Effect of Discharges on Polluted Insulators", *Proceedings of 6th International Symposium on High Voltage Engineering*, New Orleans, USA, Paper No. 30.03, 1989.

[50] Hampton, B. F., "Flashover Mechanism of Polluted Insulation", Proceedings of IEE, Vol. 11, No. 5, pp. 985-990, 1964.

[51] Hara, M. and Phan, C. L., "Leakage Current and Flashover Performance of Iced Insulators", *IEEE Transactions on Power Apparatus and Systems*, Vol. PAS-98, No. 3, pp. 849-859, 1979.

[52] Hesketh, S., "General Criterion for the Prediction of Pollution Flashover", *Proceedings of IEE*, Vol. 114, No. 4, pp. 531-532, 1967.

[53] Holtzhausen, J. P., "The Relationship between the Parameters Affecting the AC Pollution Performance of a Cylindrical Insulator", *Proceedings of 9th International Symposium on High Voltage Engineering*, Austria, Paper No. 3233, August 1995.

[54] Huang, C. et al, "Influence of Air Pressure on AC Flashover Voltage of Polluted Post Insulators", *Proceedings of 8th International Symposium on High Voltage Engineering*, Japan, Paper No. 46.01, 1993.

[55] Huang, C., "Study of the Performance of Polluted Insulation Flashover in High Altitude Area", *Thesis of PhD*, Tsinghua University, China, 1993.

[56]   Hydro-Québec Committee of Experts, "January 1998 ice storm", *Report for Hydro-Quebéc*, 1998.

[57]   Hydro-Québec, "Analysis of the Hydro-Québec System Blackout on April 1988", *Official Hydro-Québec Report*, Montreal, July 1988.

[58]   Imai, I. and Ichiro, " Studies on Ice Accretion", *Researches on Snow and Ice*, No. 1, pp.35-44, 1953.

[59]   Incropera, F. P. and Dewitt, D. P., "Fundamentals of Heat and Mass Transfer", *John Wiley & Sons, Inc.*, 1996.

[60]   International Electrotechnical Commission (IEC), "Artificial Pollution Tests on High-voltage Insulators to be Used on A.C. Systems", *International Standard 507*, 1991.

[61]   International Electrotechnical Commission (IEC), "Artificial Pollution Tests on High-voltage Insulators to be Used on D.C. Systems", *Technical Report 1245*, 1993.

[62]   International Electrotechnical Commission (IEC), "High-voltage test techniques", *IEC International standard*, Publication 60-1, 1989.

[63]   Ishii, M., Kawamura, T., Ohashi, H. and Matsumoto, T., "Observation of DC Partial Arcs on Contaminated Surface by Means of Interferometric Method", *Proceedings of 5th International Symposium on High Voltage Engineering*, Braunschweig, Germany, Paper No. 51.06, August 1987.

[64]   Ishii, M., Shimada, K., Kawamura, T., and Matsumoto, T., " Flashover of Contaminated Surfaces under Low Atmospheric Pressure", *Proceedings of 4th International Symposium on High Voltage Engineering*, Athens, Greece, Paper No. 46.02, September 1983.

[65]   Jolly, D. C., "Contamination Flashover Theory and Insulator Design", *Journal of the Franklin Institute*, Vol. 294, No. 6, 1972.

[66]   Jolly, D. C., "Contamination Flashover, Part II: Flat Plate Model Tests", *IEEE Transactions on Power Apparatus and Systems*, PAS-91, pp. 2443-2451, 1972.

[67]   Jolly, D. C., "Contamination Flashover, Part I: Theoretical Aspects", *IEEE Transactions on Power Apparatus and Systems*, PAS-91, pp. 2437-2442, 1972.

[68]   Jolly, D. C., Cheng, T. C. and Otten, D. M., "Dynamic Theory of Discharge Growth over Contaminated Insulator Surfaces", *IEEE PES Winter Power Meeting*, New York, USA, Paper, No. C74 068-3, 1974.

[69]   Jordan, J. B. and Saint-Armand, R., "Electrical corona at Ice Surface", *Proceedings of 4th International Conference on Gas Discharges*, Swansea, pp. 239-243, 1976.

[70]   Kannus, K. and Verkkonen, V., "Effect of Coating on the Dielectric Strength on High Voltage Insulators", *Proceeding of 4th International Workshop on the Atmospheric Icing of Structures*, Paris, France, pp.296-300, 1988.

[71]   Kannus, K., Lahti, K. and Nousiainen, K., "Comparisons between Experiments and Calculations of the Electrical Behaviour of Ice-Covered High Voltage Insulators", *Proceedings of 8th International Workshop on Atmospheric Icing of Structures*, Iceland, pp. 325-331, 1998.

[72]   Kawai, M., " AC Flashover Tests at Project UHV on ice-covered Insulators", *IEEE Transactions on Power Apparatus & Systems*, Vol. PAS-89, No. 8, pp. 1800-1805, Dec. 1970.

[73] Kawamura, T., Ishii, M., Akbar, M. and Nagai, K., "Pressure Dependence of DC Breakdown of Contaminated Insulators", *IEEE Transactions on Electrical Insulation*, Vol. EI-17, No. 1, February 1982.

[74] Khalifa, M. M. and Morris, R. M., "Performance of Line Insulators under Rime Ice", *IEEE Transactions on Power Application and Systems*, Vol. PAS-86, pp. 692-698, 1967.

[75] Kuffel, E. and Abdullah, M., "High Voltage Engineering", *Pergamon Press*, 1970.

[76] Kuroiwa, D., " Icing and Snow Accretion on Electric Wires", U.S Army Cold Regions Researches and Engineering Laboratory, *Research Report 123*, pp.1-10, 1965.

[77] Kuroiwa, D., " Icing and Snow Accretion", *Monograph Series of Research, Institute of Applied Electricity*, Japan, pp. 1-30, 1958.

[78] Lambeth, P. J., "Effect of Pollution on High Voltage Outdoor Insulators", *IEE Reviews*, Tome 118, No. 9R, pp. 1107-1130, 1970.

[79] Le Roy, G. Gary, C., Hutzler, B., Lalot, J. and Dubanton, C., "Les Propriétés Diélectriques de L'air et Les Très Hautes Tensions ", *Editions Eyrolles*, 1984.

[80] Lee, L. Y., Nellis, C. L. and Brown, J. E., " 60 Hz Tests on Ice-covered 500 kV Insulators Strings", *Proceedings of IEEE/PES Summer Meeting*, San Francisco, USA, Paper No. A75-499-4, 1975.

[81] Leroy, G., Simon, M. F. and Liao, T. W., "Breakdown phenomena of long gaps under switching impulse conditions", *Proceedings of IEEE/PES Summer Meeting*. Paper No. 74 CH0910-0-PRW, 1974.

[82]   Li, S., "The Mechanism of the Flashover on a Polluted Dielectric Surface under AC Voltage", *Thesis of PhD*, Tsinghua University, China, 1988.

[83]   Li, S., Zhang, R. and Tan, K., "Measurement of Dynamic Potential Distribution during the Propagation of a Local Arc along a Polluted Surface", *IEEE Transactions on Electrical Insulation*, Vol. 25, No. 4, pp. 757-761, 1990.

[84]   Li, S., Zhang, R. and Tan, K., "Measurement of the Temperature of a Local Arc Propagating", *Proceedings of 6th International Symposium on High Voltage Engineering*, New Orleans, USA, Paper No.12.05, 1989.

[85]   Li, Y., Farzaneh, M. and Zhang, J., "Effects of Voltage Type and Polarity on Flashover Performances at Low Atmospheric Pressure on an Ice Surface", *Proceedings of 8th International Offshore and Polar Engineering Conference*, Montreal, Canada, pp. 543-546, 1998.

[86]   Llewellyn-Jones, F., " Ionization and Breakdown in Gases", *Methuen & Co Ltd*, London, 1966.

[87]   Loeb, L. B. and Meek, J. M., "Mechanism of the Electric Spark", *Stanford University Press*, California, 1941.

[88]   Long, Y., "Effect of Altitude on the Flashover Voltage of External Insulation of H. V. Electrical Apparatus", *Proceedings of 4th International Symposium on High Voltage Engineering*, Athens, Greece, Paper No. 43.02, 1983.

[89]   Maikopar, A. S., "The Open Small Current Arc", *Elektrichestvo*, No. 2, pp. 22-25, 1965.

[90]   Maldonado, O. A. A. and Prado, A. J., "The Flashover Phenomenon: An Analysis with Influence of the Thickness of the Layer Pollution of the High Voltage polluted Insulators", *Conference Record of the 1994 IEEE*

International Symposium on Electrical Insulation, Pittsburgh, USA, pp. 546-549, June, 1994.

[91]   Matsuda, H., Komuro, H. and Takasu, K., "Withstand Voltage Characteristics of Insulator String Covered with Snow and Ice", *IEEE Transactions on Power Delivery*, Vol. 6, No. 3, pp. 1243-1250, July 1991.

[92]   Meek, J. M., "Phys. Rev.", 57, 722, 1940.

[93]   Meier, A. and Niggli, W. M., "The Influence of Snow and Ice Deposits on Supertension Transmission Line Insulator Strings with Special Reference to High Altitude Operation", *IEEE Conference Publ.44*, London, England, pp. 386-395, Sept. 1968.

[94]   Melo, O. T., Tam, Y. T. and Farzaneh, M., " Freezing Rain and Fog Events in Southern Ontario: Properties and Effect on EHV Transmission Systems", *Proceedings of 4th International Workshop on Atmospheric Icing of Structures*, Paris, France, pp. 70-75, 1988.

[95]   Mercure, H. P., "Insulator Pollution Performance at High Altitude: Major Trends", *IEEE Transactions On Power Delivery*, Vol. 4, No. 2, Apr. 1989.

[96]   Mercure, H. P. and Drouet, M. G., "Dynamic Measurement of the Current Distribution in the Foot of an Arc Propagation along the Surface of an Electrolyte", *IEEE Transactions On Power Apparatus and Systems*, Vol. PAS-101, No. 3, pp. 725-736, 1982.

[97]   Miller, H. C., "Surface Flashover of Insulators", *IEEE Transactions on Electrical Insulation*, Vol. 24, No. 5, pp. 765-786, October 1989.

[98]   Mizuno, Y., Kussada, H. and Naito, K., "Effect of Climatic Conditions on Contamination Flashover Voltage of Insulators", *IEEE Transactions on Dielectrics and Electrical Insulation*, Vol. 4, No. 3, pp. 286-289, 1997.

[99]   Näcke, H., "Stabilität der Fremdschichtentladungen und Theorie des Fremdschichtüberschlags", *ETZ-A*, No. 16, pp. 577-585, 1966.

[100] Naito, K., Ito, S. and Sakanishl, K., " The Effect of the Air Density on the DC Insulator Pollution Flashover Voltage", *CIGRE colloquium*, 33.87 (Coll) 11.02 IWD, 1987.

[101] Nasser, E., "Contamination Flashover of Outdoor Insulation", *ETZ-A*, Vol. 93, No. 6, pp. 321-325, 1972.

[102] Nasser, E., "Fundamentals of Gaseous Ionization and Plasma Electronics", *Wiley-Interscience*, New York, 1971.

[103] Nasser, E., "Why Contaminated Insulators Flashover at Operating Voltages", *Proceedings of IEEE Summer Power Meeting*, Paper No. 71 CP 674-PWR, 1971.

[104] Neumärker, G., " Verschmutzungszustand und Kriechweg", *Monatsber. D. Deut. Akad, Wiss.*, Berlin, Vol. 1, pp. 352-359, 1959.

[105] Obenaus, F., "Contamination Flashover and Creepage Path Length", *Disch. Electrotechnik*, 1958, vol. 12, No.4.

[106] Obenaus, F., "Die Ubersclagspannung verschmutzter Isolatoren", *ETZ*, Vol. 56, 369, 1935.

[107] Obenaus, F., "Fremdschichtüberschlag und Kriechweglänge", *Deutsche Elektrotechnik*, Vol. 4, pp. 135-136, 1958.

[108] Obenaus, F., "The Influence of Surface Coating (Fog, Salt, and Dirt) on the Flashover Voltage of Insulators", *Hescho-Mitt.*, Vol. 70, pp. 1-37, 1933.

[109] Oguchi, H. et al, " Icing on Electric Wires", *Researches on Snow and Ice*, No. 1, pp.45-49, 1953.

[110] Phan, C. L. and Matsuo, H., "Minimum Flashover Voltage of Iced Insulators", *IEEE Transactions on Electrical Insulation*, Vol. EI-18-6, pp. 605-618, 1983.

[111] Phan, C. L. et al, " Accumulation du Verglas sur les Noveaux Types d'isolateurs sous Haute Tension", *Canadian Electrical Engineering Journal*, Vol. 2, No. 4, pp. 24-28, 1977.

[112] Phan, C. L., Pirotte, P. and Trinh, N. G., "A Study of Corona Discharges at Water Drops over the Freezing Temperature Range", *IEEE Transactions on Power Apparatus and Systems*, Vol. PAS-93, No. 2, pp. 724-734, 1974.

[113] Raether, H., "Z. Phys.", 112, 464, 1939.

[114] Rahal, A. M. and Huraux, C., "Flashover Mechanism of High Voltage Insulators", *IEEE Transactions on Power Apparatus and Systems*, Vol. PAS-98, No. 6 pp. 2223-2231, 1979.

[115] Renner, P.E., Hill, H.L. and Ratz, O., "Effects of Icing on DC Insulation Strength", *Proceedings of IEEE Summer Power Meeting and EHV Conference*, Los Angeles, USA, Paper No. 70 TP 610-PWR, pp. 1201-1205, 1970.

[116] Rizk, A. M. and Rezazada, A. Q., " Modeling of Altitude Effects on AC Flashover of Polluted High Voltage Insulators", *Proceedings of IEEE/PES Winter Meeting*, Baltimore, USA, Paper No. 96 WM 104-0 PWRD, January 1996.

[117] Rizk, Farouk A. M., "Mathematical Models for Pollution Flashover", *Electra*, Vol. 78, pp. 71-103, 1981.

277

[118] Rudakova, V. M. and Tikhodeev, N. N., "Influence of Low Air Pressure on Flashover Voltages of Polluted Insulators: Test Data, Generalization Attempts and Some Recommendations", *IEEE Transactions on Power Delivery,* Vol. 4, No. 1, pp. 607-613, January 1989.

[119] Ryerson, C. C., "Atmpospheric icing with elevation on New England mountains", *Proceedings of the 4th International Workshop on Atmospheric Icing of Structures,* Paris, France, pp. 89-93, 1988.

[120] Sato, M., Saito, H., Kaga, A. and Akagami, H., " Fundamental Characteristics of AC Flashover on Contaminated Insulators Covered with Ice", *Japanese Journal of Applied Physics,* Vol. 28, No. 5, pp. 889-896, 1989.

[121] Schneider, H. M., "Artificial Ice Tests on Transmission Line Insulators-A Progress Report", *Proceedings of IEEE/PES Summer Meeting,* San Francisco, USA, Paper No. A75-491-1, pp. 347-353, 1975.

[122] Shu, L., Gu, L. and Sun, C., "A Study of Minimum Flashover Voltage of Iced-covered suspension Insulators", *Proceedings of 7th International Workshop on the Atmospheric Icing of Structures,* Chicoutimi, Canada, pp. 87-92, 1996.

[123] Shu, L., Sun, C., Zhang, J. and Gu, L., "AC Flashover Performance of Iced and Polluted Insulators for High Altitude Regions", *Proceedings of 7th International Symposium on High Voltage Engineering,* Vol. 4, Dresden, Germany, Paper 44.13, pp.303-306, August 1991.

[124] Su, F. and Jia, Y., "Artificial Rime-Covereing and Discharge Test of Long Insulator Strings", *Proceedings of 7th International Workshop on Atmospheric Icing of Structures,* Chicoutimi, Canada, pp. 369-372, 1996.

[125] Su, F. and Hu, S., " Icing on Overhead Transmission Lines in Cold Mountainous District of southwest China and Its Protection", *Proceedings of 4th International Workshop on Atmospheric Icing of Structures*, Paris, France, pp. 354-357, 1988.

[126] Su, F. and Jia, Y., "Icing on Insulator String of HV Transmission Lines and Its Harmfulness", *Proceedings of 3rd International Offshore and Polar Engineering Conference*, Singapore, pp.655-658, 1993.

[127] Sugawara, N., Hokari, K., Nosaka, T., Tatokoro, Y. and Mizumura, K., "Insulation Resistance of Transmission Line Insulators Depending on the Accretion of Ice". *Proceedings of 5th International Workshop on Atmospheric Icing of Structures*, Tokyo, Japan, Paper No. B4-9, pp. 1-6, 1990.

[128] Sugawara, N., Hokari, K., Yoshida, K., Ando, H., Hirota, M. and Tatokoro, Y., "Insulation Properties of Atmospheric Iced Insulators Installed in High Mountains", *Proceedings of 6th International Workshop on the Atmospheric Icing of Structures*, Budapest, Hungary, pp. 237-242, 1993.

[129] Sugawara, N., Takayama, K., Hokari, K., Yoshida, K. and Ito, S., "Withstand Voltage and Flashover Performance of Iced Insulators Depending on the Density of Accreted", *Proceedings of 6th International Workshop on the Atmospheric Icing of Structures*, Budapest, Hungary, pp. 231-235, 1993.

[130] Sugawara, N., Watanabe, S. and Hokari, K., "Flashover Performance of Transmission Line Insulators Covered with Salt-Contaminated Ice and Icicles", *Proceedings of 7th International Symposium on High Voltage Engineering*, Dresden, German, Paper No. 44.10, pp. 291-294, 1991.

[131] Sundararajan, R. and Nowlin, R. W., "Effect of Altitude on the Flashover Voltage of Contaminated Insulators", *Proceedings of Conference on*

Electrical Insulation and Dielectric Phenomena, San Francisco, USA, Paper No. 5A-12, pp. 433-436, 1996.

[132] Sundararajan, R., "A Computational Study of Flashover Voltage of Iced Insulators", *Proceedings of 38th American Power Conference*, Chicago, USA, pp. 6-9, 1997.

[133] Swift, D. A., "Flashover of Polluted Insulators: Electric Field in the Arc", *Proceedings of 6th International Symposium on High Voltage Engineering*, New Orleans, USA, Paper No. 30.10, 1989.

[134] Tsinghua University and Xian Jiaotong University, "High Voltage Insulation", *Power Industry Press*, China, 1980.

[135] Vuckovic, Z. and Zdravkovic, Z., "Effect of Polluted Snow and Ice Accretion on High-voltage Transmission Line Insulators", *Proceedings of 5th International Workshop on the Atmospheric Icing of Structures*, Tokyo, Japan, Paper No. B4-3, 1990.

[136] Wang, Q., "Physics of the Arc in Electrical Apparatus", *Mechanical Industry Press*, Beijing, 1982.

[137] Wang, S., "Study of Ice accumulation on transmission lines at high altitude areas of Yun Nan", *Yun Nan Province Press*, China, 1993.

[138] Watanabe, Y., "Flashover Tests of Insulators Covered with Ice or Snow", *IEEE Transactions on Power Apparatus and Systems*, Vol. PAS-97, No. 5, pp. 1788-1794, 1978.

[139] Wilkins, R. and Al-Baghdadi, A. A. J., " Arc Propagation along an Electrolyte Surface", *Proceedings of IEE*, Vol. 118, No. 12, pp. 1886-1892, 1971.

[140]   Wilkins, R., "Flashover Voltage of High Voltage Insulators with Uniform Surface Pollution Films", *Proceedings of IEE*, Vol. 116, No. 3, pp. 457-465, 1969.

[141]   Wu, C. T. and Cheng, T. C., "Formation Mechanisms of Clean Zones during the Surface Flashover of Contaminated Insulators", *IEEE Transactions on Electrical Insulation*, Vol. EI-13, No. 3, pp. 149-156, June 1978.

[142]   Wu, D., Halsan, K. A. and Fikke, S.M., "Artificial Ice Tests for Long Insulator Strings", *Proceedings of 7th International Workshop on the Atmospheric Icing of Structures*, Chicoutimi, Canada, pp. 67-71, 1996.

[143]   Zhang, J. and Farzaneh, M., "Computation of AC Critical Flashover Voltage of Insulators Covered with Ice", *Proceedings of 1998 International Conference on Power System Technology*, Beijing, China, Vol. 1, pp. 524-528, August, 1998.

[144]   Zhang, J. and Farzaneh, M., "Propagation of AC and DC Arcs on Ice Surfaces", *IEEE Transactions on Dielectrics and Electrical Insulation*, Vol. 7, No. 2, pp. 269-276, 2000.

[145]   Zhang, J. and Farzaneh, M., "Propagation of DC Arc on Ice Surfaces", *Proceedings of 8th International Offshore and Polar Engineering Conference*, Montreal, Canada, pp. 547-550, 1998.

[146]   Zhang, J., "Study on Flashover mechanism and Affecting Factors of polluted insulators", *Thesis of PhD*, Chongqing University, China, 1991.

[147]   Zhang, J., Farzaneh, M. and Chen, X., "Influence of Air Temperature on Flashover along Ice Surfaces", *Conference Record of the 1996 IEEE International Symposium on Electrical Insulation*, Montreal, Canada, Vol. 1, pp. 324-327, June 1996.

[148] Zhao, T., Zhang, R. and Xue, J., "The Influence of Pressure on AC Flashover Characteristics of Contaminated Insulators", *Proceedings of IEEE/CSEE Joint Conference on High Voltage Transmission Systems in China*, Bejing, China, pp. 291-294, 1987

[149] Zoledziowski, S., "Time-to-Flashover Characteristics of Pollted Insulators", *IEEE Transactions on Power Apparatus and Systems*, Vol. PAS-87, No. 6 pp. 1397-1404, 1966.

APPENDICES

APPENDIX 1

TECHNICAL DATA OF HIGH SPEED CAMERA

Table A.1 Technical Data of High Speed Camera

Processor	
Recording Technique	Digital images Stored in Dynamic Random Access Memory (DRAM)
Record Rates	50, 125, 250,500 and 1000 full frames per second, 2000, 3000, 4000, 6000 and 12000 split frames per second.
Image Splits	1, 2, 3, 4, 6 and 12 splits per frame. Permits record rates of up to 12000 pictures per second. Can be played back with a single image per frame or multiple images per frame.
Exposure	1/50 to 1/12000 of a second depending upon image spit and record rate.
Playback Rates	0, 1, 2, 3, 3.8, 5, 6, 7.5, 10, 15, 30, 60, 90, 120, 240, 480, 960 fps plus single step, freeze frame forward or reverse.
Data-Frame Border	Date, ID number, record rate, exposure, image split, elapsed time, playback rate, frame number, pixel depth, reticule coordinates, real time and system status messages.
Size	17" x 19.5" x 12.75" (43cm x 50 cm x 32 cm)

Standard Imager	
Control Keys	Live, Record and Stop
Sensor	192 x 239 pixel NMOS array
Spectral Response	400 to 1000 nanometers
Gray Scale	256 levels of grey
Lens Mount	C - Mount
Size	Approximately 9" x 4" x 5" (23 cm x 10 cm x 12 cm)

APPENDIX 2

CORRECTION OF FREEZING WATER CONDUCTIVITY

The conductivity correction should be made using the following formula [60]:

$$\sigma_0 = \sigma_T \left[1 - b(T - 20)\right] \tag{A.1}$$

where T is the solution temperature (°C)

σ_T is the volume conductivity at a temperature of T °C (S/m)

σ_{20} is the volume conductivity at a temperature of 20 °C (S/m)

b is the factor depending on temperature T, as given below:

Table A.2 Factor b in Equation A.1

T°C (S/m)	b
5	0.03156
10	0.02817
20	0.02277
30	0.01905

APPENDIX 3

REGRESSION ANALYSIS

The flashover phenomenon on ice-covered insulators is a stochastic process. There is a correlation between the flashover voltage and the air pressure and between the voltage along the arc and the leakage current. Therefore, regression analysis was used in this study to determine the involved coefficients such as the exponent m, the arc constant A, n, and the current density in an arc root, B.

Regression analysis consists of graphic and analytic methods for exploring relationships between one variable, referred to as a response variable, and one or more other variables, called predictor variables. The goal of this analysis is to express the response variable as a function of the predictor variables. Once such an expression is obtained it can be utilized to predict values of the response variable.

In this study, the relation between only two variables was concerned. Supposing a series of values of the predictor variable, X_1, X_2, ..., X_n , and the

corresponding values of the response variable, Y_1, Y_2, ..., Y_n, are obtained, a regression equation is then selected as:

$$Y = f(a_1, a_2, ..., a_m; X) \qquad \text{(A.2)}$$

In order to determined the coefficients a_1, a_2, ..., a_m, normally the least squares method is used. This method can be summarized as follows:

− Construct the sum of squared residuals

$$S = \sum_{i=1}^{N} r_i^2 = \sum_{i=1}^{N} [Y_i - f(a_1, a_2, ... a_m; X_i)] \qquad \text{(A.3)}$$

− Determine the coefficients a_1, a_2, ..., a_m to make the sum of squared residuals as small as possible by solving the following equations:

$$\begin{cases} \dfrac{\partial S}{\partial a_1} = 0 \\[2mm] \dfrac{\partial S}{\partial a_2} = 0 \\[2mm] ...... \\[2mm] \dfrac{\partial S}{\partial a_m} = 0 \end{cases} \qquad \text{(A.4)}$$

According to this principle, in this study, the exponent m in Equation 4.1, the arc constants A, n in Equation 6.2 and the current density in an arc root, B, in Equation 7.1 were separately determined by the following formulas:

For *m*:

$$m = \frac{\sum_{i=1}^{N}\left[\ln\left(\frac{V_i}{V_0}\right)\cdot\ln\left(\frac{P_i}{P_0}\right)\right]}{\sum_{i=1}^{N}\left[\ln\left(\frac{P_i}{P_0}\right)\right]^2} \qquad (A.5)$$

where N is the total number of tests, P_0 is the standard pressure (101.3 kPa); V_0 is the flashover voltage corresponding to the pressures P_0; P_i and V_i are the pressure and flashover voltage in the ith test.

For *n*:

$$n = \frac{\sum_{i=1}^{N}\ln(E_i)\cdot\sum_{i=1}^{N}\ln(I_i)-N\cdot\sum_{i=1}^{N}\ln(E_i)\cdot\ln(I_i)}{N\cdot\sum_{i=1}^{N}[\ln(I_i)]^2-[\sum_{i=1}^{N}\ln(I_i)]^2} \qquad ((A.6)$$

where N is the total number of tests, E_i and I_i is the flashover voltage gradient and leakage current in the ith test.

For *A*:

$$A = \frac{\sum_{i=1}^{N}E_i\cdot I_i^{-\bar{n}}}{\sum_{i=1}^{N}I_i^{-2\bar{n}}} \qquad (A.7)$$

where N is the total number of tests; E_i and I_i is the flashover voltage gradient and the leakage current obtained in the ith test; $\bar{n}$ is the average value of n at different air pressures.

For B:

$$B = \frac{\sum\limits_{i=1}^{N}(I_i)^2}{\pi \cdot \sum\limits_{i=1}^{N}(r_i^2 \cdot I_i)}$$

(A.8)

where N is the total number of tests; r_i and I_i are the arc root radius and leakage current measured in the ith test.